Accreditation by Kemdikbudristek
Decree. No.158/E/KPT/2021 (rank. SINTA 3)

ISSN 2355-5068
e-ISSN 2622-4852
Volume 10, Issue 1, April 2023

JURNAL ECOTIPE

Electronic, Control, Telecommunication, Information, and Power Engineering

https://journal.ubb.ac.id/index.php/ecotipe

Electrical Engineering Department
Bangka Belitung University

ISSN 2355-5068
e-ISSN 2622-4852

JURNAL ECOTIPE
Electronic, Control, Telecommunication, Information, and Power Engineering

Volume 10, Issue 1, April 2023
DOI : 10.33019/jurnalecotipe.v10i1

Accredited by Kemdikbudristek RI
Decree No.158/E/KPT/2021 **(rank. SINTA 3)**

Editorial Board

Publisher Address:
Electrical Engineering Department
Faculty of Engineering - Bangka Belitung University
Balunijuk, Bangka Regency, Bangka Belitung Islands Province, Indonesia
Phone (0717) 4260033 ext. 2125, 2128
Website : https://journal.ubb.ac.id/index.php/ecotipe
E-mail : jurnal.ecotipe@yahoo.com / jurnalecotipe@ubb.ac.id

Preface

Jurnal Ecotipe (Electronic, Control, Telecommunication, Information, and Power Engineering) published by the Electrical Engineering Department, Bangka Belitung University currently starting Volume 7 Number 2, October 2020 to Volume 12 Number 2, October 2025 has been accredited by the Ministry of Education, Culture, Research, and Technology of the Republic of Indonesia based on Decree No. 158/E/KPT/2021 with 3rd rank (SINTA 3).

Currently, Jurnal Ecotipe volume 10 issue 1, April 2023 has been published. In this edition of the journal, the journal articles are in full English. Starting from volume 9 issue 2 October 2022, for the next editions of the articles in Jurnal Ecotipe, articles will be published using English in their writing and presentation. The articles in this edition of the journal come from academics both from within and from outside the institution.

Our highest appreciation goes to the Reviewers, Editorial Board, Authors, and all parties involved in the preparation and publication of the Ecotipe Journal Volume 10 Issue 1 April 2023. Hopefully, this journal can provide benefits and add scientific insight into the field of Electrical Engineering in particular and engineering in general. Therefore, we still hope for suggestions and constructive criticism for improvements and improvements for the progress of this journal.

Editor-in-Chief

Indexed journal on:

ISSN 2355-5068
e-ISSN 2622-4852

Volume 10, Issue 1, April 2023
DOI : 10.33019/jurnalecotipe.v10i1

JURNAL ECOTIPE
Electronic, Control, Telecommunication, Information, and Power Engineering

Accredited by Kemdikbudristek RI
Decree No.158/E/KPT/2021 **(rank. SINTA 3)**

Table of Content

JURNAL ECOTIPE
Electronic, Control, Telecommunication, Information, and Power Engineering

Volume 10, Issue 1, April 2023, pp. 1-11
ISSN 2355-5068 ; e-ISSN 2622-4852
DOI: 10.33019/jurnalecotipe.v10i1.3357

Snack Vending Machine Using QR Code as Payment Method

Arya Jaka Maulana[1], Erna Alimudin[2], Vicky Prasetia[3], Muhammad Reza Hidayat[4]
[1,2,3]Department of Electrical Engineering, Politeknik Negeri Cilacap, Jl. Dr. Soetomo, No. 1, Cilacap 53212, Indonesia
[4]Department of Electrical Engineering,Universitas Jenderal Ahmad Yani, Jl. Terusan Jend. Sudirman, Cimahi 40531, Indonesia

ARTICLE INFO

Article historys:

Received : 05/10/2022
Revised : 23/11/2022
Accepted : 19/04/2023

Keywords:

Infrared; Obstacle Sensor; QR Code; Vending Machine

ABSTRACT

Vending machines can be used as a solution to overcome losses for selling and make the payment system easier. This study aims to design a snack vending machine with a payment system using an Android-based QR Code scan application in which there is a balance as electronic money. In the payment application, there is also an admin account to top up balances and view sales history, making it easier for sellers to monitor sales results. This snack vending machine uses ESP32 to store data as well as transmit data from every activity that occurs. There are 4 types of snacks in this vending machine. Selection of the type of snack using the Keypad and to regulate the release of the snack using a servo motor connected to a spiral wire. 16x2 LCD to display data and an Infrared Avoid Obstacle sensor to stop the servo from rotating when it detects food falling in front of it. Testing on a snack vending machine using a QR Code was carried out by trying to purchase 4 types of snacks, with each trial 10 times. The whole test is successful, the tool can issue snacks and transactions on the payment application run properly.

Corresponding Author:

Erna Alimudin
Politeknik Negeri Cilacap, Jl. Dr. Soetomo, No. 1, Cilacap 53212, Indonesia
Email: ernaalimudin@pnc.ac.id

1. INTRODUCTION

A vending machine is a machine that can automatically sell various products based on user requests. A vending machine is an automatic device that uses digital and mechanical energy or a mechanism to automatically dispense products such as medicines, groceries, tickets, or licenses to users without paying for human labor in vending machines [1, 2]. Several different drink machines user operated by inserting coins to purchase drinks [3]. Today's vending machines generally still use coins, paper money, and cards to make payments at vending machines [4]. The problem when using banknotes or coins is that they are less effective when making payments because not all buyers carry the specified amount [5].

Vending machines can now be applied to honesty canteens. Honesty canteens are a method used in schools and offices to sell something without a salesperson on duty [6]. The honesty canteen has a similar principle to a vending machine [1,7]. Buyers can make payment transactions independently without a seller, by entering money in the box provided as a place of payment at the honesty canteen [8]. However, the problem that often occurs for sellers is that the amount of sales proceeds do not match, resulting in losses [9, 10]. A vending machine can be interpreted as a tool or machine used to sell goods automatically. What is meant by automatic here is that it does not require workers to sell goods that can be purchased according to what the buyer wants [11, 12].

In its use, smartphones can read QR Codes, one of which is to provide information on data [13]. QR Code is a two-dimensional image that represents data, especially data in the form of text. QR Code has the ability to store data [14].

JURNAL ECTIPE
Electronic, Control, Telecommunication, Information, and Power Engineering
Volume 10, Issue 1, April 2023, pp. 1-11
ISSN 2355-5068 ; e-ISSN 2622-4852
DOI: 10.33019/jurnalecotipe.v10i1.3357

In this study, there are several similar studies that are used as a reference in the implementation of this research. The research and observations used as a reference are described as follows. The first research discusses an automatic food-drink vending machine with a payment system using a coin acceptor to read coins [15]. In this study, the hardware design uses ATMega8 as a microcontroller, DC motor driver, DC gearbox motor, coin selector, Bluetooth module, and buzzer. The second study discusses the design of a vending machine with a payment system entering banknotes by reading the value of the color of the banknote using a color sensor. In this study, the manufacturer of the tool uses Arduino Uno as a microcontroller and uses a 16x2 LCD, Push button, and Servo Motor [16]. The third research discusses Vending money changer machines made to help kiosks, mini markets, or banks to exchange money and make the process of converting paper money into coins easier. This device is based on the Arduino Uno microcontroller to control the equipment [17]. This tool uses a TCS3200 color sensor to detect the color of the IDR 5,000 note, a DC motor to pull out banknotes, and a servo motor to issue IDR 1,000 coins. In this device, the LCD is used to display the manual for using the vending machine and the number of coins issued. In this research, the manufacturer of the tool uses Arduino Uno as a microcontroller and uses a 16x2 LCD, TCS3200 color sensor, and a DC motor. The fourth research discusses automatic beverage vending machines that can make sales using non-cash payments by utilizing RFID as a medium for storing balances and different IDs. In this study, the manufacturer of the tool uses Arduino Uno R3 as a microcontroller and uses a 16x2 LCD, Keypad, and Servo Motor [18, 19]. The fifth study discusses the manufacture of vending machines with RFID containing balances used as a tool to make payments at the vending machine [20]. In this study, the manufacturer of the tool uses Arduino Uno as a microcontroller, Button, RFID Module, 16x2 LCD, and Motor.

This research will complement the shortcomings of previous research. The vending machine payment system this time will be done by scanning the QR Code via the camera installed on the smartphone so that buyers don't need to prepare banknotes, coins, and cards. To make payments via QR Code, smartphone users must first download the application that has been made to make payments. On the vending machine, a QR Code will be affixed which will provide information in the form of data from the snacks on the machine [21]. The QR Code scanning process is carried out through an android-based application. In the application, there are two accounts, namely the admin account user account. User accounts are used to make payment transactions which contain data in the form of user accounts and balances. The admin account is used to top-up user account balances and view snack sales history. The communication used between the vending machine and the application is through the real-time database feature on firebase. Through this application, snacks in the vending machine can be purchased. With this research, it is hoped that it can help in terms of convenience and security in transacting on snack vending machines.

2. RESEARCH METHOD

The snack vending machine made in this study consists of components that are used both software and hardware such as:

2.1. Design Block Diagram

It is one part of the design of making this tool because from this block diagram we can know the working principle of the whole circuit. Simplify the design process for making tools so that a system that is in accordance with the previous design will be formed. The following block diagram of the system can be seen in Figure 1.

Volume 10, Issue 1, April 2023, pp. 1-11
ISSN 2355-5068 ; e-ISSN 2622-4852
DOI: 10.33019/jurnalecotipe.v10i1.3357

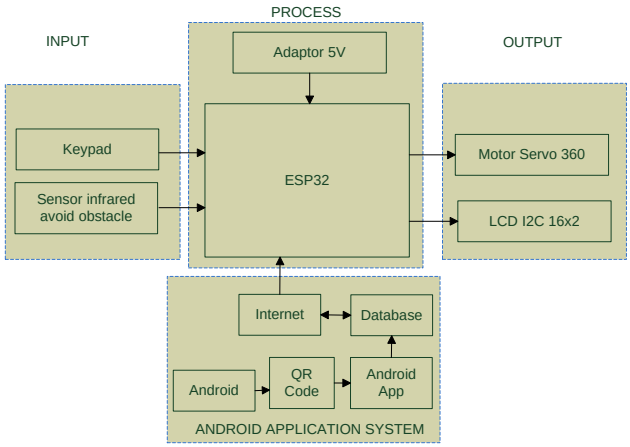

Figure 1. Design Block Diagram

The Block diagram of the system in Figure 1 can be explained as the system on a snack vending machine using ESP32 as one of those microcontrollers. ESP32 has several advantages over other microcontrollers. The main thing is the built-in WiFi module and Bluetooth which makes it easy for the ESP32 to connect to the internet. Internet connection is needed in an IoT project. ESP32 is also equipped with a GPIO Pin that can be used for various needs. There are also I2C and SPI pins which make it easy to communicate [22]. In this study, using ESP32 was the main microcontroller or data processing center used to control snack vending machines. The keypad is a series of switch buttons that have been arranged to form a row and column named in the form of numbers and letters, which serves to signal a circuit, by connecting certain lines [23]. In this study, the Keypad is used as a button to select the type of snacks available on the snack vending machine. The Infrared Obstacle Avoid Sensor is a module consisting of infrared and a photodiode that functions as a detector of obstacles or objects in front of it [24, 25]. In this study, the Infrared Obstacle Avoid sensor is used to detect food falling in front of it as a continuous servo motor rotation controller. A Servo motor is a DC motor with a closed feedback system where the position of the motor will be informed back to the control circuit in the servo motor. This motor consists of a DC motor, a series of gears, a potentiometer, and a control circuit [24]. In this study, using a continuous servo motor connected to a spiral to push snacks. As communication between the vending machine and the Android application, the real-time database feature on the firebase console is used as a database for data storage so that the vending machine and the Android application can be connected to run the work system of the snack vending machine.

2.2. Account List Flowchart

Figure 2 is a system flowchart from account registration in order to make purchases on the vending machine application. On account registration, user data after registration will be stored in the database. The data that must be filled in is the Account Name and Password. The system can also find out from the account data whether it has been used or not, if it has been used a warning will appear that the account has been registered.

2.3. Account Login Flowchart

In the design of Figure 3, namely the Account Login flowchart, the method of filling in the Account Name and Password is used, if the Account Name and Password are incorrect, the system will automatically warn that the account entry failed because the account name or password is wrong. If true then Login is successful.

JURNAL ECTIPE
Electronic, Control, Telecommunication, Information, and Power Engineering
Volume 10, Issue 1, April 2023, pp. 1-11
ISSN 2355-5068 ; e-ISSN 2622-4852
DOI: 10.33019/jurnalecotipe.v10i1.3357

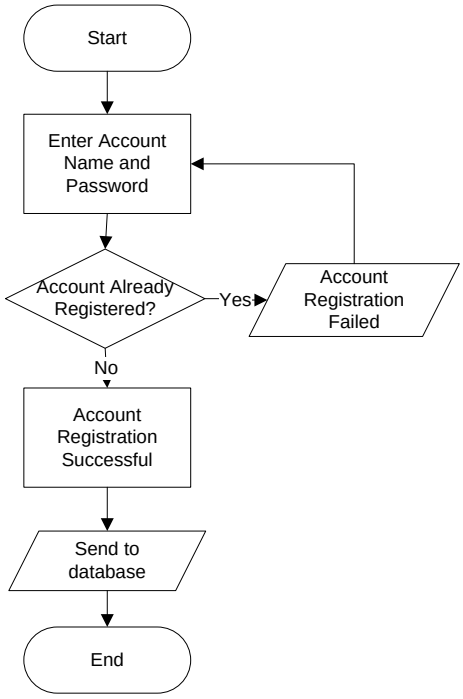

Figure 2. Account List Flowchart

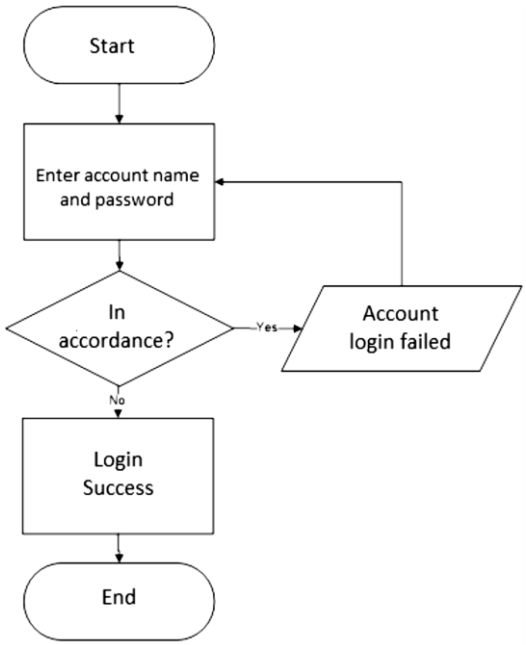

Figure 3. Account Login Flowchart

2.4. Admin Account Flowchart

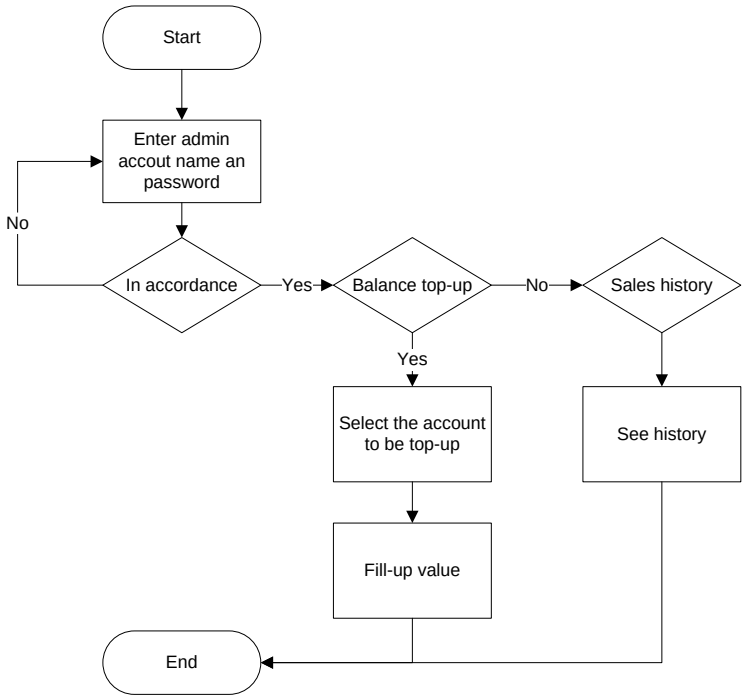

Figure 4. Admin Account Flowchart

In the design Figure 4, is a flowchart of the admin account to top-up balances and view the sales history of the vending machine. Accounts that can be top-up balances are user accounts that have been registered.

2.5. Work System Flowchart

Volume 10, Issue 1, April 2023, pp. 1-11
ISSN 2355-5068 ; e-ISSN 2622-4852
DOI: 10.33019/jurnalecotipe.v10i1.3357

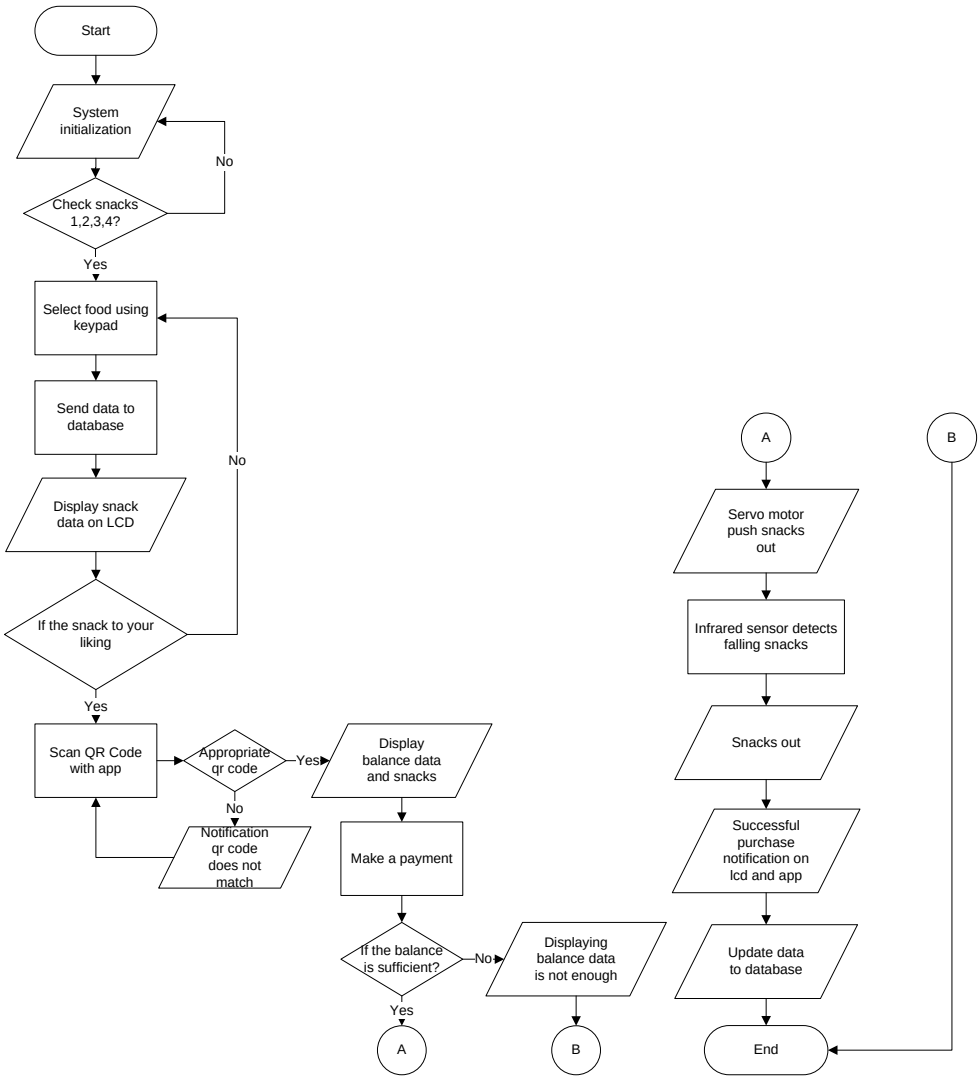

Figure 5. Work System Flowchart

From the flowchart in Figure 5, it can be explained the process of running a snack vending machine using a QR code. First, it starts with system initiation including ESP32, keypad, LCD, infrared sensor, and servo motor. The way it works starts with checking the food stock with an infrared sensor and then selecting the type of snack using the keypad. After that, the keypad input sends the food type selection data to the database which will be sent to the QR code scan payment application after scanning. After that, enter the payment application and make payments by scanning the QR code using Android. The QR code scan process is successful when the scanned QR code matches the vending machine. This QR code contains data on the price and type of snacks. Then check the balance, when the balance is sufficient then you can make purchases and when the balance is less then you can't make transactions. After the purchase transaction is successful, the latest balance data will be updated in the database. Then after the purchase is successful, the servo will push the food out. The falling food will be detected by the infrared sensor to stop the rotation of the servo motor. The buyer picks up the selected food.

2.6. Snack Vending Machine Hardware

The snack vending machine using created QR Code in Figure 6 has been tested. This is done with the aim of knowing whether the tools made are working as expected.

JURNAL ECTIPE
Electronic, Control, Telecommunication, Information, and Power Engineering
Volume 10, Issue 1, April 2023, pp. 1-11
ISSN 2355-5068 ; e-ISSN 2622-4852
DOI: 10.33019/jurnalecotipe.v10i1.3357

Figure 6. Snack Vending Machine Hardware

3. RESULTS AND DISCUSSION

This section contains the design results from testing each hardware and software used as a whole that makes up the system on the snack vending machine.

3.1. Android Application Design Results

1. Account Login Page

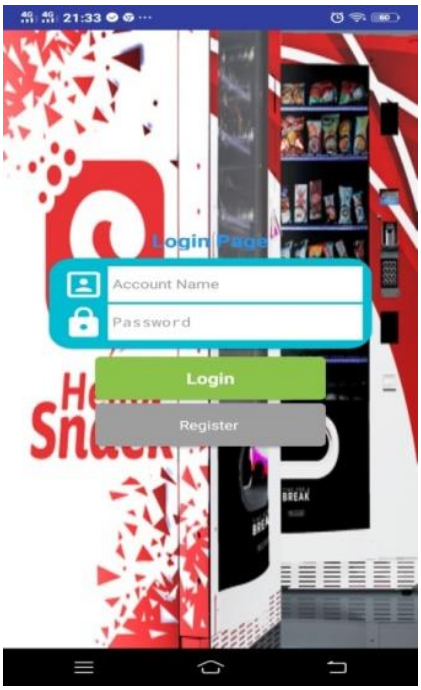

Figure 7. Account Login Page

This display in Figure 7 has two menus, namely, the first is the Login menu for an account that has been registered, then you can enter or log into the application to make transactions on the vending machine. Second, the menu for Registering a New Account, if you don't have an account, for a newly registered account, you will get an initial balance of zero rupiahs.

JURNAL ECOTIPE
Electronic, Control, Telecommunication, Information, and Power Engineering
Volume 10, Issue 1, April 2023, pp. 1-11
ISSN 2355-5068 ; e-ISSN 2622-4852
DOI: 10.33019/jurnalecotipe.v10i1.3357

2. Admin Page

Figure 8. Admin Page

On the admin page view in Figure 8, there are three menus that can be accessed, namely the Top-up Balance Menu which functions to top-up balances on member accounts or registered users so that they can make food purchases, the Snack Sales History Menu functions to view transaction history on the vending machine. Snacks that have been sold.

3. Payment Transaction Page

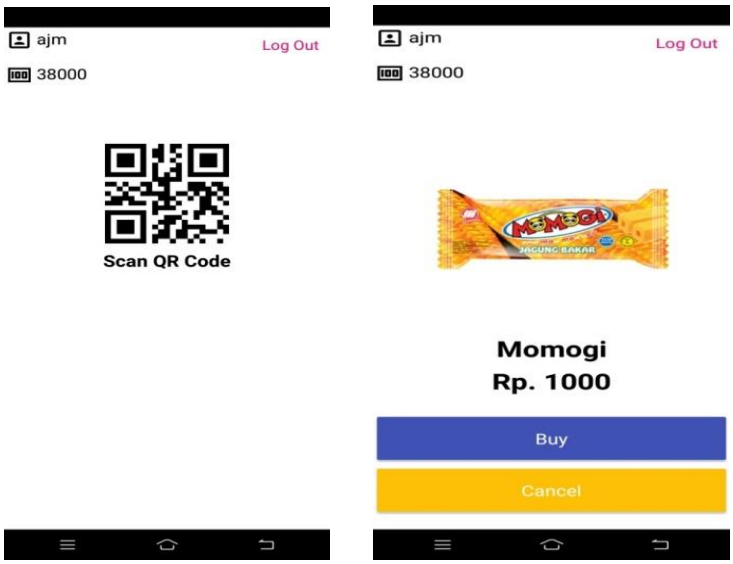

(a) (b)

Figure 9. (a) QR Code for snack and **(b)** Payment Transaction Page

On the payment transaction page in Figure 9 (b), there is an account name, balance, and a menu to scan the QR code in Figure 9 (a). After the user selects the type of snack on the machine. After that, the user scans the QR Code on the machine. When it has been scanned, the application will direct the user

JURNAL ECTIPE
Electronic, Control, Telecommunication, Information, and Power Engineering
Volume 10, Issue 1, April 2023, pp. 1-11
ISSN 2355-5068 ; e-ISSN 2622-4852
DOI: 10.33019/jurnalecotipe.v10i1.3357

or user to the menu to make payments for the snacks that have been selected. In the menu for making payments, there is price information for the selected snacks and a menu for clicking Pay Now to remove the food and the balance in the account will decrease. In addition, there is also a menu to cancel if you want other types of snacks.

2.2. System Testing Discussion

In this section is the result of a discussion of system testing carried out on snack vending machines that have been made according to the purpose or not.

1. Keypad Test and QR Code Scan

This test is carried out to determine the results of the accuracy of selecting the type of food by using the Keypad as input and scanning the QR Code according to the selected results or not. Selecting the type of food using the Keypad will be displayed on the LCD while the results of the QR Code Scan will be displayed on the Application. Keypad keys in Figure 10 used for selection are:

1. Button No. 1 in Keypad for Momogi snacks
2. Button No. 2 in Keypad for Saltcheese snacks
3. Button No. 3 in Keypad for Regal snacks
4. Button No. 4 in Keypad for Better snacks
5. Button A for Cancel

The result of the keypad test and QR code scan result is shown in Table 1.

Figure 10. Keypad Test and QR Code Scan

Table 1. Keypad Test and QR Code Scan Result

Data to-	Selection of types of snacks on the keypad	Display on LCD	QR Code scan display on the application	Description
1	Momogi	In accordance	In accordance	succeed
2	Saltcheese	In accordance	In accordance	succeed
3	Regal	In accordance	In accordance	succeed
4	Better	In accordance	In accordance	succeed

2. Infrared Obstacle Avoid Sensor Testing

This test is carried out to detect any obstacles or objects from falling snacks. Falling objects can be detected by the sensor because it has an IR Emitter that functions to reflect infrared to the object and then it is reflected and will be received by the IR Receiver. When the object in front is detected by the infrared sensor, the LED will light up. The result is in Table 2.

JURNAL ECTIPE
Electronic, Control, Telecommunication, Information, and Power Engineering
Volume 10, Issue 1, April 2023, pp. 1-11
ISSN 2355-5068 ; e-ISSN 2622-4852
DOI: 10.33019/jurnalecotipe.v10i1.3357

Table 2. Infrared Obstacle Avoid Sensor Testing

Object distance	LED condition/Sensor digital value	Status on LCD
1-4 cm	ON/0	Please take a snack
5-8 cm	ON/0	Please take a snack
9-12 cm	OFF/1	-

3. Snack Payment Test with Order

This test is done by selecting the type of food in sequence and doing the experiment repeatedly. In this test, it is expected that the tool can remove snacks on the machine according to the choice. And the balance on the account is expected to be updated after making a snack purchase at the vending machine. If the payment is succesfull, the display will show Figure 11 (b). This test is carried out using 4 different accounts and balances.

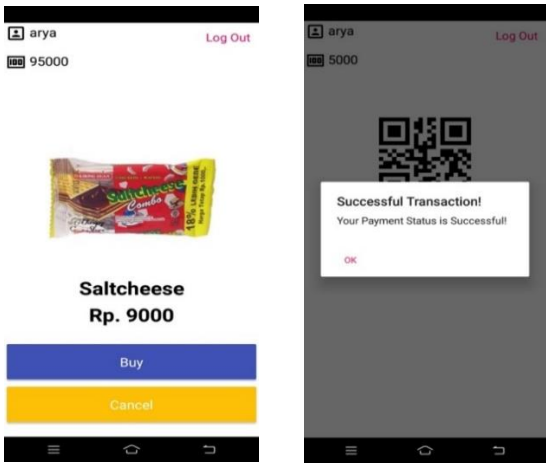

(a) (b)

Figure 11. (a) Buy a snack and **(b)** payment snack

4. Less Balance Payment Test

This test is carried out to prove when making a payment at a snack vending machine that when the balance on the account is not sufficient, it cannot process transactions and also does not issue snacks. The display will show Figure 12.

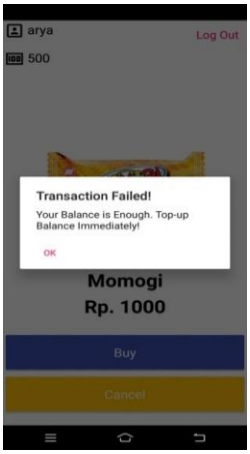

Figure 12. Less Balance Payment Test

4. CONCLUSION

Based on the results of the design, manufacture, testing, and analysis that have been carried out from the implementation of this research it can be concluded, as follows:

Volume 10, Issue 1, April 2023, pp. 1-11
ISSN 2355-5068 ; e-ISSN 2622-4852
DOI: 10.33019/jurnalecotipe.v10i1.3357

1. Snack vending machines using a scan QR code can work well marked by snacks that manage to come out of the vending machine after making a purchase transaction using a scanned QR code application.
2. Purchase of snacks using an android-based QR code scan application which includes the user's account and balance so that it is safer and makes it easier for users to make payment transactions.
3. The payment application uses an admin account to top-up balances and views the history of successful sales based on testing and analysis.

REFERENCES

[1] K. Segrave, *Vending Machine: American Social History*. North Carolina: McFarland & Company, Inc, 2002.

[2] E. Wu and D. Maslov, "Vending Machine," in *Raspberry Pi Retail Applications: Transform Your Business with a Low-Cost Single-Board Computer*, Berkeley, CA: Apress, 2022, pp. 41–70. doi: 10.1007/978-1-4842-7951-9_3.

[3] A. P. Bodhale and P. J. S. Kulkarni, "Case Study on Different Vending Machines," *Int. Res. J. Eng. Technol.*, vol. 4, no. 4, pp. 3531–3535, 2017, [Online]. Available: https://www.irjet.net/archives/V4/i4/IRJET-V4I4846.pdf

[4] R. Dijaya, E. A. Suprayitno, and A. Wicaksono, "Integrated Point of Sales and Snack Vending Machine based on Internet of Things for Self Service Scale Micro Enterprises," *J. Phys. Conf. Ser.*, vol. 1179, no. 1, 2019, doi: 10.1088/1742-6596/1179/1/012098.

[5] G. Camera, "A Perspective on Electronic Alternatives to Traditional Currencies ," *Sveriges Riksbank Econ. Rev. 1*, no. 2008, pp. 126–148, 2017, [Online]. Available: https://digitalcommons.chapman.edu/esi_working_papers/210

[6] A. Zainal, T. Sriwedari, K. Harahap, and J. Suhariyanto, "Developing a Model of Smart School Canteen: an Introduction of Self-Purchasing Technology," *J. Community Res. Serv.*, vol. 2, no. 2, p. 236, 2019, doi: 10.24114/jcrs.v2i2.13156.

[7] M. L. Caruso, E. G. Klein, and G. Kaye, "Campus-Based Snack Food Vending Consumption," *J. Nutr. Educ. Behav.*, vol. 46, no. 5, pp. 401–405, 2014, doi: https://doi.org/10.1016/j.jneb.2014.02.014.

[8] "Quick Response Mechanism Payment System Using Waterfall," vol. 9, no. 4, pp. 16–27, 2021.

[9] Transformers Committee of the IEEE Power Engineering Society, "IEEE Std C57.104™-2008, IEEE Guide for the Interpretation of Gases Generated in Oil-Immersed Transformer," 2008, doi: 10.1109/IEEESTD.2009.4776518.

[10] N. Cisse-Egbuonye, S. Liles, K. E. Schmitz, N. Kassem, V. L. Irvin, and M. F. Hovell, "Availability of Vending Machines and School Stores in California Schools," *J. Sch. Health*, vol. 86, no. 1, pp. 48–53, 2016, doi: https://doi.org/10.1111/josh.12349.

[11] A. Asgaonkar and B. Krishnamachari, "Solving the Buyer and Seller's Dilemma: A Dual-Deposit Escrow Smart Contract for Provably Cheat-Proof Delivery and Payment for a Digital Good without a Trusted Mediator," in *2019 IEEE International Conference on Blockchain and Cryptocurrency (ICBC)*, 2019, pp. 262–267. doi: 10.1109/BLOC.2019.8751482.

[12] A. Ramzan, S. Rehman, and A. Perwaiz, "RFID technology: Beyond cash-based methods in vending machine," *2017 2nd Int. Conf. Control Robot. Eng. ICCRE 2017*, pp. 189–193, 2017, doi: 10.1109/ICCRE.2017.7935068.

[13] W. Alam, D. Sarma, R. J. Chakma, M. J. Alam, and S. Hossain, "Internet of things based smart vending machine using digital payment system," *Indones. J. Electr. Eng. Informatics*, vol. 9, no. 3, pp. 719–731, 2021, doi: 10.52549/.V9I3.3133.

[14] K. H. Pandya and H. J. Galiyawala, "A Survey on QR Codes: in context of Research and

Volume 10, Issue 1, April 2023, pp. 1-11
ISSN 2355-5068 ; e-ISSN 2622-4852
DOI: 10.33019/jurnalecotipe.v10i1.3357

Application," *Int. J. Emerg. Technol. Adv. Eng. Website www.ijetae.com ISO Certif. J.*, vol. 4, no. 3, pp. 258–262, 2014.

[15] A. S. Rafika, Y. N. Hidayat, and I. Airport, "Mesin Penjual Makanan Otomatis Berbasis Mikrokontroler Atmega8 Pada Koperasi Karyawan Gmf Aeroasia Sejahtera," vol. 4, no. 2, 2016.

[16] V. M. Alkautsar and I. Husnaini, "Perancangan Vending Machine Menggunakan Uang Kertas Berbasis Arduino," vol. 2, no. 2, 2021.

[17] E. M. Firdaus, Muhammad Irmansyah, Dikky Chandra, "Rancang Bangun Vending Machine Penukar Uang Koin Berbasis Mikrokontroller," no. September, pp. 4–5, 2018.

[18] D. A. Sembiring, "Perancangan Dan Pembuatan Mesin Penjual Minuman Kaleng Otomatis Berbasis Arduino Dengan Pembayaran Menggunakan RFID Laporan," 2018.

[19] A. D. Septiadi and L. S. Alfarizi, "Pemanfaatan E-KTP Sebagai Alat Bantu Sistem Kehadiran Pegawai dalam Penanggulangan Penyebaran Covid-19," *MATRIK J. Manajemen, Tek. Inform. dan Rekayasa Komput.*, vol. 20, no. 1, pp. 159–168, 2020, doi: 10.30812/matrik.v20i1.875.

[20] S. M. Muh Luay Bagus Pamungkas, Ade Rachmawan, "Rancang Bangun Vending Machine dengan RFID Sebagai Pembayaran Elektronik Berbasis Arduino," pp. 73–78, 2021.

[21] L. Lou, Z. Tian, and J. Koh, "Tourist satisfaction enhancement using mobile QR code payment: An empirical investigation," *Sustain.*, vol. 9, no. 7, pp. 1–14, 2017, doi: 10.3390/su9071186.

[22] H. Kusumah, R. A. Pradana, P. Studi, S. Komputer, and U. Raharja, "Penerapan Trainer Interfacing Mikrokontroler dan Internet Of Things Berbasis ESP32 Pada Mata Kuliah," vol. 5, no. 2, pp. 120–134, 2019.

[23] N. D. Audji, F. Teknik, and U. N. Jakarta, "Pembuatan Vending Machine Dengan Kartu Bersaldo Untuk Transaksi Pembelian Berbasis Mikrokontroler Atmega 16 Sebagai Pengendali Pada Toko Dirgan Corner," 2018.

[24] S. Hafizhuddin, "Rancang Bangun Mesin Penjual Roti Otomatis," 2019.

[25] H. Dianty, "Mendeteksi Suhu Tubuh Menggunakan Infrared," *J. Ilmu Komput.*, vol. 3, no. 3, pp. 5–9, 2020.

JURNAL ECOTIPE
Electronic, Control, Telecommunication, Information, and Power Engineering

Volume 10, Issue 1, April 2023, pp. 12-21
ISSN 2355-5068 ; e-ISSN 2622-4852
DOI: 10.33019/jurnalecotipe.v10i1.3391

Evaluation of Follow-Up Monitoring Information System Using Hot Fit Model

Angga Anugrawan[1], Yan Rahadian[2]
[1,2] Master of Accounting, Faculty of Economics and Business, University of Indonesia, Jakarta, Indonesia

ARTICLE INFO

Article historys:

Received : 10/10/2022
Revised : 18/11/2022
Accepted : 19/04/2023

Keywords:

Follow-Up Monitoring Information System; HOT Fit; BPK RI; Human; Organization; Technology

ABSTRACT

Based on the HOT Fit Model, this study evaluates the efficiency of the Follow-Up Monitoring Information System of the Supreme Audit Agency of the Republic of Indonesia (BPK RI). The evaluation focuses on the external Follow-Up Monitoring Information System or the auditee's perspective. This research is qualitative research with a case study approach, and the object of the research is the Inspectorate of Majene Regency, West Sulawesi. Evaluations are conducted on the human, organizational, and technological components. The human side of human resources (HR) management, demonstrates the field's experience, expertise, and understanding. Passwords for every admin and Follow-Up Monitoring Information System inputer are excellent means of restricting access privileges from an organizational perspective. In terms of technology, the Follow-Up Monitoring Information System application allows for rapid page navigation and the installation of new functions. Based on the HOT Fit Model, the external Follow-Up Monitoring Information System application at the Majene Regency Inspectorate has been successful. Currently, the downsides of the Follow-Up Monitoring Information System include the lack of frequent training for users, subpar communication with users, the lack of regular password changes, and the lack of regular program upgrades.

Corresponding Author:

Angga Anugrawan
Master of Accounting, Faculty of Economics and Business, University of Indonesia, Jakarta, Indonesia
Email: angga.anugrawan@gmail.com

1. INTRODUCTION

Results of the follow-up review are categorized into 4 (four) statuses, as per BPK Regulation Number 2 of 2017 concerning Monitoring the Implementation of Follow-up on the Recommendations of BPK Examination Results: (1) the follow-up has been in accordance with the recommendations; (2) the follow-up is not in accordance with the recommendations; (3) the recommendations have not been followed up; or (4) the recommendations cannot be followed up [1]. The BPK monitors the Follow-Up to the Recommendations for Examination Results to determine that the relevant officials have implemented the recommendations on the results of the examination within the specified time limit. This system can be used by the audited entity (auditee) to submit supporting evidence documents for follow-up on recommendations from BPK examination results more quickly and well documented. The Follow-Up Monitoring Information System application is expected to speed up the process of determining the status of the recommendation. The Follow-Up Monitoring Information System application has been active for approximately five years as of 2022. On the other hand, it appears from

JURNAL ECOTIPE
Electronic, Control, Telecommunication, Information, and Power Engineering
Volume 10, Issue 1, April 2023, pp. 12-21
ISSN 2355-5068 ; e-ISSN 2622-4852
DOI: 10.33019/jurnalecotipe.v10i1.3391

Graph 1 that the growth of Follow-Up to the Recommendations for Examination Results over the period 2014-2021 is consistent with the growth of Follow-Up to the Recommendations for Examination Results before the Follow-Up Monitoring Information System application is used in 2017 and after it is used in 2021.

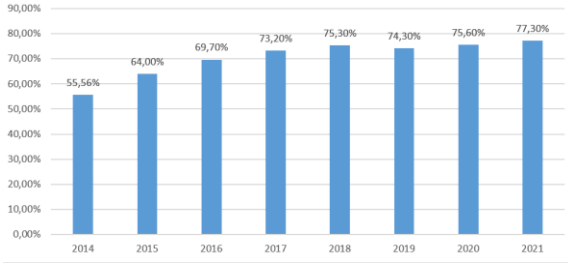

Figure 1. Follow-up Completion Progress from 2014 to 2021
(Source : IHPS Semester II, 2014 to 2021)

Using the Follow-Up Monitoring Information System application will, as previously mentioned, facilitate a more streamlined and well-documented document submission process for monitoring Follow-Up to the Recommendations for Examination Results, speed up the determination of the recommendation's status, and generate more timely, accurate, and informative data for monitoring Follow-Up to the Recommendations for Examination Results. Because Follow-Up Monitoring Information System has an indirect effect on how successfully BPK's suggestions are followed through on, this study investigates the system's effectiveness as a documentation tool from the perspective of its end users. Users of BPK's Follow-Up Monitoring Information System include both BPK, in its role as examiner (auditor), and government bodies that are the subject of examination (auditee). This study takes a case-study approach to evaluate the efficacy of the Follow-Up Monitoring Information System on a single instance. This particular item was chosen on the basis of the fact that BPK's suggestions were widely disseminated. The 2020-2021 BPK recommendation distribution is depicted in Graph 2. Figure 2 demonstrates that while the central government entity has received more BPK recommendations (23.61 trillion) than any regional government entity (55,678 recommendations), the central government entity has received a far lower value of BPK recommendations (4.82 trillion) (11,347 recommendations). Therefore, BPK makes a large number of recommendations to regional government units, but at a lesser value than to the federal government.

The reference refers to IHPS Second Semester 2021. This fact motivates the study to investigate the phenomena of monitoring outcomes in local governments in light of BPK's Follow-Up to The Recommendations For Examination Results. In this analysis, we focus on one level of governance at the provincial level: West Sulawesi. Given its status as one of Indonesia's more recent provinces, West Sulawesi was selected as the study's focus. Following through on BPK's recommendations may be difficult for the local government due to the complexity of the situation as a growing new province, particularly in the areas of human resources (HR) and technology [2]. Figure 1 displays statistics on West Sulawesi Province's progress in completing Follow-Up to the Recommendations for Examination Results from 2014 s.d. to 2021, based on which the winners were determined.

As shown in Figure 1, the Majene district saw the largest rise in the Follow-Up to The Recommendations for Examination Results completion rate after the introduction of the Follow-Up Monitoring Information System, going from 53.97 percent in 2017 to 74.7 Seventy-Four Point Seven Percent in 2018. The percentage of completion is steadily climbing; by 2021, Majene Regency will have the greatest follow-up completion rate of any district administration in Indonesia, at 81.44%.

As previously explained, it is difficult to prove the direct effect of Follow-Up Monitoring Information System implementation on the Follow-Up to The Recommendations for Examination Results completion rate in the Majene Regency. The facts show that there are still quite several BPK recommendations that have not been followed up in a period of more than 60 days. However, normatively, the use of a Follow-Up Monitoring Information System should indirectly accelerate the process of completing the Follow-Up to the Recommendations for Examination Results in the Majene Regency. The reasons why Majene Regency was chosen as the subject of this research are the facts and

JURNAL ECOTIPE
Electronic, Control, Telecommunication, Information, and Power Engineering
Volume 10, Issue 1, April 2023, pp. 12-21
ISSN 2355-5068 ; e-ISSN 2622-4852
DOI: 10.33019/jurnalecotipe.v10i1.3391

normative beliefs listed above. This study uses the Human Organization Technology Fit Model (hereinafter referred to as the "HOT Fit Model") in evaluating Follow-Up Monitoring Information System in Majene Regency. According to the HOT Fit Model, the contribution of information systems is determined by three components: human resources, organization, and technology. The HOT Fit model is suitable for evaluating Follow-Up Monitoring Information System because Follow-Up Monitoring Information System is an information system, meaning that its contribution is, of course, also influenced by these three components [3]. The HOT Fit model has been commonly used by research Soraya, which evaluates the relationship between human aspects as users, organizational aspects consisting of organizational structure and environment, and technological aspects consisting of system quality, information quality, and service quality to the benefits generated by management information systems in Indonesia [4]. General Sudirman University Hospital Pharmacy Installation. Lusiana's research also uses the HOT Fit Model to identify perceptions that influence the use of an android-based academic information system by lecturers at the University of Muhammadiyah Jember [5].

This case study research aims to evaluate the performance or effectiveness of a system that has been implemented, the sustainability of a business, or other similar evaluations. Therefore, the case study in this study belongs to the evaluation category, and the recommendation is a follow-up to improve or maintain that performance [6]. This Follow-Up Monitoring Information System evaluation case study research is very important because Follow-Up Monitoring Information System has been implemented for five years and there has never been an evaluation of its application as one of the tools or monitoring tools for the follow-up to the recommendations of the BPK examination results. This study uses the HOT Fit Model developed by Yusof, Kuljis, Papazafeiropoulou, and Stergioulasm as an evaluation framework [7]. The HOT Fit model is very appropriate to be used in this study because in previous studies it was widely used to evaluate the public sector, which is the same as the object of this research, namely Majene Regency, which is an organization that provides services to the public. This study analyzes the indirect contribution of the Follow-Up Monitoring Information System to the Follow-Up to the Recommendations for the Examination Results settlement process, namely by evaluating the effectiveness of the Follow-Up Monitoring Information System in the Majene Regency Government using the HOT Fit Model. Therefore, the formulation of the research problem is: how is the effectiveness of the Follow-Up Monitoring Information System based on the HOT Fit Model? Based on the history and problem statement above, the goal of this study is to find out how well Follow-Up Monitoring Information System works using the HOT Fit Model.

2. RESEARCH METHOD

Based on the features of qualitative research, this study may be classified as such since it generates descriptive data in the form of interviewees' opinions on the efficacy of a Follow-Up Monitoring Information System based on the HOT Fit Model. According to Sugiyono's (2005) [8] recommendations, this research looks at the Follow-Up Monitoring Information System used by the Majene Regency administration in a more natural setting. This research issue calls for an in-depth and detailed examination of the actual situations on the ground, making qualitative research the most suitable method for answering it [9, 10]. According to Sulistyanto [11], a case study is "a systematic examination of a single program, event, activity, or process as it applies to a single item." This is exactly what is needed to assess the efficacy of the Follow-Up Monitoring Information System based on the HOT Fit Model. For this reason, case studies are a valid method for investigating FMIS efficacy [12].

The main data collection technique in this study is in-depth interviews (depth interviews). Data analysis in this study was carried out through, First Grouping by category and the theme of answers at this stage, a deep understanding of the data is needed as well as full attention and openness to things that arise outside of the things to be explored [9]. The results of the interviews in the form of things expressed by the respondents were tried to be fully understood, and important themes and keywords were found, so that this study could capture experiences, problems, and dynamics that occurred in the subject [13]. Second, Put the assumptions or problems to the test. At this stage, the categories and themes that have been obtained through the analysis are reviewed in relation to the theoretical, so that the suitability of the answers to the categories and themes related to the HOT Fit model can be evaluated to answer the

Volume 10, Issue 1, April 2023, pp. 12-21
ISSN 2355-5068 ; e-ISSN 2622-4852
DOI: 10.33019/jurnalecotipe.v10i1.3391

assumptions/problems developed in this study. Third, Looking into alternative explanations for the data After the link between categories and themes of answers with assumptions and problems is realized, the research enters the explanation stage. This condition is explained with other alternatives through references or other related theories. This alternative explanation is very helpful in the discussion, conclusions, and suggestions sections [14].

3. RESULTS AND DISCUSSION

The Characteristics of Respondents Interview respondents in this study are parties who interact directly with the Follow-Up Monitoring Information System, consisting of Follow-Up Monitoring Information System Admins and Inputters as presented in Table 1.

Table 1. List of Interview Respondents for Follow-Up Monitoring Information System Application Users at the Majene Regency Inspectorate

No	Position	Task	Amount	Time
1	Staff (R1)	Admin Follow-Up Monitoring Information System	1 person	Tuesday 10 Mei 2022 at 08.00 WIB
2	Head of General Administration, Personnel, and Follow-up Sub-Division (R2)	Inputer Follow-Up Monitoring Information System	1 person	Wednesday 11 Mei 2022 at 08.00 WIB
3	Staff (R3)	Inputer Follow-Up Monitoring Information System	1 person	Friday 13 Mei 2022 at 14.00

(Source: Majene Regent Decree No. 205/HK/KEP-BUP/II/2021)

According to the prior chapter, there were a total of seven members of the Follow-Up Monitoring Information System team; however, only three respondents were questioned because the other four members of the team had no direct involvement with the system. Since these three respondents had the most dealings with the Follow-Up Monitoring Information System, the Majene Regency Inspectorate felt they were qualified to represent the system on behalf of the whole organization. The auditee's opinion on Follow-Up Monitoring Information System is derived mostly from the three interviewees' replies. Subsequently, we'll go through the findings of the tests conducted on each part of the HOT Fit Model.

3.1. Human

The following are the results of the evaluation of the components of using the Follow-Up Monitoring Information System [9, 15].

1. System Operation

Effective system functions are shown by application functions that are easy to understand and use. The evaluation results show that the Follow-Up Monitoring Information System function has been running well. This is based on the results of interviews with R1 stating that they can use the Follow-Up Monitoring Information System well, R2 stating that the features of this application are not too difficult and very easy, as well as R3, who stated the same thing. Based on the respondents' answers, it was obtained that the application functions in Follow-Up Monitoring Information System are very easy to understand and use. Information on operating system functions can be obtained through the External Follow-Up Monitoring Information System Module so that users can understand and use Follow-Up Monitoring Information System properly.

2. Training

Effective training is training that is carried out regularly, at least once a year. The results of the evaluation show that the training related to Follow-Up Monitoring Information System has not gone well. This is based on the results of an interview with R1, which stated that there was no training but at the time of launching the application there was joint input, as well as with R2, who stated the same thing. Meanwhile, R3 stated that since joining the Majene Regency Inspectorate in 2019 until 2022, there has been no training. Based on the answers of these respondents, information was obtained that the training carried out by BPK RI as the main person in charge of the Follow-Up Monitoring Information System

Volume 10, Issue 1, April 2023, pp. 12-21
ISSN 2355-5068 ; e-ISSN 2622-4852
DOI: 10.33019/jurnalecotipe.v10i1.3391

had never been carried out, either in the form of technical guidance or education and training every year. However, when the application was launched for the first time in 2017, the Majene Regency Inspectorate, together with other regencies, was guided directly by inputting together with the BPK RI team. This means that if there is a change in the Follow-Up Monitoring Information System admin and input due to a mutation or position decree, there is a possibility that the new admin or inputer will not be able to operate Follow-Up Monitoring Information System properly.

3. Understanding of System Usage

Knowledge of effective use of the system is when the user can fully understand the features that exist in the system. The evaluation results show that the knowledge of using the Follow-Up Monitoring Information System system has been running well. This is based on the results of interviews with R1, who stated that they could use the Follow-Up Monitoring Information System and felt capable even though they were not from the IT field and could learn information on system usage from the Follow-Up Monitoring Information System Module, as well as R2 and R3, who stated the same thing. Based on the answers of the respondents, it was obtained that the features used were very easy to understand. The menus and displays are very easy to use, and respondents can add knowledge about the Follow-Up Monitoring Information System based on the External Follow-Up Monitoring Information System module in the Follow-Up Monitoring Information System.

4. Hope

Effective hope is indicated by the existence of a goal to build a system that runs for the better. The results of the evaluation show that expectations have gone well. This is based on the results of interviews with R1, which stated that it was hoped that there would be a menu to bring up the completion process directly; R2, which expressed the hope to maintain speed in terms of follow-up; and R3, which expressed the hope of future training. Based on the answers of the respondents, it indicates that there is an additional hope for a menu that can show the percentage of follow-up results to be displayed more quickly in the application. The speed of the Follow-Up Monitoring Information System application is also very important in the follow-up process. In addition, it is hoped that training related to Follow-Up Monitoring Information System can be carried out regularly every year for Follow-Up Monitoring Information System users so that they can better understand and operate Follow-Up Monitoring Information System.

5. Acceptance and Rejection of The System

Weaknesses or strengths in the system are indicators of whether or not a person accepts or rejects the system. The evaluation's findings indicate a healthy balance of system acceptance and rejection. Interviewees R1 (who found the app to be extremely useful and straightforward to use right away) and R2 (who found it to be straightforward right from the 2017 release) shared these opinions, and R3 echoed them. According to the data collected, even though the BPK RI's Follow-Up Monitoring Information System application is required to monitor the implementation of its recommendations following an examination, the auditee has embraced it since 2017 thanks to its many advantages. CPC. While using the program in this manner, there is no rejection of its usage.

Based on an evaluation of the system's performance and an examination of its implementation at the Inspectorate of Majene Regency, it was determined that Follow-Up Monitoring Information System has been operating efficiently, but with some remaining flaws, most notably in its training component.

3.2. User Satisfaction

The following are the results of the evaluation of the Follow-Up Monitoring Information System user satisfaction component [9].

1. Perception of the user

An individual's impression of an information system is based on their reactions to it. Real feedback from survey takers is the best indicator of how the Follow-Up Monitoring Information System is perceived by its users. It seems like things are going well from the perspective of the users, judging by the assessment findings. Interviewees R1 and R2 both found the program useful for seeing and monitoring the status of follow-up, while interviewee R3 said the application was simpler than others since it allowed for more input options for follow-up. still, another use According to the responses of

Volume 10, Issue 1, April 2023, pp. 12-21
ISSN 2355-5068 ; e-ISSN 2622-4852
DOI: 10.33019/jurnalecotipe.v10i1.3391

these individuals, the Inspectorate of Majene Regency, which is responsible of keeping tabs on BPK Follow-Up to The Recommendations For Examination Results, will benefit greatly from the transition from paper to digital storage of this information.

2. User Advantages

User benefits are the benefits that users feel or experience when using an information system. Effective user benefits are perceived as being related to the Follow-Up Monitoring Information System system as a useful system. The evaluation results show that the user benefits have been going well. This is based on the results of interviews with R1, who stated that the general benefits were very good because they could input quickly; R2, who stated that this application was very useful, especially for reducing business travel costs and speeding up verification; and R3, who stated that this application shortened the distance with the CPC office. Based on the answers of these respondents, information was obtained that with the existence of the Follow-Up Monitoring Information System, the Majene Regency Inspectorate could minimize costs and speed up the verification process through the Follow-Up Monitoring Information System application. This application can also show information about the lack of documents needed to complete the follow-up to the recommendations of the BPK examination results so that they are in accordance with the recommendations.

The Majene Regency Inspectorate's Follow-Up Monitoring Information System effectiveness assessment of the user satisfaction part has been going well and doing its job.

3.3. Organizational Structure

The following are the results of the evaluation of the components of using Follow-Up Monitoring Information System [9].

1. Goal or Plan

The success of the system's plans and aims may be gauged by how well they are actually carried out. The evaluation demonstrates that the intended functionality of the system has been met. Interviewees R1 and R2 said the main purpose of the Follow-Up Monitoring Information System application is to facilitate follow-up monitoring by the inspectorate, and interviewee R3 said the Follow-Up Monitoring Information System application speeds up document input. According to the data collected from these respondents, the Follow-Up Monitoring Information System has successfully accomplished its primary objective of easing the burden on reporting institutions in providing ongoing monitoring of online BPK test results. It is now possible to automate the formerly manual process of entering BPK results and suggestions together with relevant follow-ups, all within the context of the Follow-Up Monitoring Information System application.

3. Standard Control (Command and Control)

The supervision of the system's use is the standard kind of control. Control standards that don't provide enough oversight or control are ineffective. Observations reveal that the established controls are functioning as expected. This is based on the responses of R1, who indicated that they only input and transmit to the admin, R2, who stated that only the admin and inspectorate input may be viewed, and R3, who stated that secrecy is preserved via email. According to the responses, the Follow-Up Monitoring Information System program controls its users by requiring them to enter unique passwords (admin and inputer). Follow-Up Monitoring Information System administrators, with input from the Majene Regency Inspectorate, are the only people who may access any given user's account, and the Inspectorate's data is never shared with any other parties. Each administrator's email address and Follow-Up Monitoring Information System data are tied together in a single account for added security and oversight over the supervision process.

4. Management

Management refers to the people who work to keep the system running. Management that is both capable and well-staffed is effective. The review indicates that the management has been functioning smoothly. This is based on an interview with R1, who said the relevant HR is a computer science graduate; moreover, R2 and R3 added up to 1 administrator and 2 inputers, all of whom said the same thing. Respondent responses indicated that the Inspectorate of Majene Regency has enough numbers and levels of expertise in its management of human resources. According to the Majene Regency Inspectorate's leadership, the current staffing level of 1 administrator and 2 inputers for the Follow-Up

Volume 10, Issue 1, April 2023, pp. 12-21
ISSN 2355-5068 ; e-ISSN 2622-4852
DOI: 10.33019/jurnalecotipe.v10i1.3391

Monitoring Information System is adequate due to the high level of follow-up in the Majene Regency. Because of this, the Follow-Up Monitoring Information System application is used more frequently and with more efficiency.

5. Communication or System Cooperation

When users and service providers work together, this is known as system communication or cooperation. When users and service providers are able to communicate and work together productively, we say that there is effective communication or system collaboration. The review shows that the system of communication or collaboration has not worked adequately. This is based on an interview with R1, who said that the information that was appropriate or not according to the recommendations was late, but that it had been completed in the Whatsapp group; an interview with R2, who said that follow-up input was not directly obtained; and an interview with R3, who said that there were network problems. internet. From the responses, it was determined that there were several communication barriers, particularly those involved in entering the BPK recommendations for examination results. It took BPK RI a few days to verify the supplied follow-up findings, by which point it was too late to submit the data. As a result, there was confusion over when and how to submit BPK Follow-Up To The Recommendations For Examination Results verification results. Because it is web-based, the Follow-Up Monitoring Information System application is particularly vulnerable to issues with the quality of the internet network during data entry. This is because the FMIS app cannot be used without an internet connection at all times. Through a Whatsapp group it developed, the BPK RI for the West Sulawesi Representative has communicated with and helped overcome these challenges.

It has been determined that the Majene Regency Inspectorate's Follow-Up Monitoring Information System has been effective in evaluating the various parts of the organization's structure; however, there are still some problems, particularly with the communication component or system collaboration, which has not been functioning optimally.

3.4. Technology (Technology)

3.4.1. System Quality

The following are the results of the evaluation of the components of using the Follow-Up Monitoring Information System [9].

1. The Simplicity of System Quality

How simple it is to utilize the system's functions is a measure of the system's usability. According to the findings of the analysis, the quality of the system's ease of use has been stable. Interviews with R1 and R2 revealed that the application provided by the Follow-Up Monitoring Information System facilitated work in processing follow-up, while those with R3 revealed that it was less of a hassle to locate data from one year to the next. From their responses, we learn that BPK examination results from LHP are archived year by year, along with any relevant follow-up recommendations. Follow-Up To The Recommendations For Examination Results BPK data entry is simplified as a result.

2. Time and Response

Time and response measure how quickly the system may be accessed and how quickly responses are generated. An efficient time and reaction is a rapid one. Timeliness and responsiveness have been excellent, as seen by the assessment results. A conversation with R1 yielded these findings; he said that reaction time is internet-dependent and that page changes happen quite quickly. Similarly, R2 and R3 make the same claim. According to the responses, the speed of the application is highly dependent on the speed of the user's internet connection. Meanwhile, switching between different application access pages in the Follow-Up Monitoring Information System was quite fluid and quick. This, however, is still contingent upon the bandwidth available to each individual utilizing the Follow-Up Monitoring Information System software. Moving to a new location with a more robust internet infrastructure will solve this problem.

3. Flexibility

The adaptability of a system depends on how well it meets the requirements of its users. What makes a system flexible is when it is adapted to each user. As can be seen from the evaluations, flexibility has been functioning as expected. Interviews with R1 and R2 and R3 yielded the same conclusion; they

Volume 10, Issue 1, April 2023, pp. 12-21
ISSN 2355-5068 ; e-ISSN 2622-4852
DOI: 10.33019/jurnalecotipe.v10i1.3391

all said that the Follow-Up Monitoring Information System application met the requirements of the Majene Regency Inspectorate. Respondent responses indicate that the software includes supplementary functionality that meets user expectations. To better meet the demands of the Majene Regency Inspectorate, the Follow-Up Monitoring Information System program has been updated to include a function that shows data on state/regional losses, for example.

4. Security

When a system is effectively secured, it can function as intended. For a system to be secure, it must employ reliable and robust safety measures. The evaluation findings indicate that the security of the Follow-Up Monitoring Information System has not been functioning optimally. R1 claims to have entered a password, R2 insists that passwords are accessible only to administrators and inputers, and R3 confirms this. The user is linked to the email addresses of all Follow-Up Monitoring Information System administrators and inputters, in addition to their passwords. Only the administrator of the Follow-Up Monitoring Information System, with approval from the Majene Regency Inspectorate, has access to the data. On the other hand, it was learned via the interviews that the administrative and Follow-Up Monitoring Information System input passwords were never consistently updated. To improve security, most programs will periodically (every 30 or 90 days, for example) change passwords, however, the Follow-Up Monitoring Information System application does not.

It appears that the Majene Regency Inspectorate has been doing a good job of evaluating the efficiency of the system quality component of the Follow-Up Monitoring Information System, but there are still some issues, particularly with the security element.

3.4.2. Information Quality (Technology)

The following are the results of the evaluation of the components of using the Follow-Up Monitoring Information System [9].

1. Information Quality Completeness

The quality of information output that offers full data is said to be complete. You may judge how complete the quality of your effective knowledge is by looking at the output you get. According to the review, the information quality and completeness have been improving. This is based on feedback from R1, who said the app's menu was comprehensive and that a tutorial was available; R2, who said it was simple to browse suggestions and LHP; and R3, who agreed. According to the responses, the Follow-Up Monitoring Information System's menu/display is packed with useful options. Information on each LHP is readily available to the Inspectorate of Majene Regency from year to year, and the output of the BPK Follow-Up to The Recommendations For Examination Results report has presented comprehensive data, including follow-up data that is in accordance with the recommendations, not in accordance with the recommendations, not in accordance with the recommendations, and cannot be followed up with the recommendations.

2. Data Accuracy

When the system generates input data accurately and without mistakes, we have high data accuracy. The system's low rate of errors translates to effective data accuracy. The data from The Follow-Up Monitoring Information System have been evaluated, and they reveal that the system is functioning smoothly. This is based on the information gleaned through conversations with R1, who said that the program was error-free and produced accurate output from the provided input. What is said in R1 is likewise stated in R2. It was determined from the responses that the data entered by the Majene Regency Inspectorate's Follow-Up Monitoring Information System inputer or administrator matched the outcomes of the application input. If the number 1000 is entered, for instance, it will also be output. The data obtained through the Follow-Up Monitoring Information System Application has been free of error circumstances to date.

Based on findings from an evaluation of the Follow-Up Monitoring Information System's information quality subsystem, the inspectorate of the Majene Regency has been successfully maintaining a high standard of information quality.

Volume 10, Issue 1, April 2023, pp. 12-21
ISSN 2355-5068 ; e-ISSN 2622-4852
DOI: 10.33019/jurnalecotipe.v10i1.3391

3.4.3. Service Quality

The following are the results of the evaluation of the components of using the Follow-Up Monitoring Information System [9].

1. Speed of Service Response

The success of a running system depends on the rapidity with which it responds to requests from its users. A system with quick data access rates can effectively respond to service requests in a short amount of time. Based on the results of the test, the service's response time appears to be stable. This is based on feedback from R1, who claims the speed of the search menu is proportional to the size of the file; R2, who claims the search menu is suitable and appropriate for LHP; and R3, who claims the search for suggestions is always appropriate. Follow-Up Monitoring Information System search functions, such as looking for LHP in a given year or looking for information like results and suggestions, may be used to gauge the responsiveness of the service based on the responses of these respondents. As a result of the FMIS app's massive data storage capacity, searching for relevant information is quick and precise. When it comes to the uploading process, the Follow-Up Monitoring Information System app is still dependent on the speed of the user's internet connection network.

2. Follow-up Service

Updates are a sort of after-care service that improves or alters the original software. Consistent system updates are essential to the success of any after-care business. Follow-up of Follow-Up Monitoring Information System services has not gone well, according to the review. A conversation with R1 yielded this conclusion; R1 confirmed that there has been no update to the Follow-Up Monitoring Information System. However, R2 said that the application has undergone further modifications because of state/regional losses, while R3 claimed that the search for recommendations was always suitable. Using their responses, we were able to determine that the Follow-Up Monitoring Information System update at the Majene Regency Inspectorate has not been audited. Version 1.0 of the Follow-Up Monitoring Information System program is still in use; however, BPK RI has added support for state/regional loss information to the application. There was a breakdown in communication due to the fact that these adjustments were not communicated in writing or through the WhatsApp group container that had been set up.

Despite positive results from the Follow-Up Monitoring Information System's evaluation of the service quality component at the Majene Regency Inspectorate, improvements are still needed.

4. CONCLUSION

This study looks at how well the Follow-Up Monitoring Information System works from the point of view of people who have been audited in the Majene District. The HOT Fit Model was used to do the evaluation. The evaluation was based on information from three respondents: one admin and two people who put information into the Follow-Up Monitoring Information System at the Majene Regency Inspectorate. Using the HOT FIT model, the evaluation shows that the Follow-Up Monitoring Information System works. The HOT Fit Model says that the Follow-Up Monitoring Information System works well in the following areas: (1) people (components of system use and satisfaction with the system); (2) organizational structure; and (3) technology (components of system quality, information quality, and service quality). Based on 18 indicators, we know that 16 have been running well: system functions, knowledge of system use, expectations, attitudes to accept or reject the system, user perceptions, user benefits, planning or goals, control standards (controlling), management, ease of system quality, time and response, flexibility, completeness of information quality, data accuracy, and speed of service response. The other 4 indicators have not been running well. The Follow-Up Monitoring Information System's flaws are shown by the three indicators that haven't worked well. There hasn't been regular training for users, communication with users hasn't been working well, passwords haven't been changed regularly, and applications haven't been updated regularly.

JURNAL ECOTIPE
Electronic, Control, Telecommunication, Information, and Power Engineering
Volume 10, Issue 1, April 2023, pp. 12-21
ISSN 2355-5068 ; e-ISSN 2622-4852
DOI: 10.33019/jurnalecotipe.v10i1.3391

REFERENCES

[1] BPK, "Peraturan BPK Nomor 2 Tahun 2017 tentang Pemantauan Pelaksanaan Tindak lanjut Rekomendasi Hasil Pemeriksaan BPK." BPK RI, 2017.

[2] BPK, "Ikhtisar Hasil Pemeriksaan Semester (IHPS) I Tahun 2021." BPK RI, 2021.

[3] M. Ayuardini and A. Ridwan, "Implementasi metode Hot Fit pada evaluasi tingkat kesuksesan sistem pengisian KRS terkomputerisasi," *Fakt. Exacta*, vol. 12, no. 2, pp. 122–131, 2019.

[4] I. Soraya, W. R. Adawiyah, and E. Sutrisna, "Pengujian model Hot Fit pada sistem informasi manajemen obat di instalasi farmasi Rsgmp Unsoed Purwokerto," *J. Ekon. Bisnis, Dan Akunt.*, vol. 21, no. 1, 2019.

[5] D. Lusiana, "Pengaruh Human Organization Technologi (Hot) Fit Model Terhadap Evaluasi Sistem Informasi Akademik Dosen," *JUSTINDO (Jurnal Sist. dan Teknol. Inf. Indones.*, vol. 5, no. 1, pp. 44–52, 2020.

[6] W. Ellet, *The case study handbook, revised edition: A student's guide*. Harvard Business Press, 2018.

[7] M. M. Yusof, J. Kuljis, A. Papazafeiropoulou, and L. K. Stergioulas, "An evaluation framework for Health Information Systems: human, organization and technology-fit factors (HOT-fit)," *Int. J. Med. Inform.*, vol. 77, no. 6, pp. 386–398, 2008.

[8] D. Sugiyono, *Memahami penelitian kualitatif*. Alfabeta, 2010.

[9] S. H. Lubis, "Evaluasi Sistem Informasi Perpustakaan IAIN Padangsidimpuan Menggunakan HOT FIT Model." Repositori Institusi Universitas Sumatera Utara, 2017.

[10] J. W. Creswell, *Research design pendekatan kualitatif, kuantitatif, dan mixed*. Yogyakarta: Pustaka Pelajar, 2010.

[11] N. B. Sulistyanto and I. G. A. Ariutama, "Evaluasi Aplikasi ST/SKI Di BPKP DKI Jakarta Dengan Pendekatan HOT-FIT Model," *EKUITAS (Jurnal Ekon. dan Keuangan)*, vol. 2, no. 4, pp. 512–530, 2018.

[12] S. Wahyuningsih, *Metode Penelitian Studi Kasus (Konsep, Teori Psikologi Komunikasi, dan Contoh Penelitiannya)*. Madura: UTM Press, 2013.

[13] A. Alijoyo, "Structured or Semi-structured interviews," 2021.

[14] M. Romney, P. Steinbart, J. Mula, R. McNamara, and T. Tonkin, *Accounting Information Systems Australasian Edition*. Pearson Higher Education AU, 2012.

[15] M. Hasibuan, *Manajemen Sumber Daya Manusia*, Cetakan Ke. Bumi Aksara, 2011.

JURNAL ECOTIPE
Electronic, Control, Telecommunication, Information, and Power Engineering

Volume 10, Issue 1, April 2023, pp. 22-31
ISSN 2355-5068 ; e-ISSN 2622-4852
DOI: 10.33019/jurnalecotipe.v10i1.3557

Application of Case Base Reasoning Algorithm in Detecting Disease in Pineapple Fruit

Nurhaeka Tou[1], Putri Mentari Endraswari[2], Nur Annisa[3]
[1,2]Information Technology, Bangka Belitung University, Balunijuk, Bangka, 33172, Indonesia
[3] Informatics, Cokroaminoto Palopo University, Jl. Latamacelling, Palopo, 91911, Indonesia

ARTICLE INFO

Article historys:

Received : 21/11/2022
Revised : 05/12/2022
Accepted : 19/04/2023

Keywords:

Expert System; CBR; Pineapple Fruit

ABSTRACT

Pineapple fruit is a type of horticultural plant that has the potential to be developed. In the process of pineapple cultivation, it is very susceptible to pests and diseases. Diseases that often attack pineapples such as; wilt disease, stem base rot, fusariosis, bacterial rot, and urethral disease. The process of identifying pineapple diseases is often done manually so it takes a long time. In addition, in the process of controlling pests and diseases, farmers only spray pesticides or other handling techniques that are not suitable for the pests and diseases that attack them. Thus, the treatment is not optimal and has an impact on the emergence of new pests and diseases in pineapple. Currently, computer technology can be used in various branches of science, one of which is artificial intelligence. The expert system is a scientific branch of artificial intelligence that can solve problems. The purpose of this research is to assist farmers in identifying pests and diseases in pineapples so that the control process can be carried out optimally, quickly and on target. The implementation of an expert system uses the Case Base Reasoning (CBR) method which will produce a diagnostic similarity value and provide recommendations for diseases that attack. This research processes data in the form of symptoms seen in pineapple plants. The test results obtained a percentage of 100%. Thus, the application of the CBR method is very relevant in identifying pests and diseases of pineapple plants.

Corresponding Author:

Nurhaeka Tou
Information Technology, Bangka Belitung University, Balunijuk, Bangka, 33172, Indonesia
Email: nurhaeka@ubb.ac.id

1. INTRODUCTION

Pineapple is a type of horticultural plant that has the potential to be developed because it can dominate the world tropical fruit trade [1]. Pineapple is a very important commodity owned by Indonesia. Indonesian people like to consume pineapple because it contains many vitamins such as; B1, B2, B3, B5, B6 and vitamin C. Pineapple can be consumed directly, or in processed forms such as: juice, pineapple jam, and cocktails [2]. In addition to the fruit which contains a lot of vitamins, the pineapple plant also has other uses, such as: (1) The leaves of the pineapple can be used as fiber (yarn) for clothing, (2) the pineapple contains the enzyme bromelain which can break down proteins, so that used for meat tenderizer, and (3) pineapple peel can be used for animal feed and as organic fertilizer [1].

Volume 10, Issue 1, April pp. 22-31
ISSN 2355-5068 ; e-ISSN 2622-4852
DOI: 10.33019/jurnalecotipe.v10i1.3557

Pineapple belongs to the bromoliaceace family category which has the property of growing in the soil using roots. Pineapple plants usually grow on home yard soil, soil that contains a lot of organic elements that can hold a lot of water, so that it can survive on dry soil for a long time [3].

In an effort to increase the productivity of pineapple fruit, various problems were found, such as the presence of plant-disturbing organisms (OPT) that cause disease. One type of disease that is dangerous in pineapple is rotting fruit disease caused by bacteria [4]. During the growth process, pineapple plants are susceptible to pests and diseases. Pest and disease disturbances in pineapples can be in the form of fruit rot, wilt disease, stem rot disease, urethritis, interknoas, and fusariosis [5]. This pest and disease attack is a concern for farmers, because it can reduce the quality of the pineapple. In addition, these pests and diseases not only attack the fruit, but also attack the pineapple crown which can affect the availability of pineapple seeds [6].

In general, if plants are attacked by pests and diseases, conventional farmers will spray pesticides or a treatment method that is not suitable for pests and diseases that attack plants. However, this method is not effective and maximal, which results in the emergence of new pests and diseases.

Based on these problems, a system is needed that is able to identify pests and diseases that attack pineapple plants, so that the control process can be carried out optimally, quickly, and on target. An expert system is a computer system that adopts human knowledge. This system can be used to solve a problem based on facts, knowledge, and reasoning like an expert or expert [7]. Until now, expert systems have been widely applied in various fields such as health, fisheries, animal husbandry, plantations, education and many more. In the problem-solving process, a suitable algorithm is needed to solve the problem, namely the Case Base Reasoning (CBR) algorithm. CBR is an algorithm that uses experience to solve a problem. The problem solving process of the CBR algorithm is to find a case that is similar to the past case and reuse it to become a new problem [8]. The CBR algorithm is applied to define the level of logical confidence in evaluating a possibility.

This research refers to several previous research studies that have implemented an expert system such as, Research conducted by [3] who created a Mobile-Based Expert System to Diagnose Pests and Diseases of Pineapple Plants Using Forward Chaining Methods. Furthermore, it was carried out by [7] to produce a system for diagnosing diseases in shallots to help farmers identify diseases in onion plants, an expert system for diagnosing diseases in gourami [9], an expert system for diagnosing infertility in men [10], and expert systems in determining healthy menus for pregnant women [11].

2. RESEARCH METHOD

2.1. Expert System

Expert System (Expert System) is a branch of artificial intelligence. An expert system is a system that adopts human knowledge to a computer or a system created to solve problems as done by an expert [12]. A good expert system is made with the aim of being able to solve certain problems by imitating the way experts work. An expert is a person who has special knowledge or expertise in solving problems that others do not have.

The purpose of the expert system is to perform problem solving in various ways such as: Interpretation, Diagnosis, Design, Planning, Monitoring, Debugging, Instryksi, and Control. Furthermore, expert systems are useful for storing knowledge from experts [13].

2.2. Case Base Reasoning

Case Base Reasoning (CBR) is a reasoning model that combines the process of problem solving, understanding. And learning. This process is carried out in various situations that have been stored in the system [14]. The process cycle of the CBR algorithm is as follows:

1. Retrieve is a process to find new cases that are similar to the old cases stored in the base case. Furthermore, it is used again to find a solution for the new case. In CBR, retrieval consists of two algorithms, namely the decision tree algorithm and the nearest neighbor algorithm.
2. Reuse is a process that reuses existing cases. This process is carried out because it is almost rare for new cases to be the same as old cases, so that solutions are made in the previous case to match the new case.
3. Revise is a process that changes and adopts the proposed solution. Revise has two main tasks, namely: Evaluation of solutions is carried out based on responses from experts, and perform error

JURNAL ECTIPE
Electronic, Control, Telecommunication, Information, and Power Engineering
Volume 10, Issue 1, April 2023, pp. 22-31
ISSN 2355-5068 ; e-ISSN 2622-4852
DOI: 10.33019/jurnalecotipe.v10i1.3557

correction (adaptation). The adaptation method can be done by, Substitution, Transformation, Re-instantiation (copying process), and using the solution from the previous case to become a solution to the new case.

4. Retain is a process of storing and validating solutions from new cases into case-based [15].

The stages of the case base reasoning process can be seen in
Figure ***1***.

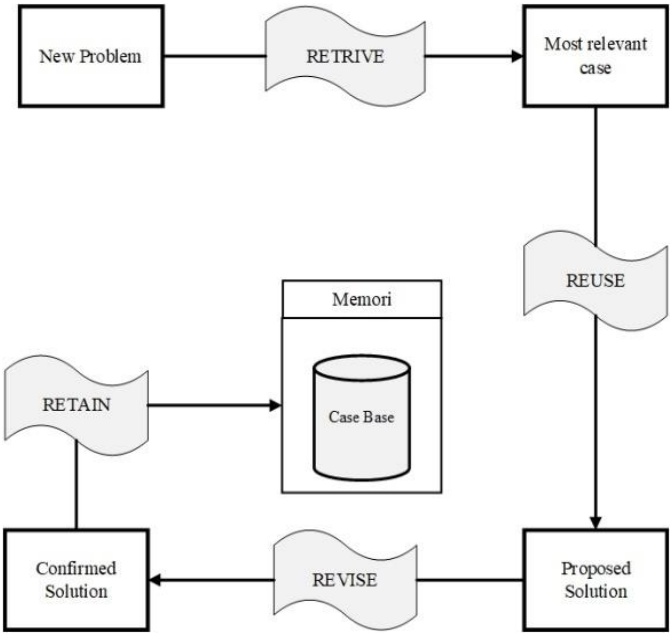

Figure 1. Process Case Base Reasoning

The equation used in the case base reasoning (CBR) algorithm is as follows:

$$Similarity(P,C) = \frac{S1+W1\ldots,(Sn+Wn)}{W1+\cdots,+Wm} \quad (1)$$

2.3. Research Stages

3.3. The stages of research carried out in this study started from the Problem Description, Literature Study, Data Collection, Data Analysis, Result Testing, and Drawing Conclusions which can be seen in
Figure ***2***.

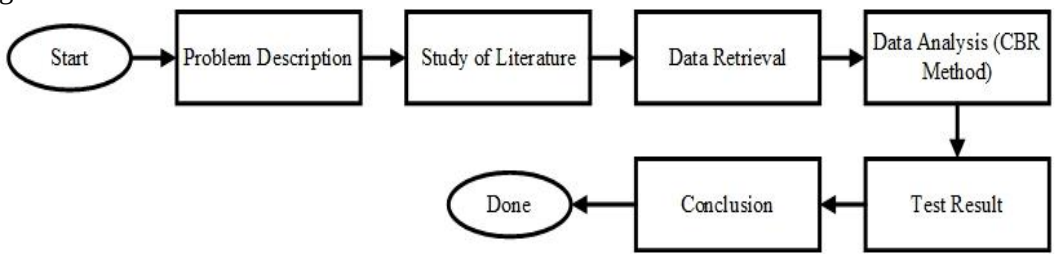

Figure 2. Research Flowchart

1. Problem Description
   Based on
   Figure ***2***, this research stage begins with the problem description stage. This stage is very important to do, to know the scope of the problem under study to find the best solution.
2. Study of Literature

JURNAL ECTIPE
Electronic, Control, Telecommunication, Information, and Power Engineering
Volume 10, Issue 1, April pp. 22-31
ISSN 2355-5068 ; e-ISSN 2622-4852
DOI: 10.33019/jurnalecotipe.v10i1.3557

The second stage in this research is literature study, to seek and study scientifically and theoretically previous studies that are relevant to the research conducted.

3. Data Retrieval
   The data collection technique used in this research is the observation data calculation technique.
4. Data Analysis (CBR Method)
   The fourth stage in this research is to analyze the data using Case Base Reasoning (CBR) method. The problem-solving process using the CBR method is carried out with the hope of finding the right similarity value based on the symptoms of the user. The following are the steps of the CBR method that will be carried out in this study:
   a. Determine the disease and symptoms
   b. Detrmine the relationship between disease and symptoms
   c. Determine the weight of each symptom
   d. Determine the similarity by the user with the disease on pineapple plants
   e. Comparing the similarity values for each disease
   f. Conclude the diseases found in pineapple fruit plants.
5. Test Result
   The next stage is to carry out the testing process using the CBR method based on criteria data, to determine the level of system accuracy with manual calculations.
6. Conclusion
   The last stage of this research is to draw conclusions based on the problems and results of research data analysis. The conclusion that is expected is to determine the type of disease from pineapple fruit plants.

In this study the determination of the type of disease in pineapple fruit using the Case Base Reasoning (CBR) algorithm. The CBR algorithm process combines the stages of problem-solving, understanding, and learning into memory processing. The flowchart of the CBR algorithm can be seen in Figure 3.

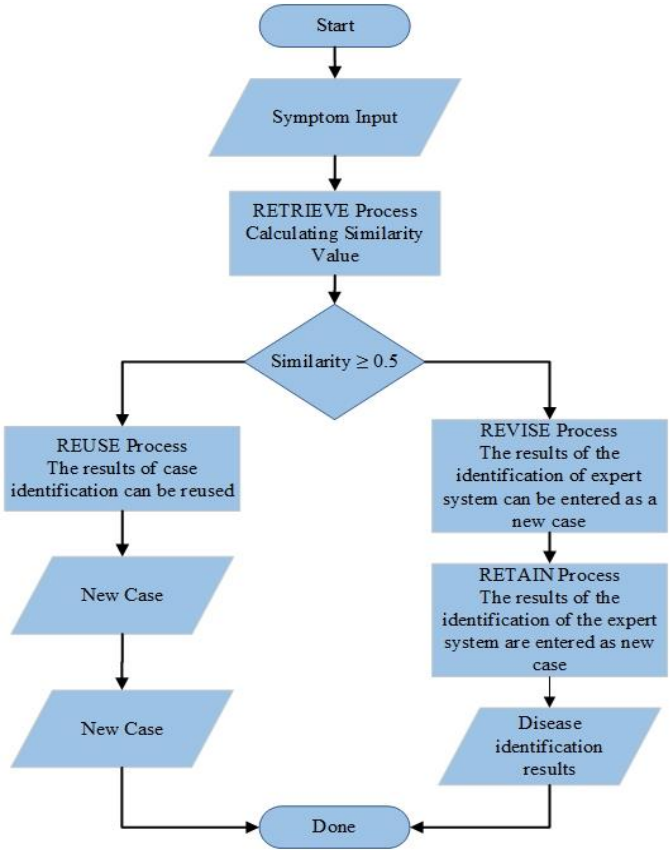

Figure 3. Expert System CBR Flowchart

Volume 10, Issue 1, April 2023, pp. 22-31
ISSN 2355-5068 ; e-ISSN 2622-4852
DOI: 10.33019/jurnalecotipe.v10i1.3557

Figure ***3*** Shows the Flowchart of the CBR process on the expert system. In the flowchart, the first thing to do is to input the symptoms of the pineapple plant. Next, the system will perform the Retrieve process by calculating the similarity value. If the similarity value obtained is more than 0.5, then the system will reuse the old case for reuse, so that the diagnosis of pineapple disease is immediately obtained. However, if the similarity value obtained is less than 0.5, the system will process Revise and Retain as a new case.

3. RESULTS AND DISCUSSION

3.1. Description of Research Data

The data used in this study were pineapple plant diseases which were used as research objects, types of diseases in pineapples and symptoms of each pineapple fruit disease.

Data on diseases and symptoms of pineapple plants were obtained from interviews with experts. Thus, information on knowledge and rules that will be used in the decision-making system based on the pineapple fruit disease category can be obtained which can be seen in Table 1.

Table 1. Pineapple Pests and Disease

Code	Disease
P1	Wither Disease
P2	Stem Rot
P3	Fusariosis
P4	Bacterial Rot
P5	Urethral Disease

Furthermore, Table 2 shows the symptoms of pests and diseases on pineapple plants:

Table 2. Symptoms of Pineapple Pests and Diseases

Code	Symptom	Weight
G01	Curved Leaves	5
G02	There are mealybugs on the roots	3
G03	Withered leaves are brown, trun yellow, and dry	5
G04	Root growth stops	5
G05	Root rot	5
G06	Rot at the base of the stem	5
G07	The base of the stem is brown	3
G08	Yellowish white leaves	3
G09	The fruit turns yellow and then black	5
G10	Leaves and fruit are easy to remove	3
G11	The rotting part smells bad	3
G12	Stunted plant grwoth (Dwarf)	5
G13	Wound at the base of the stem	3
G14	Roots and stems have urethra	3

Each disease in pineapple has symptoms that can be seen in Table 3.

Table 3. Symptoms Pineapple and Relationships

Code	P1	P2	P3	P4	P5
G01	*		*		
G02	*				
G03	*		*		*
G04	*			*	*
G05	*			*	*
G06		*	*		
G07		*			
G08	*	*			
G09		*			
G10				*	*
G11		*		*	
G12			*	*	
G13		*			*

Volume 10, Issue 1, April pp. 22-31
ISSN 2355-5068 ; e-ISSN 2622-4852
DOI: 10.33019/jurnalecotipe.v10i1.3557

G14					*

In the expert system there is an inference engine which becomes the rules for matching facts. The inference engine will start tracking by matching the facts contained in the knowledge base with the rules that have been set based on the knowledge base.

3.2 Symptom Input

The symptoms of pineapple that are inputted will be given a weight based on the answers given by the user. If the user answers YES then it will be given a weight according to the weight of each symptom, but if the user answers NO then it will be given a weight = 0. The symptom input from the user can be seen in Table 4.

Table 4. User's Answer

Code	Symptom	Answer	Weight
G01	Curved Leaves	No	0
G02	There are mealybugs on the roots	No	0
G03	Withered leaves are brown, trun yellow, and dry	No	0
G04	Root growth stops	Yes	5
G05	Root rot	Yes	5
G06	Rot at the base of the stem	No	0
G07	The base of the stem is brown	No	0
G08	Yellowish white leaves	No	0
G09	The fruit turns yellow and then black	No	0
G10	Leaves and fruit are easy to remove	Yes	5
G11	The rotting part smells bad	Yes	3
G12	Stunted plant grwoth (Dwarf)	Yes	5
G13	Wound at the base of the stem	No	0
G14	Roots and stems have urethra	No	0

Next, make the formation of rules obtained from experts, and apply them to the expert system. The experts in question are experts in the field of pests and diseases on pineapples. The following rules will be set in the expert system:

RULE 1= IF G01 AND G02 AND G03 AND G04 AND G05 THEN P01
RULE 2= IF G06 AND G07 AND G08 AND G09 AND G11 AND G13 THEN P02
RULE 3= IF G01 AND G03 AND G06 AND G12 THEN P03
RULE 4= IF G04 AND G05 AND G10 AND G11 AND G12 THEN P04
RULE 5= IF G03 AND G04 AND G05 AND G10 AND 13 AND G 14 THEN P05

After forming the rule from the expert, then execute the rule based on the answers to the symptoms selected by the user. The execution process is carried out by inputting the value of the symptom selected by the user into the predefined rule. Furthermore, from each of these symptoms, the minimum value is calculated for all symptoms that are in accordance with the rule and multiplied by the value of each rule.

3.3 Retrieve Process

The retrieval process is a process of finding similarities between new cases and cases in the knowledge base. The search process is carried out by matching the symptoms entered by the user with the symptoms contained in the knowledge base. In this retrieval process, a weighting process will be carried out using the Nearest Neighbor Retrieval (KNN) method.

In the initial stages of diagnosis, the user will input the symptoms experienced by the pineapple in the expert system. Next, the user will press the process button to find out the results of the pineapple disease diagnosis. In the next stage, the system will do the weighting by matching one by one the inputted symptoms with the symptoms contained in the knowledge base. The following equation is used to calculate the similarity of weights in the system:

$$Similarity(P,C) = \frac{s1*w1+ s2*w2+..sn+wn}{w1 +w2...,+Wn} \quad (2)$$

The process of calculating the case of wilting disease can be seen in Table 5.

Table 5. Wilt Disease Scheme

Disease Symptoms	Weight	User's Symptoms	Weight

Volume 10, Issue 1, April 2023, pp. 22-31
ISSN 2355-5068 ; e-ISSN 2622-4852
DOI: 10.33019/jurnalecotipe.v10i1.3557

Curved Leaves	5	Root growth stops	5
There are mealybugs the roots	3	Root rot	5
Withered leaves are brown, yellowes, and dry	5	Leaves and fruit are easy to remove	5
Root growth stops	5	The rotting part has an unpleasant odor	3
Root rot	5	Stunted plant growth (dwarf)	5
Yellowish-white rickshaw leaves	3		

$$S\,(P,C) = \frac{0*5+0*3+0*5+1*5+1*5}{5+3+5+5+5+3}$$

$$= \frac{10}{26} = 0.36 = 36\%$$

From the case calculation above, the user inputs 2 symptoms that have similarities with the old case. After the similarity calculation process was carried out, it was found that 43% of the diseases experienced by pineapples were wilt diseases. Furthermore, the calculation process for stem rot disease can be seen in Table 6.

Table 6. Stem Base Disease Scheme

Disease Symptoms	Weight	User's Symptoms	Weigth
Rot at the base of the stem	5	Root growth stops	5
The base of the stem is brown	3	Root rot	5
Yellowish white leaves	3	Leaves and fruit are easy to remove	5
The fruit turns yellow and then black	5	The rotting part has an unpleasant odor	3
The rotting part smells bad	3	Stunted plant growth (dwarf)	5
Wound at the base of the stem	3		

$$S\,(P,C) = \frac{0*5+0*3+0*3+0*5+1*3}{5+3+3+5+3+3}$$

$$= \frac{3}{22} = 0.13 = 13\%$$

From the case calculation above, the user inputs 1 symptom that has similarities with the old case. After the similarity calculation process was carried out, it was found that 13% of the diseases experienced by pineapples were root rot diseases. Furthermore, the process of calculating Fusariosis can be seen in Table 7.

Table 7. Fusariosis Disease Scheme

Disease Symptoms	Weight	User's Symptoms	Weight
Curved leaves	5	Root growth stops	5
Withered leaves are brown, yellowed, and dry	5	Root rot	5
Rot at the base of the stem	5	Leaves and fruit are easy to remove	5
Stunted plant growth (dwarf)	5	The rotting part has an unpleasant odor	3
		Stunted plant growth (dwarf)	5

$$S\,(P,C) = \frac{0*5+0*5+0*5+1*5}{5+5+5+5}$$

$$= \frac{5}{20} = 0.25 = 25\%$$

From the case calculation above, the user inputs 2 symptoms that have similarities with the old case. After the similarity calculation process was carried out, it was found that 50% of the diseases experienced by pineapples were Fusariosis. Furthermore, the calculation process for Bacterial Rot Disease can be seen in Table 8.

Table 8. Bacterial Rot Disease Schematic

Disease Symptoms	Weight	User's Symptoms	Weight
Root growth stops	5	Root growth stops	5
Root rot	5	Root rot	5
Leaves and fruit are easy to remove	5	Leaves and fruit are easy to remove	5
The rotting part has an unpleasant odor	3	The rotting part has an unpleasant odor	3

JURNAL ECOTIPE
Electronic, Control, Telecommunication, Information, and Power Engineering
Volume 10, Issue 1, April pp. 22-31
ISSN 2355-5068 ; e-ISSN 2622-4852
DOI: 10.33019/jurnalecotipe.v10i1.3557

Stunted plant growth (dwarf)	5	Stunted plant growth (dwarf)	5

$$S\ (P,C) = \frac{1*5+1*5+1*5+1*3+1*5}{5+5+5+3+5}$$

$$= \frac{23}{23} = 1.00 = 100\%$$

From the case calculation above, the user inputs 5 symptoms that are similar to the old case in the knowledge base. After the similarity calculation process was carried out, it was found that 100% of the diseases experienced by pineapples were bacterial rot diseases. Furthermore, the calculation process for Urethral Disease can be seen in Table 9.

Table 9. Urethral Disease Scheme

Disease Symptoms	Weight	User's Symptoms	Weight
Withered leaves are brown, yellowed, and dry	5	Root growth stops	5
Root growth stops	5	Root rot	5
Root rot	5	Leaves and fruit are easy to remove	5
Leaves and fruit are easy to remove	3	The rotting part has an unpleasant odor	3
Wounds ont the trunk	3	Stunted plant growth (dwarf)	5
Roots and stems have urethra	3		

$$S\ (P,C) = \frac{0*5+1*5+1*5+1*3+0*3}{5+5+5+3+3+3}$$

$$= \frac{13}{24} = 0.54 = 54\%$$

From the case calculation above, the user inputs 3 symptoms that have similarities with the old case. After the similarity calculation process was carried out, it was found that 54% of the diseases experienced by pineapples were Urethritis.

After calculating the similarity to the symptoms entered by the user, the identification results are obtained which can be seen in Table 10.

Table 10. Identification Results

Code	Disease	Identification Value
P01	Penyakit Layu	36%
P02	Penyakit Busuk Pangkal Batang	13%
P03	Fusariosis	25 %
P04	Busuk Bakteri	100 %
P05	Penyakit Uret	54%

Based on Table 10, obtained five types of diseases have similar values, namely wilting disease 36%, root rot 13%, fusariosis 25%, bacterial rot 100%, and urethral disease 54%. However, of the 5 similarities, the one with the greatest similarity value is Bacterial Rot Disease. So, it can be concluded that Pineapple is attacked by Bacterial Rot Disease. Then, testing with an expert system can be seen in Figure 4.

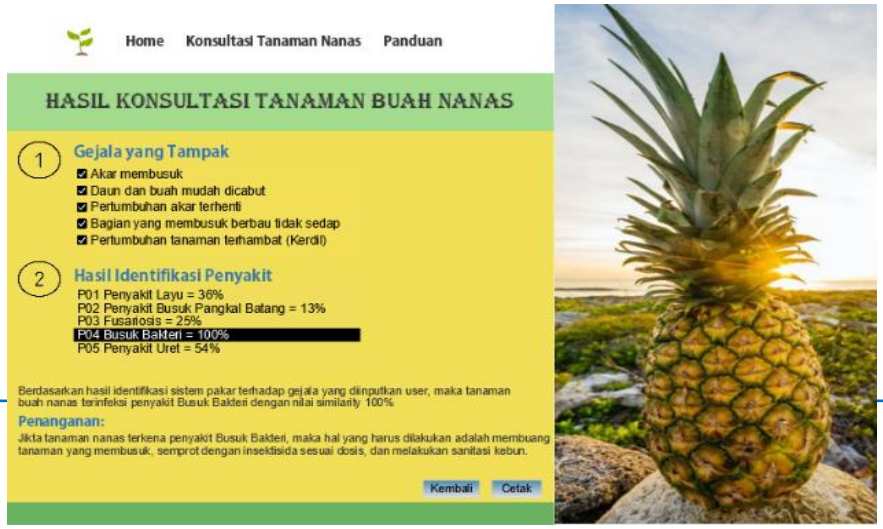

Volume 10, Issue 1, April 2023, pp. 22-31
ISSN 2355-5068 ; e-ISSN 2622-4852
DOI: 10.33019/jurnalecotipe.v10i1.3557

Figure 4. System Test Results

4. CONCLUSION

Based on the results of the research that has been done, it can be concluded that the Expert System that has been created can track the symptoms of the pineapple fruit plant selected by the user. The results of the identification of pineapple fruit plant diseases with symptoms: Root rot, Leaves, and fruit are easily removed, root growth stops, rotting parts have a bad smell, and stunted plant growth (Dwarf). Then the identification results were obtained in the form of wilting disease 36%, root rot disease 13%, fusariosis at 25%, bacterial rot 100%, and urethral disease 54%. Based on the results of the comparison of the similarity values for each disease, it can be concluded that the pineapple fruit plant was infected with bacterial rot disease with a similarity value of 100%.

REFERENCES

[1] T. Oviana, T. N. Aeny, and J. Prasetyo, "Isolasi dan Karakterisasi Penyebab Penyakit Busuk Buah pada Tanaman Nanass (Ananas Comosus [L.] Merr.)," *J. Agrotek Trop.*, vol. 3, no. 2, pp. 220–225, 2015.

[2] F. S. Sihombing, "Sistem Pakar Mendiagnosa Penyakit Pada Tanaman Nanas Dengan Menggunakan Metode Clustering," *Inf. dan Teknol. Ilm.*, vol. 7, no. 2, pp. 198–202, 2020.

[3] Nurmayanti and R. Saputra, "Implementasi Sistem Pakar Berbasis Mobile Untuk Mendiagnosa Hama Dan Penyakit Tanaman Nanas," *Sist. Inf. dan Komputerisasi Akunt.*, vol. 04, no. 02, pp. 12–16, 2018.

[4] S. Rodliyatun, S. Triyanti, S. H. Suseno, and D. A. Nugroho, "Standar Operasional Prosedur Budi Daya Nanas sebagai Upaya Penanggulangan Serangan Hama dan Penyakit pada Tanaman Nanas," *J. Pus. Inov. Masy.*, vol. 1, no. 1, pp. 13–20, 2019.

[5] R. Rachman, "Implementasi Case Based Reasoning Mendiagnosa Penyakit Stroke Menggunakan Algoritma Probabilistic Symmetric," *J. Inform.*, vol. 8, no. 1, pp. 10–16, Feb. 2021.

[6] E. Simatupang, "Jaringan syaraf tiruan menggunakan metode perceptron untuk menentukan penyakit pada tanaman buah nanas," *Maj. Ilm. INTI*, vol. 6, no. 2, pp. 55–60, 2019.

[7] Y. S. R. Nur, A. Burhanuddin, D. Aldo, and W. Lelisa Army, "Sistem Pakar Deteksi Penyakit Bawang Merah dengan Metode Case Based Reasoning," *J. MEDIA Inform. BUDIDARMA*, vol. 6, no. 3, p. 1356, Jul. 2022.

[8] Z. Nenova and J. Shang, "Chronic Disease Progression Prediction: Leveraging Case-Based Reasoning and Big Data Analytics," *Prod. Oper. Manag.*, vol. 31, no. 1, pp. 259–280, Jan. 2022.

[9] A. R. Saraswati, Y. Saintika, A. N. A. Thohari, and A. R. Iskandar, "Sistem Pakar Diagnosis Penyakit Ikan Gurami (Osphronemus Goramy) Menggunakan Case Based Reasoning," *J. Teknol. Inf. dan Ilmu Komput.*, vol. 7, no. 4, p. 779, Aug. 2020.

[10] A. Alwendi and K. Samosir, "Perancangan Aplikasi Sistem Pakar dalam Mendiagnosa Penyakit Infertilitas pada Pria Menggunakan Metode Certainty Factor Berbasis Web," *J. Inform. dan Rekayasa Perangkat Lunak*, vol. 4, no. 1, p. 24, Mar. 2022.

[11] E. Krisnanik, K. Kraugusteeliana, and V. Indriasari, "Desain Model Sistem Pakar Menu Sehat Wanita Hamil Berdasarkan Gizi Menggunakan Metode Cooper," *J. Teknol. Inf. dan Ilmu Komput.*, vol. 5, no. 6, p. 643, Nov. 2018.

[12] P. Wahyuningsih and S. Zuhriyah, "Sistem Pakar Diagnosa Penyakit Campak Rubella pada Anak

JURNAL ECOTIPE
Electronic, Control, Telecommunication, Information, and Power Engineering
Volume 10, Issue 1, April pp. 22-31
ISSN 2355-5068 ; e-ISSN 2622-4852
DOI: 10.33019/jurnalecotipe.v10i1.3557

Menggunakan Metode Certainty Factor Berbasis Website," *J. Teknol. Inf. dan Ilmu Komput.*, vol. 8, no. 1, p. 85, Feb. 2021.

[13] Asmira and Syamsul Alam, "Aplikasi Sistem Pakar Pengidentifikasi Penyakit Dan Hama Pada Tanaman Padi Berbasis Android," *SIMKOM*, vol. 5, no. 2, pp. 19–27, Jul. 2020.

[14] R. Adawiyah, "Case Based Reasoning Diagnosis Hama dan Penyakit Tanaman Nilam," *INTENSIF*, vol. 2, no. 1, p. 57, Feb. 2018.

[15] R. Adawiyah and F. Handayani, "Rancang Bangin Case Based Reasoning untuk Diagnosis Hama dan Penyakit Tanaman Nilam menggunakan Nearest Neighbor Kombinasi Certainty Factor," *J. Teknol. Inf. dan Ilmu Komput.*, vol. 7, no. 3, p. 477, May 2020.

JURNAL ECOTIPE
Electronic, Control, Telecommunication, Information, and Power Engineering

Volume 10, Issue 1, April 2023, pp. 32-41
ISSN 2355-5068 ; e-ISSN 2622-4852
DOI: 10.33019/jurnalecotipe.v10i1.3601

Design of Dual-Band Microstrip Linear Array MIMO Antenna With U Slot For 5G Communication System

Aulia Anindya Dhanyswari[1], Syah Alam[2], Indra Surjati[3]
[1,2,3]Department of Electrical Engineering, Faculty of Industrial Technology, Trisakti University, Jl. Kyai Tapa No.1, Jakarta, 11440, Indonesia

ARTICLE INFO

Article historys:

Received : 28/11/2022
Revised : 12/12/2022
Accepted : 19/04/2023

Keywords:

5G, Array; Microstrip Antenna; MIMO; U Slot

ABSTRACT

The development of 5G technology is expected to result in high data rate communication, low power consumption, and larger network capacity. Microstrip antenna is an antenna that can support 5G technology because it can work at high frequencies but has the disadvantage of producing a small gain and narrow bandwidth. The use of array and MIMO methods can increase the gain value. The addition of the U slot method aims to increase bandwidth and can produce multi-frequency. In this study, the antenna was designed using an epoxy substrate (FR-4) with a rectangular U-slot patch arranged in a 4×2 MIMO array and fabricated. From the simulation results, the return loss parameter (S11) is -12.49 dB, (S12) is -88.17 dB, the bandwidth is 610 MHz, the gain is 15.70 dB, the envelope correlation coefficient is 3.85 × 10-10. and diversity gain of 10 dB. From the fabrication results, two working frequencies are obtained, namely at a frequency of 3.2 GHz and 3.62 GHz with each return loss value (S11) of -25.96 dB and -29.22 dB, (S12) of -48.61 dB and -51.78 dB, a bandwidth of 50 MHz. The independence of each antenna is indicated by the envelope correlation coefficient of 6.48 × 10-6 and 1.5 × 10-6, and a diversity gain of 10 dB. This antenna can be recommended as a receiving antenna in 5G communication systems.

Corresponding Author:

Aulia Anindya Dhanyswari
Department of Electrical Engineering, Faculty of Industrial Technology, Trisakti University, Jl. Kyai Tapa No.1, Jakarta, 11440, Indonesia
Email: aulia062002004026@std.trisakti.ac.id

1. INTRODUCTION

5G technology is the next phase of wireless network communication development [1]. One of the candidates for the radio frequency range for 5G trials in Indonesia is in the 3.3 – 4.2 GHz (3.5 GHz radio frequency band) [2]. The adaptation of the Multiple Input Multiple Output (MIMO) technique into 5G technology is used to produce high data rate communication and low power consumption compared to 4G technology and the radiation pattern can be in several directions. The MIMO technique can take advantage of multipath fading depending on the number of antennas it uses [3].

One type of antenna that can support 5G technology is the microstrip antenna because it has a small size, is easy to store, and can operate at high frequencies, but the microstrip antenna has drawbacks, namely small gain, poor directionality, and poor bandwidth efficiency resulting in poor quality and the signal reception level is not optimal. The gain value can be increased by the array method, namely by arranging several patch microstrip antennas that are connected to the supply line [4].

In Research [5], a 2×2 MIMO array microstrip antenna has been designed using the slot method at a frequency of 37 GHz for 5G with return loss ≤ 10 dB, VSWR ≤ 2, gain 18.7 dBi and bandwidth 2.12 GHz. However, in this study the frequency used was different from the radio frequency band for testing in the range of 3.3 – 4.2 GHz.

JURNAL ECOTIPE
Electronic, Control, Telecommunication, Information, and Power Engineering
Volume 10, Issue 1, April 2023, pp. 32-41
ISSN 2355-5068 ; e-ISSN 2622-4852
DOI: 10.33019/jurnalecotipe.v10i1.3601

In Research [6], the design of a 4x2 planar microstrip antenna array at a center frequency of 3.55 GHz with a return loss of -20.8 dB, VSWR 1.2, a bandwidth of 123.3 MHz, and gain of 10.4 dB was carried out. However, in this study, the antenna arrangement has not been arranged in MIMO. Furthermore, in research [7], a rectangular array microstrip MIMO antenna has been designed with a 2x2 u slot at a frequency of 3.5 GHz for 5G with a bandwidth value of 188 MHz, minimum return loss -23.65 dB, gain 8.528 dB and mutual coupling -63.16 dB. However, in this study, the working frequency of the antenna still operates at one working frequency.

In research [8], the design and realization of a dual-band microstrip antenna using a u-shaped slot has been carried out to produce frequencies of 2.4 GHz and 3.6 GHz, each having VSWR values of 1.56 and 1.33, a bandwidth of 124 MHz and 125 MHz with unidirectional radiation pattern. However, in this study, the antenna only had one patch and was not applied to 5G.

Based on previous research that has been carried out, this study uses a frequency of 3.5 GHz referring to [6, 7], adopting a linear MIMO array form in [5] and replacing the center load of the patch using a U slot like [7, 8], as well as developing research [7] become MIMO 4×2. The purpose of adding the U slot is to increase the reflection coefficient while the array method is used to increase the gain. Furthermore, the U-slot and array method also serves to generate double frequencies [8].

2. RESEARCH METHOD

In the antenna design process, starting from determining the desired antenna working frequency, which is 3.5 GHz, determining the substrate to be used, namely epoxy FR-4 with a dielectric constant value of 4.3, a thickness of 1.6 mm and a loss tangent of 0.0265, the selection FR-4 epoxy substrate material aims to improve antenna performance.

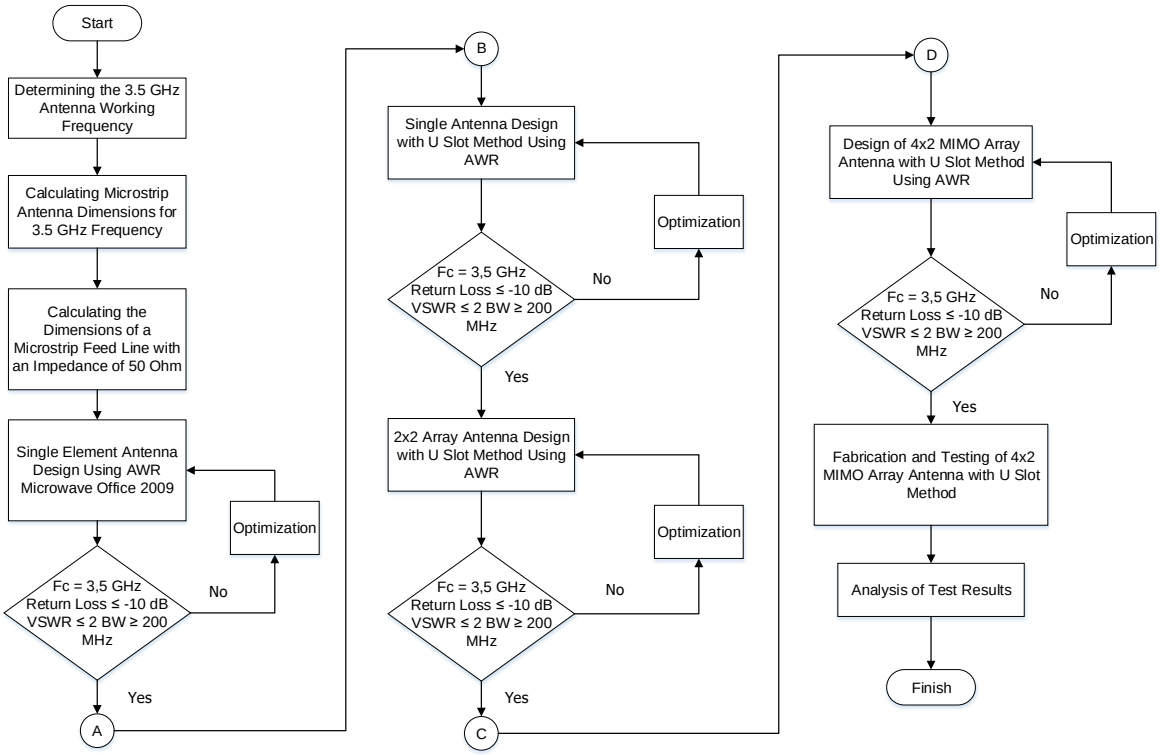

Figure 1. Design Flowchart

Figure 1 shows the antenna design process. Before the simulation process is carried out, first determine the dimensions of the antenna, namely patch dimensions, enclosure dimensions, and supply line dimensions. Next, perform a simulation of the antenna that has been designed using the software. In the simulation process it is possible to optimize several parameters by adjusting the dimensions of the antenna until it reaches the specified limit, namely return loss ≤ -10 dB, bandwidth ≥ 200 MHz, VSWR ≤ 2, gain ≥ 5 dB, directional radiation pattern, isolation loss ≤ -20 dB, envelope correlation coefficient ≤ 0.5 and diversity gain 10 [7]. From the simulation results that have been optimized, the

JURNAL ECTIPE
Electronic, Control, Telecommunication, Information, and Power Engineering
Volume 10, Issue 1, April 2023, pp. 32-41
ISSN 2355-5068 ; e-ISSN 2622-4852
DOI: 10.33019/jurnalecotipe.v10i1.3601

antenna fabrication process can then be carried out. Fabrication is carried out to analyze whether the design is following the desired. After being fabricated, the antenna will be measured, analyzed, and compared with the simulation results. This analysis process is carried out to see the performance of the proposed antenna and its feasibility to be applied to 5G communication systems.

Antenna design begins with calculating the dimensions of a single-element antenna. Figure 2 shows the shape of the single-element design and the dimensions of the antenna can be calculated using equations (1) to (7) [9, 10].

$$W = \frac{c}{2f}\sqrt{\frac{\varepsilon_r + 1}{2}} \quad (1)$$

W/h > 1 (2)

$$\varepsilon_{reff} = \frac{\varepsilon_r + 1}{2} + \frac{\varepsilon_r - 1}{2}\left(1 + \frac{12h}{w}\right)^{-\frac{1}{2}}$$

$$\mathrm{L}_{eff} = \frac{c}{2f\sqrt{\varepsilon_{reff}}} \quad (3)$$

$$\Delta\mathrm{L} = 0.412h\left(\frac{\varepsilon_{reff} + 0.3}{\varepsilon_{reff} + 0.258}\right)\left(\frac{\frac{W}{h} + 0.264}{\frac{W}{h} + 0.8}\right) \quad (4)$$

$$L = \mathrm{L}_{eff} - 2\Delta\mathrm{L} \quad (5)$$

$$Wg = 6h + W \quad (6)$$

$$Lg = 6h + L \quad (7)$$

W is antenna patch width in mm, *εreff* is effective dielectric constant, *Leff* is the effective length of patch antenna in mm, Δ*L* is patch length increase in mm, *h* is substrate thickness in mm, *f* is a frequency in Hz, *Wg* is enclosure width in mm, *Lg* is enclosure length mm, and *L* is antenna patch length in mm.

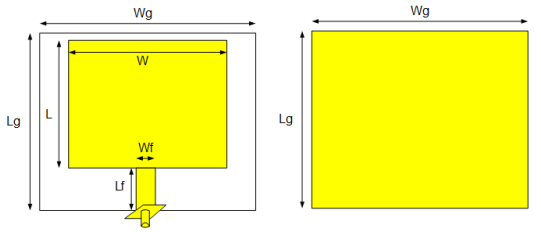

(a) (b)

Figure 2. Single Element Antenna Design; (a) Front View, (b) Back View

To get a higher bandwidth value, it is necessary to add a method to the antenna, namely the U slot method. Figure 3 shows the shape of the antenna design by adding a U-slot and the dimensions of the U-slot, it can be calculated using equations (8) to (13) [11, 12].

$$\mathrm{F} = \mathrm{E} = \frac{\lambda}{60} \quad (8)$$

$$C = 0.3 \times W \quad (9)$$

$$\mathrm{D} = \frac{c}{f_{low}\sqrt{\varepsilon_{reff}}} - 2(L + \Delta\mathrm{L} - \mathrm{F}) \quad (10)$$

$$\varepsilon_{reff}(pp) = \frac{\varepsilon_r + 1}{2} + \frac{\varepsilon_r - 1}{2}\left(1 + 12\frac{h}{D - 2F}\right)^{-\frac{1}{2}} \quad (11)$$

$$2\boldsymbol{\Delta}_{L-E-H} = \frac{\left(\varepsilon_{reff}(pp) + 0{,}3\right)\left(\frac{D - 2F}{h} + 0{,}264\right)}{\left(\varepsilon_{reff}(pp) - 0{,}258\right)\left(\frac{D - 2F}{h} + 0{,}8\right)} \quad (12)$$

$$H \approx L - E + 2\boldsymbol{\Delta}_{L-E-H} - \frac{1}{\sqrt{\varepsilon_{reff}(pp)}}\left(\frac{C0}{fhigh} - (2C + D)\right) \quad (13)$$

JURNAL ECTIPE
Electronic, Control, Telecommunication, Information, and Power Engineering
Volume 10, Issue 1, April 2023, pp. 32-41
ISSN 2355-5068 ; e-ISSN 2622-4852
DOI: 10.33019/jurnalecotipe.v10i1.3601

F/E is slot sleeve width in mm, *C* is vertical slot length in mm, *D* is horizontal slot length in mm, and *H* is slot distance from the base in mm.

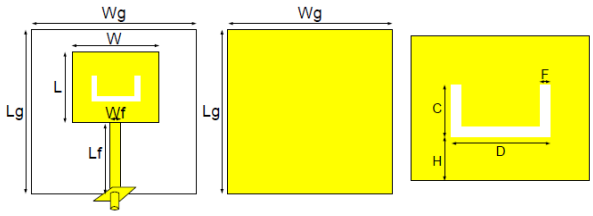

(a) (b) (c)

Figure 3. Single Element Antenna Design with U Slot; (a) Front View, (b) Back View ; (c) U slots

To increase the gain value, an antenna array technique can be used. The calculation of the array required calculations for the width of the feeder 50 Ω, 70,7 Ω, 100 Ω using equations (14) to (15) and the calculation of the distance between the radiating elements (patches) contained in equation (16) [4].

$$Wf = \frac{2h}{\pi}\left\{B - 1 - \ln(2B-1) + \frac{\varepsilon r - 1}{2\varepsilon r}\left[\ln(B-1) + 0{,}39 - \frac{0{,}61}{\varepsilon r}\right]\right\} \quad (14)$$

$$B = \frac{60\pi^2}{Z_0\sqrt{\varepsilon r}} \quad (15)$$

$$d = \frac{\lambda}{2} = \frac{c}{2f} \quad (16)$$

Wf is feed channel width in mm, *B* is microstrip feed line constant, *εr* is dielectric constant, and *d* is the distance between patch elements in mm.

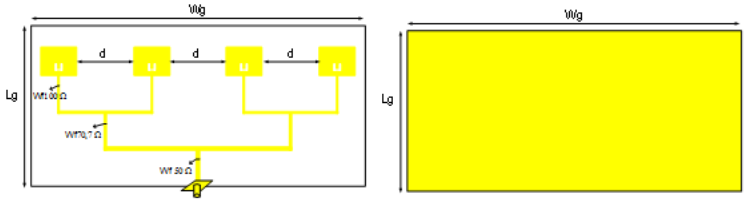

(a) (b)

Figure 4. 2×2 U Slot Array Design; (a) Front View, (b) Back View

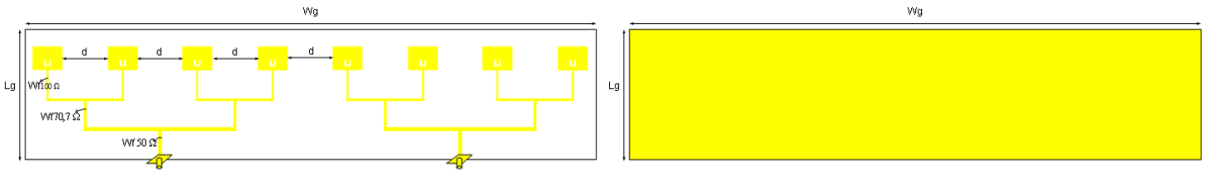

(a) (b)

Figure 5. Design of 4×2 U Slot MIMO Array Antenna; (a) Front View, (b) Back View

Based on the equations and the appropriate parameters the have been obtained, a 2×2 microstrip array antenna with the U slot method can be designed as shown in Figure 4, and to increase the bandwidth value and obtain a directional radiation pattern, the MIMO technique can be used. Figure 5 shows the design of the MIMO 4×2 Slot U, Array Antenna. Table 1 shows the dimensions of the designed antenna array and MIMO.

JURNAL ECTIPE
Electronic, Control, Telecommunication, Information, and Power Engineering
Volume 10, Issue 1, April 2023, pp. 32-41
ISSN 2355-5068 ; e-ISSN 2622-4852
DOI: 10.33019/jurnalecotipe.v10i1.3601

Table 1. Dimensions of Array Antenna 2×2 U Slot

Parameter	Description	Dimension (mm)
W	Patch width	26
L	Patch length	20.5
Wg	Groundplane width	250
Lg	Groundplane length	120
Wf	Width of power supply line 50 Ω	2.1
Lf	Length of power supply line 50 Ω	28
D	Slot length	5.1
C	Slot width	4.8
E/F	Slot thickness	0.9
H	Slot distance from base	3.5
d	Distance between elements	43
$Wf_{70,7\Omega}$	Width of power supply line 70,7 Ω	1.1
$Lf_{70,7\Omega}$	Length of of power supply line 70,7 Ω	28
$Wf_{100\Omega}$	Width of power supply line 100 Ω	1
$Lf_{100\Omega}$	Length of of power supply line 100 Ω	28

3. RESULTS AND DISCUSSION

3.1. Simulation Results

The antenna design process is simulated using AWR Microwave Office 2009 software to see the results of the antenna parameters that have been designed. The comparison of return loss and bandwidth can be seen in Figure 6.

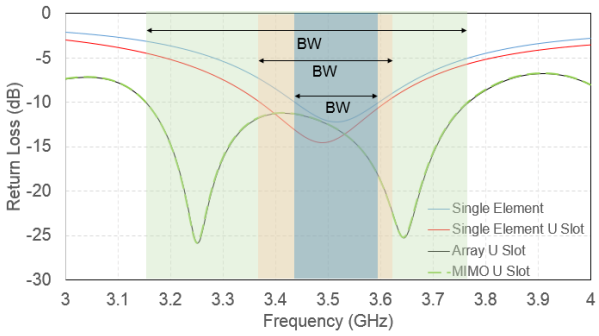

Figure 6. Comparison of Return Loss Simulation of Each Antenna

Figure 6 shows the comparison of the return loss and bandwidth of each antenna. It can be seen that the 4×2 slot U MIMO array antenna has a return loss value of -12.49 dB, a decrease compared to a single-element antenna. This decrease in return loss is due to the addition of patch elements, array methods, and MIMO so that power absorption is also better. For comparison of VSWR, results can be seen in Figure 7.

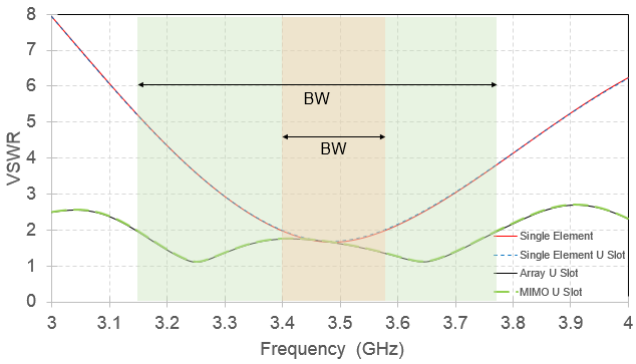

Figure 7. Comparison of the Overall Simulation VSWR of the Antenna

JURNAL ECTIPE
Electronic, Control, Telecommunication, Information, and Power Engineering
Volume 10, Issue 1, April 2023, pp. 32-41
ISSN 2355-5068 ; e-ISSN 2622-4852
DOI: 10.33019/jurnalecotipe.v10i1.3601

Figure 7 shows the comparison of the VSWR values for each antenna. It can be seen that the MIMO 4×2 slot U antenna array has a VSWR value of 1.62, a decrease compared to a single-element antenna. The decrease in VSWR is due to the addition of patch elements, array methods, and MIMO so that power absorption is also better.

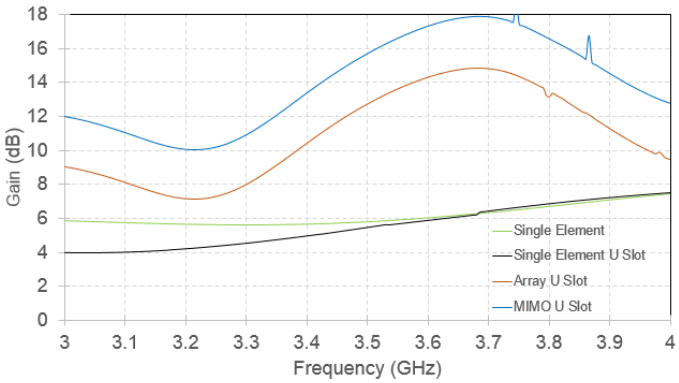

Figure 8. Comparison of Overall Antenna Simulation Gain

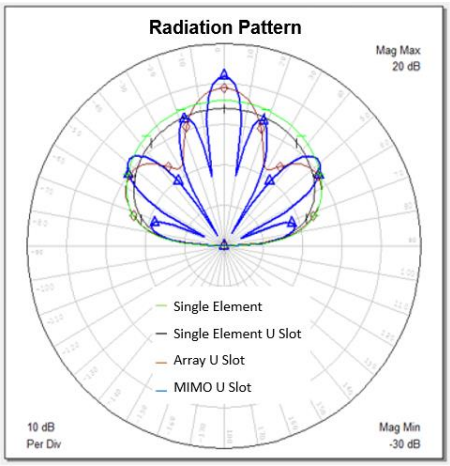

Figure 9. Comparison of Overall Antenna Simulation Radiation Patterns

Figure 8 shows the comparison of the overall gain value of the antenna. It can be seen that the overall gain value of the antenna increases and the MIMO 4×2 slot U antenna array has the highest gain value of 15.70 dB. Figure 9 shows the overall radiation pattern of the antenna. It can be seen that the antenna with a single element has a unidirectional radiation pattern and the addition of a patch using the array and MIMO method can produce a directional radiation pattern in which the beam becomes narrower. Figure 10 shows the overall impedance comparison of the antenna.

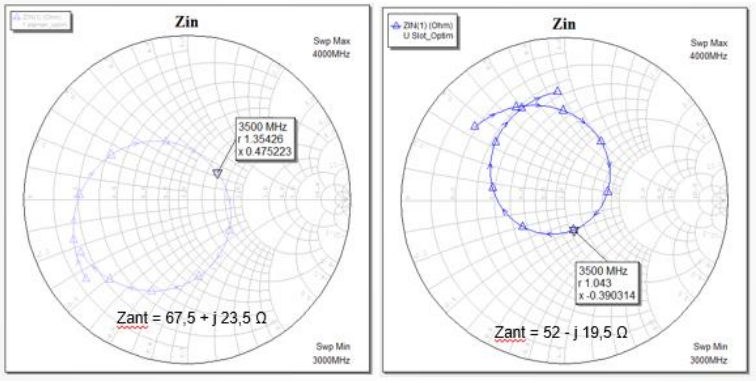

(a) (b)

JURNAL ECTIPE
Electronic, Control, Telecommunication, Information, and Power Engineering
Volume 10, Issue 1, April 2023, pp. 32-41
ISSN 2355-5068 ; e-ISSN 2622-4852
DOI: 10.33019/jurnalecotipe.v10i1.3601

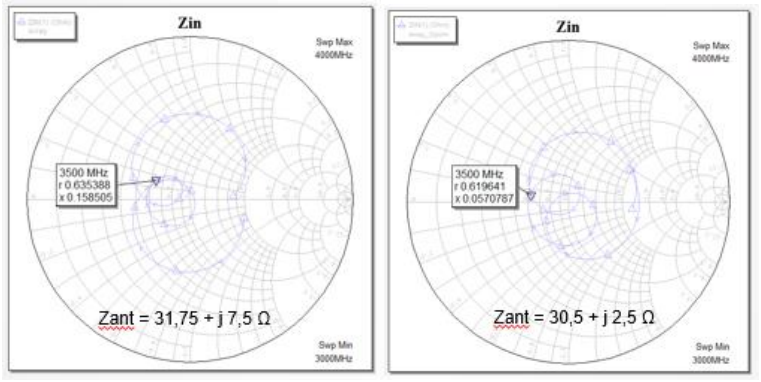

(c) (d)

Figure 10. Simulation Impedance Comparison of All Antennas; (a) Single Element Antenna, (b) Single Element U Slot Antenna, (c) 2×2 Array U Slot Antenna, (d) 4×2 MIMO Array U Slot Antenna

Figure 10 shows the overall impedance ratio of the antenna. The comparison value of the overall antenna parameters can be seen more clearly in Table 2.

Table 2. Comparison of Overall Antenna Simulation Parameters

Antenna	Parameter					
	Return loss (dB)	**Bandwidth (MHz)**	**VSWR**	**Gain (dB)**	**Impedance**	**Radiation Pattern**
Single Element	-12,15	155	1,65	5,82	67,5 + j 23,5 Ω	Unidirectional
Single Element U Slot	-14,48	235	1,68	5,48	52 - j 19,5 Ω	Unidirectional
2×2 Array U Slot	-12,50	3765 - 3155 = 610	1,62	12,75	31,75 + j 7,5 Ω	Directional
4×2 MIMO Array U Slot	-12,49	3765 - 3155 = 610	1,62	15,70	30,05 + j 2,5 Ω	Directional

From Table 2 it can be seen that the overall results of the antenna simulation parameters that have been designed have met the criteria, namely return loss ≤ -10 dB, bandwidth ≥ 200 MHz and VSWR ≤ 2.

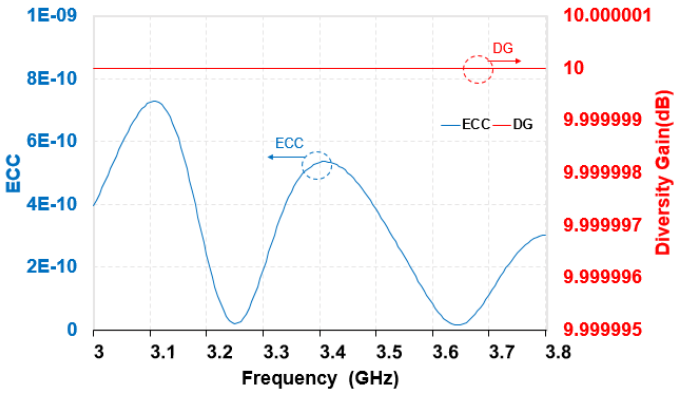

Figure 11. Envelope Correlation Coefficient (ECC) and Diversity Gain (DG) Simulation 4×2 MIMO Array U Slot *Antenna*

Figure 11 illustrates the value of the envelope correlation coefficient (ECC) and the diversity gain (DG) of the simulation results. It can be seen that the ECC value obtained is $3{,}85 \times 10^{-10}$ and the DG is 10 dB at a frequency of 3.5 GHz. From these two results, it can be stated that the antenna design has met the required ECC and DG limit values for MIMO antennas, namely the value of ECC < 0.5 and DG ≥ 10 dB.

After the results of the antenna simulation parameters match the desired criteria, the next step for the antenna can be the fabrication process.

JURNAL ECOTIPE
Electronic, Control, Telecommunication, Information, and Power Engineering
Volume 10, Issue 1, April 2023, pp. 32-41
ISSN 2355-5068 ; e-ISSN 2622-4852
DOI: 10.33019/jurnalecotipe.v10i1.3601

3.2. Antenna Fabrication Measurement Results

After obtaining the simulation and optimization results that match the criteria, then the fabrication process can be carried out and measurements of the antenna parameters of the fabricated results can be carried out. Fabrication is the process of realizing the simulation model into the original form of the antenna. The results of antenna fabrication will be measured using a Network Analyzer. In Figure 12, can be seen fabrication results of the 4×2 MIMO Array U Slot Antenna.

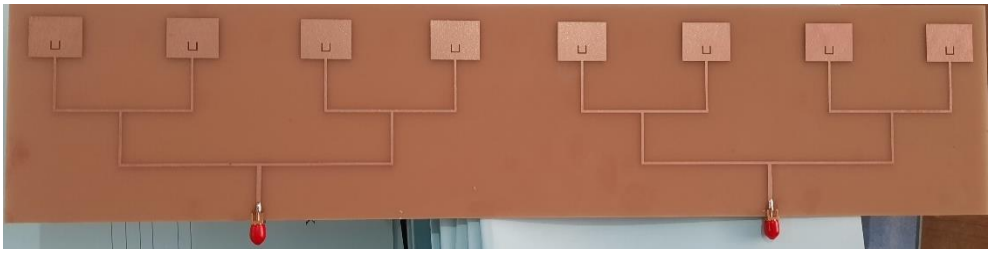

Figure 12. Fabrication Results of 4×2 MIMO Array U Slot Antenna

Measurement of the fabricated antenna obtained the parameters of return loss, bandwidth, VSWR, and impedance shown in Figure 13.

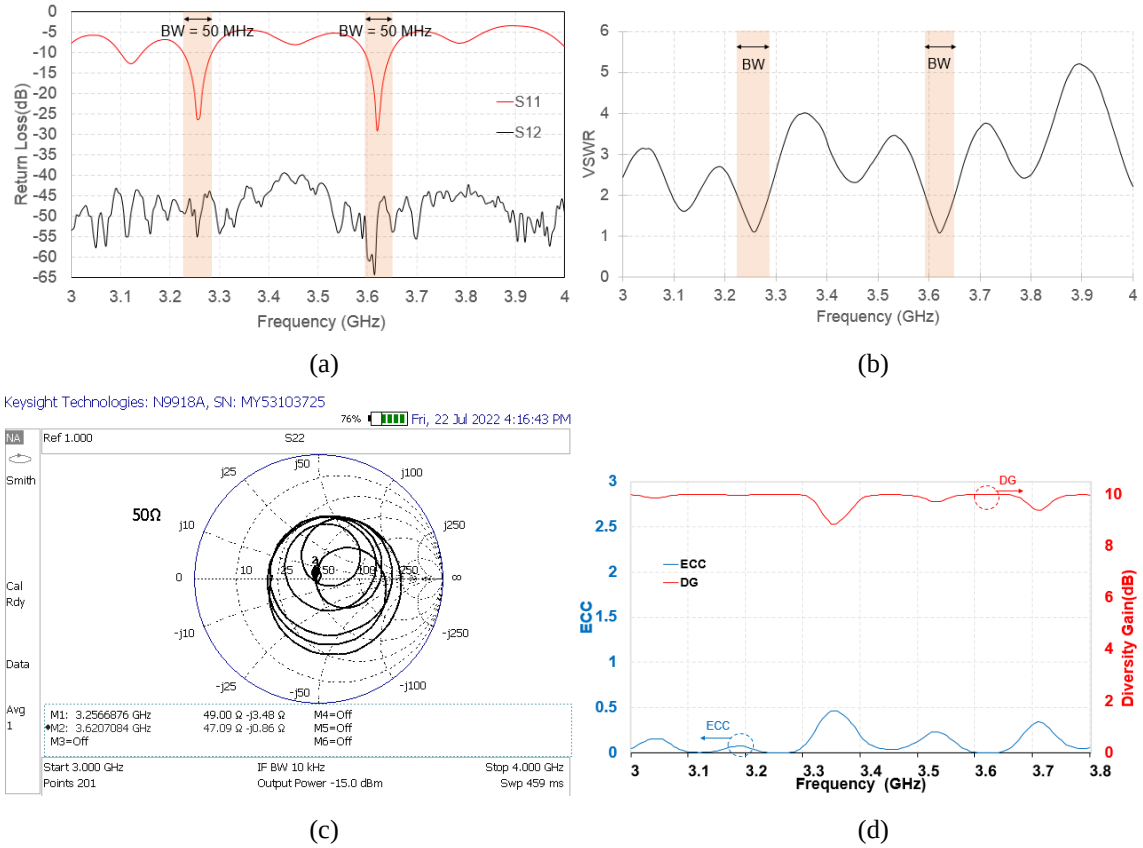

Figure 13. Parameters of 4×2 MIMO Array U Slot Antenna Fabrication; (a) Return loss, (b) VSWR, (c) Impedance, (d) Envelope Correlation Coefficient (ECC) and Diversity Gain (DG)

Figures 13 shows the results of measuring return loss, bandwidth, VSWR, impedance, envelope correlation coefficient (ECC), and diversity gain (DG) from 4×2 MIMO Array U Slot Antenna Fabrication. The results of the measurement of the return loss parameter (S11) of -6.03 dB, (S12) -42.78 dB, VSWR of 2.99, ECC of 0.12, and DG of 9.92 dB at a frequency of 3.5 GHz. Based on the measurement results of antenna fabrication, the parameters obtained at a frequency of 3.5 GHz do not match the desired criteria. This is caused by several factors including losses in connectors, soldering results, or poor dissolving of the antenna. However, it can be seen in Figures 12 to 15 that 2 valley points

Volume 10, Issue 1, April 2023, pp. 32-41
ISSN 2355-5068 ; e-ISSN 2622-4852
DOI: 10.33019/jurnalecotipe.v10i1.3601

meet the desired antenna criteria, namely at a frequency of 3.26 GHz and 3.62 GHz. The results of the antenna parameters at the frequency of 3.26 GHz and 3.62 GHz will be described in Table 3.

Table 3. Measurement Results of 4×2 MIMO Array U Slot Antenna Fabrication at 3.26 GHz and 3.62 GHz

Parameter	Frequency	
	3,26 GHz	3,62 GHz
Return loss (S11)	-25,96 dB	-29,22 dB
Return loss (S12)	-50,90 dB	-51,78 dB
Bandwidth	50 MHz	50 MHz
VSWR	1,10	1,06
Impedance	49,00 – j0,48 Ω	47,09 – j0,86 Ω
ECC	$6{,}48 \times 10^{-6}$	$1{,}45 \times 10^{-6}$
DG	10 dB	10 dB

Table 3 shows the measurement of 4×2 MIMO Array U slot antenna fabrication at a frequency of 3.26 GHz and 3.62 GHz. It can be seen that 3.62 GHz frequency is the frequency that has the lowest value for return loss (S11) of -29.22 dB, (S12) -51.78 dB, VSWR of 1.06, an impedance of 47.09 - j 0.86 Ω, ECC of 1.45×10^{-6} and DG of 10 dB.

3.3. Analysis and Comparison of Antenna Parameters

Research [7] with a 2×2 MIMO array U slot antenna with a frequency of 3.5 GHz obtained the lowest return loss value (S11) -21.98 dB, (S12) -63.16 dB, Bandwidth 188 MHz, VSWR ≤ 2, ECC of 3.97 × 10-7 and a DG of 10 dB. Based on research simulation data using a 4×2 MIMO array U slot antenna, it shows an increase in the bandwidth value of 422 MHz and a return loss value of -25.01 dB when compared to the research results [7]. The increase in bandwidth and return loss is due to the addition of patch elements to the antenna so that power absorption is also better.

A Comparison of the results of simulation and fabrication studies of the 4×2 MIMO array U slot antenna shows slightly different results. The return loss value generated by the antenna fabrication is higher than the simulation results which causes the parameter value at a frequency of 3.5 GHz not to meet the antenna specifications. This is caused by several factors including losses in connectors, soldering results, or poor dissolving of the antenna. However, it can be seen at a frequency of 3.62 GHz that the antenna parameter values meet the criteria for return loss ≤ -10 dB, VSWR ≤ 2, gain ≥ 5 dB, directional radiation pattern, isolation loss ≤ -20 dB, envelope correlation coefficient ≤ 0.5 and diversity gain 10 dB.

A complete comparison of previous studies, simulation results, and fabrication studies of the 4×2 MIMO array U slot antenna is shown in Table 4.

Table 4. Comparison of Simulation Result Parameters and Antenna Fabrication

Parameter	2×2 MIMO Array Slot U [7]	Simulation	Fabrication	
Frequency	3.5 GHz	3.5 GHz	3.5 GHz	3.62 GHz
Return loss (S11)	-21.98 dB	-12.49 dB	-6.03 dB	-29.22 dB
Return loss (S12)	-63.16 dB	-88.17 dB	-42.78 dB	-51.78 dB
Bandwidth	188 MHz	610 MHz	-	50 MHz
VSWR	≤ 2	1.62	1,10	1.06
Impedance	-	31 + j 2.5 Ω	-	47,09 – j0,86 Ω
ECC	3.97×10^{-7}	3.85×10^{-10}	0.12	1.45×10^{-6}
DG	10 dB	10 dB	9.92 dB	10 dB

4. CONCLUSION

Based on the simulation, fabrication, and analysis results in this final project, it can be concluded that the design and simulation of the MIMO linear microstrip antenna array at a frequency of 3.5 GHz for 5G technology have successfully met the desired specifications for 5G technology with a return loss of -12.49 dB, a bandwidth of 610 MHz, VSWR of 1.62, a gain of 15.70 dB, an envelope correlation coefficient of 3.85×10^{-10} and diversity gain of 10 dB at a frequency of 3.5 GHz. Giving slots and increasing the number of patches has the effect of forming two resonant frequencies and forming a

Volume 10, Issue 1, April 2023, pp. 32-41
ISSN 2355-5068 ; e-ISSN 2622-4852
DOI: 10.33019/jurnalecotipe.v10i1.3601

directional radiation pattern. From the results of the fabrication of the MIMO linear array antenna with a U slot at a frequency of 3.5 GHz, it has not met the desired specifications with a return loss of -6.03 dB and a VSWR of 2.99. However, two working frequencies meet the desired specifications for 5G technology, namely at frequencies of 3.2 GHz and 3.62 GHz with each return loss value (S11) of -25.96 dB and -29.22 dB, (S12) of -48.61 dB and -51.78 dB, a bandwidth of 50 MHz. The independence of each antenna is indicated by the envelope correlation coefficient of 6.48×10^{-6} and 1.5×10^{-6}, and a diversity gain of 10 dB.

REFERENCES

[1] H. U. Mustakim, "Tantangan Implementasi 5G di Indonesia," *INTEGER J. Inf. Technol.*, vol. 4, no. 2, pp. 1–10, 2019, doi: 10.31284/j.integer.2019.v4i2.561.

[2] Dinas Kominfo, *Studi Lanjutan 5G Indonesia 2018 Spektrum Outlook dan Use Case untuk Layanan 5G Indonesia*. 2018.

[3] Y. W. Fauzia Kurnia Hadist, Heroe Wijanto, "Antena Mikrostrip Mimo 4×4 Bowtie 2,4 GHz Untuk Aplikasi Wifi 802.11n," *Angew. Chemie Int. Ed. 6(11), 951–952.*, vol. 13, no. April, pp. 15–38, 2017.

[4] R. F. N. Alam syah, "Meningkatkan Gain untuk Aplikasi LTE pada Frekuensi 2.300 Mhz," *Tek. dan Ilmu Komput.*, vol. 07, pp. 365–378, 2018.

[5] M. Sholeh and Y. Rahayu, "Perancangan Antena MIMO Array 37 Ghz Untuk Jaringan Komunikasi 5G," *J. Nas. Tek. Elektro*, vol. 5, no. 2, pp. 1–9, 2018.

[6] M. R. Sumpena, H. Madiawati, and Elisma, "Desain Antena Susun Mikrostrip Rectangular Patch 4x2 Untuk Aplikasi 5G," *Pros. 11th Ind. Res. Work. Natl. Semin.*, pp. 591–595, 2020.

[7] Z. A. Sanaz, S. Alam, and I. Surjati, "Perancangan Antena MIMO Microstrip Rectangular Array dengan Slot U," vol. 16, no. 2, pp. 40–45.

[8] T. A. Riza, Y. Wahyu, F. T. Elektro, U. Telkom, and K. Kunci, "Perancangan dan Realisasi Antena Mikrostrip Dual-Band Menggunakan Slot Berbentuk U Untuk Aplikasi Wifi Design And Realization Dual-Band Microstrip Anntena Using U- Shaped Slot For Wifi Application," 2015.

[9] C. A. Balanis, *Antenna Theory: Analysis and Design, 3rd Edition*. 2005.

[10] M. Erifiandi, "Universitas Sumatera Utara Skripsi," *Ranc. Bangun Antena Mikrostrip Patch Segiempat 1x8 Linier Array Dengan Pencatuan Aperture Coupled Untuk Apl. Radar Marit. Frekuensi 3,2 GHZ*, 2018.

[11] K. Jones A.S., L. Olivia N., and B. Syihabuddin, "Perancangan Antena MIMO 2×2 Array Rectangular Patch dengan U-Slot untuk Aplikasi 5G," *J. Nas. Tek. Elektro dan Teknol. Inf.*, vol. 6, no. 1, 2017, doi: 10.22146/jnteti.v6i1.299.

[12] P. Bhattacharjee, V. Hanumante, and S. Roy, "Design of U-Slot Rectangular Patch Antenna for Wireless LAN at 2 . 45GHz," no. December, 2014.

JURNAL ECOTIPE
Electronic, Control, Telecommunication, Information, and Power Engineering

Volume 10, Issue 1, April 2023, pp. 42-51
ISSN 2355-5068 ; e-ISSN 2622-4852
DOI: 10.33019/jurnalecotipe.v10i1.3704

ZigBee-Based Wireless Sensor Network Topology Design and Comparison in Residential Areas

Muh. Aristo Indrajaya[1], Rizana Fauzi[2], Erwin Adrias[3]
[1,2,3]Department of Electrical Engineering, Engineering Faculty, Tadulako University, 94118, Indonesia.

ARTICLE INFO

Article historys:

Received : 25/12/2022
Revised : 17/01/2023
Accepted : 19/04/2023

Keywords:

End-To-End Delay, Hop Number, Media Access Delay, Opnet, Packet Dropped, Throughput, ZigBee

ABSTRACT

When designing a ZigBee-based wireless sensor network, choosing the right network topology is important, especially in networks with multiple nodes. Choosing the wrong topology will have an impact on the performance of the wireless sensor network as a whole because it will cause a large delay value. This research has the main objective to find the right type of topology that can be applied to densely populated residential areas with a large number of houses and a large area of land. This research will provide benefits for housing developers who want to implement a ZigBee-based wireless sensor network for various purposes in each unit in their residential area, such as recording electricity and water usage, security systems, and so on. This research will use three types of ZigBee topologies, namely star, tree, and mesh topologies. The housing used for the simulation in this study is Citraland Waterfront City Housing located in Palu City, Central Sulawesi Province, Indonesia. By using simulation-based calculations using the Opnet Modeler 14.5 application, it is known that the star topology on the ZigBee network is suitable for application to residential areas with a large number of nodes and areas. This can be seen from the highest throughput and media access delay, end-to-end delay, number of hops, and the lowest packet drop value compared to the tree and mesh topologies.

Corresponding Author:

Muh. Aristo Indrajaya
Department of Electrical Engineering, Engineering Faculty, Tadulako University, 94118, Indonesia.
Email: aristo90c@gmail.com

1. INTRODUCTION

The application of wireless sensor networks, especially in residential areas, is currently experiencing rapid development, along with the increasing number of home features offered by developers. One of the smart home features owned by several housing estates which are starting to be implemented at this time, among others, is the electronic recording of electricity and water consumption. So far, the recording of the use of electricity and water is carried out by authorized officers. This is of course a waste of human resources amid very high demands for efficiency. Microcontroller-based electronic recording supported by wireless sensor networks can be recorded online. One type of device that is often used in wireless sensor networks is ZigBee. With ZigBee, all data belonging to the microcontroller can be sent directly to the server.

ZigBee is an IEEE 802.15.4 standard for data transmission between commercial and consumer electronic devices [1,2,3]. ZigBee is made to operate on low-level personal networks and consumes less power [4,5]. Devices with ZigBee technology are frequently used as wireless sensors or to control other devices [6,7]. A feature of ZigBee allows it to control both its network and the flow of data on the network [8,9]. ZigBee also has the benefit of requiring little power, making it suitable for use as a wireless control system that only needs to be installed once [10,11,12]. ZigBee has the advantage of

Volume 10, Issue 1, April 2023, pp. 42-51
ISSN 2355-5068 ; e-ISSN 2622-4852
DOI: 10.33019/jurnalecotipe.v10i1.3704

very low power consumption and if it is not operating, then ZigBee will always be in sleep mode and has a maximum data rate of 250 Kbps [13,14]. With these advantages, ZigBee is suitable to be placed in applications that require devices with low power consumption [15]. Compared to other WPANs like Bluetooth, which has a transmission rate of 1 Mbps, ZigBee has a transfer rate of roughly 250 Kbps [16]. The operating range or distance of ZigBee is around 76 m, which is greater than Bluetooth. Like a LAN network, ZigBee also has a network topology which is the concept of the ZigBee network infrastructure. Based on the IEEE 802.15.4 standard, ZigBee has three network topologies, namely Star, Mesh, and Tree. [17].

Numerous research has been conducted about the topology of the ZigBee network. Hamdy [18] has assessed how the ZigBee topology affects throughput and end-to-end latency when used in the IoT space. The result obtained from the tree topology can produce the greatest results at a frequency of 2.4 GHz, while the star topology can produce the best results at frequencies of 915 and 868 MHz, according to testing including the star, mesh, and tree topologies. Opnet Modeler 14.5 was also used for this test's execution. Other studies have also been carried out by Söğüt [19] by comparing the performance of star, mesh, and tree topologies. Through the simulations carried out, it can be seen that by considering a large number of hob values, the star topology can provide the best end-to-end delay results. Research related to other ZigBee network topologies was also carried out by Ibrahim [10]. Through his research, he examines the effect of response time on the three types of ZigBee topologies. The results of his research show that the mesh topology can provide better throughput and latency values compared to the star and tree topologies.

Based on previous research, a simulation of the ZigBee network is carried out in this study by spreading out the number of nodes over a greater area that includes residential areas. This is done to determine which topology is appropriate for use given the location and node count. The findings of this study can be used as a guide for developers to choose the best wireless sensor network topology for use in residential areas with a lot of densely populated homes and a variety of purposes. Citraland Waterfront City Housing, a middle- to upper-class housing model situated in Palu City, Central Sulawesi Province, Indonesia, was selected as the housing model. This residential area was chosen as a reference not only because the housing design is characterized by today's housing, it is also supported by the number of units and a very large area.

2. RESEARCH METHOD

2.1. Site Survey

The first step in this research is a site survey. This survey was conducted to determine the area of housing, the location of each house, and the number of units in it. The design and simulation of the wireless sensor network in this paper take the design of the existing residential area model at Citraland Waterfront City Housing in Palu City, Central Sulawesi Province, Indonesia. Citraland Waterfront City housing consists of several blocks of houses, shops, and public areas. Overall Citraland Waterfront City Housing has a total of 160 shop units and 352 housing units. The design of Citraland Waterfront City Residential can be seen in Figure 2.

The design of the ZigBee network topology will focus on residential areas located in blocks B6, B5, B3, B7, and A1. Each house will have one end device unit and in this model, it is assumed that each end device is placed in the front yard of each house and every house in Citraland Waterfront City is next to each other. The total simulated houses are 113 units.

JURNAL ECTIPE
Electronic, Control, Telecommunication, Information, and Power Engineering
Volume 10, Issue 1, April 2023, pp. 42-51
ISSN 2355-5068 ; e-ISSN 2622-4852
DOI: 10.33019/jurnalecotipe.v10i1.3704

Figure 1. Citraland Waterfront City Residential Master Plan

2.2. Topology Design

The second stage of this research is topological design. After the site survey and house mapping have been completed, the next step is to design the topology used. In this study, a comparison of three types of topology owned by ZigBee was carried out, namely star, mesh, and tree. Topology design will refer to the three types of topology.

2.2.1. ZigBee Component

ZigBee is made up of three major components: the ZigBee Coordinator, the ZigBee End Device, and the ZigBee Router [8]. The ZigBee coordinator coordinates overall network actions and is in charge of network bootstrapping [18]. The ZigBee routers create a network among themselves to exchange packets [6]. The ZigBee end device is in charge of requesting any outstanding messages from its parent [16]. If an end device moves, it must notify the network that it has rejoined a new parent.

2.2.2. Star Topology

The first topology is the star topology. The star topology is made up of a coordinator and a few end devices. It is the most basic and limited ZigBee protocol. All devices are linked to a single coordinator node, through which all communication is routed. The star topology is significant because it is defined by the underlying 802.15.4 specification on which ZigBee is based [9]. The disadvantage of this architecture is that there is no alternative path from the source to the end devices, which may be a hindrance.

Based on the star topology concept, a star topology design was developed and used for the Citraland Waterfront City Residential area, as shown in Figure 2. It can be seen in Figure 2, that in the star topology model, each house block will have one coordinate unit. This coordinator will control every ZigBee device that acts as an End Device in every resident's house. Each coordinator will have a different PAN ID (Personal Area Network Identifier). So that all existing end devices will only connect to the coordinator with the same PAN ID. This is done to minimize delay and the possibility of collisions in the network caused by the number of nodes in it.

JURNAL ECOTIPE
Electronic, Control, Telecommunication, Information, and Power Engineering
Volume 10, Issue 1, April 2023, pp. 42-51
ISSN 2355-5068 ; e-ISSN 2622-4852
DOI: 10.33019/jurnalecotipe.v10i1.3704

Figure 2. Design of star topology

2.2.3. Tree Topology

Tree topology is the second type of ZigBee topology. It is made up of a coordinator, a few routers, and end devices that work together to form a central node or root tree. Routers extend network coverage. Children are end nodes that are linked to the parent (coordinators or routers) [6]. Only the end devices have access to the parent. The disadvantage of the tree topology is that if one parent is disabled, the disabled parent's children cannot connect with other devices in the network, even if they are close to one another [9]. Figure 3 depicts a tree topology design for the Citraland Waterfront City Residential area based on the tree topology concept.

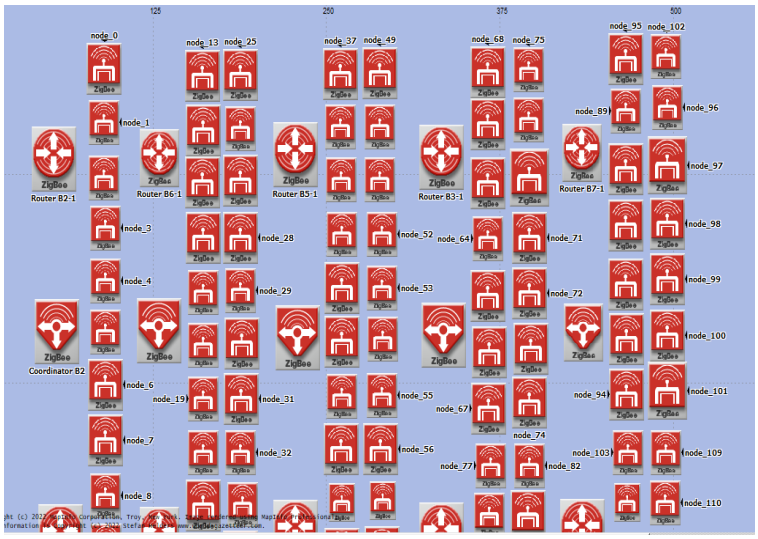

Figure 3. Design of tree topology

The tree topology applied to this housing model uses two routers and one coordinator for each house block. Each end device in each home will be connected to both routers, and both routers will be connected to a coordinator who will control the network as a whole. As in the star topology, each coordinator in each block will have a different PAN ID so that the end devices and routers in each house will only be connected to the coordinator who has the same PAN ID as theirs.

2.2.4. Mesh topology

The third and final topology is peer-to-peer or mesh topology. This topology is made up of a coordinator, a few routers, and an end device [3]. The coverage area can be expanded by adding new devices to the network. If one of the paths fails during transmission, the node will find another path to

JURNAL ECOTIPE
Electronic, Control, Telecommunication, Information, and Power Engineering
Volume 10, Issue 1, April 2023, pp. 42-51
ISSN 2355-5068 ; e-ISSN 2622-4852
DOI: 10.33019/jurnalecotipe.v10i1.3704

the destination, reducing dead zones [9]. Users can easily add or delete devices when using this mesh topology because they can connect to any target device in the network [6]. Figure 4 depicts a mesh topology design based on the mesh topology concept for the Citraland Waterfront City Residential area.

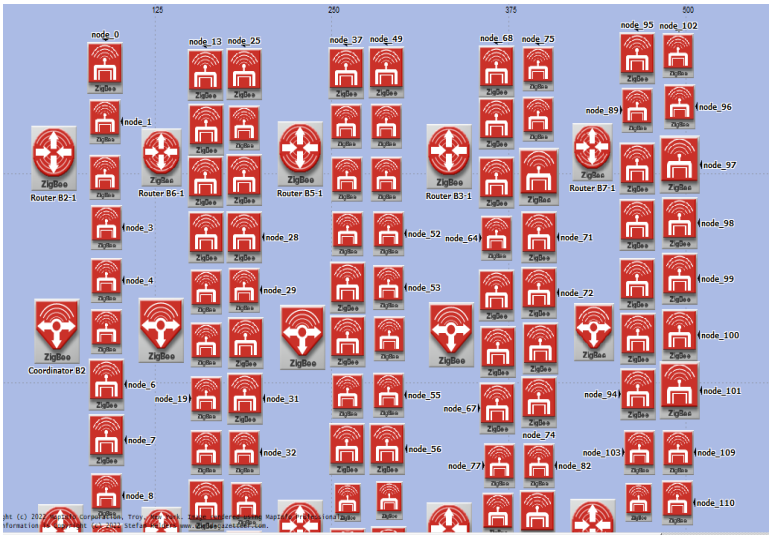

Figure 4. Design of mesh topology

The components used in the mesh topology are the same as those used in the tree topology, involving two routers and one router. The difference between the two lies only in the connecting path between the two routers and the topology configuration of the unit that acts as a coordinator.

2.3. Topology Simulation

The next stage is simulation. The simulation is carried out to determine the performance of the three ZigBee network topology designs. This simulation also aims to collect data based on the specified parameters to find out which topological design is appropriate to be applied to residential areas.

The design along with the ZigBee-based wireless sensor network topology simulation in this study uses the Opnet Modeler 14.5 application. This application itself is widely used by students and researchers who focus on research related to communication between devices and telecommunication networks, computer networks, and wireless sensor networks [20].

2.4. Evaluation

The last stage is evaluation. Evaluation is carried out by looking at all the results of parameter measurements that have been carried out through a simulation process which will then be analyzed to find out the causes and determine what type of topology is suitable for use as a ZigBee network topology in residential areas.

3. RESULTS AND DISCUSSION

The three topology designs were simulated using the Opnet Modeler 14.5 application. Parameter settings in Opnet can be seen in Table 1:

Table 1. Simulation parameter.

Parameter	Value
Area size	1000 m x 1000 m
Destination	Parent
Packet size	Constant (200 bytes)
Frequency	2.4 GHz
Start time	Uniform (20,21)
Simulation time	1 Hour
Number of units	113

JURNAL ECOTIPE
Electronic, Control, Telecommunication, Information, and Power Engineering
Volume 10, Issue 1, April 2023, pp. 42-51
ISSN 2355-5068 ; e-ISSN 2622-4852
DOI: 10.33019/jurnalecotipe.v10i1.3704

Testing is done by looking at parameters: throughput, media access delay, end-to-end delay, hop number, and packet dropped. The results of the tests carried out on the three topological designs can be seen as follows.

3.1. Throughput

Throughput is the total number of bits (in bits/sec) forwarded from the 802.15.4 MAC to higher layers in all network WPAN nodes. The simulation results are shown in Figure 5.

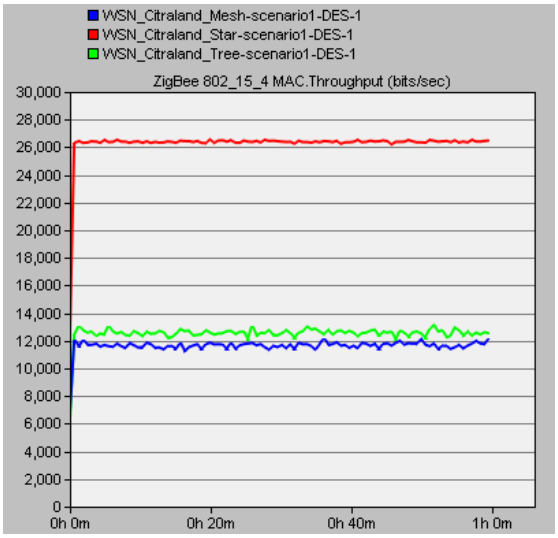

Figure 5. Throughput from the three topologies

The throughput measurement results show that the star topology can pass more data within a certain period compared to the tree and mesh topologies. It can be seen from the graph that the star topology has a throughput value of 26000 kbps, far superior to the tree and mesh topologies. This is because the star topology has a simpler design so that data can be passed more easily and quickly.

3.2. Media Access Delay

The sum of the contention and queuing delays for all 802.15.4 MACs is known as the media access delay. This delay is determined for each frame as the amount of time that passes between the time the frame is added to the transmission queue, which is the arrival time for higher layer data packets and the creation time for all other frame types, and the time the frame is sent to the physical layer for the first time. The media access delay value obtained from the three topologies can be seen in Figure 6.

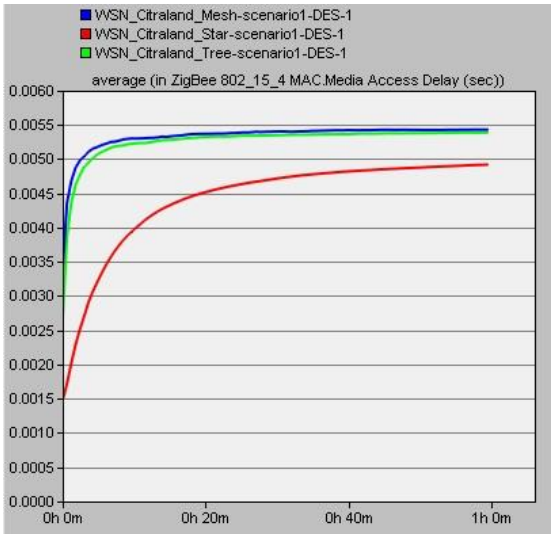

Figure 6. Media access delay parameter of the three topologies

JURNAL ECTIPE
Electronic, Control, Telecommunication, Information, and Power Engineering
Volume 10, Issue 1, April 2023, pp. 42-51
ISSN 2355-5068 ; e-ISSN 2622-4852
DOI: 10.33019/jurnalecotipe.v10i1.3704

From the results of the tests carried out, the design with a star topology still provides advantages compared to a tree with a mesh where the star topology has the smallest media access delay value.

3.3. End-to-End Delay

The end-to-end delay depicts the total amount of delay experienced when sending data from the sender to the recipient. Figure 7 displays the end-to-end delay measurement results for the three topology designs.

From the simulation results carried out on the three topologies designs, it can be seen that the star topology can provide better performance than the tree and mesh. This can be seen from the end-to-end delay value of the star topology which is much lower than the tree and mesh topology.

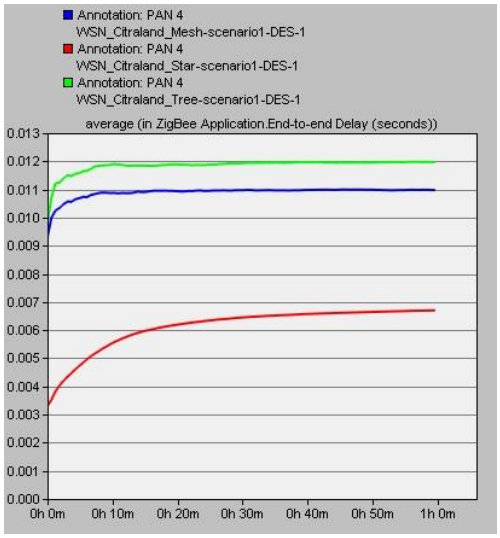

Figure 7. End-to-end delay parameters from the three topologies

3.4. Hop Number

The hop number refers to the number of intermediate devices that data must pass through for transmission from the source node to the destination node to be successful. Figure 8 depicts the hop number measurement results for the three topology designs. The simulation results show that the star topology has the fewest hops when compared to the mesh and tree topologies.

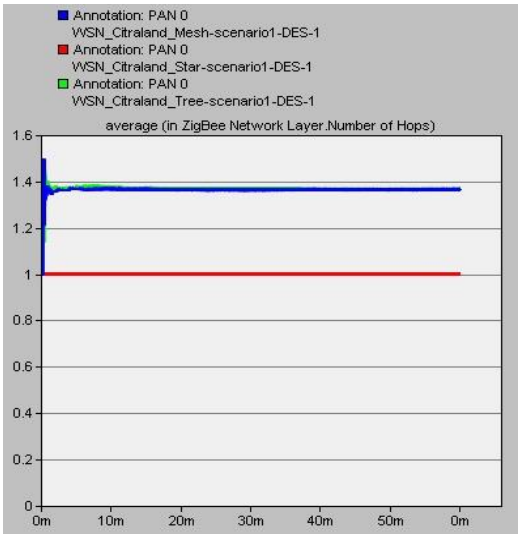

Figure 8. Hop number parameter from the three topologies

JURNAL ECTIPE
Electronic, Control, Telecommunication, Information, and Power Engineering
Volume 10, Issue 1, April 2023, pp. 42-51
ISSN 2355-5068 ; e-ISSN 2622-4852
DOI: 10.33019/jurnalecotipe.v10i1.3704

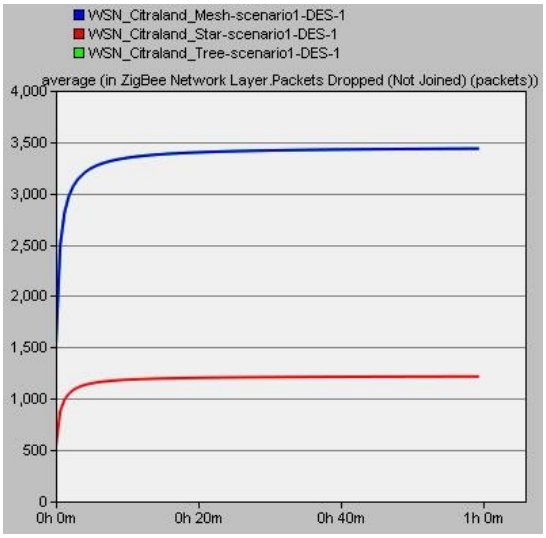

Figure 9. Packet dropped parameter from the three topologies

3.5. Packet Dropped

Packets dropped to show the number of data packets lost during the data transmission process. Based on the simulations performed, the star topology appears to have the smallest packet drop value compared to the mesh and tree topologies. The values in the tree and mesh topologies have the same packet dropped values. The values of packet dropped from the three topologies can be seen in Figure 9.

3.6. Result Evaluation

Through the results of all parameter simulations, it can be seen that a network with a star topology has its advantages when compared to a network with a tree or mesh topology. This can be caused because the star topology has simpler components when compared to the tree and mesh topologies, where the star topology does not use routers. Just like on a LAN network, routers on a ZigBee network also work by using a routing table. The router works to receive each data packet it receives and matches the information in it with its routing table. On a network with a small number of nodes, the resulting delay is not large, but the delay value will increase as the number of nodes in the network increases [21]. It can also be seen from the hop number parameter that data packets in the mesh and tree topologies must pass through more nodes to reach their destination compared to the star topology. This will further increase the existing delay, thereby reducing the overall network capacity. Phenomena like this can also be seen in the research conducted by Hamdy [18] and Ibrahim [10] where when the number of nodes and the area used is relatively small, the tree and mesh topologies can provide better results. However, for large-scale networks with a large number of nodes, star topology can provide better results, as in the research conducted by Söğüt [19].

4. CONCLUSION

The purpose of this study is to find the best type of ZigBee network topology that is suitable for use in residential areas. From the calculation results obtained through the simulation process, by looking at parameters such as throughput, media access delay, end-to-end delay, hop number, and packet dropped, it can be concluded that the ZigBee network with a star topology is suitable for residential areas. This is possible because the component design is simpler so that it minimizes the possibility of large latencies that impact network performance. However, it is known that the star topology has a drawback where because all the communication that runs is centered on the coordinator device, this topology will be prone to interference if the coordinator has problems and does not have a backup line. Further research is needed to enable the star topology to have a backup path like that of the mesh and tree topologies.

Volume 10, Issue 1, April 2023, pp. 42-51
ISSN 2355-5068 ; e-ISSN 2622-4852
DOI: 10.33019/jurnalecotipe.v10i1.3704

REFERENCES

[1] H.-Y. Chang, "A connectivity-increasing mechanism of ZigBee-based IoT devices for wireless multimedia sensor networks," *Multimed Tools Appl*, vol. 78, no. 5, pp. 5137–5154, Mar. 2019, doi: 10.1007/s11042-017-4584-2.

[2] A. Haka, V. Aleksieva, H. Valchanov, and D. Dinev, "Analysis of ZigBee Network Using Simulations and Experiments," in *2020 International Conference Automatics and Informatics (ICAI)*, Varna, Bulgaria, Oct. 2020, pp. 1–4. doi: 10.1109/ICAI50593.2020.9311328.

[3] C. A. G. Silva, E. L. Santos, A. C. K. Ferrari, and H. T. S. Filho, "A Study of the Mesh Topology in a ZigBee Network for Home Automation Applications," *IEEE Latin Am. Trans.*, vol. 15, no. 5, pp. 935–942, May 2017, doi: 10.1109/TLA.2017.7910209.

[4] V. D. Vaidya and P. Vishwakarma, "A Comparative Analysis on Smart Home System to Control, Monitor and Secure Home, based on technologies like GSM, IOT, Bluetooth and PIC Microcontroller with ZigBee Modulation," in *2018 International Conference on Smart City and Emerging Technology (ICSCET)*, Mumbai, Jan. 2018, pp. 1–4. doi: 10.1109/ICSCET.2018.8537381.

[5] P. Mounika, "Performance analysis of wireless sensor network topologies for Zigbee using riverbed modeler," in *2018 2nd International Conference on Inventive Systems and Control (ICISC)*, Coimbatore, Jan. 2018, pp. 1456–1459. doi: 10.1109/ICISC.2018.8399050.

[6] T. Nimi and P. Samundiswary, "Comparative analysis of ZigBee network with tree and mesh topology for different range of frequencies," in *2017 2nd International Conference on Communication and Electronics Systems (ICCES)*, Coimbatore, Oct. 2017, pp. 560–564. doi: 10.1109/CESYS.2017.8321140.

[7] S. W. Nourildean, M. D. Hassib, and Y. A. Mohammed, "Internet of things based wireless sensor network: a review," *IJEECS*, vol. 27, no. 1, p. 246, Jul. 2022, doi: 10.11591/ijeecs.v27.i1.pp246-261.

[8] B. Rajesh kanna and M. Anitha, "Congruent routing protocols in diverse tree topology ZigBee built home area networks," *Materials Today: Proceedings*, vol. 33, pp. 4592–4601, 2020, doi: 10.1016/j.matpr.2020.08.194.

[9] Ompal, V. M. Mishra, and A. Kumar, "Zigbee Internode Communication and FPGA Synthesis Using Mesh, Star and Cluster Tree Topological Chip," *Wireless Pers Commun*, vol. 119, no. 2, pp. 1321–1339, Jul. 2021, doi: 10.1007/s11277-021-08282-w.

[10] S. A. Abdulhussien and S. K. Ibrahim, "Effects of Wireless Sensor Network Topology on Response Time," in *2020 International Conference on Electrical, Communication, and Computer Engineering (ICECCE)*, Istanbul, Turkey, Jun. 2020, pp. 1–5. doi: 10.1109/ICECCE49384.2020.9179353.

[11] G. Liang and X. Xu, "Residential area streetlight intelligent monitoring management system based on ZigBee and GPRS," presented at the MATERIALS SCIENCE, ENERGY TECHNOLOGY, AND POWER ENGINEERING I: 1st International Conference on Materials Science, Energy Technology, Power Engineering (MEP 2017), Hangzhou, China, 2017, p. 020213. doi: 10.1063/1.4982578.

[12] Y. Zhao, "Research on Wireless Sensor Network System Based on Zigbee Technology for Short Distance Transmission," *J. Phys.: Conf. Ser.*, vol. 1802, no. 2, p. 022008, Mar. 2021, doi: 10.1088/1742-6596/1802/2/022008.

[13] M. F. Shaik, M. M. Subashini, and N. Swathi, "Implementation of a ZigBee Based Network for WBAN," in *2021 7th International Conference on Advanced Computing and Communication*

Volume 10, Issue 1, April 2023, pp. 42-51
ISSN 2355-5068 ; e-ISSN 2622-4852
DOI: 10.33019/jurnalecotipe.v10i1.3704

Systems (ICACCS), Coimbatore, India, Mar. 2021, pp. 188–192. doi: 10.1109/ICACCS51430.2021.9442016.

[14] B. Pavkovic, N. Matic, D. Glisic, L. Berbakov, and I. Pap, "Simple detection of network anomalies and topology control in ZigBee networks," in *2017 25th Telecommunication Forum (TELFOR)*, Belgrade, Nov. 2017, pp. 1–4. doi: 10.1109/TELFOR.2017.8249346.

[15] R. Das and J. N. Bera, "ZigBee based Small-World Home Area Networking for Decentralized Monitoring and Control of Smart Appliances," in *2021 5th International Conference on Smart Grid and Smart Cities (ICSGSC)*, Tokyo, Japan, Jun. 2021, pp. 66–71. doi: 10.1109/ICSGSC52434.2021.9490482.

[16] S. F. Shende, R. P. Deshmukh, and P. D. Dorge, "Performance improvement in ZigBee cluster tree network," in *2017 International Conference on Communication and Signal Processing (ICCSP)*, Chennai, Apr. 2017, pp. 0308–0312. doi: 10.1109/ICCSP.2017.8286367.

[17] M. A. Moridi, Y. Kawamura, M. Sharifzadeh, E. K. Chanda, M. Wagner, and H. Okawa, "Performance analysis of ZigBee network topologies for underground space monitoring and communication systems," *Tunnelling and Underground Space Technology*, vol. 71, pp. 201–209, Jan. 2018, doi: 10.1016/j.tust.2017.08.018.

[18] Y. R. Hamdy and A. I. Alghannam, "Evaluation of ZigBee Topology Effect on Throughput and End to End Delay Due to Different Transmission Bands for IoT Applications," *J. commun. softw. syst. (Online)*, vol. 16, no. 3, pp. 254–259, Sep. 2020, doi: 10.24138/jcomss.v16i3.975.

[19] E. Söğüt and O. A. Erdem, "Performance Comparison of the IEEE 802.15.4 Standard (ZigBee) Topologies".

[20] M. G. Al-Hamiri, H. J. Abd, and H. M. Al Abboodi, "Performance evaluation of WLAN in enterprise WAN with real-time applications based on OPNET modeler," *IJEECS*, vol. 21, no. 2, p. 911, Feb. 2021, doi: 10.11591/ijeecs.v21.i2.pp911-918.

[21] A. S. Tanenbaum and D. Wetherall, *Computer networks*, 5th ed. Boston: Pearson Prentice Hall, 2011.

JURNAL ECOTIPE
Electronic, Control, Telecommunication, Information, and Power Engineering

Volume 10, Issue 1, April 2023, pp. 52-60
ISSN 2355-5068 ; e-ISSN 2622-4852
DOI: 10.33019/jurnalecotipe.v10i1.3723

Control Mass-Spring-Damper Based on Tuning Trade-off PID Controller

Adi Mulyadi[1], Muhammad Zainal Roisul Amin[2], Muhamad Khoirul Anam[3]
[1,2] Electrical Engineering, PGRI Banyuwangi University, Street Ikan Tongkol No. 22, Kertosasi, Banyuwangi, and 68416, Indonesia
[3] Mechanical Engineering, PGRI Banyuwangi University, Street Ikan Tongkol No. 22, Kertosasi, Banyuwangi, and 68416, Indonesia

ARTICLE INFO

Article historys:

Received : 01/01/2023
Revised : 03/02/2023
Accepted : 19/04/2023

Keywords:

Mass-Spring-Dumper, Setpoint Tracking, PID Controller, Tuning 1-2 DOF Controller, Trade-off PID Controller

ABSTRACT

This paper discusses the control mass-spring-dumper (MSD) system used in vehicle suspensions. The vehicle suspension consists of mass, coil (spring), and shock absorber (dumper). MSD provided a shock effect when the vehicle was caused by the frictional force on the load. The difficulty to achieve the stability of the suspension and the following of set-point tracking. Therefore, Therefore, the proportional-integral-derivative (PID) controller, tuning 1 and 2 degrees of freedom (1-2 DOF), and tuning trade-off PID controller were proposed for stability when the disturbance occurs. The MSD equation was obtained by using the Laplace transform and validated in Matlab Simulink. The result shows that the tuning trade-off PID control reduces disturbance rejection by the smaller set point tracking peak amplitude of 1.01, overshoot of 0.682%, and settling time of 0.318 seconds. The PID controller achieved set point tracking and disturbance rejection with a peak amplitude of 1.52, overshoot of 51.7%, and settling time of 2.23 seconds, and the tuning 1-2 DOF PID controller achieved set point tracking and disturbance rejection with a peak amplitude of 1.07, overshoot 6.53%, settling time 0.524 seconds. The tuning trade-off PID control has the best performance than tuning 1-2 DOF PID and PID controller.

Corresponding Author:

Adi Mulyadi
Electrical Engineering, PGRI Banyuwangi University, Street Ikan Tongkol No. 22, Kertosari, Banyuwangi, Banyuwangi, 68416, Indonesia
Email: adimulyadi@unibabwi.ac.id

1. INTRODUCTION

Mass-spring-damper (MSD) suspension systems are used in automobiles and motorcycles [1]. The system consists of mass, coil (spring), and shock absorber (dumper). MSD creates a shock effect caused by friction between the wheels and the load [2]. The vehicle load is used as a support for the suspension of the steering system [3], wheels, and chassis [4]. Important components that must be considered in the suspension such as transmission force, torque, comfort, and stability [5]. The Suspension has three classifications such as passive, semi-active, and active systems [6]. A Semi-active system has the characteristics of stability, balance [7], and low energy consumption [8]. The passive system limits the movement of the car body and wheels at speed for a comfortable ride [9]. The active system consists of actuators, mechanical springs, dampers, actuators, and mechanical springs [10]. The difference between active and passive systems is the controlling force. The controlling force reduces the vibrations that are affected by the entire surface of the vehicle and produce more comfort for the occupant than a driver is comfortable [11]. The comfort of the steering system and road estimation is a concern for controlling

Volume 10, Issue 1, April 2023, pp. 52-60
ISSN 2355-5068 ; e-ISSN 2622-4852
DOI: 10.33019/jurnalecotipe.v10i1.3723

the suspension system. The greater the suspension system is disturbed, the MSD will experience vibrations felt by the driver and passengers [12].

The conventional active suspension is mounted in parallel with the spring dumper, hydraulic, and actuator to generate vertical force between the sprung (chassis) [13] and unsprung (wheels) [14]. Active suspension with variable geometry is proposed to reduce mass unsprung gradually and power demand is limited [15]. The adaptive neural scheme is applied to active suspension with vertical mass sprung replacement limits and actuator saturation. Then radial basis function neural networks (RBFNNs) are used to predict the indeterminate body mass and pneumatic spring. So the prescribed performance function (PFF) control is designed for fault tracking from constrained sprung changes [16]. Ride height control (RHC) functions for semi-active air suspension and processes air in or out of the spring. RHC plays a role in improving vehicle performance. Non-linear predictive model control and proportional-integral-derivative are used to evaluate the performance of the car system [17]. Car system performance is analyzed by fuzzy logic for active suspension systems. The suspension system is reviewed for unknown parameters, actuator errors, and displacement limitations. Fault Tolerance Control (FTC) is proposed as an estimation control for external disturbances. External disturbances are analyzed using fault approximation techniques, and actuator errors. FTC is designed to address the output performance of a vehicle's suspension. The proposed control can overcome the problems of fault tolerance and tracking errors [18]. Control Electronic Suspension (ESC) is applied to the suspension to improve the yaw-roll-pitch motion of the vehicle. The vehicle pitch movement is used as a control for each degree of freedom (DOF) movement. The control algorithm consists of an integrated vehicle observer (IVO) for condition estimation, an integrated target generator (ITG), an integrated vehicle controller (IVC), and an optimal distribution controller (ODC). ITG is used as a target for roll, pitch, and yaw angles. IVC detects roll, pitch, and yaw states. The ODC determines the damping force to be applied to each method. The results show that the proposed algorithm can improve roll, yaw, and pitch vehicle movements [19]. Adaptive control is implemented for active suspension vehicles with nonlinearities (spring, and damper). Performance that describes the convergence, maximum overshoot, and steady-state error of the vertical and pitch motion control design. Vertical control performance and transient angle changes, and vehicle steady-state result in error changes [20].

The performance of the mass-spring-damper from transient to steady state is influenced by the spring force and mass transfer to return slowly when shocks occur. This is caused by inertia and vehicle body displacement systems and DOF motion [21]. A single-degree-of-freedom MSD has one mode of oscillation, the mass of which is connected by a single spring. But a single mass connected to two parallel springs causes oscillations back and forth at high frequencies. Meanwhile, the natural frequency experiences more oscillations per second, because a combination of springs arranged in parallel has greater stiffness than a single spring. Parallel springs experience the same displacement, but the resulting force is not the same. MSD system displacement with DOF in dynamic vehicles [22]. In dynamic vehicles, the system response must reach the initial point condition before the disturbance occurs [23], [24]. This study designed a mass-spring-dumper control system for vehicle suspension to dampen oscillations caused by disturbance. The system is designed with a proportional-integral-derivative (PID) control trade-off of 1-DOF and 2-DOF for tracking disturbance rejection. Tracking disturbance using PID tuning.

PID provides reliable control and stability in both linear and non-linear systems. Non-linear systems with proportional (Kp), integral (Ki), and derivative (Kd) constants have limitations in obtaining parameters that can adjust to changes in load [25]. A tuning control is proposed to control an unstable system with a design difference in increased closed-loop response [26].

The development of PID control is fast, but the control produces delays and disturbances that cannot be detected quickly [27]. PID tuning is used to regulate Kp, Ki, and Kd constants in achieving the values required by linear loads [28]. The linear PID system provides a tracking reference and reduces interference. Meanwhile, an unstable system can affect tracking reference and interference. PID also has a large overshoot and settling time [29]. Complex processes such as vehicle suspension require a PID tuning control to overcome the oscillatory response [30]. So, the PID controller control scheme, 1-2 DOF PID, and PID trade-off tuning for setpoint tracking and disturbance rejection are proposed. The control scheme is designed to reduce the oscillatory response of the mass-spring-damper under load and

JURNAL ECTIPE
Electronic, Control, Telecommunication, Information, and Power Engineering
Volume 10, Issue 1, April 2023, pp. 52-60
ISSN 2355-5068 ; e-ISSN 2622-4852
DOI: 10.33019/jurnalecotipe.v10i1.3723

without interference. System testing was carried out on Matlab software to validate the design and the resulting response.

2. RESEARCH METHOD

In this section, you should explain how the research was conducted, including research design, research procedure (in the form of algorithms, Pseudocode or other), how to acquire the data and how to perform any test. The description of the course of research should be supported by references, so the explanation can be accepted scientifically.

2.1. PID Controller

The research method uses proportional-integral-derivative (PID) control. PID control corrects the error value between input and output to achieve the response required by the load. If the input and output responses are not the same, then the controller will correct them with a feedback system [31]. The PID control feedback is tuned to disturbance rejection or fast response with good attenuation to change the input set point. Figure 1 describes the P(s), and C(s) process control and transfer functions respectively. On the system r (s) set point, u (s) control output, d (s) output signal, d (s) load disturbance, and y (s) controlled variable [32] described in formula (1).

$$u_{(s)} = P_{(s)}(r(s) - y(s)) \tag{1}$$

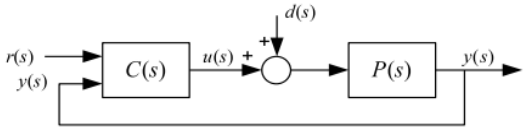

Figure 1. PID Controller [32]

2.2. Tuning 1-DOF dan 2-DOF PID

The 1-DOF and 2-DOF PID controls are used to set the value of the proportional constant (Kp), integral constant (Ki), and derivative constant (Kd) parameters based on variations in the input set point in a closed loop system [26]. Changes in the value of the set point parameter will be monitored (tracking) by reducing the resulting oscillation response (disturbance rejection). Then, the response results are fed back to the u control to find out the error value. The error value is obtained by calculating the difference between the reference input and the response output. The calculation of the error value is explained as follows [29]. 1-DOF control relates to input set point (r), disturbance (d), plant (Po), and output (y). Set point (r) and disturbance (d) have an impact on the error value (u). If (r) and (d) vary in the same way, then control (K) can be selected to reduce the small error value. Input (r) and disturbance (d) have different properties in the control system to provide tracking and disturbance rejection responses [33].

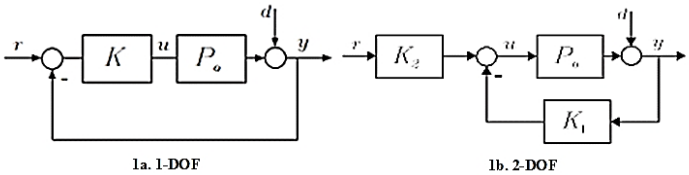

Figure 2. Degree of Freedom (DOF) [33]

The 2-DOF control is explained as input set point (r) on control (K2), error value (u), plant (Po), disturbance (d), output (y), and control feedback (K1). The 2-DOF compensator has a trade-off between feedback and reference tracking. The feedback control system is ensured with a degree of freedom, tracking reference indicated on the control pre-filter. Then the degree of freedom is determined by the open loop of the input reference [34]. The conventional control approach uses feedback to regulate the desired response. in a linear control system, the use of a reference model will determine the desired response from the controlled system [35].

$$u = K\begin{bmatrix} r \\ y \end{bmatrix} = K_2 r - K_1 y \tag{2}$$

JURNAL ECOTIPE
Electronic, Control, Telecommunication, Information, and Power Engineering
Volume 10, Issue 1, April 2023, pp. 52-60
ISSN 2355-5068 ; e-ISSN 2622-4852
DOI: 10.33019/jurnalecotipe.v10i1.3723

2.3. Tunning Trade-Offs PID

The PID tuning trade-offs are designed to achieve good tracking and fast disturbance rejection at the same time. Assuming a constant control bandwidth, disturbance rejection requires a lot of gains (amplifier) so that the slope of the crossover can be achieved. If the slope is greater, the response will overshoot at the set point. Equation (3) is described as a tuning control where r is the system input, y is the actual output, d is the disturbance, e is defined as the error value, and u is the error signal [36]. The trade-off PID tuning controller can reduce noise quickly without significantly increasing overshoot in set-point tracking. The PID controller trade-off is also useful to reduce the influence of changes in the reference signal on the control signal. Figure 2 shows the control architecture with a trade-off PID controller [37]. The relationship between the trade-off control output (u) and the two inputs (r and y) can be represented in parallel or standard form. The two forms differ in the parameters used to express proportional, integral, and derivative actions. The relationship between the trade-off PID control output (u) and the two inputs (r and y) can be represented by the following equation [38]. The MSD plant system with PID controller tuning control, 1-DOF and 2-DOF PID tuning, and PID trade-off tuning are described in Figure 3. The system was designed using PID tuning parameters and compared based on tracking and disturbance rejection and frequency to obtain the correct overshoot. small in set point tracking and can reduce changes in the reference signal.

$$u = K_p(br - y) + \frac{K_i}{s}(r - y) + \frac{K_d s}{T_f s + 1}(cr - y) \tag{3}$$

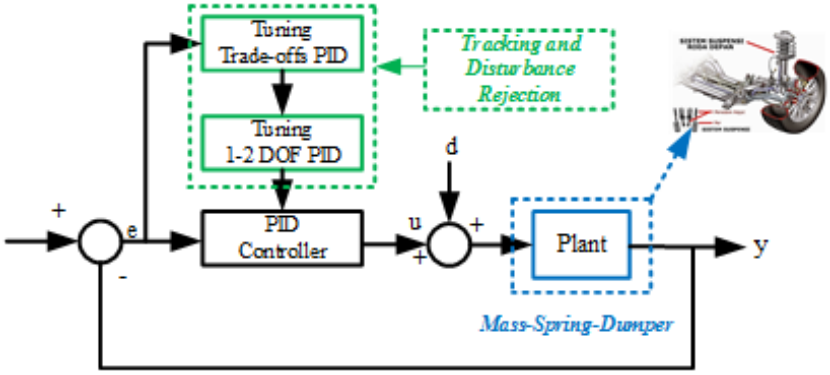

Figure 3. MSD Plant Control System

3. RESULTS AND DISCUSSION

Figure 4 a, b, and c are the MSD (mass-spring-dumper) output responses, where the MSD response on a stable road has a rise time of 2.55 seconds and a settling time of 4.48 seconds. The response to reach a stable 2.5 seconds requires a rise time and a long settling time. This is influenced by the mass-spring to return to its original point when a shock occurs. The output starts with zero to 2.5 seconds describing the state of the wheel and spring shock absorbers. The MSD is installed between the wheels and the vehicle body to reduce shaking and shock. The MSD system is applied to open-loop control. When an MSD disturbance occurs, the system does not provide feedback in the form of variables which will be processed according to the magnitude of the load and physical characteristics. The sudden resistance generated by the response will start to rise and slow down the vehicle according to the decrease in the response and inertia of the car.

JURNAL ECTIPE
Electronic, Control, Telecommunication, Information, and Power Engineering
Volume 10, Issue 1, April 2023, pp. 52-60
ISSN 2355-5068 ; e-ISSN 2622-4852
DOI: 10.33019/jurnalecotipe.v10i1.3723

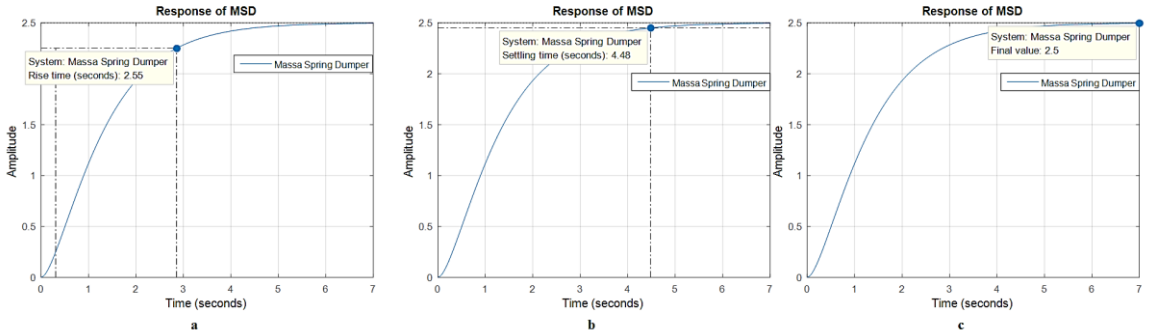

Figure 4. (a) Rise Time, (b) Setling Time, and (c) Steady State Respon Open Loop MSD

The control system uses feedback control in the comparison of tracking and disturbance rejection which is explained in Figures 5 a and b. The control system is designed to reduce interference that will occur and will return to the desired tracking setpoint. The tracking error at peak gain is 1.68 abs and the frequency is 8.12 rad/s. The maximum loop gain of 3.45 dB with a frequency of 6.25 rad/s. Meanwhile, the minimum loop gain occurs at a frequency of 0.00697 rad/s, and a single value of 63 dB. Open-loop tracking and gain are used to determine the frequency domain tracking between predetermined inputs and outputs. The purpose of the setting will determine the maximum error (error) value of the reference input to the tracking error value.

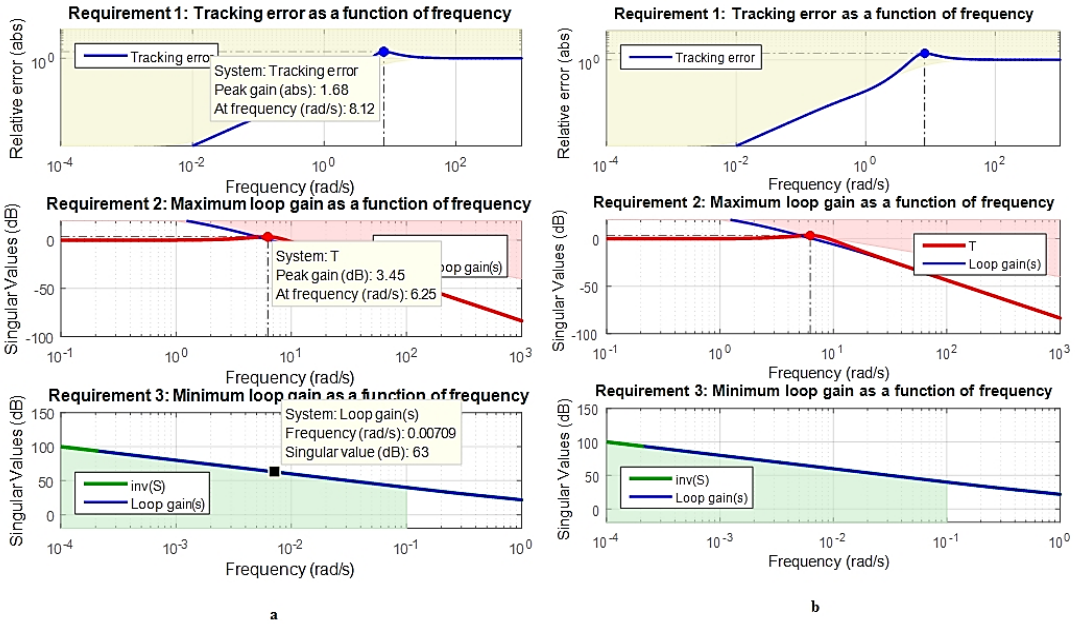

Figure 5. (a) Tracking and (b) Disturbance Rejection

Figure 6a and b show a comparison between the response of setpoint tracking using a PID controller, 1-2 DOF PID tuning, and PID trade-off tuning. The open loop response with a wide frequency is [0, 0, 1] rad/second by adding the value of α. The value of α is the frequency amplifier which is set from 1, 2, and 4 to increase disturbance rejection at a certain point. Setpoint Tracking (a) The PID controller has a settling time of 1.19 seconds, a 1-2 DOF PID tuning of 1.95 seconds, and a PID trade-off tuning of 2.23 seconds. Figure (b) describes the PID controller tracking setpoint overshoot, 1-2 DOF PID tuning, and PID trade-off tuning. The results of the overshoot setpoint tracking using the PID controller have an overshoot of 30.6%, and a peak amplitude of 1.31. Tuning 1-2 DOF PID has an overshoot of 43.3%, a peak amplitude of 1.43. While the PID trade-off tuning gets 51.7% overshoot and 1.52 peak amplitude. The PID controller's settling time response is faster due to the search for Kp, Ki, and Kd parameters that can adjust the load requirements when a disturbance occurs. However, the 1-2 DOF PID tuning and the PID trade-off tuning experienced a delay with the PID parameter search of

Volume 10, Issue 1, April 2023, pp. 52-60
ISSN 2355-5068 ; e-ISSN 2622-4852
DOI: 10.33019/jurnalecotipe.v10i1.3723

0.443 seconds, 0.533 seconds, and 0.479 seconds. In addition, the overshoot on the three controls affects the MSD to return to its initial state before the disturbance occurs. This indicates that the system is unstable to reach a steady state.

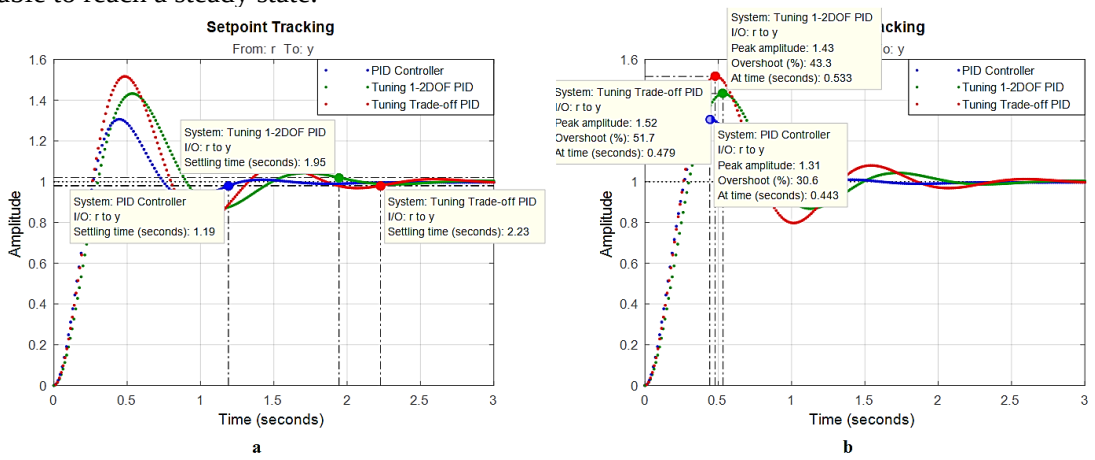

a b

Figure 6. (a) Settling Time and (b) Overshoot Set Point Tracking

Figure 7 (a) and (b) explain the comparison of the PID controller's disturbance rejection response, 1-DOF PID and 2-DOF PID tuning, as well as the PID trade-off tuning to increase shock absorption when the driver is at high speed and can return to the point start stably in case of trouble on the road. The open loop response is affected by changes in the mass-spring dumper load. Disturbance rejection Figure (a) PID controller has a setting time of 6.34 seconds, 1-2 DOF PID tuning with a setting time of 2.1 seconds, and a PID trade-off settling time tuning of 2.13 seconds. Figure (b) PID controller disturbance rejection has a peak amplitude of 0.087, an overshoot of 3.132%. Tuning 1-2 DOF PID has a peak amplitude of 0.201, overshoot of 1.022%, and tuning trade-off PID has a peak amplitude of 10.174, overshoot of 0.39%. This is caused by changes in load and search for the values of the tuning parameters Kp, Ki, and Kd to obtain parameters that match the load requirements.

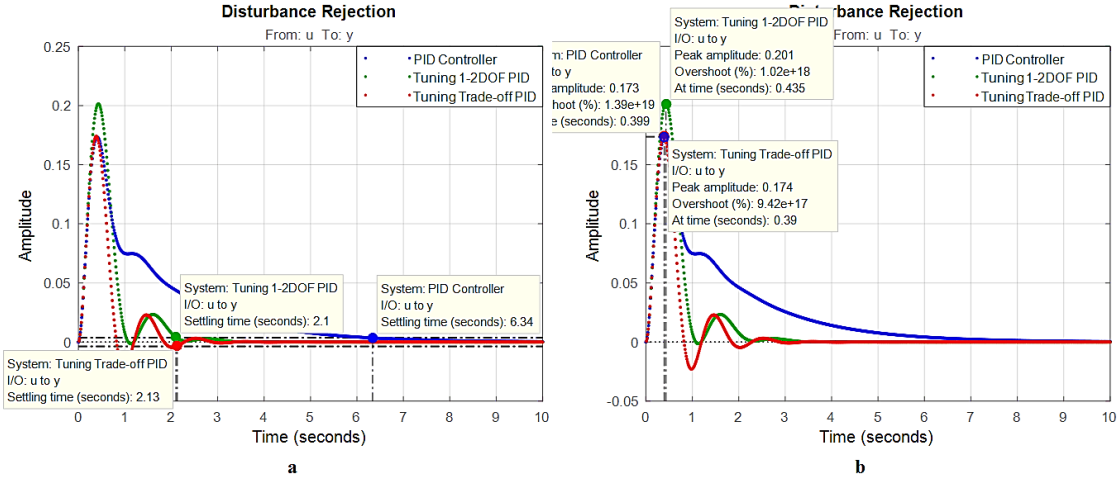

a b

Figure 7. (a) Settling Time Disturbance Rejection, (b) Overshoot Disturbance Rejection

Figure 8 (a) and (b) show a comparison of the PID controller setpoint tracking control, 1-2 DOF PID tuning, and PID trade-off tuning. The results of the comparison of the PID controller in figure (a) produce a settling time of 2.23 seconds, 0.524 seconds of 1-2DOF PID tuning, and 0.318 seconds of PID trade-off tuning. While figure (b) shows a comparison of the results of the three control setpoint tracking with a PID controller overshoot of 51.7% and a peak amplitude of 1.52, 1-2DOF PID overshoot tuning of 6.53%, and a peak amplitude of 1.07. Meanwhile, the PID trade-off tuning achieves an overshoot of 0.682% and a peak amplitude of 1.01. The time to reach a steady state condition at the tracking setpoint achieved by the PID trade-off tuning control is faster than the other controls. This

JURNAL ECOTIPE
Electronic, Control, Telecommunication, Information, and Power Engineering
Volume 10, Issue 1, April 2023, pp. 52-60
ISSN 2355-5068 ; e-ISSN 2622-4852
DOI: 10.33019/jurnalecotipe.v10i1.3723

proves that the proposed control can reduce disturbance rejection to adjust to changes in mass-spring-dumper load.

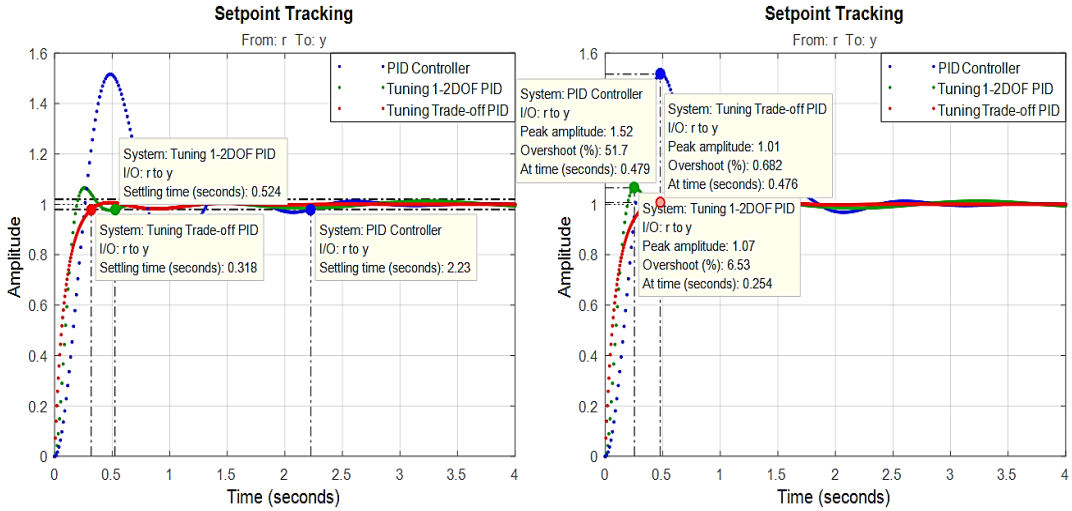

Figure 8. Set Point Tracking 1-DOF, 2-DOF, and Proposed Method

3.1. PID Value Comparison Table

The comparison of PID controller tuning parameters is described in Table 1. The comparison of PID control parameters, 1-2DOF PID tuning, and PID trade-off tuning with each proportional gain control, (K_p) integral gain (K_i), and derivative gain (K_d) can affect the peak amplitude, settling time, and overshoot response in the event of a disturbance. The calculation of the parameters PID controller, 1-2 DOF PID, and tuning trade-off PID is obtained from the equation below. The PID controller parameter is Kp + Ki * s + Kd * Tf*s+1 with Kp = 5.67, Ki = 12.2, Kd = 7.21, Tf = 72.1, The 1-2-DOF PID tuning parameter is u = Kp (b*r-y) + Ki*s (r-y) + Kd*Tf*s+1(c*r-y) with Kp = 0.0615, Ki = 20.2, Kd = 1.85, Tf = 0.106, and the trade-off PID tuning is u = Kp (b*r-y) + Ki*s (r-y) + Kd*Tf*s+1 (c*r-y) with Kp = 9.18, Ki = 45.5, Kd = 0.969, Tf = 2.14e-05.

Table 1. The Comparison of PID Controller Tuning Parameters

PID	The Controller PID Tuning		
	PID Controller	**1-DOF dan 2-DOF PID**	**Trade-off PID**
Kp	5.67	0.0615	9.18
Ki	12.2	20.2	45.5
Kd	7.21	1.85	0.969

4. CONCLUSION

MSD (mass-spring-dumper) suspension is used in car or motorcycle vehicle systems. Models of vehicle suspension in the form of mass, coil (spring), and shock absorber (dumper). MSD provides a shock effect when the vehicle is running which is caused by frictional forces on the load. The response must quickly return to a stable point when shocks occur. The MSD equation is obtained by Laplace transform, then validated in Matlab Simulink. Three PID controllers, 1-2 DOF PID tuning, and PID trade-off tuning are proposed to obtain the set point tracking and disturbance rejection. The simulation results show that the PID trade-off tuning control can reduce disturbance rejection to a smaller extent with a set point tracking peak amplitude of 1.01, an overshoot of 0.682%, and a setting time of 0.318 seconds. While the PID controller has a set point tracking and disturbance rejection each larger with a peak amplitude of 1.52, overshoot of 51.7%, settling time of 2.23 seconds, and tuning of 1-2 DOF PID has a peak amplitude of 1.07, overshoot of 6.53%, settling time of 0.524 seconds.

Volume 10, Issue 1, April 2023, pp. 52-60
ISSN 2355-5068 ; e-ISSN 2622-4852
DOI: 10.33019/jurnalecotipe.v10i1.3723

REFERENCES

[1] S. M. Savaresi, C. Poussot-Vassal, C. Spelta, O. Sename, and L. Dugard, *Semi-Active Suspension Control Design for Vehicles*, 1st Ed. Oxford: Elsevier Ltd, 2010.

[2] H. Arrosida and A. Sudaryanto, "Perancangan Metode Kontrol Linear Quadratic Integral Tracking (LQIT) untuk Pengendalian Posisi Sistem Suspensi Sederhana (Mass-Spring-Damper)," *J. Nas. Tek. Elektro*, vol. 6, no. 2, p. 111, 2017.

[3] C. Canudas-de-Wit, F. R. Rubio, and M. A. Corchero, "D-OSKIL: A new mechanism for controlling stick-slip oscillations in oil well drillstrings," *IEEE Trans. Control Syst. Technol.*, vol. 16, no. 6, pp. 1177–1191, 2008.

[4] B. Amstrong, "A Survey of Models, Analysis Tools and Compensation Methods for the Control of Machines with Friction," *Automatica*, vol. 56, no. 2, pp. 158–159, 1994.

[5] D. Wang, D. Zhao, M. Gong, and B. Yang, "Research on Robust Model Predictive Control for Electro-Hydraulic Servo Active Suspension Systems," *IEEE Access*, vol. 6, pp. 3231–3240, 2017.

[6] X. Ma, P. K. Wong, J. Zhao, J. H. Zhong, H. Ying, and X. Xu, "Design and Testing of a Nonlinear Model Predictive Controller for Ride Height Control of Automotive Semi-Active Air Suspension Systems," *IEEE Access*, vol. 6, pp. 63777–63793, 2018.

[7] Y. Qin, F. Zhao, Z. Wang, L. Gu, and M. Dong, "Comprehensive analysis for influence of controllable damper time delay on semi-active suspension control strategies," *J. Vib. Acoust. Trans. ASME*, vol. 139, no. 3, 2017.

[8] Y. Qin, C. Xiang, Z. Wang, and M. Dong, "Road excitation classification for semi-active suspension system based on system response," *JVC/Journal Vib. Control*, vol. 24, no. 13, pp. 2732–2748, 2018.

[9] A. R. Bhise, R. G. Desai, M. R. N. Yerrawar, A. C. Mitra, and D. R. R. Arakerimath, "Comparison Between Passive And Semi-Active Suspension System Using Matlab/Simulink," *IOSR J. Mech. Civ. Eng.*, vol. 13, no. 04, pp. 01–06, 2016.

[10] A. F. Mohd Riduan, N. Tamaldin, A. Sudrajat, and F. Ahmad, "Review on active suspension system," *SHS Web Conf.*, vol. 49, p. 02008, 2018.

[11] Y. Zhang, Y. Liu, and L. Liu, "Adaptive Finite-Time NN Control for 3-DOF Active Suspension Systems With Displacement Constraints," *IEEE Access*, vol. 7, pp. 13577–13588, 2019.

[12] N. Aisyiyah, "Pemodelan Sistem Suspensi Kendaraan Dengan Menggunakan Software Solidwork," Institut Teknologi Sepuluh November, 2016.

[13] W. Sun, H. Gao, and B. Yao, "Adaptive robust vibration control of full-car active suspensions with electrohydraulic actuators," *IEEE Trans. Control Syst. Technol.*, vol. 21, no. 6, pp. 2417–2422, 2013.

[14] T. P. J. Van Der Sande, B. L. J. Gysen, I. J. M. Besselink, J. J. H. Paulides, E. A. Lomonova, and H. Nijmeijer, "Robust control of an electromagnetic active suspension system: Simulations and measurements," *Mechatronics*, vol. 23, no. 2, pp. 204–212, 2013.

[15] M. Yu, C. Arana, S. A. Evangelou, D. Dini, and G. D. Cleaver, "Parallel Active Link Suspension: A Quarter-Car Experimental Study," *IEEE/ASME Trans. Mechatronics*, vol. 23, no. 5, pp. 2066–2077, 2018.

[16] C. M. Ho, D. T. Tran, C. H. Nguyen, and K. K. Ahn, "Adaptive Neural Command Filtered Control for Pneumatic Active Suspension with Prescribed Performance and Input Saturation," *IEEE Access*, vol. 9, pp. 56855–56868, 2021.

[17] J. Zhao, P. K. Wong, Z. Xie, C. Wei, and F. He, "Integrated variable speed-fuzzy PWM control for ride height adjustment of active air suspension systems," *Proc. Am. Control Conf.*, vol. 2015-July, pp. 5700–5705, 2015.

[18] C. M. Ho and K. K. Ahn, "Design of an Adaptive Fuzzy Observer-Based Fault Tolerant Controller

Volume 10, Issue 1, April 2023, pp. 52-60
ISSN 2355-5068 ; e-ISSN 2622-4852
DOI: 10.33019/jurnalecotipe.v10i1.3723

for Pneumatic Active Suspension with Displacement Constraint," *IEEE Access*, vol. 9, pp. 136346–136359, 2021.

[19] W. Cho, J. Suh, and S. H. You, "Integrated Motion Control Using a Semi-Active Damper System to Improve Yaw-Roll-Pitch Motion of a Vehicle," *IEEE Access*, vol. 9, pp. 52464–52473, 2021.

[20] J. Na *et al.*, "Active Adaptive Estimation and Control for Vehicle Suspensions With Prescribed Performance," vol. 26, no. 6, pp. 1–15, 2017.

[21] B. Hirzinger, C. Adam, and P. Salcher, "Dynamic response of a non-classically damped beam with general boundary conditions subjected to a moving mass-spring-damper system," *Int. J. Mech. Sci.*, vol. 185, no. June, 2020.

[22] P. Salcher and C. Adam, "Modeling of dynamic train–bridge interaction in high-speed railways," *Acta Mech.*, vol. 226, no. 8, pp. 2473–2495, 2015.

[23] N. Zhang, H. Xia, W. W. Guo, and G. De Roeck, "A Vehiclebridge Linear Interaction Model and Its Validation," *Int. J. Struct. Stab. Dyn.*, vol. 10, no. 2, pp. 335–361, 2010.

[24] M. Barreau, S. Tarbouriech, and F. Gouaisbaut, "Lyapunov Stability Analysis of a Mass–Spring System Subject to Friction," *Syst. Control Lett.*, vol. 150, p. 104910, 2021.

[25] V. Rajinikanth and K. Latha, "Setpoint weighted PID controller tuning for unstable system using heuristic algorithm," *Arch. Control Sci.*, vol. 22, no. 4, pp. 481–505, 2012.

[26] H. Taguchi and M. Araki, "Two-Degree-of-Freedom PID Controllers — Their Functions and Optimal Tuning," *IFAC Proc. Vol.*, vol. 33, no. 4, pp. 91–96, 2000.

[27] N. Hidayah, J. Juwari, and R. Handogo, "Maximum Peak-Gain Margin 2DOF-IMC Tuning for a 2DOF-PID Filter Set Point Controller Under Parametric Uncertainty," *IPTEK J. Proc. Ser.*, vol. 0, no. 1, pp. 8–16, 2014.

[28] A. Mulyadi, "Desain Sistem Kendali Kecepatan Motor Induksi Pada Cane-Carier Based on Cohen-Coon Method," *J. Zetroem*, vol. 02, no. 01, pp. 16–20, 2020.

[29] M. A. Johnson and M. H. Moradi, *PID Control: New Identification and Design Methods*. 2005.

[30] F. Naz *et al.*, "PID Tuning with reference tracking and plant uncertainty along with disturbance rejection," *Syst. Sci. Control Eng.*, vol. 9, no. 1, pp. 160–166, 2021.

[31] A. Mulyadi, Wijono, and B. Siswojo, "Kecepatan Motor Penggerak Quadcopter," *J. Transm.*, vol. 22, no. 4, pp. 107–116, 2020.

[32] V. M. Alfaro and R. Vilanova, "Optimal robust tuning for 1DoF PI/PID control unifying FOPDT/SOPDT models," *IFAC Proc. Vol.*, vol. 2, no. PART 1, pp. 572–577, 2012.

[33] S. Alcantara, C. Pedret, and R. Vilanov, "A Model Reference Based 2-DOF Robust Observer-Controller Design Methodology," *New Approaches Autom. Robot.*, no. May, 2008.

[34] D. C. Youla and J. J. Bongiorno, "A Feedback Theory of Two-Degree-of-Freedom Optimal Wiener-Hopf Design," *IEEE Trans. Automat. Contr.*, vol. 30, no. 7, pp. 652–665, 1985.

[35] V. M. Alfaro and R. Vilanova, "Simple robust tuning of 2DoF PID controllers from a performance/robustness trade-off analysis," *Asian J. Control*, vol. 15, no. 6, pp. 1700–1713, 2013.

[36] M. Clever, "PID Setpoint Tracking and Disturbance Rejection," *Matwork*, 2012. [Online]. Available: https://www.mathworks.com/help/control/ug/pid-tuning-for-setpoint-tracking-vs-disturbance-rejection.html.

[37] R. Kurokawa, N. Inoue, T. Sato, O. Arrieta, R. Vilanova, and Y. Konishi, "Simple optimal PID tuning method based on assigned robust stability - Trade-off design based on servo/regulation performance," *Int. J. Innov. Comput. Inf. Control*, vol. 13, no. 6, pp. 1953–1963, 2017.

[38] B. Astrom, K.J. & Wittenmark, *Computer-Controlled Systems - Theory and Design*. Prentice-Hall, 1967.

JURNAL ECOTIPE
Electronic, Control, Telecommunication, Information, and Power Engineering

Volume 10, Issue 1, April 2023, pp. 61-68
ISSN 2355-5068 ; e-ISSN 2622-4852
DOI: 10.33019/jurnalecotipe.v10i1.3807

Smart Room Design As A Concrete Step Towards A Sustainable Smart Campus At The Institut Teknologi Sumatera

Sabhan Kanata[1], Sabar[2], Amrina Mustaqim[3], Gde KM Atmajaya[4], M. Rizky Hikmatullah[5], Muhammad Asrofi[6], Asmar[7]

[1,4,6]Electrical Engineering, Institute of Teknologi Sumatera, Lampung Selatan, 35365, Indonesia
[2]Instrumentation and Automation Engineering, Institute of Teknologi Sumatera, Lampung Selatan, 35365, Indonesia
[3]Physics Engineering, Institute of Teknologi Sumatera, Lampung Selatan, 35365, Indonesia
[5]Telecommunications Engineering, Institute of Teknologi Sumatera, Lampung Selatan, 35365, Indonesia
[7]Electrical Engineering, Bangka Belitung University, Bangka Belitung, 33172, Indonesia

ARTICLE INFO

Article historys:

Received : 27/01/2023
Revised : 19/02/2023
Accepted : 19/04/2023

Keywords:

Energy, Internet of Things, Smart-campus, SMARTERA

ABSTRACT

Institut Teknologi Sumatera (ITERA) is one of the new PTN campuses in Indonesia. As a campus that carries the smart-campus motto, ITERA will continue to create smart services, including saving electrical energy. One of the programs to support a sustainable campus is innovation in electrical energy management so that electrical energy efficiency can be maximized. The ITERA smart-room product called SMARTERA is one of the campus's tangible manifestations to control electrical equipment using Internet-based intelligent control of Things (IoT). The initial stage in this research is automatic control of the two most widely used electrical equipment in the campus environment, namely lights and air conditioning (AC).

Corresponding Author:

Sabhan Kanata
Electrical Engineering, Institut Teknologi Sumatera, Lampung Selatan, 35363, Indonesia
Email: sabhan.kanata@el.itera.ac.id

1. INTRODUCTION

The rapid development of digital technology has greatly helped people to get limitless services. This also happens in universities as a become of science and technology. Smart campus programs must be pushed forward so that the campus can become a pioneer in a smart technology-based environment. Currently, awareness of the utilization of energy-saving technology has not been widely applied in managing energy usage in campus environments in Indonesia [1]. Automation processes to manage frequently used electrical equipment are often considered unimportant. If this unawareness is left to continue, then the campus as a green energy pioneer can only be a symbol.

Digital technologies have been an immense boon to the educational realm, with multiple applications designed to enhance the teaching and learning experience from preschool to university levels [2]. The latest advancements in intelligent control and communication systems have brought about a situation where heterogeneous devices can form an integrated network. The integration of short-range cellular transceivers into everyday objects has enabled new forms of communication between objects and between people and objects. A concept where an object can send data over a network without the assistance of a computer device or a human is called the Internet of Things (IoT) [3].

Universities provide great opportunities to apply various smart solutions as they are considered to have a complex ecosystem. Universities have an openness to do experiments as they have multidisciplinary expertise, scientific knowledge, and innovative developments. Moreover, Universities are considered small-scale cities for the usage of smart technologies such as smart transportation, smart

Volume 10, Issue 1, April 2023, pp. 61-68
ISSN 2355-5068 ; e-ISSN 2622-4852
DOI: 10.33019/jurnalecotipe.v10i1.3807

buildings, smart parking, and so on [4].

The application of a smart home or smart room can increase the efficiency of electricity usage due to the increased use of electricity networks and the pattern of users or humans in the use of this electricity network. The implementation of the smart home concept may involve using technologies such as the Internet of Things (IoT) platform, computing, control, visual presentation, and communication [5].

The Institute of Technology of Sumatera (ITERA) is a new university with a mission to empower the potential in the Sumatera region and Indonesia as well as the world through excellence in education, research, and community service in the field of science, technology, art, and humanities. Programs to support the campus slogan of a smart, friendly, and forrest campus need to be continuously supported to prepare human resources that are ready to compete nationally and internationally.

Smart Room is a real manifestation of ITERA Institute of Technology's initiative as Smart Green Campus. This is aimed at creating sustainable development in the ITERA campus environment. The utilization of technology and knowledge built is the automatic control of existing electrical equipment in a room within the campus environment based on IoT. This implementation is expected to help electricity saving on the campus.

2. RESEARCH METHOD

In this study, we used applied research where applied research is done with the aim of implementing, testing, and evaluating the ability of a theory to be applied in solving practical problems [5]. This research method has several stages, which are designing SMARTERA System Architecture, creating schematic diagrams, creating flowcharts, implementing the SMARTERA monitoring and automation prototype, and testing the system.

2.1. The ITERA Smart Room Architecture System

The ITERA Smart Room Architecture (SMARTERA) is a concept in automatic control of the two utilities as shown in Figure 1. The working principle of the SMARTERA layout is that the Relay and NodeMCU ESP8266 module will be supplied with voltage from the AC/DC power supply so that all equipment can work and function. PIR sensor can detect motion, especially coming from the man while in range (range) sensor, PIR sensor only responds to energy and passive IR rays possessed by each object detected by it [6]. PIR sensors work by capturing heat energy produced from passive infrared rays that are possessed by each object with an object temperature above 0 degrees celsius [7]. The PIR sensor will send information about the presence or absence of human movement then read by the NodeMCU ESP82766 and then send data to the server in TCP / IP format so that it can be displayed on the smartphone [8].

Likewise, the DHT11/22 sensor will send the temperature/humidity condition to the NodeMCU ESP8266 microcontroller. The DHT11 module works on serial communication and is single-wire communication. This module sends data in form of a pulse train of the specific period. Before sending data to Arduino, it needs some initialization command with a time delay. And the whole process time is about 4 ms [9]. Subsequently, the microcontroller will read both conditions and then send the data to the server in TCP/IP format so that it can be displayed on the smartphone.

Then, the microcontroller will read the commands sent to the server using TCP/IP format and then change to form a "high" and "low" logic, when the sensor is at a HIGH (1) level, digital data is sent from the DHT22 to the MCU, allowing it to process the data for display. Conversely, when the sensor is not active at a LOW (0) level, the digital data transmission is stopped and the MCU will not process it. The voltage connected to the 3.3V pin is linked to the VDD pin, whilst the GND pin is connected to the NodeMCU ESP8266 V3's GND pin. Then, the relay will be commanded to be on when it is of "high" logic and vice versa [10].

JURNAL ECOTIPE
Electronic, Control, Telecommunication, Information, and Power Engineering
Volume 10, Issue 1, April 2023, pp. 61-68
ISSN 2355-5068 ; e-ISSN 2622-4852
DOI: 10.33019/jurnalecotipe.v10i1.3807

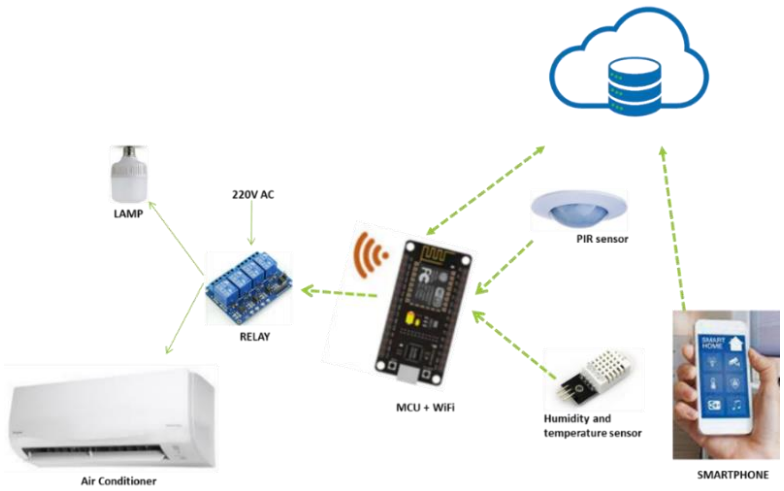

Figure 1. SMARTERA System Architecture

2.2. Schematic Diagram

The circuit design in Figure 2 illustrates the connectivity of the device to process and generate the desired output simultaneously. The researchers maximized the small space for the chosen microcontroller. With the compact circuit design, the device won't take up much space, making it easy to move. The circuit connection involves the Data OUT Pin of the PIR Sensor and DHT11 connected to the microcontroller with the ESP8266 pins. The LED has connected pins indicating the current status of the light as either ON or OFF. Each IN pin of the relay switch is connected to the pins marked D on the MCU. The Relay NO pin is connected to the electric equipment control cable while the COM pin is connected to the AC supply line. This design allows the components to work together following the desired functionality of the system as a whole. The final design itself can work in any kind of lighting set in any building. Furthermore, the researchers also designed a PCB as a realization form of the SMARTERA prototype to be installed in the ITERA General Lecture Building. The design of ITERA's PCB product is shown in Figure 2 below.

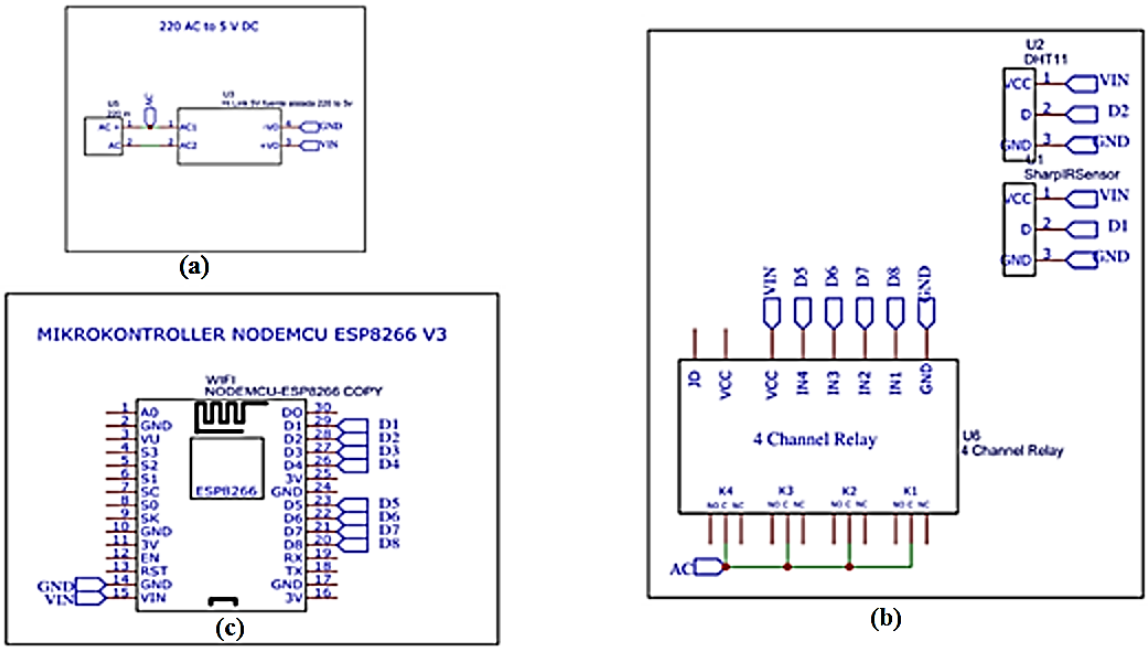

Figure 2. SMARTERA Schematic Diagram; (a) AC to DC Converter, (b) 4 Channel Relay, (c) NodeMCU ESP8266

JURNAL ECTIPE
Electronic, Control, Telecommunication, Information, and Power Engineering
Volume 10, Issue 1, April 2023, pp. 61-68
ISSN 2355-5068 ; e-ISSN 2622-4852
DOI: 10.33019/jurnalecotipe.v10i1.3807

Figure 2. (a) shows an AC to DC (Alternating Current to Direct Current) Converter which is an electronic device used to convert alternating current (AC) into direct current (DC) in the circuit. Then Figure 2. (b) shows 4 channels in which an electronic device is used to control a larger electrical load by using a small electrical signal. It has four channels or channels, each of which can control a separate electrical load. The last part figure 2. (c) explains NodeMCU ESP 8266 which is a microcontroller development board based on the ESP8266 chip. The ESP8266 is a system on a chip (SoC) integrated with a WiFi module that enables the use of wireless networks in electronics projects such as the smartera prototype.

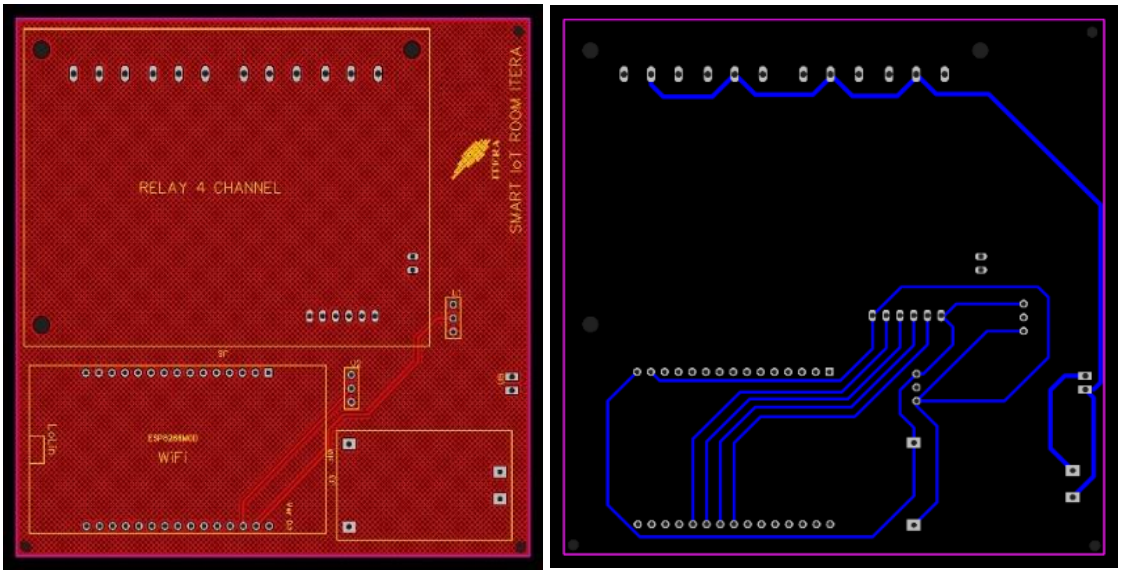

(a) (b)

Figure 3. SMARTERA PCB Design: (a) Top view (red) (b) Bottom view (black)

Figure 3. (a) provides information about smartera PCB design from the top View and Figure 3. (b) explains PCB design from the bottom view.

2.3. Flowchart Design

The stages of this system are detailed in the flowchart diagram as shown in Figure 4 below. Figure 4 provides information about the logic of the system can be seen in the flowchart Figure 4. The system work starts when the equipment is turned on and then immediately initializes the air conditioner and lamp. In the next step, the system will control the temperature, and humidity and detect the presence of humans in the room. Furthermore, it works for the measurement target in the room. If there is a measurement error, the system will be calibrated to avoid larger errors.

The procedures carried out in this study were carried out in several stages, as follows: (1) Simulation of design outcomes. This step is to ensure the wiring process, sensors, and connections to the IoT are in line with the desired output, (2) Laboratory scale testing phase. At this stage, researchers will conduct experiments on the laboratory scale prototype to ensure the hardware device runs according to the simulation results, (3) Limited space testing phase. The prototype that has been tested in the laboratory will be tested in the field (small scale) to observe the response in a limited environment, (4) the multi-room scale testing phase. The prototype that has been tested in the laboratory will be tested in the field (multi-room scale) to observe the response in a wider environment.

JURNAL ECTIPE
Electronic, Control, Telecommunication, Information, and Power Engineering
Volume 10, Issue 1, April 2023, pp. 61-68
ISSN 2355-5068 ; e-ISSN 2622-4852
DOI: 10.33019/jurnalecotipe.v10i1.3807

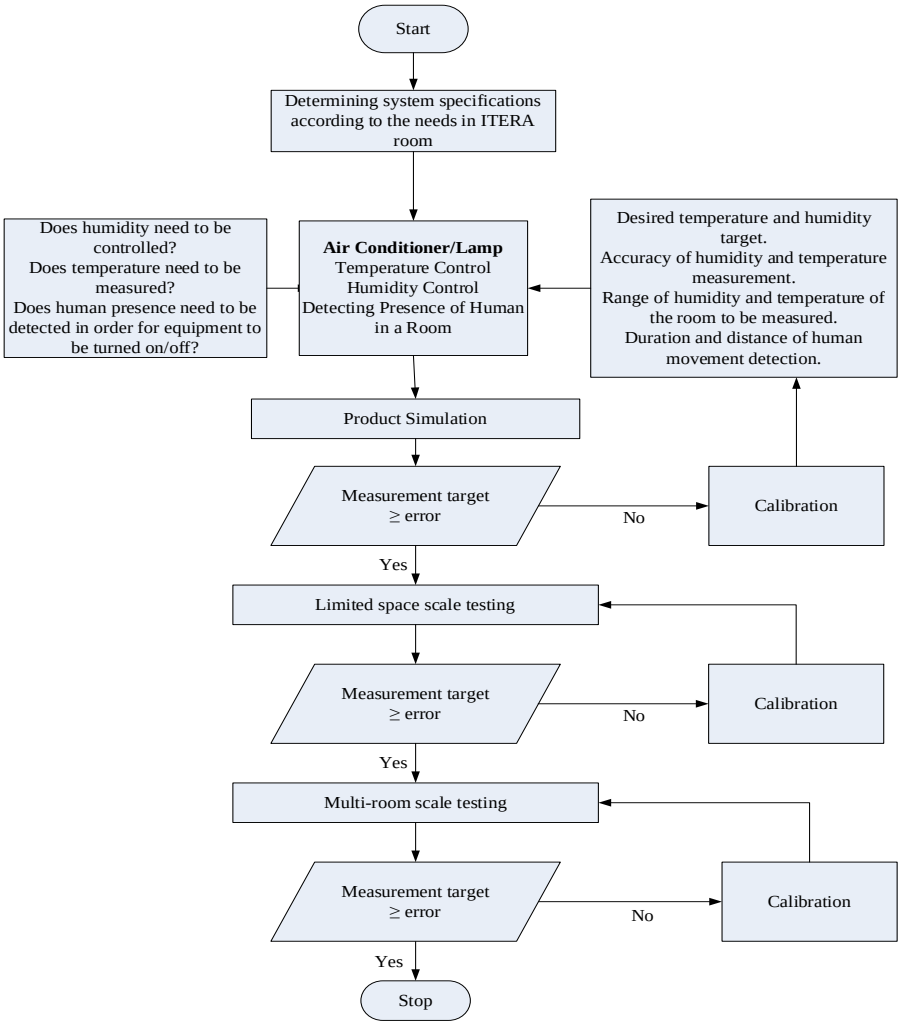

Figure 4. SMARTERA Flowchart Diagram

3. RESULTS AND DISCUSSION

3.1. Prototype Realization

The SMARTERA product of ITERA Smart Room is a tangible manifestation of campus for controlling electrical equipment using intelligent control-based Internet of Things (IoT) control. The initial stage of this research is automatic control of two most commonly used electrical appliances in the campus environment, namely lamps and air conditioning (AC). The researcher will conduct 3 test stages, namely laboratory scale, limited room scale, and multi-room scale. In the process of testing the three test stages, the researcher will validate the accuracy of the input parameters, process, and output.

The results of the product in the research produced the design of the SMARTERA Chasing Smart Room ITERA which will later be installed in the room to be tested. The picture of the product SMARTERA is shown in Figure 5 below.

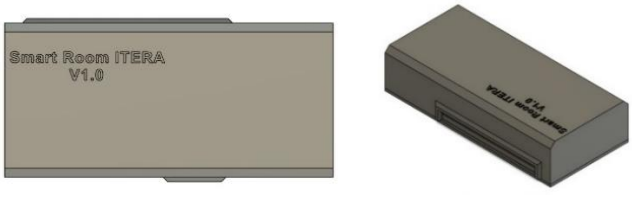

(a) (b)

Figure 5. SMARTERA Casing of Products (a) Top view; (b) Bottom view

JURNAL ECTIPE
Electronic, Control, Telecommunication, Information, and Power Engineering
Volume 10, Issue 1, April 2023, pp. 61-68
ISSN 2355-5068 ; e-ISSN 2622-4852
DOI: 10.33019/jurnalecotipe.v10i1.3807

Figure 5 shows the design of easing Smart Room ITERA will be used as cover and protect the system. Figure 5 (a) is the view from the top and figure 5 (b) is the view from the bottom.

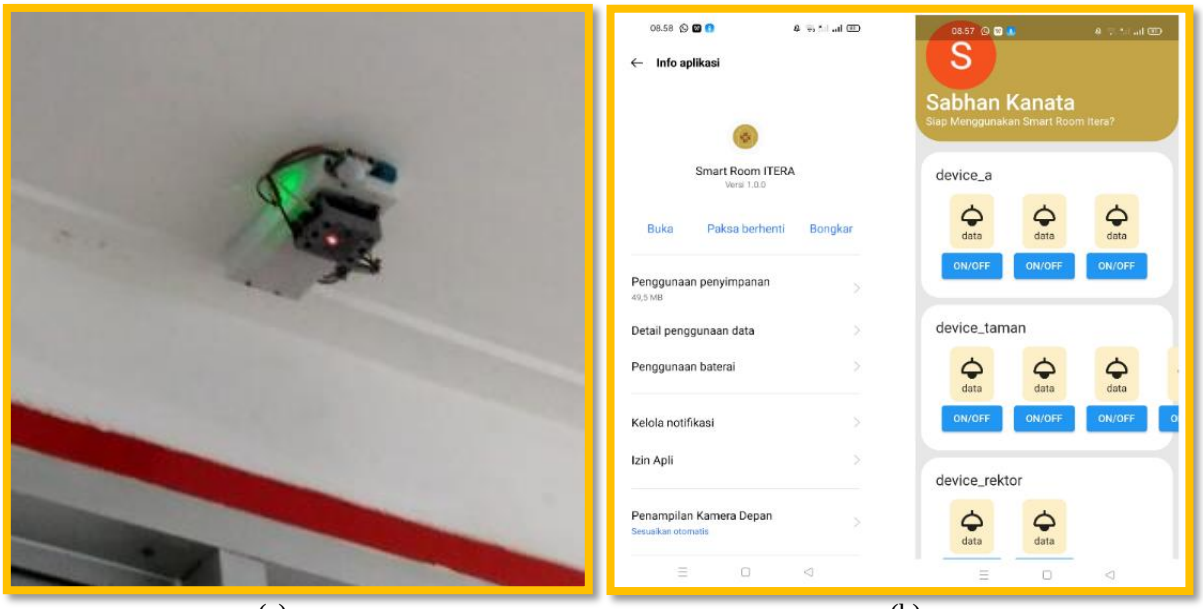

(a) (b)

Figure 6. (a) Implementation of SMARTERA in the ITERA lecture room (b) Display of the SMARTERA Application from a smartphone

Figure 6 (a) provides information on the prototype which had been applied in the ITERA lecture room. The system has the function to control and regulate the usage of lights and AC automatically based on IoT in the room that will be tested. Figure 6 (b) describes the interface display via smartphone such as picture 6 (b). Then the function of SMARTERA provides information that the lecture room could be controlled and monitored with this SMARTERA application System. So, users can easily control the temperature and monitor the room from a remote location with the aim of efficiency of electrical energy.

3.2. System Testing

First, we test the system on the power supply device which serves as the resource provider for SMARTERA devices. Therefore, an electrical power supply is necessary to convert the current. Testing the power supply circuit serves to convert 220V AC voltage to DC voltage. The SMARTERA prototype is fitted with an IC specifically designed as a voltage regulator to deliver a stable 12-volt output voltage. The circuit is tested using a multimeter. The scale used to measure voltage is attained by connecting the VCC circuit with the positive cable. The test results are indicated in Table 1 below.

Table 1. Supply Testing

IC	Input PLN	Output (Vdc)
SMARTERA	220 Volt	11,54 volt

Next, sensor testing is carried out to find out the output voltage of the PIR sensor when it is in logic 1 and 0. This testing is also required to find out the output voltage value of the passive infrared (PIR) sensor when it detects human movement and when it does not detect human movement. The way to carry out this testing is for the sensor should get an input voltage of 5 Vdc. Then measure the input and output voltage of the sensor using a voltmeter. From Table 2, the PIR sensor testing was obtained.

Table 2. PIR Sensor Testing

No	Sensor	V_{in}	V_{out}	Logic
1	Motion detected	5,00	3,31	1
2	No Motion detected	5,00	0	0

JURNAL ECTIPE
Electronic, Control, Telecommunication, Information, and Power Engineering
Volume 10, Issue 1, April 2023, pp. 61-68
ISSN 2355-5068 ; e-ISSN 2622-4852
DOI: 10.33019/jurnalecotipe.v10i1.3807

The same was done to the DHT11/22 sensors to check their condition. To check the level of error, a comparison was done between the temperature readings and the room's standard thermomet [11,12]. The results of the experiment, done 5 times, are shown in table 3 below.

Table 3. Temperature Sensor Testing

No	Sensor DHT11 (^{0}C)	Thermometer (^{0}C)	Error (^{0}C)
1	23,5	24,5	1
2	24,8	25,5	0,7
3	25,3	26,3	1
4	25,7	26,5	0,8
5	25,9	26,6	0,7

The system testing includes verifying the PIR, temperature, and microcontroller along with its electronic devices running properly. The main purpose of this system testing is to ensure the components mounted on the device can run and function properly as well as the dashboard display. This sensor testing also aims to determine the good or bad settings of the infrared sensor sensitivity. This sensor is located above the room door and so on. The mechanism of system testing is illustrated in figure 8 below.

Figure 8. Testing the SMARTERA device system

After making sure that all components are in good condition, the overall system testing is conducted. We turn on the electrical switch of the room, then electricity provides voltage to the microcontroller and runs the program on the SMARTERA device that will be executed. The program runs the PIR and Temperature sensors to detect movement and room temperature. Microcontroller program to run the PIR sensor to detect the motion of objects passing by. As for the PIR sensor in the classroom, it has functions to turn on the lights. The relay will be active if the PIR sensor is given the motion when the lights will turn on simultaneously as an active SMARTERA system. When there is no movement in the classroom, the lights will be off. When an object enters the classroom, the sensor detects the movement of the object, and the SMARTERA device will re-initialize the program. The next step SMARTERA runs the program to turn on the lights. Furthermore, temperature of the sensors reaches the set points of the system setting, while the AC will turn on according to the program that has been set in the SMARTERA device.

4. CONCLUSION

This research has the purpose to create and test a control and monitoring system for room temperature, light as well as the presence of humans based on the Internet of Things using the NodeMCU ESP8266 microcontroller and the SMARTERA application. The core of the system made is based on detecting the room temperature threshold with a DHT11 sensor and identifying light and dark conditions and the system after that detects the presence of a human in a room. Then from these two conditions, the Node MCU as a processor will instruct the relay to turn on or turn off the AC and the light according to the conditions required. Furthermore, all parameters will be sent and displayed on the SMARTERA application in real time. This prototype system has worked well and can be further developed to include more controllable parameters for smart room and automation industry.

Volume 10, Issue 1, April 2023, pp. 61-68
ISSN 2355-5068 ; e-ISSN 2622-4852
DOI: 10.33019/jurnalecotipe.v10i1.3807

Acknowledgments

Thank you to the Research and Community Service Institute (LPPM) ITERA for funding this SMARTERA research.

REFERENCES

[1] G. M. S. B. Pracasitaram, L. and R. S. Hartati, "Konsep Dan Penerapan Green Computing di Lingkungan Kampus," *Majalah Ilmiah Teknologi Elektro,* vol. 18, no. 3, pp. 299-302, 2019.

[2] N. Min-Allah and S. Alrashed, "Smart campus—A sketch," *Sustainable Cities and Society 59 (2020),* vol. 59, 2020.

[3] G. Sfikas, C. Akasiadis and E. Spyrou, "Creating a Smart Room using an IoT approach," in *Proceedings of the Workshop on AI and IoT (AI-IoT), 9th Hellenic Conference on Artificial Intelligence*, Thessaloniki, 2016.

[4] E. Gilman, S. Tamminen, R. Yasmin, E. Ristimella, E. Peltonen, M. Harju, L. Lauri, J. Riekki and S. Pirttikangas, "Internet of Things for Smart Spaces: A University Campus Case Study," *Sensors,* vol. 20, no. 13, 2020.

[5] R. Y. Endra, A. Cucus and F. N. Affandi, "The Concept and Implementation of Smart Room using Internet of things (IoT) for Cost Efficiency and Room Security," *Journal of Physics: Conference Series,* vol. 1381, no. 1, 2019.

[6] J. Nasir, "Web-Based Scheduling Application and Motion Sensor Using Arduino Mega," *JISA (Jurnal Informatika dan Sains),* vol. 04, no. 01, pp. 28-32, 2021.

[7] E. Darmawan and R. Taufan, "Space Security System using Motion Sensor and Notification of Short Message Service with Arduino-Based Fuzzy Logic Algorithm," *Journal of Physics: Conference Series,* vol. 1179, no. 1, 2019.

[8] M. R. Hidayat, C. and B. S. Sapudin, "Perancangan Sistem Keamanan Rumah Berbasis IoT Dengan NodeMCU ESP8266 Menggunakan Sensor PIR HC-SR501 Dan Sensor Smoke Detector," *KILAT,* vol. 7, no. 2, pp. 139-148, 2018.

[9] F. Z. E. Mashonjowa and E. Matandirotya, "DHT11 Based Temperature and Humidity Measuring System," *Journal of Electrical Engineering and Electronic Technology,* vol. 11, no. 5, 2022.

[10] F. Hendajani, A. Mughni, I. P. Wardhani and A. Hakim, "Modeling Automatic Room Temperature and Humidity Monitoring System with Fan Control on the Internet of Things," *ComTech: Computer, Mathematics and Engineering Applications,* vol. 13, no. 2, pp. 75-85, 2022.

[11] F. Puspasari, T. P. Satya, U. Y. Oktiawati, I. Fahrurozi and H. Prisyanti, "Analisis Akurasi Sistem Sensor DHT22 berbasis Arduino terhadap Thermohygrometer Standar," *JURNAL FISIKA DAN APLIKASINYA,* vol. 16, no. 1, pp. 42-45, 2020.

[12] Azhari, D. Simanjuntak, L. Hakim, and Sabar, "Design and control system of temperature and water level in hydroponic plants," *J. Phys. Conf. Ser.*, vol. 2193, no. 1, 2022, doi: 10.1088/1742-6596/2193/1/012018.

JURNAL ECOTIPE
Electronic, Control, Telecommunication, Information, and Power Engineering

Volume 10, Issue 1, April 2023, pp. 69-77
ISSN 2355-5068 ; e-ISSN 2622-4852
DOI: 10.33019/jurnalecotipe.v10i1.3852

Rain Process Education as Interactive Multimedia in Early Childhood using the Multimedia Development Life Cycle (MDLC)

Yohani Setiya Rafika Nur[1], Dasril Aldo[2], Annisaa Utami[3]
[1,2,3] Department of Informatics Engineering, Faculty of Informatics, Institut Teknologi Telkom Purwokerto,
Jl. DI Panjaitan No.128, Jawa Tengah 53147, Indonesia

ARTICLE INFO

Article historys:

Received : 09/02/2023
Revised : 19/02/2023
Accepted : 19/04/2023

Keywords:

Early Childhood; Multimedia; Learning Media; MDLC; Rain; Teachers

ABSTRACT

Learning media has a positive impact because it can be fun, increase students' interest in learning, and be interactive. The learning method in Early Childhood Education (PAUD) Ratnanigsih uses a Sentra approach and the environment by playing sambal learning to develop the intelligence of a potential child. The facts in PAUD Ratnaningsih found obstacles in the teaching and learning process. These obstacles occur due to the lack of visualization or media for teachers, and the absence of variations in learning can cause saturation in children. Users in this study are early childhood teachers in PAUD Ratnaningsih. Based on these problems, a learning press is needed for teacher and child relations educated at PAUD Ratnaningsih. The learning media design method in this study uses the Multimedia Development Life Cycle (MDLC) approach and learning media using Macromedia Flash 8. The results of this study are in the form of storyboard design, visualization of interface design, implementation of learning media, and testing with *Blackbox Testing*. Based on the conclusions of this study shows that all components and features of learning media function properly and can be used by teachers in the learning process "Universe" with the sub-theme "Rain".

Corresponding Author:

Yohani Setiya Rafika Nur
Teknik Informatika, Fakultas Informatika, Institut Teknologi Telkom Purwokerto,
Jl. DI Panjaitan No.128, Jawa Tengah 53147, Indonesia
Email: yohani@ittelkom-pwt.ac.id

1. INTRODUCTION

Education is one of the essential things for the future of individuals or society. The general explanation of education has been contained in Law No. 20 of 2003 Section 1, and it is explained that education is a conscious and planned effort to create a learning atmosphere and learning process so that students actively develop their potential, have spiritual, mental strength, self-control, personality, wisdom, noble character, and skills [1]. According to Munirah in Rahmi [2], there are several components in national education, such as the environment, facilities and infrastructure, resources, and the community, so they support each other to achieve an education. The development of technology can make it easier for us to do everything and do daily activities. As a result, technology can facilitate information delivery to anyone without time restrictions [3]. Technology can also play a role in helping students succeed in understanding learning topics from teachers [4].

Each educational institution, almost all of them use technology to support the process of implementing learning. One such technology is interactive-based multimedia. Interactive multimedia is used to assist students in accepting the knowledge delivered by the teacher [5]. If interactive-based technology is not used in a learning medium, it will be difficult for teachers and parents to provide an

JURNAL ECOTIPE
Electronic, Control, Telecommunication, Information, and Power Engineering
Volume 10, Issue 1, April 2023, pp. 69-77
ISSN 2355-5068 ; e-ISSN 2622-4852
DOI: 10.33019/jurnalecotipe.v10i1.3852

excellent lessons to students [5]. Learning media is a significant factor in learning because learning media is related to the student's learning experience. One of the objectives of implementing learning using interactive multimedia is to replace and complement the objectives, materials, methods, and assessment tools that exist in the teaching and learning process as much as possible. The importance of learning media is to provide convenience in achieving a learning goal and increase students' interest in learning. The application of learning with multimedia will be more interesting, and this is under the statement of Ida Bagus Ketut Trinawindu et al. in the research of Wahyu Tisno Atmojo et al. [6] that the essence of using multimedia today must be more dynamic Because of the existence of multimedia, this is not only reading in the form of text but can be by using voice or audio, music, video, and images [6].

Many studies related to learning media have been carried out. Research conducted by Andrian Syahputra et al. related to learning media in introductory physics courses obtained results that the material was entirely feasible and the suitability and depth of the material with a percentage value of 82.85% that the learning media in the study could function, and use it in the learning process well [7]. The research conducted by Hidayatu Munawaroh et al. on interactive learning media on the theme of the universe for early childhood 4 to 6 years, results in the study found that interactive media is effective in the learning process in the classroom. An evaluation was carried out on the early childhood with an E-Test PR score with an average of 2.07 to 2.73 in the post-test with an achievement result of 80% so that it experienced a significant increase [8]. Early Childhood Education (PAUD) Ratnaningsih is one of the places of educational institutions or early childhood education facilities before the elementary school (SD) education level is implemented. PAUD Ratnaningsih is located in the Bantul area, DI Yogyakarta province. PAUD Ratnaningsih has created students who excel and have a noble characters. The learning method carried out at PAUD Ratnaningsih is currently the Center & Circle Approach, which is a method of playing while learning at a child-centered center to develop all the potential of children's intelligence (multi-intelligence).

One of the themes in the curriculum at PAUD Ratnaningsih is "The Universe" with the sub-theme "Rain." Based on the results of an interview with PAUD Ratnaningsih, the primary approach method, and the "Universe" curriculum circle experienced obstacles in the teaching and learning process. These obstacles are caused by the lack of visualization or media for teachers, and the absence of variations in learning can be possible to encounter saturation in children. Not only learning materials but learning media can also add games. The game indicates structured and semi-structured activities with the aim of entertainment and can sometimes be used as a means of education to evaluate the understanding of learning [9]. The game's fun, motivating, and collaborative character makes this activity popular with many people. Based on these problems, the purpose of this study is to create a learning media in the process of rain based on Macromedia Flash 8. Furthermore, with this learning media making it easier for students to learn the process of forming rain, it is hoped that it can increase students' interest in learning and facilitate the delivery of material.

2. RESEARCH METHOD

2.1. Development Method

In this section, this research used the *Multimedia Development Life Cycle* (MDLC) method. The MDLC method is a method for interactive multimedia development with six stages. The six stages are concept, design, material collecting, assembly, testing, and distribution [10]. The flow of the research stages of the method can be seen in Figure 1.

JURNAL ECOTIPE
Electronic, Control, Telecommunication, Information, and Power Engineering
Volume 10, Issue 1, April 2023, pp. 69-77
ISSN 2355-5068 ; e-ISSN 2622-4852
DOI: 10.33019/jurnalecotipe.v10i1.3852

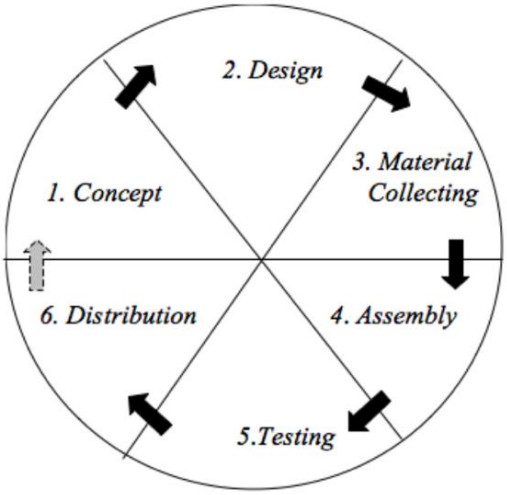

Figure 1. MDLC Method Stage Flow

As shown in Figure 1 f is an explanation of the steps of the Multimedia Development Life Cycle (MDLC) development method concept:

1. Concept
   The first stage is to conceptualize by determining the initial goal, end output, and end users who will use the learning media for the process of this rain. Concept design is the overall determination stage of designing the concept of an interactive multimedia program to be built to have a clear goal.
2. Design
   The second stage is to do a detailed sketch per the theme of delivering the material. The design stage in this study begins with the design of the menu structure architecture, learning content pages (main or homepage display, learning materials, evaluation games), storyboards, and interface design so that it can be continued to the implementation stage.
3. Material Collecting
   The third stage is the stage of collecting necessities. The materials used in this study use materials that are appropriate (relevant) to the learning media to be made. These materials include images, animations, audio, learning materials, and other materials.
4. Assembly
   The fourth stage in the study divided the two sub-components. First, the storyboard and interface design that have been designed are implemented into multimedia materials using Macromedia flash professional 8 software. Second, the creation of material along with the audio dubbing that has been available.
5. Testing
   The fifth stage of this study was completed after all the components in the fourth stage were completed. Based on these results, testing was carried out to test the feasibility of this learning media from the user side using the Blackbox testing concept.
6. Distribution
   At the distribution stage in this study, the first step is to socialize with teachers at PAUD Ratnaningsih to ensure that the learning media that has been done is appropriate and there are no errors.

2.2. Designing The Concept of Learning Media Components

The concept of learning media in this study consists of several components of the flow of use from beginning to end. The details of the pipeline can be seen in Figure 2.

JURNAL ECOTIPE
Electronic, Control, Telecommunication, Information, and Power Engineering
Volume 10, Issue 1, April 2023, pp. 69-77
ISSN 2355-5068 ; e-ISSN 2622-4852
DOI: 10.33019/jurnalecotipe.v10i1.3852

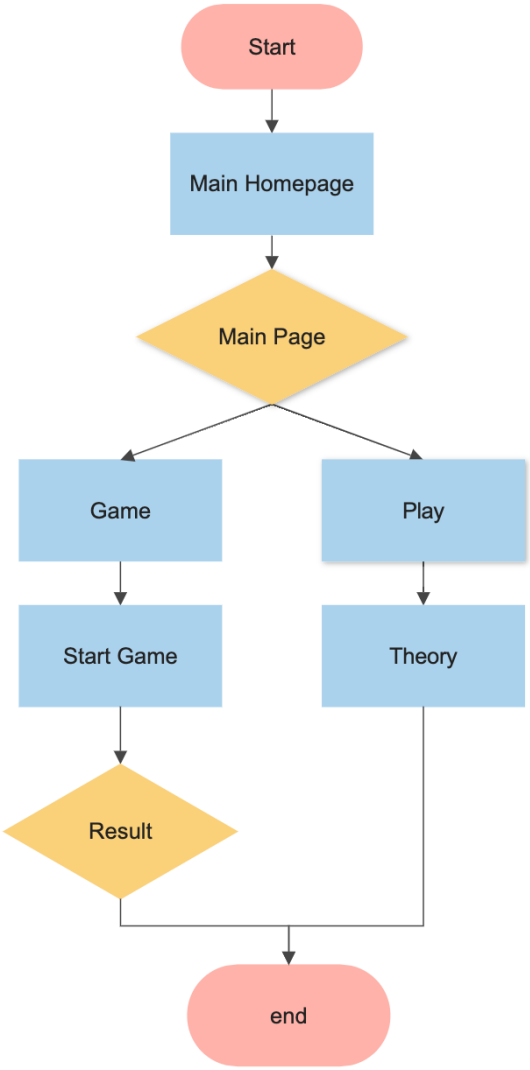

Figure 2. Learning Media Flow

Figure 2 describes the components or features available in the learning media in this study. The segment consists of the main homepage. The main homepage serves as the main page that will appear for the first time when users use this learning media, and the main homepage also has a game menu button and a play menu button for learning materials.

3. RESULTS AND DISCUSSION

3.1. Concept Results

The creation of this media takes the concept from the background of the problem, namely "How to Make Learning Media the Process of Rain," to facilitate the teaching and learning process. At this stage generates several formulations of concepts in the study, as follows:

1. The purpose of learning media in the rain process is to provide information and educate early childhood about rain formation.
2. Users of this learning media are teachers and early childhood students at PAUD Ratnaningsih.
3. The description of this learning media provides information related to the process of this rain that can be operated on a computer device. Learning media consists of material that is presented visually, animated, and audio, as well as games that can be done to attract early childhood interest.

3.2. Design Results

This design stage resulted in the design of the menu structure, storyboard, and interface design of each menu in the learning media in this study. These designations include:

JURNAL ECTIPE
Electronic, Control, Telecommunication, Information, and Power Engineering
Volume 10, Issue 1, April 2023, pp. 69-77
ISSN 2355-5068 ; e-ISSN 2622-4852
DOI: 10.33019/jurnalecotipe.v10i1.3852

1. Menu Structure Design

The design of the menu aims to create a chart. It is a significant part of demonstrating the capabilities and facilities for the user. The design of the menu structure can be seen in Figure 3.

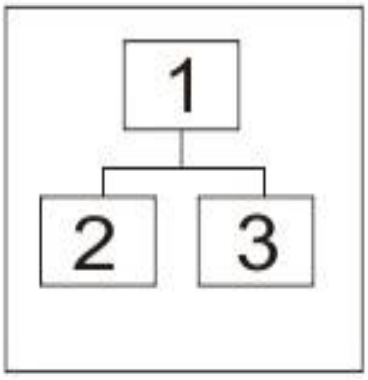

Figure 3. Menu Structure

Based on Figure 3 above, there are 3 main components, namely:

1.) Main View (Home)
Generally, a learning application or other applications presents an overview of the application on the main page. This is useful for leading users to understand the multimedia application's purpose. In this draft, the main page will contain the application's navigation buttons and main menus. Later there will be a Material menu and a Game menu. Each menu on the main page will have a different submenu for each stage.

2.) Learning Materials Menu
This menu was created based on an analysis conducted at PAUD Ratnaningsih. In this menu, learning materials are placed with explanations using voice (audio). In the material menu, a submenu will direct the user to the student's learning page. After that, a game menu on the front page will require users to use the game as an evaluation.

3.) Menu Game
As explained above, a game menu (evaluation) of students is intended to evaluate the user's ability to master the material that has been given.

2. Storyboard and Interface Design

The design of the storyboard, in this case, is to create a script. Storyboards are used to depict storylines according to the story's content, accompanied by explanations of the storyline in each frame of the learning media so that the application program created becomes user-friendly. The storyboard in this study consists of frames 1 to 3, which can be seen in Figure 4, Figure 5, and Figure 6 below:

1.) Visual Frame 1
Frame 1 is a design for the main page in the learning media by containing the appearance of the menus contained in this learning media. The visualization in frame 1 can be seen in Figure 4.

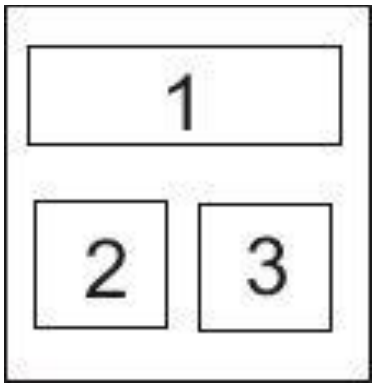

Figure 4. Visual Frame 1

JURNAL ECOTIPE
Electronic, Control, Telecommunication, Information, and Power Engineering
Volume 10, Issue 1, April 2023, pp. 69-77
ISSN 2355-5068 ; e-ISSN 2622-4852
DOI: 10.33019/jurnalecotipe.v10i1.3852

Based on figure 4 above, it is the design of The main page consists of a background image, title (number 1), game menu (number 2), and material menu (number 3).

2.) Visual Frame 2

In frame 2 is the design of the material page. The visualization in frame 2 can be seen in Figure 5.

Figure 5. Visual Frame 2

Based on Figure 5 above, the Frame is an animated design (number 1) for the material presentation page. The user will be directed to the material explaining how the rain process will be studied.

3.) Visual Frame 3

Visual Frame 3 is a game page containing a simple puzzle game that is useful as a user's evaluation after seeing the material that has been presented. The visualization in frame 3 can be seen in Figure 6.

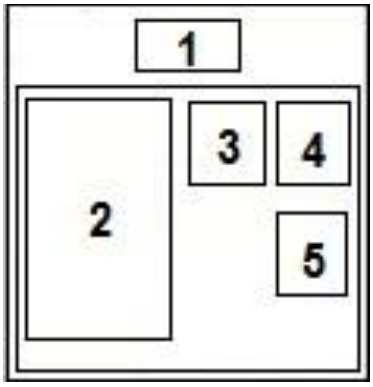

Figure 6. Visual Frame 3

Based on Figure 6 above, it is the design of the main page of this learning media, the animation design (number 1) for the material presentation page. This page consists of the title (number 1), puzzle board (number 2), puzzle box (number 3), game processing time (number 4), and score (number 5).

3.3. Material Results

This study collected materials by conducting interviews with teachers at PAUD Ratnaningsih and collecting material from several sources that support the pattern of providing suitable material for early childhood. Related to the materials for making interactive multimedia collected are images for backgrounds, buttons, and other components online, as well as voice (audio) dubbing for material presentation. Creation of learning media using Macromedia flash professional 8 and Corel Draw X5 software to create and process learning media.

3.4. Assembly Results

At this stage, the implementation of making learning media using Macromedia flash software professional 8, then creating designs using Corel Draw X5 Software. The final results of the performance of making learning media in this study are based on the design design at the design stage, as follows:

1. Main Page View

JURNAL ECOTIPE
Electronic, Control, Telecommunication, Information, and Power Engineering
Volume 10, Issue 1, April 2023, pp. 69-77
ISSN 2355-5068 ; e-ISSN 2622-4852
DOI: 10.33019/jurnalecotipe.v10i1.3852

This main page view is displayed first when the learning media is run. The main menu display has menus that can be selected. The main menu has a game menu and a material menu. Here's a look at the main menu that can be seen in Figure 7.

Figure 7. Main Page View

Based on Figure 7 above, there are two buttons. The "Game" button, if a click action is performed, will lead to a simple game page in the form of compiling puzzles. However, acting on the "Play" button will redirect to the learning materials page. The choice of full color is a consideration in the background setting to attract children's attention using this learning medium.

2. Material Page View

The material page display contains an animation of the delivery of material from the rain process and is accompanied by sound (audio) in the presentation. The function of the audio is so that early childhood can understand easily. The following view of the material page is seen in Figure 8.

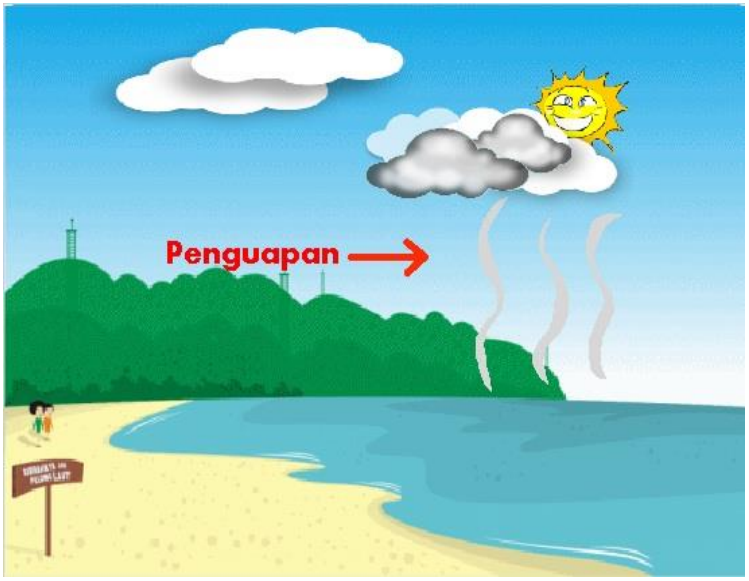

Figure 8. Material Page View

Based on Figure 8 above is a page of material presentation. The process of delivering material by creating an animation that can move to explain better the details of the operation of the rain and each of these processes is also accompanied by a sound (audio) that can be heard directly by the user.

Volume 10, Issue 1, April 2023, pp. 69-77
ISSN 2355-5068 ; e-ISSN 2622-4852
DOI: 10.33019/jurnalecotipe.v10i1.3852

3. Game Page View

Game page view is an animated display of puzzel games in this learning medium. The following display of the game page can be seen in Figure 9. The following view of the game page can be seen in Figure 9.

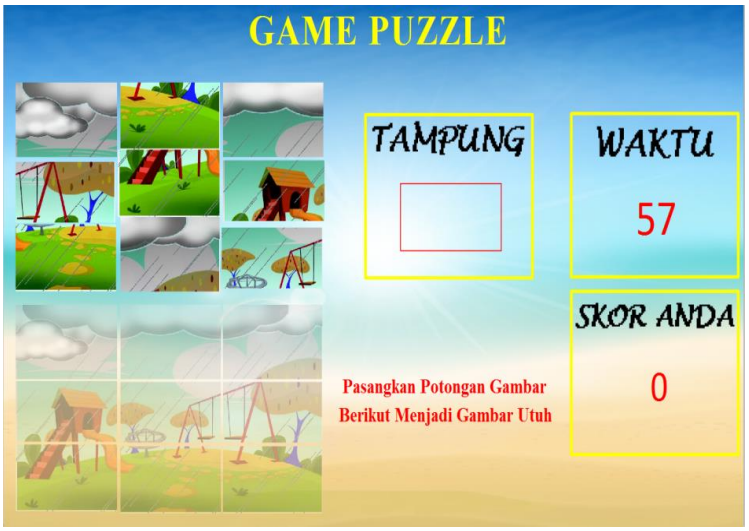

Figure 9. Game Page View

Based on Figure 9 above is the puzzel game page. The game page display is an evaluation page for users, in this puzzle-shaped game students are invited to pair puzzle pieces into a complete picture. Puzzel games serve as a medium for evaluating the achievement of material understanding from students.

3.5. Testing Results

The testing stage is carried out after the completion of the assembly stage process. The test is performed using a beta test. The beta test method will test the learning media of the user series (in this test, the user is a teacher) before the learning media can be used for early childhood students in PAUD Ratnaningsih. Blackbox test tests focus on the functionalities and components in this learning media and whether they can function correctly. Testing consists of several activities. The activity consists of testing audio or sound, animations, and buttons in the media. Details of the Blackbox test results in this study can be seen in Table 1.

Table 1. *Blackbox* Test Results

No	Component	Testing Activities	Test Results
1	Sound/Audio	Sound testing when delivering material	Ok
		Sound testing on buttons when clicked	Ok
2	Animation	Testing on loading	Ok
		Animation testing on material discussion	Ok
3	Knob	Test on the game button when clicked	Ok
		Test on the play button of the material when clicked	Ok

3.6. Distribution Result

The results at the distribution stage of this study, learning media have been socialized to teachers at PAUD Ratnaningsih for their use, and it has been confirmed in the test results that the learning media that has been made is appropriate and there are no errors.

4. CONCLUSION

Based on the results of research on interactive learning media for early childhood at PAUD Ratnaningsih, in understanding the process of rain, it was concluded that the media learning using

JURNAL ECOTIPE
Electronic, Control, Telecommunication, Information, and Power Engineering
Volume 10, Issue 1, April 2023, pp. 69-77
ISSN 2355-5068 ; e-ISSN 2622-4852
DOI: 10.33019/jurnalecotipe.v10i1.3852

the Multimedia Development Life Cycle method could function properly. It can also be viewed based on the test results using a Blackbox, getting the results of all feature components such as sound or audio of material delivery and on the button when clicked, animations in the delivery of material, as well as game buttons and buttons, can run properly. With this learning medium, children at an early age can help to understand the occurrence process in the "Universe" subtheme of an event. Rain by adding audio to make it easier for early childhood to understand the material.

REFERENCES

[1] P. R. Indonesia, "Law of the Republic of Indonesia Number 20 of 2003 concerning the National Education System," 2003

[2] M. S. M. R. Rahmi, M. A. Budiman, and A. Widyaningrum, "Development of Macromedia Flash 8 Interactive Learning Media on Thematic Learning My Experience Theme," International Journal of Elementary Education, vol. 3, no. 2, pp. 178–185, 2019.

[3] G. A. Purnomo, F. Maulana, F. S. N. Amanah, A. R. Ardi, and D. Aldo, "Interactive Multimedia Media-Based Drug Recognition and Countermeasures Information System," Journal of Information Systems and Management, vol. 10, no. 1, pp. 78–85, 2022.

[4] P. A. O. Gde, Media and Multimedia Learning, 1st ed. Pascal Books, 2022.

[5] E. Z. Arnada and R. W. Putra, "Implementation of Interactive Multimedia in Paud Nurul Hikmah as a Learning Media," IDEALIS Journal, vol. 1, no. 5, pp. 393–400, 2018.

[6] W. T. Atmojo, F. Fitri Nurwidya, and E. Dazki, "Learning Media for Introducing Indonesian Cultural Diversity with the Multimedia Development Life Cycle Method," 2019.

[7] A. Shaputra, S. Suparno, M. Giatman, and R. Maulida, "Designing Interactive Learning Media Based on Problem Based Learning Learning Models for Basic Physics Courses," Journal of Informatics Media Budidarma, VOL. 4, NO. 1, P. 245, Jan. 2020, doi: 10.30865/mib.v4i1.1974.

[8] H. Munawaroh, A. Y. E. Widiyani, and R. Muntaqo, "Development of Interactive Multimedia Themes of the Universe in Children Aged 4-6 Years,"Journal of Obsession: Journal of Early Childhood Education, vol. 5, no. 2, pp. 1164–1172, Oct. 2020, doi: 10.31004/obsession.v5i2.619.

[9] F. Yulianto, Y. T. Utami, and I. Ahmad, "Educational Game for the Introduction of Vitamin C Fruits for Early Childhood," 2018.

[10] M. Mustika, E. P. A. Sugara, and M. Pratiwi, "Development of Interactive Learning Media using the Multimedia Development Life Cycle Method," Journal of Online Informatics, vol. 2, no. 2, p. 121, Jan. 2018, doi: 10.15575/join.v2i2.139.

JURNAL ECOTIPE
Electronic, Control, Telecommunication, Information, and Power Engineering

Volume 10, Issue 1, April 2023, pp. 78-85
ISSN 2355-5068 ; e-ISSN 2622-4852
DOI: 10.33019/jurnalecotipe.v10i1.3855

Analysis of the Utilization of Tofu Liquid Waste as a Biogas Electricity Power Plant

(Case Study of BK Tofu Industry at Payakumbuh City West Sumatra)

Galuh Putra Rajabya[1], Novi Gusnita[2]
[1,2]Sultan Syarif Kasim State Islamic University Riau, HR. Soebrantas Street, Pekanbaru, Riau, Indonesia

ARTICLE INFO

Article historys:

Received : 10/02/2023
Revised : 28/03/2023
Accepted : 19/04/2023

Keywords:

Biogas, Liquid Tofu Waste, PLTBG, Superpro Designer

ABSTRACT

The increase in population from year to year causes an increase in the need for food such as Tofu. This also has an impact on the number of tofu industries in Indonesia. Nevertheless, it arises that the environmental problems posed by the tofu industry are waste generated from the liquid tofu waste manufacturing process. When discharged into the environment, it can cause a foul odour and pollute the environment. The utilization of tofu liquid waste into electrical resources is one of the steps that can be developed in reducing pollution and increasing electrification. This study aims to determine the potential value of tofu liquid waste and electrical energy for PLTBG fuel as an effort to apply clean technology. The method in this study using anaerobic fermentation with SuperPro Designer simulation. The results of this study, from 500 litres per day of tofu liquid waste can produce methane gas (CH4) of 141,97 m^3 per day and total electrical energy of 129,03 kWh. It can be concluded from this study. tofu liquid waste can be used as biogas to fuel a generator set with an output power of 12.000 Watts which fulfills industrial electricity needs for 11,73 hours.

Corresponding Author:

Galuh Putra Rajabya
Sultan Syarif Kasim State Islamic University, Riau, HR. Soebrantas Street, Pekanbaru, Riau, Indonesia
Email: galuhrajabya@gmail.com

1. INTRODUCTION

The increase in population has an impact on food needs, such as primary needs in the form of tofu. Tofu is a traditional food made from soybeans. The development of tofu consumption from 2002 to 2018 fluctuated with an average value of 7.41. Tofu consumption is estimated at 8.38, 8.52, and 8.67 in 2019, 2020, and 2021, respectively [1]. This has caused an increase in the tofu industry. The increase in the tofu industry has an impact on the accumulation of waste has increased [2].

The tofu industry in its formulation produces two wastes, namely liquid waste and solid waste. Liquid waste comes from the process of washing, boiling, and molding while solid liquid waste in the form of dregs arises from the way of filtering soybean porridge [3]. Tofu liquid waste with a high organic matter composition, if discharged directly into the water, can harm the environment around the industry. The amount of tofu industry in Indonesia is quite large, with around 84,000 small and medium-scale tofu industries, and usually family-owned with a total yearly production of more than 2.56 million tons [2]. Payakumbuh city, West Sumatra has 7 tofu industries. BK Tofu Industry is one of them. It is located on the riverbank of Batang Agam. After making observations with the owner, in one day it can produce tofu liquid waste around 500 liters and 2000 kg of tofu solid waste. Solid waste in the BK tofu industry is sold as livestock feed while liquid tofu waste in the BK tofu industry has no further process. So the industry needs a waste processing that aims to reduce the negative impact of tofu liquid waste [4].

JURNAL ECOTIPE
Electronic, Control, Telecommunication, Information, and Power Engineering
Volume 10, Issue 1, April 2023, pp. 78-85
ISSN 2355-5068 ; e-ISSN 2622-4852
DOI: 10.33019/jurnalecotipe.v10i1.3855

Based on observations and interviews with Mr. Yusril as the owner, his tofu industry has not been able to process tofu waste and waste disposal is not following existing regulations, causing pollution. This pollution will negatively affect the health of the people around the industry. This issue involves many groups that use tofu liquid waste to be processed into various useful products, thereby reducing the risk of pollution [2]. Biogas fuel is one product that can reduce the risk of pollution. The use of tofu liquid waste to produce biogas can be made using the anaerobic fermentation method. The fermentation method is a process of processing organic ingredients through fermentation without the use of oxygen. The main components of biogas are carbon dioxide and methane gas. This methane gas will be used as fuel for a generator set that converts it into electricity [4].

Related research on biogas from tofu liquid waste has been done several times, these studies include examining the potential of tofu liquid waste in clean technology endeavors [5]. This study [6] The study examined the results of one-stage and two-stage anaerobic treatment of organic matter shrinkage as seen from the Chemical Oxygen Demand (COD) parameter, bacterial development monitored from the Volatile Suspended Solid (VSS) parameter, Volatile Fatty Acid (VFA) production, and biogas production. This study [7] has a topic of calculating the potential biogas that can be produced, the duration of fermentation, and the construction of the reactor.

Based on these studies, all studies only focus on the processing and production of biogas from tofu liquid waste. Therefore, this study calculates the potential of electrical energy from tofu liquid waste biogas and electrical energy for the manufacture of wind power plant fuel by anaerobic fermentation method. Utilization of tofu liquid waste can increase the efficiency of waste that is not used anymore. Tofu liquid waste which is the raw material produced by the BK Tofu Industry then used to form biogas, then converted into electrical energy. This study uses an anaerobic fermentation method with the help of Superpro Designer Software to produce biogas. This study takes advantage of the anaerobic fermentation process combined with Superpro Designer software to produce biogas. The potential benefits of biogas were calculated and the value of electrical energy produced from tofu liquid waste was established.

2. RESEARCH METHOD

The substance of this study is to calculate the potential of biogas and electrical energy of tofu liquid waste with an anaerobic fermentation method assisted by Superpro Designer Software to produce biogas. Where the results of the potential biogas from tofu liquid waste are converted into electrical energy.

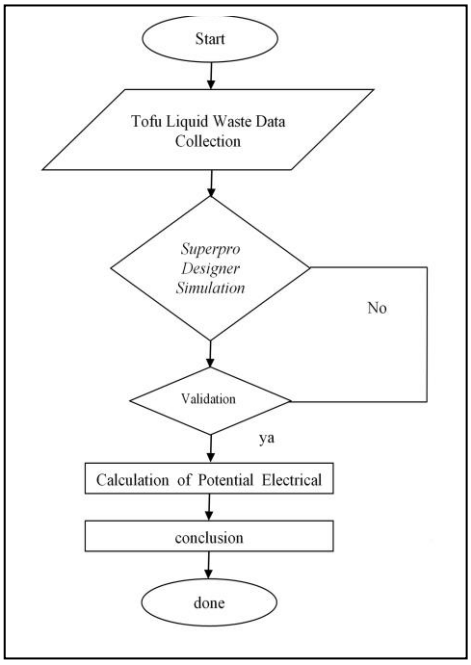

Figure 1. Research Series

JURNAL ECOTIPE
Electronic, Control, Telecommunication, Information, and Power Engineering
Volume 10, Issue 1, April 2023, pp. 78-85
ISSN 2355-5068 ; e-ISSN 2622-4852
DOI: 10.33019/jurnalecotipe.v10i1.3855

2.1. Collection of Research Data and Process Parameters

Stages of data collection and process parameters were carried out in two stages, namely by survey (interviews with resource persons) at the BK Tofu Industry location in Payakumbuh City and with related parameter data from the literature review.

2.1.1. Data Collection

According to the Payakumbuh City Industry and Trade Office, the tofu industry has 7 tofu industries. The development of the tofu industry in Payakumbuh City has increased from year to year.

Table 1. Data of Tofu Industry Liquid Waste Payakumbuh

Number	Tofu Industry Liquid Waste Data	
	Industries	Total Waste (L/day)
1	Industri Tahu BK	500
2	Industri Tahu Urang Awak	300
3	Industri Tahu DF	300
4	Industri Tahu Jaya Bersama	250
5	Industri Tahu Kapatar	450
6	Industri Tahu AA	130
7	Industri Tahu Sumedang Saitana	110

BK Tofu Industry is one of the tofu industries in Payakumbuh City, it is located on the riverbank of Batang Agam which is operating from 06.00 WIB to 18.00 WIB. After a survey with the industry owner, in one day the BK Tofu Industry can produce 500 liters of tofu liquid waste.

The BK Tofu Industry has an electric power of 11.000 VA and has electrical equipment consisting of 5 units of 1-phase electric motors, 3 units of water pumps, and 7 units of lamps. So that the total electrical load of the industry is 94,383 Watt or 94,383 kWatt. The equipment operates for around 10 hours per day.

Table 2. BK Tofu Industry Expense Data

Number	Industry Expense Data				Power Amount (Watt)
	Equipments	Active Time (Hours)	Power (Watt)	Total (Unit)	
1	Motor 1 Phase	9	1850	5	83.250
2	Water Pump	9	372	3	10.125
3	LED Light	10	18	7	1.008

2.1.2 Process Parameters

The parameters used in this biogas formation process are parameters that help in applying simulations to form biogas. Tofu liquid waste has a high nutrient and organic content consisting of water, carbohydrates, protein, and fat. The percentage content of tofu liquid waste can be seen in Table 2.

Table 3. Tofu Liquid Waste Levels

Number	Tofu Liquid Waste Levels	
	Parameters	Levels (%)
1	Water	90,72
2	Carbohydrate	6,28
3	Protein	1,8
4	Fat	1,2

2.2. Simulation of Superpro Designer Producing Biogas

2.2.1 Superpro the Flow of Making Tofu Liquid Waste Biogas with the Superpro Software

The potential of tofu liquid waste to become biogas is determined by an anaerobic fermentation method facilitated by SuperPro Designer Software. The procedure is shown in Figure 2 [8].

JURNAL ECOTIPE
Electronic, Control, Telecommunication, Information, and Power Engineering
Volume 10, Issue 1, April 2023, pp. 78-85
ISSN 2355-5068 ; e-ISSN 2622-4852
DOI: 10.33019/jurnalecotipe.v10i1.3855

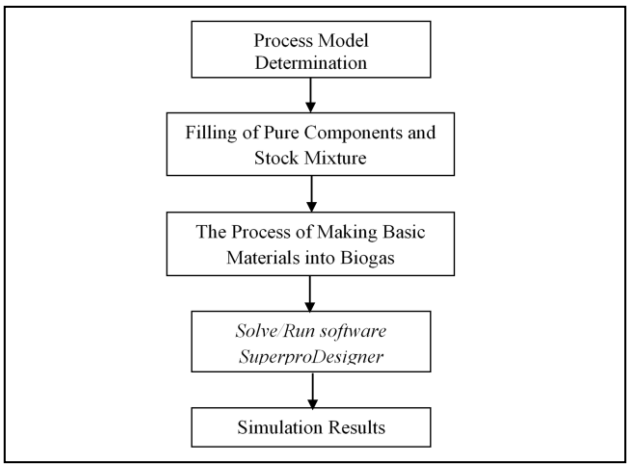

Figure 2. Biogas Production Series from Tofu Liquid Waste with Superpro Software

2.2.2 Determination of the Process Model

In the process of forming biogas with Superpro Software, there are several steps used in the process model, which is a process that is done after determining the value of the pure component. In simulating the software, it uses a Batch process with a duration of according to the Superpro Software recommendation of 336 days. Because of this method, the processing time can be changed while the primary process is in progress. The use of cycles in the anaerobic fermentation process. The unit procedure used is fermentation using Anaerobic Digestion.

2.2.3 Filling of Pure Components and Stock Mixture

Components consist called Pure Components are compounds that are reacted during simulation, while Stock Mixture is a compound in the raw material that will be processed into biogas.

2.2.4 Process of Manufacturing the Basic Materials Into Biogas

In this procedure, the preparation and processing of raw materials in the Anaerobic Digester are carried out. This procedure will produce methane and CO2 through chemical processes helped by bacteria, including hydrolysis, acidogenesis, acetogenesis, and methanogenesis. Biogas processing from wastewater requires an Anaerobic Digester component, which is a closed process that lacks free oxygen to produce biogas gas. The output of this process is tofu liquid waste. The end product is biogas, which consists of methane gas and carbon dioxide.

2.2.5 Validation of Simulation Results

The validation that was done in this study was to compare with research [7] that has the topic of study to calculate the potential biogas that can be produced, the duration of fermentation, and the construction of the reactor.

Table 4. Levels of Tofu Liquid Waste

Number	**Validation of Simulation Results**		
	Parameters	**Researchs** [7]	**Validation**
1	Raw Material	Tofu Liquid Waste	Tofu Liquid Waste
2	Composition	Water 90,72%, Carbohydrate 6,28%, Protein 1,8%, and Fat 1,2%	Water 90,72%, Carbohydrate 6,28%, Protein 1,8%, and fat 1,2%
3	Inputs value	90 Liter/days	90 Liter/day
4	Biogas Levels	80,57% methane, 19,42%carbon dioxide	80,57% methane, 19,42%carbon dioxide
5	Volumetric Flow	31,7193 m^3	31,7193 m^3

The validation of the simulation results showed that in the research [7] volume of tofu liquid waste was 90 liters and 500 liters. The Superpro simulation results in this study produce biogas which has a composition of 80.57% methane and 19.42% carbon dioxide. This simulation produces biogas that has

JURNAL ECOTIPE
Electronic, Control, Telecommunication, Information, and Power Engineering
Volume 10, Issue 1, April 2023, pp. 78-85
ISSN 2355-5068 ; e-ISSN 2622-4852
DOI: 10.33019/jurnalecotipe.v10i1.3855

a composition of 80.57% methane and 19.42% carbon dioxide. From the results of the biogas composition parameters, it can be seen that there are no inaccuracies in the values, which means that this research is valid because it does not have an error value of more than 10%.

2.3. Calculation of Electric Potential

Determine the working duration of the generator per day, we can use (1) [4].

$$\text{Operation Time} = \frac{\text{Volumetric Flow} \times \text{Mass Comp Gas Methan}}{\text{Fuel Consumption}} \quad (1)$$

Where operating time is the duration of generator set work that can be obtained, volumetric flow is the volume flow rate of methane gas obtained from simulation, fuel consumption is the amount of fuel consumption with 100% load.

Calculation of potential electrical energy can use (2) [4], as follows:

$$\text{Total electrical energy} = \text{operating time} \times \text{generator power} \quad (2)$$

Total electrical energy is the total potential electrical energy generated from tofu liquid waste, electrical power is the generator specification power, and operating time is the time in operating the generator set.

3. RESULTS AND DISCUSSION

In this section, the authors explain the results of the research as well as provide a comprehensive explanation of the discussion.

3.1. Biogas Potential from Tofu Liquid Waste

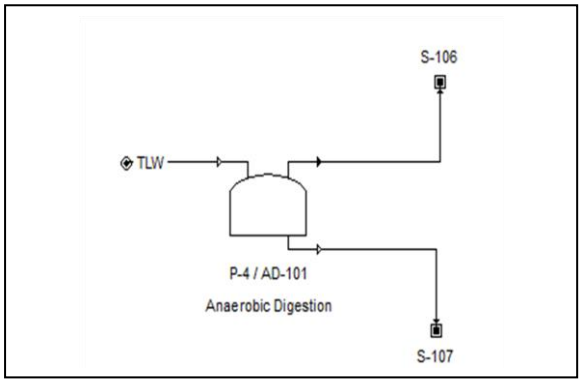

Figure 3. Single Line Diagram Anaerobic Fermentation Process

The first process of tofu liquid waste of 500 liters from the BK Tofu Industry in Payakumbuh City is included in the Anaerobic Digestion section. In Anaerobic Digestion, the formation of methane gas happens. The final results of the simulation are shown in the output.

Table 5. Levels of Tofu Liquid Waste

Number	Levels of Tofu Liquid Waste	
	Parameters	**Result**
1	Tofu Liquid Waste Volume	500 L/day
2	Volumetric flow	176218,54 L/day
3	Biogas levels	Methane 80,57% and CO^2 19,42%

The results of the simulation using Superpro software with the input of tofu liquid waste with a daily volume produced biogas with a Volumetric Flow of 176218.54 Liters or 176.21 m3 in a day with levels of 80.57% Methane Gas and 19.42% Carbon dioxide.

3.2. Potential of Electrical Energy from Biogas

In calculating the potential of electrical energy, we must choose the capacity of the generator set. The generator used for this PLTBG analysis is a Jet Power generator set. Based on the electrical energy

Volume 10, Issue 1, April 2023, pp. 78-85
ISSN 2355-5068 ; e-ISSN 2622-4852
DOI: 10.33019/jurnalecotipe.v10i1.3855

capability of the BK Tofu Industry in Payakumbuh city and the amount of potential biogas formed, the details of the generator set used are shown in Table 4.

Table 6. Tofu Liquid Waste Generator Specifications

Number	Generator Specifications	
	Parameters	**Result**
1	Manufacture	Jet Power
2	Model No	NG-17
3	Output Power	12 kW
4	Speed	1500/1800rpm
5	Frequency	50Hz/60Hz
6	Currency	40A-1000A
7	Phase	1 Phase/3 phase
8	Fuel Consumption	12,1 m^3/h
9	Manufacture	Jet Power

After knowing the specifications of the generator set that will be utilized as a generator, the next step is to calculate the electrical potential of tofu liquid waste using (1) and Equation (2).

$$Operating\ time = \frac{176{,}21\ \ m^3 \times 80{,}57\%}{12.1\ m^3/hours}$$

$$Operating\ time\ = \frac{141{,}97\ m^3}{12.1\ m^3/hour}$$

$$Operating\ time\ =\ 11{,}73\ hour$$

In 500 liters of tofu liquid waste mass, it can produce about 141.97 m^3 of methane gas and the operating time of the biogas generator is about 11,73 hours

$$Total\ Electrical\ energy =\ 11{,}73\ hours \times 12.000\ watt = 140{,}76\ kWh$$

Table 7. Electrical Energy Comparison

Number	Electrical Energy Comparison		
	Parameters	**Researchs** [7]	**Validation**
1	Raw material	Tofu Liquid Waste	Tofu Liquid Waste
2	Inputs value	90 Liter/days	500 Liter/day
4	Operating time	2,11 hour	11,73 hour
5	Total Energy	25,32 kWh	140,76 kWh

Previous research has that 90 liters/day of tofu liquid waste can produce total electrical energy of 25.32 kWh while from this study,500 liters/day of tofu liquid waste produces electrical energy of 140.76 kWh and can turn on the generator for 11.73 hours using a 12,000 Watts biogas generator. BK Tofu Industry operates from 06.00 WIB to 18.00 WIB, so that the potential electrical energy generated from tofu liquid waste can be utilized as fuel for PLTBG to the maximum during the operational time of BK Tofu Industry in Payakumbuh City.

4. CONCLUSION

Based on the results obtained, it is concluded that with the amount of 500 liters of tofu liquid waste can be processed into biogas by anaerobic fermentation method with Superpro Designer simulation, the results of biogas output with methane gas content of 82.257% and carbon dioxide of 19.42% and volumetric flow of 176218.54 liters per day or 176.21 m^3, with a total gas produced of 141.97 m3. From the potential of methane gas, it can operate the biogas generator for 11,73 hours with a total energy of 140.76 kWh.

Volume 10, Issue 1, April 2023, pp. 78-85
ISSN 2355-5068 ; e-ISSN 2622-4852
DOI: 10.33019/jurnalecotipe.v10i1.3855

REFERENCES

[1] B. Budiyono, I. Syaichurrozi, S. Suhirman, T. Hidayat, and J. Jayanudin, "Experiment and modeling to evaluate the effect of total solid on biogas production from the anaerobic co-digestion of Tofu liquid waste and rice straw," *Polish J. Environ. Stud.*, vol. 30, no. 4, pp. 3489–3496, 2021, doi: 10.15244/pjoes/127277.

[2] S. Sally, Y. P. Budianto, M. W. K. Hakim, and W. El Kiyat, "Potensi Pemanfaatan Limbah Cair Tahu Menjadi Biogas Untuk Skala Industri Rumah Tangga Di Provinsi Banten," *Agrointek*, vol. 13, no. 1, p. 43, 2019, doi: 10.21107/agrointek.v13i1.4715.

[3] K. Rajagukguk, "Pengolahan Limbah Cair Tahu Menjadi Biogas Menggunakan Reaktor Biogas Portabel," *Quantum Tek. J. Tek. Mesin Terap.*, vol. 1, no. 2, 2020, doi: 10.18196/jqt.010210.

[4] A. Wahyudi and M. Jelita, "Analisis Potensi Energi Listrik dan Biaya Limbah Rumen Sapi Rumah Potong Hewan Kota Pekanbaru," *JTEV (Jurnal Tek. Elektro dan Vokasional)*, vol. 8, no. 2, p. 263, 2022, doi: 10.24036/jtev.v8i2.117622.

[5] H. Nisrina and P. Andarani, "Pemanfaatan Limbah Tahu Skala Rumah Tangga Menjadi Biogas Sebagai Upaya Teknologi Bersih Di Laboratorium Pusat Teknologi Lingkungan – Bppt," *J. Presipitasi Media Komun. dan Pengemb. Tek. Lingkung.*, vol. 15, no. 2, p. 139, 2018, doi: 10.14710/presipitasi.v15i2.139-140.

[6] Florence T.N. Silalahi, Halimatuddahliana, and Amir Husin, "Pengolahan Limbah Cair Tahu Menggunakan Bioreaktor Anaerob Satu Tahap Dan Dua Tahap Secara Batch," *J. Tek. Kim. USU*, vol. 7, no. 1, pp. 34–40, 2018, doi: 10.32734/jtk.v7i1.1634.

[7] K. Ridhuan, "Pengolahan Limbah Cair Tahu Sebagai Energi Alternatif Biogas yang ramah lingkungan," *Turbo J. Progr. Stud. Tek. Mesin*, vol. 1, no. 1, pp. 1–9, 2016, doi: 10.24127/trb.v1i1.81.

[8] M. Hasan, *Potensi Dari Limbah Cair*, 1st ed. mahmudzone, 2013.

[9] J. and F. D. Clark, *Introduction to Chemicals From Biomass*, 2nd ed. United Kingdom: Wiley, 2015.

[10] W. Nurjuwita, A. Sasongko, T. J. Hartanto, and M. Purwanto, "Potential and characterization biogas from tofu liquid waste with addition cow dung and effective microorganisms 4 as biocatalyst," *Mater. Today Proc.*, vol. 46, pp. 1908–1912, 2020, doi: 10.1016/j.matpr.2021.02.025.

[11] Y. Kurniati, A. Rahmat, B. I. Malianto, D. Nandayani, and W. S. W. Pratiwi, "Review Analisa Kondisi Optimum Dalam Proses Pembuatan Biogas," *Rekayasa*, vol. 14, no. 2, pp. 272–281, 2021, doi: 10.21107/rekayasa.v14i2.11305.

[12] F. Arifan, Abdullah, and S. Sumardiyono, "Methane gas production from a mixture of cow manure, chicken manure, cabbage waste, and liquid tofu waste using the anaerobic digestion method," *IOP Conf. Ser. Earth Environ. Sci.*, vol. 623, no. 1, pp. 0–6, 2021, doi: 10.1088/1755-1315/623/1/012036.

[13] Nurjannah, L. Ifa, F. Jaya, and M. Lamo, "Produksi Bahan Bakar Gas Biomassa dari Limbah Organik Industri (Molases)," *Primordia*, vol. 12, no. 2, pp. 87–94, 2016.

[14] M. Mira, T. Iskandar, and ..., "Pra Rancang Bangun Pabrik Biogas Dari Limbah Padat Pembuatan Tahu Dengan Kapasitas 4.865, 664 Liter/Tahun," *eUREKA J. Penelit. ...*, vol. 2, no. 1, pp. 122–128, 2018, [Online]. Available: https://publikasi.unitri.ac.id/index.php/teknik/article/view/1157

[15] B. Outlook Energi, *Outlook Energi Indonesia 2021 Perspektif Teknologi Energi Indonesia: Tenaga Surya untuk Penyediaan Energi Charging Station*. 2021.

[16] M. B. Katjo and I. Irwansyah, "Pemanfaatan Air Limbah Tahu Sebagai Bahan Bakar Biogas Pada Kompor," *J. Tek. MESIN*, 2018, [Online]. Available: http://ojs.ustj.ac.id/mesin/article/view/610

Volume 10, Issue 1, April 2023, pp. 78-85
ISSN 2355-5068 ; e-ISSN 2622-4852
DOI: 10.33019/jurnalecotipe.v10i1.3855

[17] J. C. Akunna, *Anaerobic Waste-Wastewater Treatment and Biogas Plants*. Boca Raton: CRC Press, 2019. [Online]. Available: https://www.ptonline.com/articles/how-to-get-better-mfi-results

[18] T. Mesin, F. Teknik, U. Panca, and M. Probolinggo, "Cermin : Jurnal Penelitian Pengaruh Penambahan Bioaktivator Em-4 Terhadap Produksi Biogas Dari Limbah Cair Industri Tahu The Effect Of Additional Em-4 Bioactivator On Biogas Production From Tofu Industrial Liquid Waste Pendahuluan Jumlah industri tahu di ," vol. 5, pp. 362–372, 2021.

[19] A. R. I. Utami, R. A. Ryantara, E. D. Sumaryatie, and I. Chandra, "Analysis of the effect of internal gas pressure of an anaerobic digester on biogas productivity of a mixture of cow dung and tofu liquid waste," *AIP Conf. Proc.*, vol. 2320, 2021, doi: 10.1063/5.0037446.

[20] A. Afrizal, F. Yandari, S. Kurniawan, N. Yanqoritha, F. Razi, and Munajat, "Biogas production from tofu wastewater substrate using HUASB reactors with addition of trace metal," *IOP Conf. Ser. Mater. Sci. Eng.*, vol. 801, no. 1, 2020, doi: 10.1088/1757-899X/801/1/012059.

[21] D. Dieter, *Biogas From Waste And Reneweble Resources*. Deggendorf, 2008.

[22] M. Nurhilal, P. Purwiyanto, and G. M. Aji, "Pengaruh Komposisi Dan Waktu Fermentasi Campuran Limbah Industri Tahu Dan Kotoran Sapi Terhadap Kandungan Gas Methane Pada Pembangkit Biogas," *JTT (Jurnal Teknol. Ter.*, vol. 6, no. 1, p. 47, 2020, doi: 10.31884/jtt.v6i1.239.

[23] N. Herdiana, S. Hardina, and U. Hasanuddin, "Potential for Management and Utilization of Lampung Province of Tofu Industrial Waste," no. 2015.

[24] F. Saputra, S. Sutaryo, and A. Purnomoadi, "Pemanfaataan Limbah Padat Industri Tahu sebagai Co-Subtrat untuk Produksi Biogas Utilization of Tofu Cake as Co-Substrate in Biogas Production," *J. Apl. Teknol. Pangan*, vol. 7, no. 3, pp. 117–121, 2018, doi: 10.17728/jatp.2315.

JURNAL ECOTIPE
Electronic, Control, Telecommunication, Information, and Power Engineering

Volume 10, Issue 1, April 2023, pp. 86-94
ISSN 2355-5068 ; e-ISSN 2622-4852
DOI: 10.33019/jurnalecotipe.v10i1.3896

K-means and K-medoids Algorithm Comparison for Clustering Forest Fire Location in Indonesia

Ichwanul Muslim Karo Karo[1], Sri Dewi[2], Mardiana[3], Fanny Ramadhani[4], Putri Harliana[5]
[1,2,4,5]Computer Science, Medan State of University, Medan, 20221, Indonesia
[3]Electrical Engineering, Medan State Polytechnic, Medan, 20221, Indonesia

ARTICLE INFO

Article historys:

Received : 01/03/2023
Revised : 01/04/2023
Accepted : 19/04/2023

Keywords:

Clustering, K-Means, K-Medoids, Feature Importance, Silhouette Coefficient

ABSTRACT

Forest fires are the most common cause of deforestation in Indonesia. This condition hurts the survival of living things. Of course, this has received special attention from various parties. One effort that can be made for prevention is to group these points into areas with the potential for fire using the clustering method. In this research, a comparative study of the clustering algorithm between K-Means and K-Medoids was conducted on hotspot location data obtained from Global Forest Watch (GFW). Besides that, important variables that affect the clustering process are also analyzed in terms of feature importance. There are nine important variables used in the clustering process, of which the Acq_time variable is the most important. The clustering quality of both algorithms is evaluated using the silhouette coefficient (SC). Both algorithms are capable of producing strong clusters. The best number of clusters is six clusters. The K-medoids algorithm is better at grouping data than K-means.

Corresponding Author:

Ichwanul Muslim Karo Karo
Compute Science, Medan State University, Medan, 20221, Indonesia
Email: ichwanul@unimed.ac.id

1. INTRODUCTION

Indonesia is one of the world's lungs, with a total area of 94.1 million hectares [1]. However, Indonesia's deforestation threat is 17% annually [2]. Forest fires are the most common cause of deforestation. Global Forest Watch (GFW) is an organization in the environmental sector that has noted Indonesia as the country most frequently affected by forest fires. The impact is that air quality in Indonesia deteriorates over time, causing damage to the world's lungs due to global warming. In addition, the destruction of forests results in the instability of flora and fauna ecosystems, so many species are threatened with extinction.

The negative repercussions of forest and land fires encourage various parties to take early prevention measures. Given that the volume of forest and land fires will increase as the dry season approaches, one of the anticipatory steps that can be taken is to predict the distribution of hotspots and classify these points into areas with the potential for forest or land fires [3]. The distribution of hotspots indicates the likelihood of forest fires' occurrence in a given area [3,4].

Hotspots are areas with higher temperatures than the surrounding surface areas. Hotspots could be detected as locations for forest and land fires. It uses the MODIS sensors on the Terra/Aqua satellite and the SNP VIIRS satellite[5]. Hotspot datasets can be grouped depending on their information similarity using data mining techniques, and these techniques can process data on a large scale [6]. One approach to data mining is clustering. The clustering algorithm will group the data into the same cluster based on their similarity.

JURNAL ECTIPE
Electronic, Control, Telecommunication, Information, and Power Engineering
Volume 10, Issue 1, April 2023, pp. 86-94
ISSN 2355-5068 ; e-ISSN 2622-4852
DOI: 10.33019/jurnalecotipe.v10i1.3896

A study applied a data mining approach in its category of clustering to identify areas susceptiblto forest fires in West Kalimantan Province [3]. The K-means algorithm is used to cluster the forest fire dataset. The dataset was obtained from the Institute of Aeronautics and Space (LAPAN). Evaluation of clustering results using the Davies Bouldin Index. Based on the results of the grouping, there are three with information on fire-prone, non-prone, and fire areas. By using identical algorithm, study by [6] clustering points of forest fires on the island of Sumatra. Forest fire hotspot data was obtained from the EOSDIS website. In addition, the study also analyzes the comparison of the K-means algorithm with the Isodata algorithm. Cluster results were evaluated using the silhouette coefficient (SC). Based on the results of their study, the K-means and Isodata algorithms are able to cluster data with very strong cluster quality, with SC values above 0.9. The results of further analysis show that the K-means algorithm is better at producing clusters, with a greater SC value than the Isodata algorithm.

Another popular clustering algorithm is K-medoids. Research by [7] clusters hotspots in the Saravan Forest, Iran. The dataset was obtained from the local Ministry of Forestry. The study also analyzes the comparison of K-medoids with the fuzzy c-means (FCM) algorithm. Clustering results are evaluated with the silhouette coefficient. Both algorithms are capable of clustering hotspots with quite a good cluster quality. By using the same algorithm, a work clusters areas with the potential for forest/land fires based on hotspots [8]. The distribution of hotspots covering the Southeast Asia region was obtained from the database of the NASA LANCE –FIRM MODIS Active Fire website. The data used contains information in the form of brightness temperature, FRP, latitude, longitude, and confidence values. To evaluate the cluster results, they use the silhouette coefficient. The K-medoids algorithm can cluster the data. However, the quality of the cluster results in the low-quality range is quite good.

Based on the conditions and facts above, this study analyzes two partitioning clustering algorithms, these are K-means and K-medoids. Both algorithms cluster forest fire hotspot data. There are two kinds of datasets, each obtained from a distinct source [1, 5]. Furthermore, this study also provides information on the most important variables in the research using the important feature.

2. RESEARCH METHOD

This section describes several research processes (Figure 1). The process begins with collecting data, followed by pre-processing. The next process entails that every dataset be clustered with the K-means and K-medoids algorithms. The silhouette coefficient is used to evaluate clustering results.

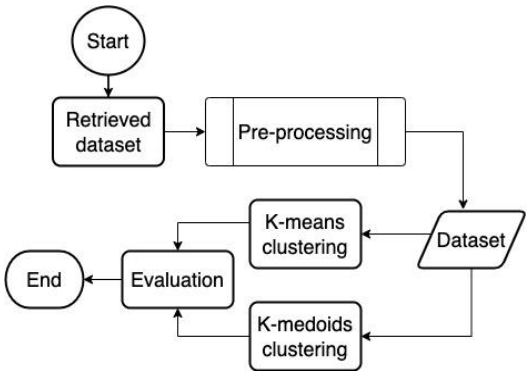

Figure 1. Research flowchart

2.2. Dataset

There are two types of datasets used in this study. Global Forest Watch (GFW) provided the first dataset (Dataset I). GFW is a data and tool platform available online to monitor forest fires [5]. The second dataset (Dataset II) is obtained from the research sampling [1]. The dataset I have 185 287 hotspot records and Dataset II consists of 25 000 records. Dataset II is a sampling from Dataset I. Both datasets have the same variable and there are twelve variables in dataset Table 1.

JURNAL ECOTIPE
Electronic, Control, Telecommunication, Information, and Power Engineering
Volume 10, Issue 1, April 2023, pp. 86-94
ISSN 2355-5068 ; e-ISSN 2622-4852
DOI: 10.33019/jurnalecotipe.v10i1.3896

Table 1. Variable description

Variable	Description
latitude	Latitude
longitude	Longitude
bright_ti4	The brightness temperature is I-4 in kelvins
scan, track	Scan size in pixels
acq_date	Track size in pixels
acq_time	Date of acquisition of VIIRS
instrument	Instrument
confidence	N= Suomi National Polar-orbiting Partnership (Suomi NPP), 1=NOAA-20 (designated JPSS-1 prior to launch)
satellite	satellite
version	Version
frp	Hot spot radiative strength
bright_ti5	The brightness temperature is I-5 in kelvins

2.3. Pre-processing

This is a vital phase of the data mining process[9]. Most of the energy of research is consumed by this process. In addition to preparing data, this process can also improve the performance of the resulting model [15]. Several procedures are executed at this stage to obtain a ready dataset. The processes are raw selection, normalization, and variable selection. Raw selection is selecting used records or deleting unused records. This study employs the principle of deleting unused records. This study removes invalid records that contain the value "X" on variable longitude and "Y" on latitude. Of course, the record deletion does not have a significant impact because the number is small in comparison to the raw dataset size.

Some values of the variables in this study dataset have non-standard ranges of values and high gaps. Therefore, process normalization is required. The data normalization process is carried out to standardize the data scale for each variable. This study uses the z-score method because the method is proven reliable for numeric and integer data types[10], [11]. Equation (1) is a z-score formula, Z notation represents normalized values, x is data, μ is the mean of data and σ is the standard deviation.

$$Z = \frac{x - \mu}{\sigma} \quad (1)$$

This study dataset has many features. These conditions make it difficult to build a model [12], [13]. This research performs feature selection using feature importance. There have been many studies using this method to solve dataset variety problems [1,12,13]. This study also used the feature importance method by threshold 0.5, which is refer to [1].

2.4. *Clustering*

Clustering is known as unsupervised learning to partition data into several clusters [14]. A cluster is a group of objects with a high degree of similarity. The quality of the clustering results is dependent on the method used. Generally, clustering algorithms are divided into three categories[4]: hierarchical, density, and partitioning. Partitioning clustering is a clustering algorithm that partitions data into k clusters [15]. The k clusters by the partitioning clustering method are frequently of higher quality than the k clusters by the hierarchical or density methods [3,14,16,17]. The popular partitioning clustering algorithms are K-means and K-Medoids [18].

2.5. K-Means Algorithm

The K-means algorithm is a non-hierarchical cluster analysis method that partitions objects into one or more groups based on similar characteristics, objects that have characteristics that are closer to being grouped in the same cluster are grouped into that cluster [19]. In other words, the K-Means algorithm goal is to minimize variation within a cluster while increasing variation with existing data in other clusters. Without knowing the target class, the learning algorithm divides the data into k clusters based on the similarity value closest to the cluster's center (centroid). This learning is included in

Volume 10, Issue 1, April 2023, pp. 86-94
ISSN 2355-5068 ; e-ISSN 2622-4852
DOI: 10.33019/jurnalecotipe.v10i1.3896

unsupervised learning [18]. The number of clusters (*k*) is assigned manually at the beginning of the clustering process. This algorithm has been widely used in any case because it is simple to implement and has a minimum computational complexity [14].

K-means algorithm
1. Define *k* as the number of clusters
2. Determine the *k* initial centroid
3. Calculated similarity between centroid to each data
4. Allocate each object to the nearest centroid based
5. Update the centroid by finding the average value of the cluster members
6. Repeat steps 3 to 5 until there is no change in the centroid

2.6. K-Medoids Algorithm

Leonard Kaufman and Peter J. Rousseeuw provided the K-Medoids algorithm, which is an enhanced version of the K-Means algorithm [11] byproduct, the two algorithms are very similar. The distinction between the K-Means and the K-Medoids algorithm is in identifying the centroid; the K-Means algorithm applies the mean value of each cluster as the centroid, whilst the K-Medoids algorithm uses data objects as representatives (medoids) as the centroid.

K-medoids algorithm
1. Initialize *k* (number of clusters) centroid
2. Allocate each data (object) to the closest centroid based on similarity
3. Choose an object randomly from the members of each cluster as a new centroid candidate
4. Calculate distance of each object to the new centroid candidate in each cluster
5. Calculate the cost (*S*) by calculating the new total distance – the old total distance
6. If *S*<0, then swap centroid by new centroid
7. Repeat step 2-7 until there is no change in centroid

2.7. Evaluation Silhouette Coefficient

This study uses the silhouette coefficient (*SC*) to evaluate clustering results. SC is a technique for determining the quality and strength of clusters. The Silhouette Coefficient Method is a hybrid of the Cohesion and Separation Methods [13]. The cohesion method measures the closeness of relationships between objects in a cluster. While the separation method determines how far or close a cluster is to other clusters. Let *A* be a cluster, randomly select an object *i* from a member of cluster A, and then the steps for calculating the silhouette coefficient are as follows [19]:

1. Calculate the mean distance from an object ($a(i)$) to all other objects in a cluster using equation (2). Where *j* is another object in cluster A and $d(i,j)$ is distance object *i* to object *j*

$$a(i) = \frac{1}{|A|-1}\sum_{j\in A, j\neq i} d(i,j) \quad (2)$$

2. Calculate the mean distance from object *i* to all data in other clusters using equation (3), and take the smallest value *b(i)*. Where $d(i,C)$ is the object's distance to all objects in cluster C, where C is not the same as *A*.

$$d(i,C) = \frac{1}{|A|}\sum_{j\in C,} d(i,j) \quad (3)$$

3. Calculate the Silhouette Coefficient value by using equation (4).

$$S(i) = \frac{b(i)-a(i)}{\max(a(i),b(i))} \quad (4)$$

The range of SC values is 0 to 1. SC values represent cluster quality. Table 2 shows the SC description.

JURNAL ECTIPE
Electronic, Control, Telecommunication, Information, and Power Engineering
Volume 10, Issue 1, April 2023, pp. 86-94
ISSN 2355-5068 ; e-ISSN 2622-4852
DOI: 10.33019/jurnalecotipe.v10i1.3896

Table 2. Interval Silhouette Coefficient

Interval SC	Description
0.71 - 1	Strong cluster
0.51 – 0.71	Reasonable cluster
0.26 – 0.5	Weak cluster
< 0.25	Wrong cluster

3. RESULT AND DISCUSS

This chapter describes the results and discusses four main points of discussion; the results of selecting variables with feature importance, clustering using the K-Means algorithm, clustering using the K-Medoids algorithm, and studying the comparison of the two algorithms.

3.1. Feature Selection

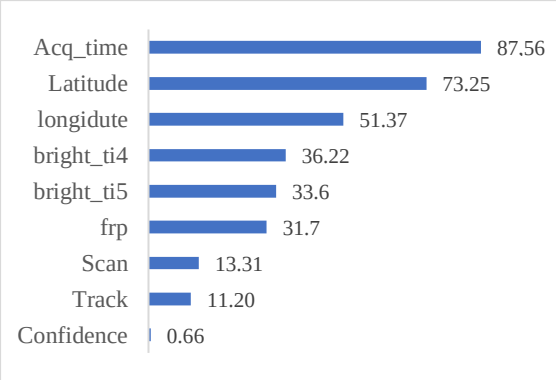

Figure 2. Feature importance value of variables

There are twelve features in this study dataset. According to the findings of this study, nine features fulfill the threshold requirements Figure 2. These are acq_time, latitude, longitude, bright_ti4, bright_ti5, FRP, scan, track, and confidence. The acq_time variable has the highest value, and the confidence variable has the lowest feature importance value. The higher the value, the greater the influence on building the model later, and vice versa. These nine variables are used to build the clustering model.

3.1. Clustering using K-Means

This section presents the results of implementing the K-means algorithm on two datasets. The K-means algorithm tests a number of clusters (k), including k = 2, 3, 4, 5, and 6, respectively. The clustering results were evaluated using the silhouette coefficient (*SC*). Evaluation results can be seen in Table 3.

Table 3. Cluster quality by K-means algorithm

k	SC Dataset I	SC Dataset II
2	0.729	0.7286
3	0.729	0.7287
4	0.777	0.776
5	0.776	0.742
6	0.794	0.754

Based on the information in the table, the K-means algorithm is able to produce strong clusters for both datasets. It means that the algorithm is capable to clusters a small or large number of records. Even though all the k tests produced strong clusters, six and four are the best number of clusters for dataset I and dataset II. In addition, k = 2 has lowest SC for both datasets, the number of cluster does not recommended as an insight of problem.

JURNAL ECTIPE
Electronic, Control, Telecommunication, Information, and Power Engineering
Volume 10, Issue 1, April 2023, pp. 86-94
ISSN 2355-5068 ; e-ISSN 2622-4852
DOI: 10.33019/jurnalecotipe.v10i1.3896

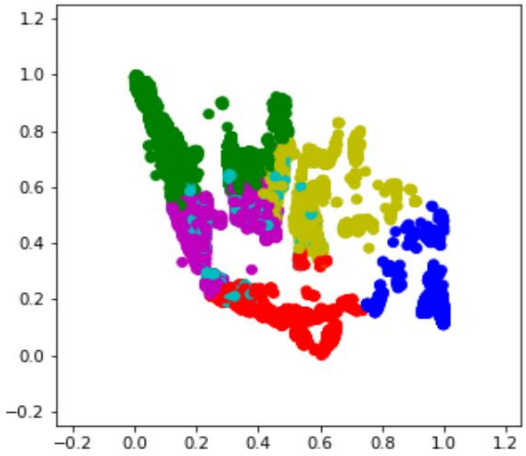

Figure 3 K-means visualization result for dataset I

The dataset I have a higher quality of clusters than Dataset II. This study argues that dataset sampling affects cluster quality. This study presents a visualization of the results of cluster dataset I depending on the attributes of latitude and longitude (Figure 3). There are six different colors, each representing a cluster. Even though the K-means algorithm produces strong clusters, there is one Tosca blue cluster with disjoint conditions between its members.

3.2. Clustering using K-Medoids

This section discusses the results of implementing the K-Medoids algorithm on both datasets. The K-medoids algorithm was also tested and evaluated using the same number of clusters and techniques that were used in the previous experiment. The evaluation results can be found in Table 4. Based on the table, $k = 2$ has the lowest SC for both datasets, while $k = 6$ has the highest SC for both datasets. It means that the number of clusters with the lowest SC is not a recommendation for grouping hotspots. On the other hand, the number of clusters with the highest SC could provide insight into grouping hotspots.

Table 4. Cluster quality by K-medoids algorithm

k	SC Dataset I	SC Dataset II
2	0.729	0.723
3	0.776	0.776
4	0.794	0.777
5	0.794	0.806
6	0.813	0.810

Based on all the numbers of k tested, K-medoid is also able to produce strong clusters for both datasets. Even though both clustering results show the same number of best clusters, the SC of the best number of clusters from dataset I is greater than the SC of the best number of clusters from dataset II. On other hand, the cluster quality of dataset I is still more reliable than dataset II. This condition reinforces the argument from this study that sampling datasets affect cluster quality. This argument is reinforced by the results of the visualization in Figure 4, the figure shows that the disjoint member of the cluster is less than the previous clustering results.

JURNAL ECTIPE
Electronic, Control, Telecommunication, Information, and Power Engineering
Volume 10, Issue 1, April 2023, pp. 86-94
ISSN 2355-5068 ; e-ISSN 2622-4852
DOI: 10.33019/jurnalecotipe.v10i1.3896

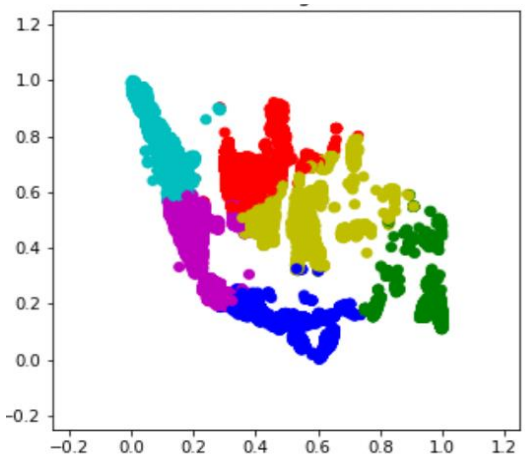

Figure 4 K-medoids visualization result for dataset I

3.3. Comparison of Two Algorithms

Based on the best cluster visualization results for both datasets in the previous section, it can be seen that the K-medoids clustering results are more compact than the K-means results. Further investigation results can be seen in Figure 5 (a) and (b). Figure 5 (a) is the SC comparison graph of algorithms for dataset I and Figure 5 (b) is the SC comparison graph of algorithms for dataset II. SC of K-medoids ≥ SC of K-means for a dataset I. The highest SC value of K-medoids is 0.813, while the K-means algorithm is less than 0.8. Similar conditions exist for dataset II, with the K-means algorithm only being superior when $k = 2$.

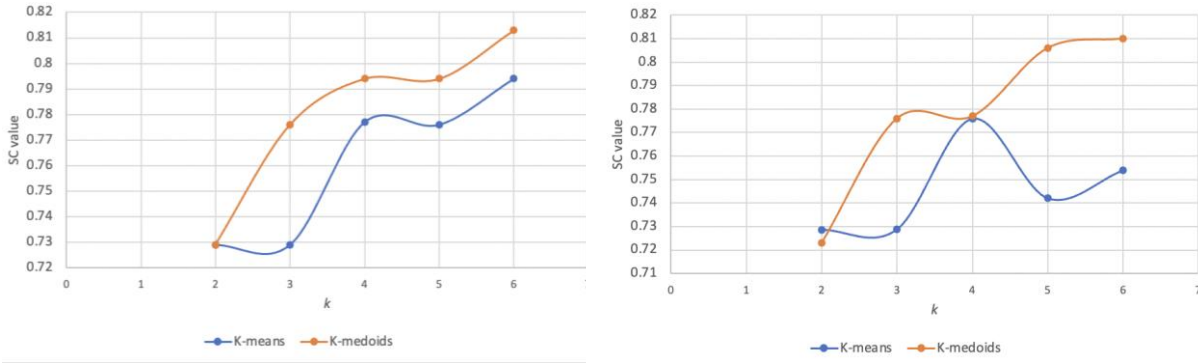

(a) (b)

Figure 5 Comparison SC value of algorithms

Lastly, both algorithms can produce strong clusters for both datasets. This can be seen from the SC value, which is always above 0.71. The facts show that the SC value of the K-medoids algorithm is greater than the SC value of the K-means algorithm for both datasets. It means that the performance of the K-medoids algorithm is superior to that of the K-means algorithm.

4. CONCLUSION

Based on the results and discussion, nine attributes are most influential in building a fire forest clustering model, these are Acq_time, longitude, latitude, bright_ti4, bright_ti5, FRP, scan, track, and confidence. Both algorithms can be implemented for grouping data on the location of forest/land fires in Indonesia based on the distribution of hotspots. Both algorithms produce strong clusters for large and small data sizes. Although the size of the dataset also affects the quality of the cluster, six clusters are the most numerous in both datasets. The quality of the clustering results of the K-medoids algorithm is superior to K-means.

Volume 10, Issue 1, April 2023, pp. 86-94
ISSN 2355-5068 ; e-ISSN 2622-4852
DOI: 10.33019/jurnalecotipe.v10i1.3896

REFERENCES

[1] I. M. K. Karo, "Implementasi Metode XGBoost dan Feature Importance untuk Klasifikasi pada Kebakaran Hutan dan Lahan," *Journal of Software Engineering, Information and Communication Technology*, vol. 1, no. 1, pp. 10–16, 2020.

[2] H. Wahyuni and S. Suranto, "Dampak Deforestasi Hutan Skala Besar terhadap Pemanasan Global di Indonesia," *JIIP: Jurnal Ilmiah Ilmu Pemerintahan*, vol. 6, no. 1, 2021, doi: 10.14710/jiip.v6i1.10083.

[3] N. A. Khairani and E. Sutoyo, "Application of K-Means Clustering Algorithm for Determination of Fire-Prone Areas Utilizing Hotspots in West Kalimantan Province," *International Journal of Advances in Data and Information Systems*, vol. 1, no. 1, pp. 9–16, Apr. 2020, doi: 10.25008/ijadis.v1i1.13.

[4] K. Pratama Simanjuntak and U. Khaira, "MALCOM: Indonesian Journal of Machine Learning and Computer Science Hotspot Clustering in Jambi Province Using Agglomerative Hierarchical Clustering Algorithm Pengelompokkan Titik Api di Provinsi Jambi dengan Algoritma Agglomerative Hierarchical Clustering," vol. 1, pp. 7–16, 2021.

[5] World Resources Institute, "Forest Monitoring, Land Use & Deforestation Trends | Global Forest Watch," *Global Forest Watch*. 2021.

[6] E. F. Sirat, B. D. Setiawan, and F. Ramdani, "Comparative Analysis of K-Means and Isodata Algorithms for Clustering of Fire Point Data in Sumatra Region," in *2018 4th International Symposium on Geoinformatics, ISyG 2018*, 2019. doi: 10.1109/ISYG.2018.8611879.

[7] M. Kurniawan, R. R. Muhima, and S. Agustini, "Comparison of Clustering K-Means, Fuzzy C-Means, and Linkage for Nasa Active Fire Dataset," *International Journal of Artificial Intelligence & Robotics (IJAIR)*, vol. 2, no. 2, 2020, doi: 10.25139/ijair.v2i2.3030.

[8] Laboratoire lorrain de recherche en informatique et ses applications and Institute of Electrical and Electronics Engineers, *1st IEEE International Workshop on Arabic Script Analysis & Recognition : April 3-5, 2017, LARIA, Nancy, France.*

[9] M. U. Salur and I. Aydin, "The Impact of Preprocessing on Classification Performance in Convolutional Neural Networks for Turkish Text," in *2018 International Conference on Artificial Intelligence and Data Processing, IDAP 2018*, 2019. doi: 10.1109/IDAP.2018.8620722.

[10] H. Henderi, "Comparison of Min-Max normalization and Z-Score Normalization in the K-nearest neighbor (kNN) Algorithm to Test the Accuracy of Types of Breast Cancer," *IJIIS: International Journal of Informatics and Information Systems*, vol. 4, no. 1, 2021, doi: 10.47738/ijiis.v4i1.73.

[11] I. M. Karo Karo and H. Hendriyana, "Klasifikasi Penderita Diabetes menggunakan Algoritma Machine Learning dan Z-Score," *Jurnal Teknologi Terpadu*, vol. 8, no. 2, pp. 94–99, 2022.

[12] S. Khalid, T. Khalil, and S. Nasreen, "A survey of feature selection and feature extraction techniques in machine learning," in *Proceedings of 2014 Science and Information Conference, SAI 2014*, 2014. doi: 10.1109/SAI.2014.6918213.

[13] I. M. Karo Karo, S. Nadia Amalia, and D. Septiana, "Klasifikasi Kebakaran Hutan Menggunakan Feature Selection dengan Algoritma K-NN, Naive Bayes dan ID3," *Journal of Software Engineering, Information and Communication Technology*, vol. 3, no. 1, pp. 121–126, 2022.

[14] E. Schubert and P. J. Rousseeuw, "Fast and eager k-medoids clustering: O(k) runtime improvement of the PAM, CLARA, and CLARANS algorithms," *Inf Syst*, vol. 101, 2021, doi: 10.1016/j.is.2021.101804.

Volume 10, Issue 1, April 2023, pp. 86-94
ISSN 2355-5068 ; e-ISSN 2622-4852
DOI: 10.33019/jurnalecotipe.v10i1.3896

[15] M. A. Ahmed, H. Baharin, and P. N. E. Nohuddin, "Analysis of K-means, DBSCAN and OPTICS Cluster algorithms on Al-Quran verses," *International Journal of Advanced Computer Science and Applications*, vol. 11, no. 8, 2020, doi: 10.14569/IJACSA.2020.0110832.

[16] E. Lidrawati, S. Bahri, U. F. Zubaedi, V. P. Carolina, K. Kusrini, and D. Maulina, "Kebakaran Hutan Implementasi Metode CLARA Clustering Untuk Pengelompokan Data Potensi Kebakaran Hutan/Lahan Berdasarkan Persebaran Titik Panas (Hotspot)," *Journal of Computer System and Informatics (JoSYC)*, vol. 3, no. 4, 2022, doi: 10.47065/josyc.v3i4.2006.

[17] I. M. K. Karo and A. F. Huda, "Spatial clustering for determining rescue shelter of flood disaster in South Bandung using CLARANS Algorithm with Polygon Dissimilarity Function," in *Proceedings - 2016 12th International Conference on Mathematics, Statistics, and Their Applications, ICMSA 2016: In Conjunction with the 6th Annual International Conference of Syiah Kuala University*, 2017. doi: 10.1109/ICMSA.2016.7954311.

[18] S. Gultom, S. Sriadhi, M. Martiano, and J. Simarmata, "Comparison analysis of K-Means and K-Medoid with Ecluidience Distance Algorithm, Chanberra Distance, and Chebyshev Distance for Big Data Clustering," in *IOP Conference Series: Materials Science and Engineering*, 2018, vol. 420, no. 1. doi: 10.1088/1757-899X/420/1/012092.

[19] I. M. Karo Karo, A. Yusmanto, and R. Setiawan, "Segmentasi Nasabah Kartu Kredit Berdasarkan Perilaku Penggunaan Kartu Kreditnya Menggunakan Algoritma K-Means," *Journal of Software Engineering, Information and Communication Technology*, vol. 2, no. 2, pp. 101–107, 2021, [Online]. Available: https://www.kaggle.com/arjunbhasin2013/ccdata.

JURNAL ECOTIPE
Electronic, Control, Telecommunication, Information, and Power Engineering

Volume 10, Issue 1, April 2023, pp. 95-102
ISSN 2355-5068 ; e-ISSN 2622-4852
DOI: 10.33019/jurnalecotipe.v10i1.3919

Development of IoT-Based Temperature and Relative Humidity Monitoring System for Mushroom Cultivation House

Laurentius Kevin Hendinata[1], Ahmad Ilham Rokhul Fikri[2]
[1, 2] Department of Nuclear Engineering and Engineering Physics, Faculty of Engineering, Universitas Gadjah Mada,
Jl. Grafika No.2, Senolowo, Sinduadi, Kec. Mlati, Kabupaten Sleman, Daerah Istimewa Yogyakarta, 55281, Indonesia

ARTICLE INFO

Article historys:

Received : 12/03/2023
Revised : 10/04/2023
Accepted : 21/04/2023

Keywords:

Mushroom cultivation; monitoring system; IoT; Thinger.io; NodeMCU

ABSTRACT

Mushrooms are one of the agricultural products that are in great demand because of their high nutritional content and healthy and delicious taste. Nowadays, mushroom cultivation is increasingly widespread and focuses on understanding the optimal environmental conditions for good mushroom production. The main parameters that affect the growth of fungi are the temperature and humidity of the environment, where the fungus will grow optimally at a temperature of 20 to 30°C and a humidity of 60 to 90%RH. But unfortunately, mushroom farmers often find it difficult to monitor at any time the environmental conditions where the mushrooms grow. For this reason, an IoT-based temperature and humidity monitoring system was developed for use in mushroom cultivation rooms. This system is assembled using a DHT11 temperature and humidity sensor, a NodeMCU ESP3866 microcontroller and WiFi module, and an LCD screen. IoT development is carried out using the Thinger.io platform which allows mushroom farmers as users to monitor room conditions directly through a web page. The efficiency of the IoT-based monitoring system in providing the appropriate growth conditions for mushroom cultivation, despite the existence of variable environmental factors, has been demonstrated. The system has been shown to measure temperature and relative humidity levels within the range of 19.4°C to 31.5°C and 43%RH to 82%RH, respectively.

Corresponding Author:

Laurentius Kevin Hendinata
Department of Nuclear Engineering and Engineering Physics, Faculty of Engineering, Universitas Gadjah Mada, Jl. Grafika No.2, Senolowo, Sinduadi, Kec. Mlati, Kabupaten Sleman, Daerah Istimewa Yogyakarta, 55281, INDONESIA
Email: kevinhendinata@mail.ugm.ac.id

1. INTRODUCTION

However, in practice mushroom cultivation often has obstacles, one of which is the environment that cannot be monitored properly so that the quality of the mushrooms produced is not good. Besides that, mushroom farmers often experience crop failure when environmental conditions are not properly monitored [10,11]. With the advancement of technology, the internet of things (IoT) offers an opportunity to develop a more efficient and reliable monitoring system for mushroom cultivation houses. Therefore, it is necessary to develop a mushroom cultivation system that is integrated with technology that can monitor the environmental conditions of the mushroom growing media so that it is always in accordance with their habitat.

This article will discuss the development of an IoT-based temperature and relative humidity monitoring system for mushroom cultivation houses. This system utilizes state-of-the-art sensors and wireless communication technology to collect and transmit environmental data in real-time. The

JURNAL ECTIPE
Electronic, Control, Telecommunication, Information, and Power Engineering
Volume 10, Issue 1, April 2023, pp. 95-102
ISSN 2355-5068 ; e-ISSN 2622-4852
DOI: 10.33019/jurnalecotipe.v10i1.3919

collected data can be accessed remotely, allowing growers to monitor and control environmental conditions more effectively. The hope is, by accurately monitoring and controlling the environmental conditions, such as temperature and relative humidity, growers can achieve better crop yield, quality, and consistency. Additionally, this system can help reduce labor costs and minimize the risk of crop failure due to environmental factors, ultimately leading to a more sustainable and profitable mushroom cultivation industry.

2. SYSTEM DESIGN

This temperature and humidity monitoring tool is designed with a sensor device with a simple microcontroller and uses the Internet of Things (IoT) protocol. In more detail this system is described as follows.

2.1. System Overview

This temperature and humidity monitoring tool that was developed simply consists of several components, namely components of sensors, displays, microcontrollers, and wireless communication modules. Here, the sensor will sense the environmental conditions of the mushroom cultivation room. The sensor reading results will be displayed on a simple display screen near the device, and the data will be sent to the cloud server via the internet. Later, users will be able to see directly the results of sensor readings through the dashboard on the web page.

The working scheme of this system is shown in the block diagram in Figure 1 below.

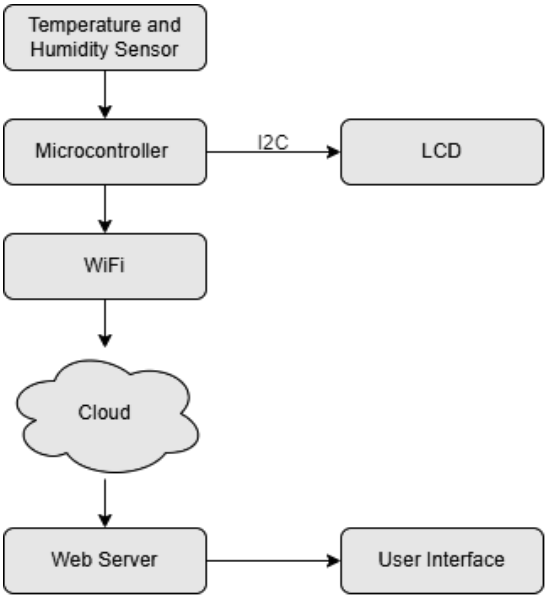

Figure 1. Block diagram of the proposed monitoring system

As shown in Figure 1, the sensor will sense the environmental conditions according to the parameters of temperature and relative humidity (RH) and transmit it to the microcontroller device. Here, the microcontroller will send data based on the I2C protocol to be displayed on the liquid crystal display (LCD). In addition, the microcontroller also sends data on the internet network via WiFi to the cloud and web server, to then display the sensor readings on the dashboard on the web page directly.

2.2. System Architecture

The design of this IoT-based temperature and humidity monitoring system encompasses a comprehensive structure that comprises several essential components, each of which serves a specific function and contributes to the overall functionality of the system. The architecture of this system consists of several constituent components, which are described in Table 1.

JURNAL ECOTIPE
Electronic, Control, Telecommunication, Information, and Power Engineering
Volume 10, Issue 1, April 2023, pp. 95-102
ISSN 2355-5068 ; e-ISSN 2622-4852
DOI: 10.33019/jurnalecotipe.v10i1.3919

Table 1. Components Used in Sensor Board and Control Board

No.	Components	Remarks
1	NodeMCU ESP8266	Microcontroller and UART WiFi Module
2	DHT11	Temperature and relative humidity sensor
3	LCD I2C	Display
4	Micro USB	Power circuitry
5	Adapter	220 V (AC) to 5 V (DC)

As described in Table 1, the system comprises a NodeMCU ESP8266, which serves as both the microcontroller and the UART WiFi module. This low-cost microcontroller is widely used in IoT applications due to its compact size and built-in WiFi capabilities. The DHT11 temperature and relative humidity sensor is used to measure the temperature and relative humidity of the mushroom cultivation house environment, providing growers with accurate environmental data. The LCD I2C display serves as a visual interface that displays the current temperature and relative humidity data collected by the DHT11 sensor. The use of the Micro USB and the adapter, a 220 V (AC) to 5 V (DC) power adapter, provide the necessary power to the system.

These components are assembled on the board as shown in Figure 2.

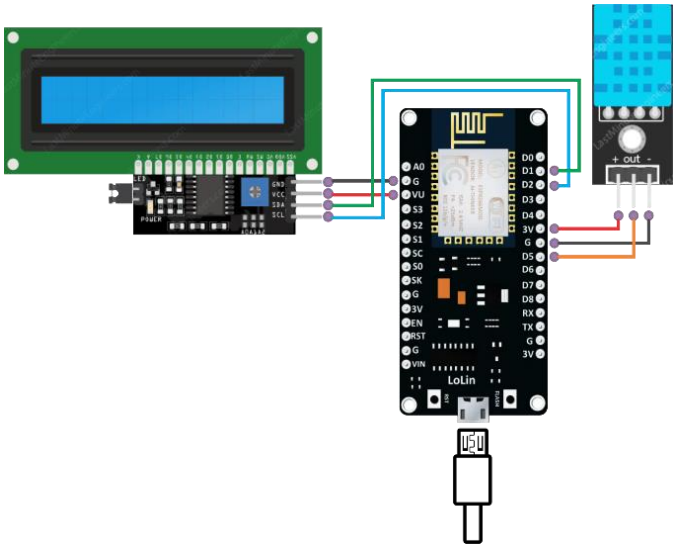

Figure 2. Wiring diagram of the temperature and humidity monitoring system on the NodeMCU module

The assembly of the five components, including the NodeMCU ESP8266, DHT11, LCD I2C, Micro USB, and Adapter, on the board as shown in Figure 2 enables the creation of a reliable and efficient IoT-based monitoring system for mushroom cultivation houses. The compact and streamlined design of the board ensures ease of use and integration with existing cultivation house infrastructure.

2.3. Cloud Configuration

The cloud used in this research is Thinger.io. This platform provides a ready to use cloud service for connecting devices to the Internet to perform any remote sensing or actuation over the Internet [12]. How Thinger.io works is shown in Figure 3.

JURNAL ECOTIPE
Electronic, Control, Telecommunication, Information, and Power Engineering
Volume 10, Issue 1, April 2023, pp. 95-102
ISSN 2355-5068 ; e-ISSN 2622-4852
DOI: 10.33019/jurnalecotipe.v10i1.3919

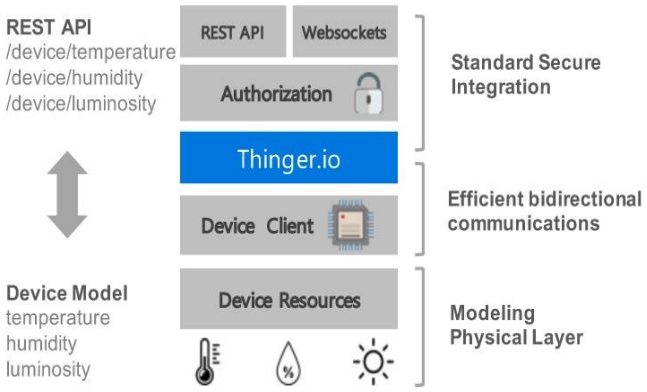

Figure 3. Mechanism of data transfer from device model with REST API [12]

Thinger.io platform allows device models to be defined which are automatically converted to REST APIs and can be deployed from any external application in real time.

3. RESULTS AND DISCUSSION

3.1. System Installation

The proposed system is installed in a mushroom cultivation house located in Cangkringan District, Sleman Regency, Yogyakarta Special Region Province, Indonesia. Sleman Regency itself is the largest mushroom producing area in the Special Region of Yogyakarta [2]. Here, the tool is installed in a mushroom house belonging to a small business private cultivator on a pole at the edge of the cultivation room. This installation is shown in Figure 4.

Figure 3. Installation of monitoring tools in mushroom cultivation house

3.2. Data Interfacing

The temperature and humidity monitoring system developed for mushroom cultivation rooms includes two types of displays: an on-site display using an LCD screen installed in the cultivation room and a virtual dashboard screen created on the Thinger.io platform. The LCD screen is designed to display the current temperature and relative humidity values based on the readings from the DHT11 temperature and humidity sensor, as well as an indicator showing the status of the WiFi network connection. The screen layout of the LCD display is depicted in Figure 5, providing users with real-time environmental data that can be used to adjust and optimize growing conditions for mushroom cultivation.

JURNAL ECOTIPE
Electronic, Control, Telecommunication, Information, and Power Engineering
Volume 10, Issue 1, April 2023, pp. 95-102
ISSN 2355-5068 ; e-ISSN 2622-4852
DOI: 10.33019/jurnalecotipe.v10i1.3919

Figure 5. LCD screen display on mushroom cultivation house to display sensor readings and WiFi connection status

As shown in Figure 5, the LCD display not only shows the temperature and relative humidity readings obtained from the DHT11 sensor, but it also displays a WiFi network connection status indicator, which indicates whether the device is connected to the network or not. This indicator serves as a helpful feature for growers, as it allows them to quickly identify any connectivity issues with the device, such as intermittent connection loss, and take necessary measures to resolve them. The WiFi network connection status indicator on the LCD display provides growers with real-time information on the connectivity of the device, showing whether it is currently connected or disconnected from the network. This feature helps ensure that the data obtained from the device is accurate and reliable, enabling growers to make informed decisions based on real-time data.

In addition, sensor measurement results are also displayed on a dashboard created from the Thinger.io IoT platform. The dashboard displays sensor measurement results, which include temperature and humidity values, as well as graphs showing changes in temperature and humidity over the last 24 hours. Figure 6 illustrates the display of the dashboard. This allows for continuous and remote monitoring of the environmental conditions in the mushroom cultivation room, providing valuable data to ensure optimal growth conditions for mushrooms.

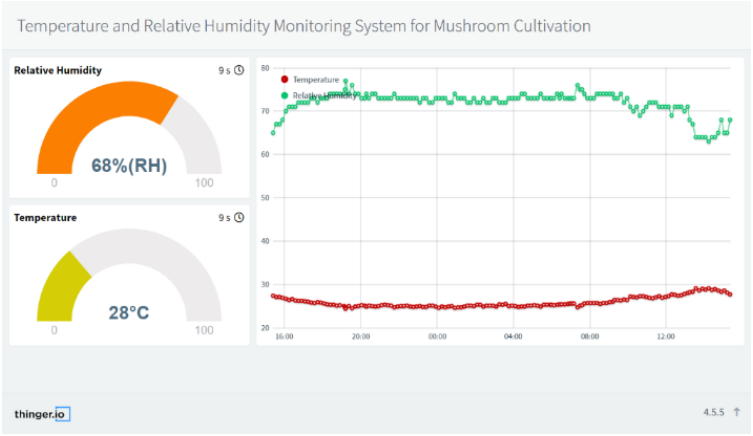

Figure 6. Dashboard display on the developed web page

The dashboard display created as part of this system has been evaluated by mushroom farmers who have reported finding it user-friendly and easy to read, allowing for easy access to the sensor measurement results through a web page interface. This feature enables farmers to quickly obtain valuable data on environmental conditions, which is essential for optimal mushroom growth. At the same time, the developers of this system can also continuously monitor its performance and status through the same platform, which can provide them with valuable information to improve the system's functionality and reliability.

The user-friendly dashboard display allows farmers to obtain an overview of the current environmental conditions in their mushroom cultivation room, including temperature and humidity readings, as well as graphs depicting changes over time. The continuous and remote monitoring capability of the system provides real-time updates on the room's conditions, enabling farmers to quickly

Volume 10, Issue 1, April 2023, pp. 95-102
ISSN 2355-5068 ; e-ISSN 2622-4852
DOI: 10.33019/jurnalecotipe.v10i1.3919

respond to changes and take action if necessary. The ability for developers to monitor the system's performance through the same platform also enhances the system's reliability, as they can identify and address any issues that arise promptly.

3.3. Data Measurement

The temperature and humidity monitoring tool that has been made has been installed in the mushroom cultivation house. For testing purposes, the temperature and humidity monitoring tool was installed in a mushroom cultivation house for 7 days, from August 10, 2022 to August 17, 2022. During this period, the temperature and relative humidity of the mushroom cultivation room were continuously measured using a data logger module on the Thinger.io platform.

To ensure the quality of the recorded data, a time step of 10 minutes was chosen to record the temperature and humidity levels in the mushroom cultivation house. This time step was selected because it is relevant to the mushroom cultivation process, where sudden changes in temperature and humidity can adversely affect mushroom growth. The temperature and humidity data collected were then presented as daily graphs, as shown in Figure 7 and Figure 8, respectively. These graphs provide a detailed view of the daily temperature and humidity variations, which can be useful in optimizing the growth conditions for mushrooms.

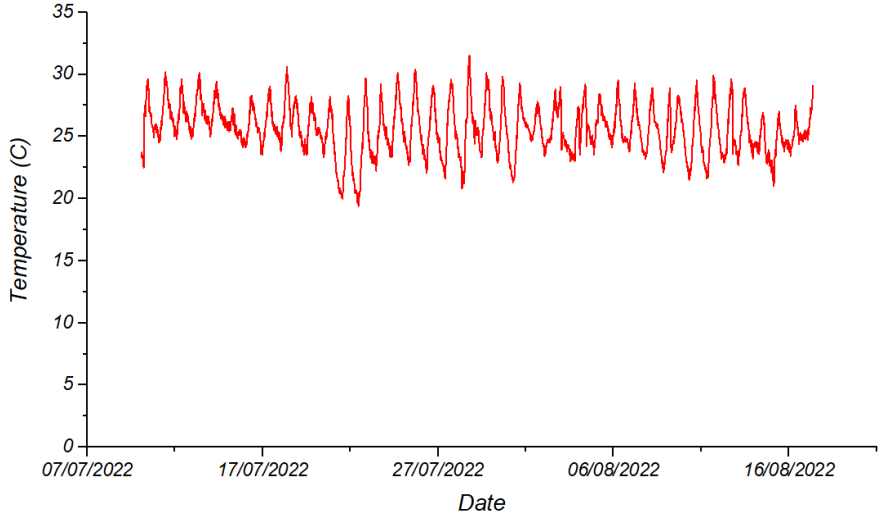

Figure 7. Daily graph of temperature in mushroom cultivation room

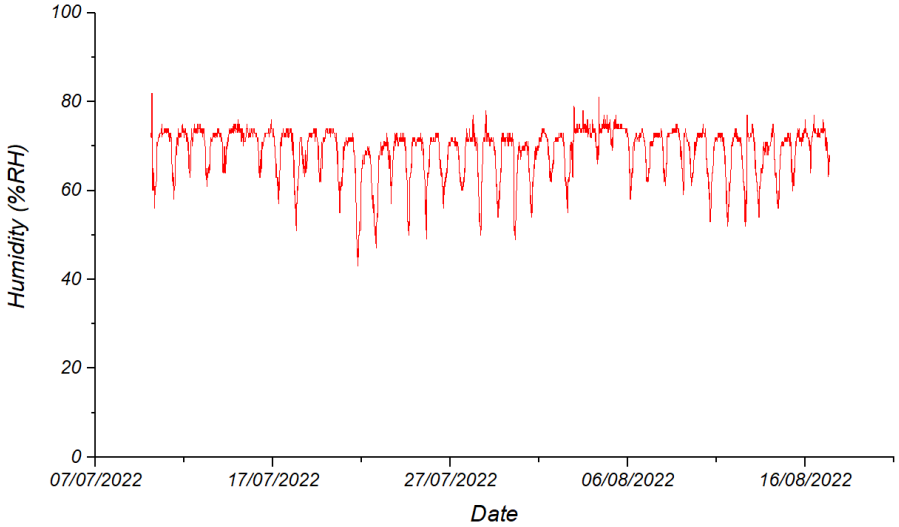

Figure 8. Daily graph of relative humidity in mushroom cultivation room

Volume 10, Issue 1, April 2023, pp. 95-102
ISSN 2355-5068 ; e-ISSN 2622-4852
DOI: 10.33019/jurnalecotipe.v10i1.3919

According to the data presented in Figure 7 and Figure 8, the measured temperature and humidity in the mushroom cultivation house are in the range of 19.4 °C to 31.5 °C and 43%$_{RH}$ to 82%$_{RH}$, respectively. These measurements are well within the recommended range for mushroom cultivation, which typically requires a temperature range of 20 to 25 °C and relative humidity between 70% to 90%. The accuracy and consistency of these measurements are essential to ensure optimal growing conditions and prevent the growth of harmful microorganisms.

Furthermore, the measured temperature and humidity in the mushroom cultivation house are relevant to the local climate conditions. The temperature and humidity levels in the mushroom cultivation house must be monitored and controlled to compensate for fluctuations in the local climate, such as changes in temperature and humidity due to weather patterns or seasonality. By monitoring and controlling the environmental conditions in the mushroom cultivation house, growers can ensure a stable and consistent growing environment, regardless of external climate conditions. Overall, the data presented in Figure 7 and Figure 8 demonstrate the effectiveness of the IoT-based monitoring system in maintaining optimal environmental conditions for mushroom cultivation, even in the face of changing environmental conditions.

4. CONCLUSION

The design and implementation of a temperature and humidity monitoring system for mushroom cultivation using the IoT platform is already presented. Sensor readings in the form of temperature and humidity parameters obtained from the DHT11 sensor are sent to the NodeMCU ESP8266 and displayed on the LCD screen and virtual dashboard on a web page developed on the Thinger.io IoT platform. The experimental results obtained indicate that in general the system can run well and can sense, record data, transmit, and display data on both displays. The IoT-based monitoring system has been shown to be highly effective in ensuring the optimal growth conditions for mushroom cultivation, even in the presence of fluctuating environmental variables. Seeing its promising performance and very helpful for mushroom farmers, further development is needed to connect it to the sensor network and integrate it with the actuator system.

Acknowledgments

This research did not receive any specific grant from funding agencies in the public, commercial or not-for-profit sectors.

REFERENCES

[1] J. Raman, S.-K. Lee, J.-H. Im, M.-J. Oh, Y.-L. Oh, and K.-Y. Jang, "Current prospects of mushroom production and industrial growth in India," 한국버섯학회지, vol. 16, no. 4, pp. 239–249, Dec. 2018.

[2] N. Rahmawati and Marbudi, "Analysis of Oyster Mushroom Farming in Highlands (A Case Study in Sleman and Temanggung Indonesia)," *E3S Web Conf.*, vol. 232, p. 01012, 2021.

[3] A. Assemie and G. Abaya, "The Effect of Edible Mushroom on Health and Their Biochemistry," *Int. J. Microbiol.*, vol. 2022, p. 8744788, Mar. 2022.

[4] S. W. You, R. T. Hoskin, S. Komarnytsky, and M. Moncada, "Mushrooms as Functional and Nutritious Food Ingredients for Multiple Applications," *ACS Food Sci. Technol.*, vol. 2, no. 8, pp. 1184–1195, Aug. 2022.

[5] P. Klinlek, N. Samattapapong, and V. D. Cadenet, "Design of Temperature and Humidity Sensor in Mushroom Houses Displayed via Wi-Fi," Art. no. 4641, Nov. 2020, Accessed: Aug. 09, 2022. [Online]. Available: https://easychair.org/publications/preprint/gtW8

[6] A. Najmurrokhman, Kusnandar, U. Komarudin, A. Daelami, and F. Adiputra, "Design and Implementation of Temperature and Humidity Control System in Oyster Mushroom Cultivation

Volume 10, Issue 1, April 2023, pp. 95-102
ISSN 2355-5068 ; e-ISSN 2622-4852
DOI: 10.33019/jurnalecotipe.v10i1.3919

using Fuzzy Logic Controller," in *2019 International Conference on Computer, Control, Informatics and its Applications (IC3INA)*, Oct. 2019, pp. 146–150.

[7] M. A. M. Ariffin *et al.*, "Automatic Climate Control for Mushroom Cultivation using IoT Approach," in *2020 IEEE 10th International Conference on System Engineering and Technology (ICSET)*, Nov. 2020, pp. 123–128.

[8] G. P. Cikarge and F. Arifin, "Oyster Mushrooms Humidity Control Based On Fuzzy Logic By Using Arduino ATMega238 Microcontroller," *J. Phys. Conf. Ser.*, vol. 1140, p. 012002, Dec. 2018.

[9] E. Istiyanti, F. R. Fivintari, and M. Syaftiana, "Potential development of oyster mushrooms in the lowlands of Bantul Regency, Special Region of Yogyakarta, Indonesia," *IOP Conf. Ser. Earth Environ. Sci.*, vol. 423, no. 1, p. 012037, Jan. 2020.

[10] A. H. Bramantara, A. S. Wicaksono, M. Setiawan, M. Q. Yuliyana, and A. P. W. W, "IoT-Based Mushroom Cultivation Monitoring Information System," *Solid State Technol.*, vol. 63, no. 4, Art. no. 4, Nov. 2020.

[11] D. A. Setiawati, S. G. Utomo, Murad, and G. M. D. Putra, "Design of temperature and humidity control system on oyster mushroom plant house based on Internet of Things (IoT)," *IOP Conf. Ser. Earth Environ. Sci.*, vol. 712, no. 1, p. 012002, Mar. 2021.

[12] A. Luis Bustamante, M. A. Patricio, and J. M. Molina, "Thinger.io: An Open Source Platform for Deploying Data Fusion Applications in IoT Environments," *Sensors*, vol. 19, no. 5, p. 1044, Mar. 2019.

JURNAL ECTIPE
Electronic, Control, Telecommunication, Information, and Power Engineering

Volume 10, Issue 1, April 2023, pp. 103-110
ISSN 2355-5068 ; e-ISSN 2622-4852
DOI: 10.33019/jurnalecotipe.v10i1.3924

On the Spectral and Energy Efficiency Analysis of Statistical Clustered-Based MIMO Channel

Uri Arta Ramadhani[1], Purwono Prasetyawan[2]
[1,2]Electrical Engineering, Institut Teknologi Sumatera, Jalan Terusan Ryacudu, Lampung Selatan, 35365, Indonesia

ARTICLE INFO

Article historys:

Received : 15/03/2023
Revised : 10/04/2023
Accepted : 21/04/2023

Keywords:

Clustered Channel; Energy Efficiency; Multiple-Input Multiple-Output; Spectral Efficiency

ABSTRACT

The Multiple-Input Multiple-Output technology played a key role in the accomplishment of user-high data rates. In the evolution of cellular technology to future wireless communication and beyond, the utilization of millimeter waves has been projected to deliver a better performance in terms of capacity and latency. However, the development of this technology is limited by the system's power consumption. The purpose of this study is to examine the impact of clustered channels utilization in terms of spectral and energy efficiency. In this paper, we study the performance of clustered-based channel using multiple antennas by evaluating the spectral efficiency, throughput, and energy efficiency in macrocell (UMa), microcell (UMi), indoor office, and indoor shopping mall scenarios. The simulation result shows that the performance of the system in the UMi type of environment scenario outperforms other scenarios in which 90% of bandwidth utilization reaches 24 bits/s/Hz. Furthermore, the result shows, in UMi deployment, the increase of spectral efficiency is in line with the escalation of the number of antennas and transmit power, which achieves the best spectral utilization at 16x40 antennas and 10 dB, respectively. However, these scenarios consumed most power among others, which is the trade-off of the system.

Corresponding Author:

Uri Arta Ramadhani
Electrical Engineering, Institut Teknologi Sumatera, Jalan Terusan Ryacudu, Lampung Selatan, 35365
Email: uri.ramadhani@el.itera.ac.id.

1. INTRODUCTION

The amount of communication traffic carried by the wireless network has been significantly increasing, which includes and is not limited to video streaming services, online gaming, instant messaging, and Voice over Internet Protocol (VoIP). These types of services are highly dependent on the reliability of the network connectivity which is supported by Multiple-Input Multiple-Output (MIMO) technology. The MIMO technology enables the communication system to transmit several signals from multiple antennas as transmitters and receivers, in a single radio channel [1]. To add more, as cellular technology has moved to 5G, the use of millimeter waves will open the opportunity to achieve multi-Gigabit-per-second [2,3]. The spectrum of millimeter waves technically ranges from 30 to 300 GHz. With smaller wavelengths, the traffic transmission through millimeter waves may use a new spatial processing technique that can provide greater capacity. However, communication through millimeter waves requires a new understanding of channel propagation as the behavior of the channel is different from the currently used frequency spectrum, ranging from 700 MHz to 2.6 GHz [4].

Similar to spectrum frequency as a scarce resource, the availability of energy resources is also one of the main concerns of cellular technology development. The limitation of energy resources is unavoidable causing the restriction to bandwidth expansion [5,6]. Therefore, it is essential to investigate

Volume 10, Issue 1, April 2023, pp. 103-110
ISSN 2355-5068 ; e-ISSN 2622-4852
DOI: 10.33019/jurnalecotipe.v10i1.3924

the performance of wireless communication in the relation to the system energy usage. Better schemes of power consumption is continuously worked on to achieve more efficient energy usage.

Several works have been conducted related to utilizing millimeter waves in 5G communication. The feasibility of utilizing millimeter waves in 5G communication has been put forward by [6] and the technical aspect of millimeter utilization has been discussed in [7, 8, 9, 10]. Jijo et al. has done a comprehensive study on the challenges of 5G millimeter wave [11]. The propagation parameters and channel models for understanding millimeter wave propagation are investigated by [12, 13, 14]. The statistical procedure for generating a clustered MIMO channel model operating at a millimeter wave is proposed in [15]. The study to find the comparison between energy efficiency and spectral efficiency in a heterogeneous network is conducted by [16, 17, 18, 19, 20]. However, the study of energy and spectra on clustered-based channels is still lacking. At this point, it is important to also investigate the relationship between energy and spectral efficiency in a clustered MIMO network operating in millimeter waves, which is the main purpose of this work.

2. RESEARCH METHOD

The work of this study focuses on the performance evaluation of the channels propagation of clustered MIMO channel operating at millimeter waves, concerning spectral efficiency and energy efficiency. The research is conducted by simulating the MIMO channel matrix for linear time-invariant clustered channel model, along with their path loss components. Next, the achievable user rate can be obtained and the spectral efficiency of the system can be measured. Finally, after measuring the throughput and power consumption, the system's energy efficiency is accomplished.

2.1. Clustered MIMO Channel Model

MIMO array is commonly spacious in size, especially massive MIMO which consists of more than eight antennas to offer benefits to multiple simultaneous users. Consequently, as mentioned in [21], a certain amount of cluster paths of the MIMO channel are only visible to some parts of the array, referred to as non-common clusters. However, there are also cluster paths that contain all the signal paths from the whole multiple antennas, namely common clusters. As shown in Figure 1, a single cluster consists of several signal rays and there can be several clusters for an instantaneous time frame. Multipath clusters are defined as propagation paths that have similar angles and delays [21].

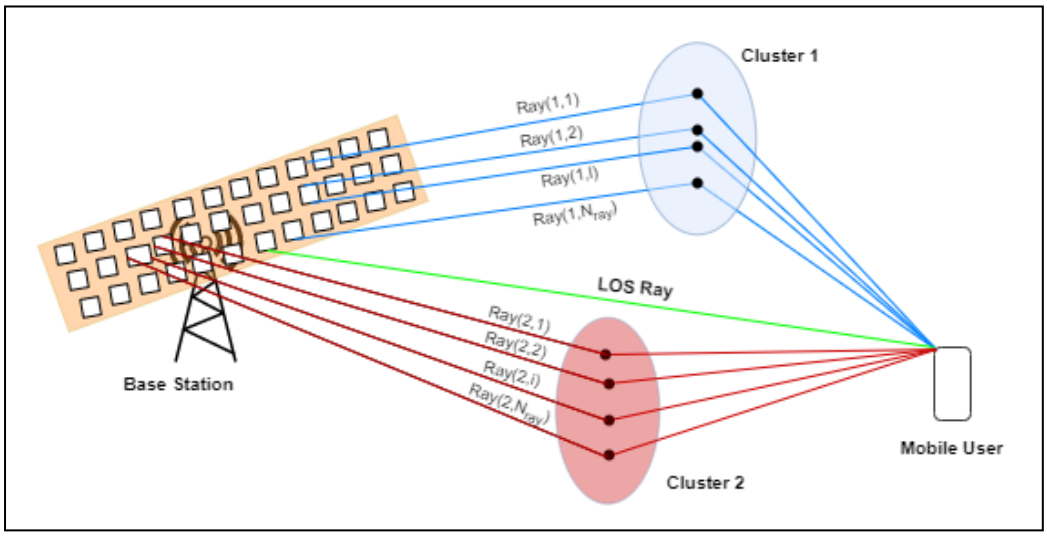

Figure 1. Illustration of clustered-based MIMO channel

In this work, the simulation environment is built based on the work by [15] which consists of a MIMO network with several multiple antennas, N_{TX} and N_{RX}, as the number of transmitter antennas, and receiver antennas, respectively. During the transmission of the signal, there will be several channel clusters, N_{cl}, and each cluster contains several N_{ray} signal paths. The propagation environment is the combination of Line of Sight (LOS) components and Non-LOS (NLOS) components associated with

JURNAL ECTIPE
Electronic, Control, Telecommunication, Information, and Power Engineering
Volume 10, Issue 1, April 2023, pp. 103-110
ISSN 2355-5068 ; e-ISSN 2622-4852
DOI: 10.33019/jurnalecotipe.v10i1.3924

distinct scatters. On the user's side, when there is a communication link from the BS to the user, i.e. downlink communication, a signal which arrived at the user fashions an azimuth angle and elevation angle, denoted by $\Phi_{i,l}^{r}$ and $\theta_{i,l}^{r}$, respectively, for l^{th} signal ray and i^{th} cluster. When the user's mobile phone transmits signals to the BS, the signals also form an azimuth angle and elevation angle, denoted by $\Phi_{i,l}^{t}$ and $\theta_{i,l}^{t}$. The linear-time-invariant channel matrix, $\boldsymbol{H}(\tau)$, can be written as:

$$\boldsymbol{H}(\tau) = \gamma \sum_{i=1}^{N_{cl}} \sum_{l=1}^{N_{ray}} \alpha_{i,l} \sqrt{PL(f, r_{(i,l)})} \boldsymbol{a}_r(\Phi_{i,l}^{r}, \theta_{i,l}^{r}) \times \boldsymbol{a}_t^{H}(\Phi_{i,l}^{t}, \theta_{i,l}^{t}) h(\tau - \tau_{i,l}) + \boldsymbol{H}_{LOS}(\tau) \quad (1)$$

Where γ is a normalization factor to linearly scale signal power with the product of $N_{RX}N_{TX}$, whose value is based on [22]. $\alpha_{i,l}$ is the complex path gain, $\boldsymbol{a}_r(\Phi_{i,l}^{r}, \theta_{i,l}^{r})$ and $\boldsymbol{a}_t^{H}(\Phi_{i,l}^{t}, \theta_{i,l}^{t})$ are the normalized array response vectors evaluated at the corresponding angle of arrival and departure signal, respectively. $h(\tau - \tau_{i,l})$ is the $\tau_{i,l}$ delayed version of channel response which is attained by a convolution between the channel baseband of transmit waveform, $h_{(TX)}(t)$, and the channel baseband of the receive filter signal waveform $h_{(RX)}(t)$. $PL(f, r_{(i,l)})$ is the path loss (PL) associated with the (i,l)-th propagation path, which will be specified in the next section. $\boldsymbol{H}_{LOS}(\tau)$ is the channel matrix for the LOS condition, which is written as [15]:

$$\boldsymbol{H}_{LOS}(\tau) = I_{LOS}(d) \sqrt{N_{RX}N_{TX}} e^{j\eta} \sqrt{PL_{LOS}} \boldsymbol{a}_r(\Phi_{LOS}^{r}, \theta_{LOS}^{r}) \times \boldsymbol{a}_t^{H}(\Phi_{LOS}^{t}, \theta_{LOS}^{t}) h(\tau - \tau_{LOS}) \quad (2)$$

With η is uniformly distributed phase, PL_{LOS} is the attenuation of a signal transmitted from the transmitter and receiver without the existence of obstructions, which is called free space loss (FSPL). $I_{LOS}(d)$ is a parameter that indicates if there is a LOS link between BS and the user. The setting p is the probability of LOS link occurrence, which will give $I_{LOS}(d) = 1$. The existence of the LOS link will depend on the deployment scenarios. In this paper, the scenarios are simulated for four different types, i.e. Urban Macrocellular (UMa), Urban Microcellular (UMi), Indoor Hotspot (InH) Office, and InH Shopping Mall. The value of p for each scenario follows [23] which is written in Table 1.

Table 1. Calculation of p for different scenarios

UMa	$p = \left(min\left(\frac{18}{d}, 1\right)\left(1 - e^{-\frac{d}{63}}\right) + e^{-\frac{d}{63}}\right), for\ receiver\ height = 1\ meter$
UMi	$p = min\left(\frac{20}{d}, 1\right)\left(1 - e^{\frac{-d}{39}}\right) + e^{\frac{-d}{39}}$
InH	$p = \begin{cases} 1, d \le 1.2 \\ e^{-\left(\frac{d-1.2}{4.7}\right)}, 1.2 \le d \le 6.5 \\ 0.32e^{-\left(\frac{d-6.5}{32.6}\right)}, d \ge 6.5 \end{cases}$

where d is the distance between the transmitter and the receiver.

2.2. Path Loss Model

Path loss is defined as the signal power lost due to the dissipation of the transmitter power and the effects of the propagation channel [24, 25]. The simplest path loss model for signal propagation is FSPL which the signal propagation path between transmitter and receiver forms a straight line, without any obstacles. The other common path loss models are the Ray-tracing model and the empirical model. The ray-tracing model depends on the geometry and the dielectric properties of the region where the signal propagates. The empirical model is built upon the realistic measurement of the indoor and outdoor propagation channels.

As the technology of wireless communication is continuously evolving, the path loss model for 5G communication is also developed. The channel models for the 5G network for frequency up to 100 GHz has been derived [23]. The path loss model for the system that is used in this work is a close-in free (CIF) space reference distance model with frequency-dependent path loss exponent [23, 26], given by:

$$PL(f, r_{(i,l)})[dB] = FSPL(f, 1\ m) + 10n\left(1 + b\left(\frac{f - f_0}{f_0}\right)\right) log_{10}\left(\frac{r_{(i,l)}}{1\ m}\right) + X_{\sigma} \quad (3)$$

JURNAL ECTIPE
Electronic, Control, Telecommunication, Information, and Power Engineering
Volume 10, Issue 1, April 2023, pp. 103-110
ISSN 2355-5068 ; e-ISSN 2622-4852
DOI: 10.33019/jurnalecotipe.v10i1.3924

Where $PL(f, r_{(i,l)})$ is the path loss for cluster i-th and array l-th, $FSPL\ (f, 1\ m)$ is the free space path loss (FSPL) for d is 1 meter, n is the path loss exponent, b denotes the system parameter that captures the slope, f_0 is the reference frequency, $r_{(i,l)}$ is the path length for a signal path in cluster i-th and array l-th, and X_σ is the shadow fading in dB. $r_{(i,l)}$ is calculated based on the geometrical properties, depending on the height of BS and user's terminal.

The values for the parameters in (3) for each scenario are based on the previous related works [23], [26], as presented in Table 2.

Table 2. Model Parameters for Different Scenarios

Scenario	Value Parameter n	Value Parameter b	Value Parameter f_0	Value Parameter X_σ
UMa	3.0	0	49 GHz	6.8 dB
UMi	3.19	0	49 GHz	8.2 dB
InH Office	3.19	0.06	24.2 GHz	8.29 dB
InH Shopping Mall	2.59	0.01	39.5 GHz	7.40 dB

2.3. Spectral Efficiency

Based on [27], spectral efficiency is defined as the average number of bits that can be transmitted per complex-valued sample, measured in bit/s/Hz. For the complex-baseband signal representation, B complex-valued samples per second are legitimate [28]. The maximum spectral efficiency is determined by the channel capacity which relates to the information rate of the system.

The baseband equivalent of the received signal at time sampling n is written as [15]:

$$\boldsymbol{r}(n) = \sum_{l=0}^{P-1} \boldsymbol{D}^H \boldsymbol{H}(l) \boldsymbol{Q} \boldsymbol{s}(n-l) + \boldsymbol{D}^{\boldsymbol{H}} \boldsymbol{w}(n) \quad (4)$$

Where P is the length of the channel, $\boldsymbol{D}$ is the combining matrix and $\boldsymbol{Q}$ is the precoding matrix. The dimension of $\boldsymbol{D}$ and $\boldsymbol{Q}$ depend on the dimension of antenna elements in the BS and the user's terminal, respectively. $\boldsymbol{s}(n)$ is the vector of the data symbol, transmitted from the BS at the time n, with the dimension of M the number of information symbols. $\boldsymbol{w}(n)$ is the additional noise vector. To obtain the estimation of $\boldsymbol{s}(n)$, i.e. $\hat{s}(n)$, the Linear Minimum Mean-Squared Error (LMMSE) using a matrix estimator $\boldsymbol{E}$, which aims to minimize mean-squared error (MSE) $\mathbb{E}\|\boldsymbol{s}(n) - \hat{\boldsymbol{s}}(n)\|^2$. $\hat{\boldsymbol{s}}(n)$ can be written as $\hat{\boldsymbol{s}}(n) = \boldsymbol{E}^H \boldsymbol{A} \boldsymbol{s}(n) + \boldsymbol{E}^H \boldsymbol{A}_I \boldsymbol{s}_I(n) + \boldsymbol{E}^H \boldsymbol{B} \boldsymbol{w}$. The first term contains $\boldsymbol{A}$, as the desired symbols. The second term consists of $\boldsymbol{A}_I$ and $\boldsymbol{s}_I(n)$ are a signature matrix and the symbol, respectively, appeared due to interference. The third term is the noise component. The information rate at the user's terminal is expressed as [15], [29]:

$$\mathcal{R} = log_2 det \left[\boldsymbol{I}_M + \left| \boldsymbol{E}^H \left(\frac{P_T}{M} \boldsymbol{A}_I \boldsymbol{A}_I^H + \sigma_N^2 \boldsymbol{B}\ \mathbb{E}[\boldsymbol{w}(n) \boldsymbol{w}^H(n) \boldsymbol{B}^H] \right) \boldsymbol{E} \right|^{-1} \left(\frac{P_T}{M} \boldsymbol{E}^H \boldsymbol{A} \boldsymbol{A}^H \boldsymbol{E} \right) \right] \quad (5)$$

Where P_T is the transmit power and $\boldsymbol{B}$ is the available bandwidth. By normalizing the user's information rate to the bandwidth $\boldsymbol{B}$, the achievable spectral efficiency can be obtained.

2.4. Energy Efficiency

"The energy efficiency of a cellular network is the number of bits which can reliably transmitted per unit energy" [27]. The energy efficiency can be measured by:

$$\text{Energy Efficiency (bit/}Joule) = \frac{Bandwidth \times Spectral\ Efficiency\ (bit/s)}{Power\ Consumption\ (Watt)} \quad (6)$$

Equation (6) shows that the energy efficiency indicates the efficiency of delivering bits from the transmitter and the receiver. The power consumption (PC) of the system is calculated by [27]:

$$PC = ETP + CP \quad (7)$$

Where ETP is effective transmit power, i.e. transmit power of the BS, and CP is the circuit power. In this work, the CP model of a BS follows [27] which is composed of power consumption of fixed power, transceiver chains, channel estimation, signal processing, coding/decoding, load-dependent

JURNAL ECTIPE
Electronic, Control, Telecommunication, Information, and Power Engineering
Volume 10, Issue 1, April 2023, pp. 103-110
ISSN 2355-5068 ; e-ISSN 2622-4852
DOI: 10.33019/jurnalecotipe.v10i1.3924

backhaul, and signal processing. The values of those parameters are based on [27] for the MMSE scheme. The total CP in single cell MMSE is 26.51 Watts for 100 multiple antennas.

3. RESULTS AND DISCUSSION

This section provides the simulation results of the system model described in prior. In this work, we consider 73 GHz carrier frequency and there are 6 data symbols in each transmission. In the Uma scenario, the height of BS h_{TX}, is 30 meters, and the height of the user's terminal, h_{RX}, is 1 meter, and d is 60 meters. For UMi, InH Office, and InH Shopping Mall scenario, h_{TX} is 7 meters, h_{RX} is 1 meter and d is 5 meters.

Figure 2 presents the Cumulative Distribution Function (CDF) of the spectral efficiency for four different scenarios simulated in this work when the user's terminal has 20 multiple antennas and there are 40 multiple antennas in the BS. It can be observed that the spectral efficiency of UMi scenario outperforms other scenarios. In UMi deployment, 90% of bandwidth utilization reaches 24 bits/s/Hz. However, those value is not much different for the InH Shopping Mall scenario. In the scenario of InH Office, there is around 18 bits/s/Hz for the same portion of bandwidth usage. The last performance occurs in the UMa scenario in which 90% of users receive around 7 bits/s/Hz, and achieve only 10 bits/s/Hz at maximum. The distinguished performance of the UMi deployment can be the result of a shorter range of BS's transmit power hence the propagation is less. While for indoor deployment, the performance is influenced by the walls blocking the signals and the materials of the building.

The performance of the clustered-based channel is also evaluated by varying the number of antenna elements having a UMi scenario. In Figure 3, it can be observed that as the amount of antenna elements increases, the user is able to achieve a higher data rate. For 16x40 MIMO, the user's achievable rate is the highest as many as 17 Mbps, compared to other MIMO schemes. The increase of user data rate in this work is similar to the spectral efficiency performance in [15], in which the rise of spectral efficiency is in line with the increment of the number of antennas. However, for a 16x40 MIMO scenario, the energy efficiency only reaches around 1 Mbit per Joule, which is the lowest performance. By using 16x16 MIMO, the system is able to perceive the most efficient energy usage with 1.5 Mbit per Joule. This happens in line with the fact that the system power consumption escalates in magnitude as the rise of number of antenna elements. Although the user's rate can be improved by adding multiple antennas, the efficiency of the energy in power usage will be the trade-off.

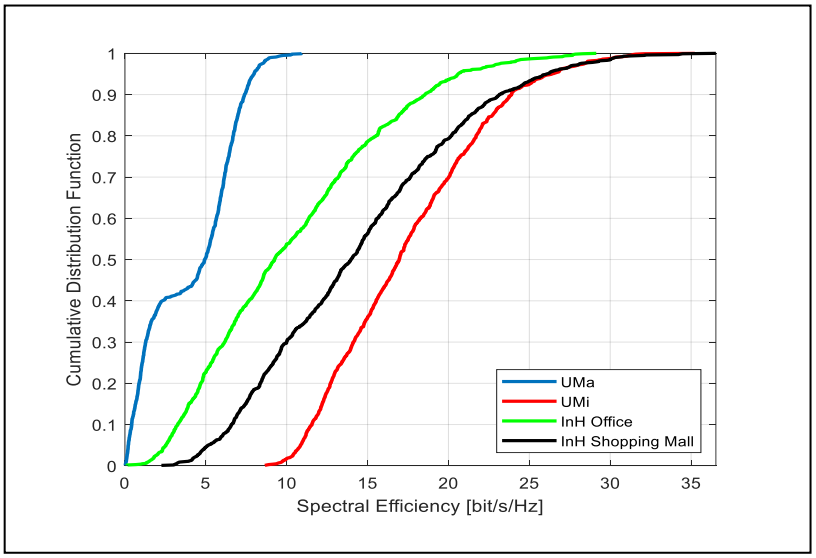

Figure 2. CDF of spectral efficiency for different deployment scenarios

JURNAL ECTIPE
Electronic, Control, Telecommunication, Information, and Power Engineering
Volume 10, Issue 1, April 2023, pp. 103-110
ISSN 2355-5068 ; e-ISSN 2622-4852
DOI: 10.33019/jurnalecotipe.v10i1.3924

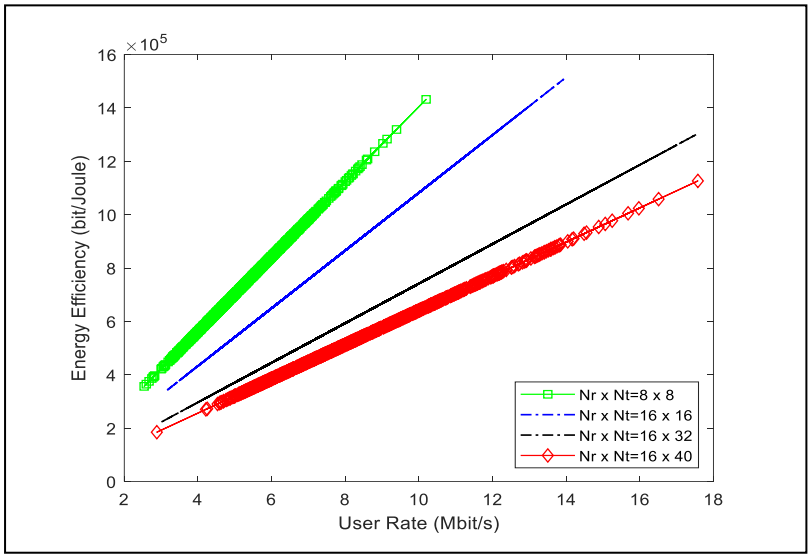

Figure 3. Energy efficiency as a function of achievable user rate for different number of antenna elements

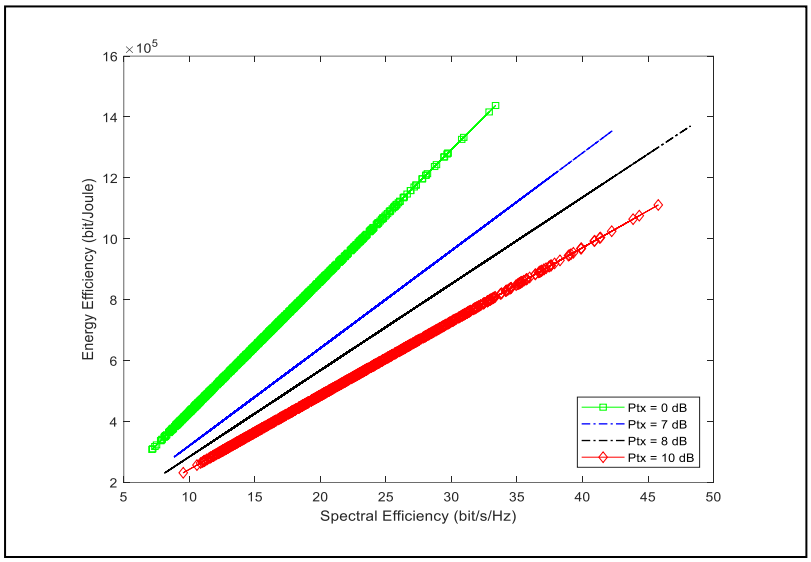

Figure 4. Energy efficiency versus spectral efficiency for different cases of BS transmit power

Figure 4. presents the spectral and energy efficiency considering different schemes of transmit power with fixed 40x40 antenna elements in MIMO. With higher power transmitted by the BS, the spectral efficiency also scales up as the user experiences a better information rate. Among various values of transmit power simulated in this work, using 8 dB transmit power results in a spectrum efficiency of 48 bit/s/Hz which outperforms other transmit power schemes, while having around 1.3 Mbit per Joule which is not much different when using 0 dB and 7 dB transmit power. This result is similar to the one conducted by [30] which for higher transmit power there is a trade-off between spectral and energy efficiency for cell-free massive MIMO. However, the simulation conducted in this study does not include the velocity of moving users which is the limitation of this work.

4. CONCLUSION

This research is conducted to investigate the performance of the cluster-based channel in the MIMO system operating in millimeter waves in terms of spectral and energy efficiency. Based on the simulation on UMa, UMi, InH Office, and InH Shopping Mall scenarios, the deployment of the clustered channel on UMi has the best performance where 90% of users can achieve 24 bits/s/Hz spectral efficiencies,

Volume 10, Issue 1, April 2023, pp. 103-110
ISSN 2355-5068 ; e-ISSN 2622-4852
DOI: 10.33019/jurnalecotipe.v10i1.3924

which can be caused by the shorter range of BS's transmit power. Moreover, by controlling several system parameters in the simulation including schemes of environment type, the number of antenna elements in MIMO, and the power transmitted by the BS, it can be concluded that there is a trade-off between spectral efficiency and energy efficiency. Having a good efficiency in spectrum utilization, there will be the price in the low efficiency of energy usage. However, by increasing the number of antennas and BS transmit power, the performance of energy efficiency does not always surpass those with lower power, as shown in the simulation result above that by using 16x40 MIMO antennas and 10 dB transmit power, the performance of energy efficiency is the least among others. Hence, this research has contribution in the selection of values of related parameters considered when designing the cluster-based channel MIMO system.

REFERENCES

[1] C. Cardona, *Cooperative Radio Communication for Green Smart Environments*. River Publishers, 2022.

[2] R. Y. Li, B. Gao, X. Zhang, and et al., "Beam Management in Millimeter-Wave Communications for 5G and Beyond," *IEEE Access*, vol. 8, pp. 13282–13293, 2020.

[3] R. Mittra, A. Nasri, and R. K. Arya, "Wide-Angle Scanning Antennas for Millimeter-Wave 5G Applications," *Engineering*, vol. 11, pp. 60–71, 2022, doi: 10.1016/j.eng.2021.10.017.

[4] T. S. Rappaport, S. Sun, R. Mayzus, and et al., "Millimeter Wave Mobile Communications for 5G Cellular: It Will Work!," *IEEE Access*, vol. 1, pp. 335–349, 2013, doi: 10.1109/ACCESS.2013.226081.

[5] I. Ezeh and I. A. Ezenugu, "Challenges of Bandwidth and Power Limitations in Cellular Communication: A Review," *IOSR J. Mob. Comput. Appl. IOSR-JMCA*, vol. 7, no. 4, pp. 01–11, 2020, doi: 10.9790/0050-07040111.

[6] J. Yi, B. Huang, and et al., "Edge-Based Collaborative Training System for Artificial Intelligence-of-Things," *IEEE Trans. Ind. Inform.*, vol. 18, no. 10, pp. 7162–7173, 2022, doi: 10.1109/TII.2022.3147831.

[7] Sehrai, D. Ali, and et al., "A novel high gain wideband MIMO antenna for 5G millimeter wave applications," *Electronics*, vol. 9, no. 6, p. 1031, Jun. 2020, doi: https://doi.org/10.3390/electronics9061031.

[8] M. Sung, J. Kim, and et al., "5G Trial Services Demonstration: IFoF-Based Distributed Antenna System in 28 GHz Millimeter-Wave Supporting Gigabit Mobile Services," *J. Light. Technol.*, vol. 37, no. 14, pp. 3592–3601, 2019, doi: 10.1109/JLT.2019.2918322.

[9] Y. Hong, I. Hwang, and et al., "Design of Single-Layer Metasurface Filter by Conformational Space Annealing Algorithm for 5G mm-Wave Communications," *IEEE Access*, vol. 9, pp. 29764–29774, 2021, doi: 10.1109/ACCESS.2021.3059019.

[10] H. Askari, N. Hussain, and et al., "A Wideband Circularly Polarized Magnetoelectric Dipole Antenna for 5G Millimeter-Wave Communications," *Sens. 2*, vol. 22, no. 6, 2022, doi: https://doi.org/10.3390/s22062338.

[11] A. Gupta, A. V. H. Vardhan, and et al., "Performance Analysis at different millimetre wave frequencies for indoor shopping complex and outdoor UAV applications towards 5G," *Microprocess. Microsyst.*, vol. 9, 2022, doi: https://doi.org/10.1016/j.micpro.2022.104506.

[12] Jijo, B. Taha, and et al., "A Comprehensive Survey of 5G mm-Wave Technology Design Challenges," *Asian J. Res. Comput. Sci.*, vol. 8, no. 1, pp. 1–20, 2021, doi: 10.9734/ajrcos/2021/v8i130190.

[13] D. Liu, W. Hong, T. S. Rappaport, and et al., "What will 5G antennas and propagation be?," *IEEE Trans. Antennas Propag.*, vol. 65, no. 12, pp. 6205–6212, doi: 10.1109/TAP.2017.2774707.

[14] Y. Zhang, J. Zhang, and L. Yu, "Cluster-Based Fast Time-Varying MIMO Channel Fading Prediction in the High-Speed Scenario," *IEEE Access*, 2019, doi: 10.1109/ACCESS.2019.2946881.

Volume 10, Issue 1, April 2023, pp. 103-110
ISSN 2355-5068 ; e-ISSN 2622-4852
DOI: 10.33019/jurnalecotipe.v10i1.3924

[15] R. He and et al., "Propagation Channels of 5G Millimeter-Wave Vehicle-to-Vehicle Communications: Recent Advances and Future Challenges," *IEEE Veh. Technol. Mag.*, vol. 15, no. 1, pp. 16–26, 2020, doi: 10.1109/MVT.2019.2928898.

[16] S. Buzzi and C. D'Andrea, "On Clustered Statistical MIMO Millimeter Wave Channel Simulation," *IEEE Wirel. Commun. Lett.*, 2016, doi: https://doi.org/10.48550/arXiv.1604.00648.

[17] C. C. Coskun and E. Ayanoglu, "Energy- and Spectral-Efficient Resource Allocation Algorithm for Heterogeneous Networks," *IEEE Trans. Veh. Technol.*, vol. 67, no. 1, pp. 590–603, Jan. 2018, doi: 10.1109/TVT.2017.2743684.

[18] Ruan, Y. Li, Y. Wang, and et al., "Power allocation in cognitive satellite-vehicular networks from energy-spectral efficiency tradeoff perspective," *IEEE Trans. Cogn. Commun. Netw.*, vol. 5, no. 2, pp. 318–329, 2019, doi: 10.1109/TCCN.2019.2905199.

[19] L. Sboui, Z. Rezki, and M. Alouini, "A New Relation Between Energy Efficiency and Spectral Efficiency in Wireless Communications Systems," *IEEE Wirel. Commun.*, vol. 26, no. 3, pp. 168–174, Jun. 2019, doi: 10.1109/MWC.2019.1800161.

[20] A. Khazali, S. Sobhi-Givi, and et al., "Energy-spectral efficient resource allocation and power control in heterogeneous networks with D2D communication," *Wirel. Netw.*, vol. 26, pp. 253–267, 2020, doi: https://doi.org/10.1007/s11276-018-1811-3.

[21] D. Li, "How Many Reflecting Elements Are Needed for Energy- and Spectral-Efficient Intelligent Reflecting Surface-Assisted Communication," *IEEE Trans. Commun.*, vol. 70, no. 2, pp. 1320–1331, Feb. 2022, doi: 10.1109/TCOMM.2021.3128544.

[22] J. Li, B. Ai, R. He, and et al., "A Cluster-Based Channel Model for Massive MIMO Communications in Indoor Hotspot Scenarios," *IEEE Trans. Wirel. Commun.*, vol. 18, no. 8, pp. 3856–3870, Aug. 2019, doi: 10.1109/TWC.2019.2919026.

[23] O. E. Ayach, S. Rajagopal, and et al., "Spatially Sparse Precoding in Millimeter Wave MIMO Systems," *IEEE Trans. Wirel. Commun.*, vol. 13, no. 3, pp. 1499–1513, Mar. 2014, doi: 10.1109/TWC.2014.011714.130846.

[24] "5G Channel Model for bands up to100 GHz." [Online]. Available: http://www.5gworkshops.com/2015/5G_Channel_Model_for_bands_up_to100_GHz(2015-12-6).pdf

[25] A. Goldsmith, *Wireless Communication*. Cambridge University Press, 2005.

[26] A. Goldsmith, D. Gunduz, and et al., *Machine Learning and Wireless Communications*. New York: Cambridge University Press, 2022.

[27] G. R. Mccartney, T. S. Rappaport, and S. Sun, "Indoor Office Wideband Millimeter-Wave Propagation Measurements and Channel Models at 28 and 73 GHz for Ultra-Dense 5G Wireless Networks," *IEEE Access*, vol. 3, pp. 2388–2424, Oct. 2015, doi: 10.1109/ACCESS.2015.2486778.

[28] E. Bjornson, J. Hoydis, M. Kountouris, and M. Debbah, "Massive MIMO Systems With Non-Ideal Hardware: Energy Efficiency, Estimation, and Capacity Limits," *IEEE Trans. Inf. Theory*, vol. 60, no. 11, pp. 7112–7139, Nov. 2014, doi: 10.1109/TIT.2014.2354403.

[29] R. Sobot, *Wireless Communication Electronics*. Springer International Publishing, 2020.

[30] F. Negro, S. P. Shenoy, I. Ghauri, and D. T. M. Slock, "On the MIMO interference channel," presented at the 2010 Information Theory and Applications Workshop (ITA), La Jolla, CA, USA, La Jolla, CA, USA: IEEE, 2010, pp. 1–9. doi: 10.1109/ITA.2010.5454085.

[31] N. Li, Y. Gao, and K. Xu, "On the optimal energy efficiency and spectral efficiency trade-off of CF massive MIMO SWIPT system," *EURASIP J. Wirel. Commun. Netw.*, 2021, doi: 10.1186/s13638-021-02035-w.

JURNAL ECOTIPE
Electronic, Control, Telecommunication, Information, and Power Engineering

Volume 10, Issue 1, April 2023, pp. 111-120
ISSN 2355-5068 ; e-ISSN 2622-4852
DOI: 10.33019/jurnalecotipe.v10i1.3925

Direct Torque Control Design with Fuzzy Sugeno-Propotional Derivative for 3-Phase Induction Motor Speed Control

Ahmad Faizal[1], Agustiawan[2], Nanda Putri Miefthawati[3], Mulyono[4], Rudy Kurniawan[5], Elfira Safitri[6], Corry Corazon Marzuki[7], Rahmadeni[8]

[1,2,3,4]Electrical Engineering, UIN Sultan Syarif Kasim Riau, Jl.HR. Soebrantas No. Km 15, Riau, 28923
[5]Electrical Engineering, Bangka Belitung University, Balunijuk, Bangka, 33172, Indonesia
[6,7,8]Mathematics, UIN Sultan Syarif Kasim Riau, Jl.HR. Soebrantas No. Km 15, Riau, 28923

ARTICLE INFO

Article historys:

Received : 17/03/2023
Revised : 10/04/2023
Accepted : 21/04/2023

Keywords : 3 Phase Inductor Motor; Direct Torque Control; Fuzzy Sugeno; Proportional-Derivative

ABSTRACT

An induction motor is an electric motor that works based on induction currents. In general, induction motors are more used in the industry than DC motors due to the characteristics of induction motors, which are robust, reliable, easy to maintain, and relatively inexpensive. Rotational speed changes with load changes can lead to induction motor speed regulation, and slowing response time, but overshoot caused by external environmental factors should be minimized. Due to interference, a controller is needed that can work properly to optimize performance. The purpose of this research is to design a Kanno PD Fuzzy DTC controller that provides a fast and strong response on DTCs mounted on AC motors. Based on the research result obtained Fuzzy Sugeno provides a short computation time and its inference contains enough data and PD to speed up reaction time results. Therefore, the proposed method produces the rotational speed of the induction motor according to the specified settings of 100 rad/s with a settling time of 0.45 s, a rise time of 0.2 s, and no steady-state error. Based on the predicted state of the output response before it is sent to the controller, the steady-state error is obtained at 5 rad/s with a maximum overshoot of 5.4111%, a settling time of 0.1554 seconds, and a rise time of 0.1554 seconds.

Corresponding Author:

Ahmad Faizal
Electrical Engineering, Faculty of Science and Technology, UIN Sultan Syarif Kasim Riau, 28129, Pekanbaru
Email: ahmad.faizal@uin-suska.ac.id

1. INTRODUCTION

Since the 19th century, induction motors have undergone improvements to the present. These improvements are made so that the operation works more optimally, for example by operating it as a synchronous-asynchronous machine, changing the number of poles in the stator winding, controlling with electronic systems, and so on [1]. Progress in the industrial sector in our country is growing rapidly, both large and small industries. Large industries use induction motors, because of their simple construction, robustness, relatively easy maintenance, lighter weight, high efficiency, and low cost compared to other motors such as DC motors. In an induction motor, there is no contact between the stator and the rotor except the bearing, then the power is quite large, the electric power is low and there is almost no maintenance [2,3]. In directing the speed of an induction motor at a decent speed and variable speed, frequency or torque is needed [4]. The power converter is used to set the induction motor parameters so that the motor speed can be affected by setting the input motor parameters [5].

Efforts to improve the limitations of the alternating current motor for control purposes consist of two methods, namely scalar and vector settings. In this study, the authors used vector control, in which

Volume 10, Issue 1, April 2023, pp. 111-120
ISSN 2355-5068 ; e-ISSN 2622-4852
DOI: 10.33019/jurnalecotipe.v10i1.3925

the vector control method to separate the flux from the rotor so that the speed control could work in a steady state and could not only adjust the speed angle and magnitude, but also the current, voltage, and flux [6]. This 3-Phase induction motor has a weak point, namely one of them, if it is disturbed, the speed is not constant. Giving this disturbance will cause changes in motor parameters so that the speed of the induction motor drops and does not reach the setpoint value [7,8].

To make the motor speed stable or have good performance, requires a controller to regulate the speed of a 3-Phase induction motor. There is research on 3-Phase induction motors that have been carried out, one of which uses DTC-based Fuzzy but there is still an overshoot of 2.67% with a rise time of 0.025 seconds and a settling time of 0.2 seconds When the motor changes, the rotation reference becomes 74.51 rad/second with of 12.64 N-m occurs 94.6% overshoot, rise time 0.018 seconds and settling time 0.325 seconds [2]. In this study, there is still an overshoot and it is still oscillating, but the overshoot when the rotation reference changes occur is very large. In another study using the Flux Vector Control method based on PI Self Tuning. In this study, controlling the speed of an induction motor using a self-tuning PI controller for quadrature currents was able to reduce the motor speed overshoot from 132.8 rad/s to 119.2 rad/s [3]. So in this study, there is still overshoot, but the overshoot using self-tuning pi is smaller than the overshoot with conventional PI.

In another study, 3-Phase induction motors have been studied using Fuzzy Mamdani based on field-oriented control methods. In this study the test results and responses showed that the settling time was around 0.27 seconds, the rise time was around 0.29 seconds, the overshoot was around 2.7%, the undershoot was 0.5% and the steady state error was around 2% [7]. So in this study, there is still a fairly large overshoot and the steady state is close to 0. DTC is a control method based on adjusting the magnetic flux and stator torque and provides a fast and powerful response installed in AC motors. DTC was proposed by Isao Takahashi and Toshihiko Noguchi in 1980. DTC has easier construction, less computational requirement, and higher performance and execution. The DTC method makes it possible to directly set the switching conditions on the inverter with Space Vector Modulation. Even so, the conventional DTC setting scheme still uses a PI controller so that if there is a change in the load on the motor, the motor's speed response will decrease, not according to the given reference speed. [9].

As for the research regarding 3-Phase induction motors using DTC modeling, namely in this study the DTC controller settings can provide the performance is quite good where the overshoot and steady state are close to 0 and the rise time and settling time are quite fast but in this study oscillations still occur [10]. According to Cox (1994), there are several reasons why Fuzzy logic is used is because the idea of Fuzzy logic is easy, fully customizable, can bear wrong information, can show very complex nonlinear capabilities, and can help. usual control methods and given the normal language [11]. In Fuzzy logic there are usually several methods, namely the Mamdani method and the Sugeno method, However, in this study, the authors wanted to use Fuzzy Sugeno because the calculation time was short and the reasoning included quite extensive data [12].

Research using the Sugeno Fuzzy controller is a comparison between Fuzzy Sugeno and Fuzzy Mamdani on DC motors that do not have overshoot and to reach a set point, and when compared to computing between Fuzzy Sugeno and Mamdani to reach a steady state, Fuzzy Sugeno is faster. However, to reach the steady state mean (SE), Mamdani is faster than Sugeno and the delta error Mamdani is more stable than Fuzzy Sugeno.[12] In the research above, Fuzzy Sugeno has been able to get good results, but to further optimize better results, in this study adding a PD controller to speed up the system response in reaching the set point [13]. Based on the background description above, the authors are interested in conducting research using the Fuzzy Sugeno-PD DTC control for controlling 3-Phase induction motors.

2. RESEARCH METHOD

The flow of research begins with literature study, problem identification, data collection, variable determination in the form of transfer functions of 3-Phase induction motor systems, validation of mathematical models, designing DTC controllers, Fuzzy Mamdani controllers, combining DTC controllers, Fuzzy Mamdani with PD, analyzing the design results controller and the last is to draw conclusions based on the results of the research.

JURNAL ECOTIPE
Electronic, Control, Telecommunication, Information, and Power Engineering
Volume 10, Issue 1, April 2023, pp. 111-120
ISSN 2355-5068 ; e-ISSN 2622-4852
DOI: 10.33019/jurnalecotipe.v10i1. 3925

2.1 3-Phase Motor Induction

3-Phase induction motor is one of the motors in which an electric device converts electrical energy into mechanical energy with the converted electric power being 3-Phase electricity. This 3-Phase induction motor is quite widely used in today's industries and has also been used in households. This machine is used because it is very strong, and straightforward and the price is relatively cheap. According to the findings of experts towards the end of the 19th century, it is said to be an induction motor because the motor rotor current is an induced current as a result of the difference between the rotor rotation and the rotating field generated by the stator current. In general, there are 2 main construction parts in an induction motor, namely the stator and the rotor. The stator is the stationary part and the rotor is the rotating part. The construction of an induction motor can be seen in Figure 2.1 [1].

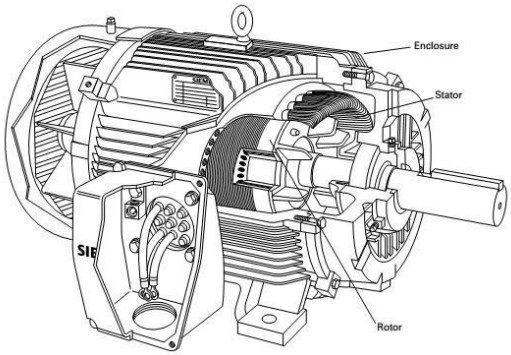

Figure 1. General structure of an ac motor

2.2 Mathematical Modeling

Table 1 is the parameter values that will be used to calculate the mathematical model of a 3-Phase induction motor.

Table 1. Parameter 3-Phase induction motor [25]

No	Name	Value
1	Motor Power (Hp)	3/2,4 Kw
2	Motor Voltage (line to line)(Volt)	460
3	Frekuensi (Hz)	60
4	Nomber Of Pole	4
5	Stator Resistance(Ohm)	1,77
6	Tahanan Resistance (Ohm)	1,34
7	Sator Inductance(mH)	0,3829
8	Rotor Inductance (mH)	0,3811
9	Magnetic Inductance (mH)	0,369
10	Moment of Inertia (Kg.M^2)	0,025
11	Full Load Current (A)	4
12	Full Load Speed (RPM)	1750
13	Full Load Efficiency (%)	88,5
14	Power Faktor (%)	80
15	Full Load Slip (%)	1,72

After doing the writing research, a mathematical model of the plant was obtained, especially the induction motor so that it tends to be simulated by the plant and the quality of the plant in the product used. The mathematical model of the induction motor used in this design can be obtained from formula (1). Equation (1) needs to be simplified again so that the simulation in Matlab is easy to manufacture. The simplification process is:

$$\begin{bmatrix} V_{qs} \\ V_{ds} \\ V_{qr} \\ V_{dr} \end{bmatrix} = \begin{bmatrix} R_s+pL_s & \omega_e.L_s & pL_m & \omega_e.L_m \\ -\omega_e.L_s & R_s+pL_s & -\omega_e.L_m & pL_m \\ pL_m & (\omega_e-\omega_r)L_m & R_r+pL_r & (\omega_e-\omega_r)L_r \\ -(\omega_e-\omega_r)L_m & pL_m & -(\omega_e-\omega_r)L_r & R_r+pL_r \end{bmatrix} \begin{bmatrix} i_{qs} \\ i_{ds} \\ i_{qr} \\ i_{dr} \end{bmatrix} \quad (1)$$

JURNAL ECTIPE
Electronic, Control, Telecommunication, Information, and Power Engineering
Volume 10, Issue 1, April 2023, pp. 111-120
ISSN 2355-5068 ; e-ISSN 2622-4852
DOI: 10.33019/jurnalecotipe.v10i1.3925

A separation is made between variables that contain their derivatives, so that the form of the equation becomes:

$$\begin{bmatrix} V_{qs} \\ V_{ds} \\ V_{qr} \\ V_{dr} \end{bmatrix} = \begin{bmatrix} R_s & \omega_e.L_s & 0 & \omega_e.L_m \\ -\omega_e.L_s & R_s & -\omega_e.L_m & 0 \\ 0 & (\omega_e-\omega_r)L_m & R_r & (\omega_e-\omega_r)L_r \\ -(\omega_e-\omega_r)L_m & 0 & -(\omega_e-\omega_{r)} & R_r+pL_r \end{bmatrix} \begin{bmatrix} i_{qs} \\ i_{ds} \\ i_{qr} \\ i_{dr} \end{bmatrix} + \begin{bmatrix} pL_s & 0 & pL_m & 0 \\ 0 & pL_s & 0 & pL_m \\ pL_m & 0 & pL_r & 0 \\ 0 & pL_m & 0 & pL_r \end{bmatrix} \begin{bmatrix} i_{qs} \\ i_{ds} \\ i_{qr} \\ i_{dr} \end{bmatrix} \quad (2)$$

In another form, the above equation can be as follows:

$$\begin{bmatrix} V_{qs} \\ V_{ds} \\ V_{qr} \\ V_{dr} \end{bmatrix} = \begin{bmatrix} R_s & \omega_e.L_s & 0 & \omega_e.L_m \\ -\omega_e.L_s & R_s & -\omega_e.L_m & 0 \\ 0 & (\omega_e-\omega_r)L_m & R_r & (\omega_e-\omega_r)L_r \\ -(\omega_e-\omega_r)L_m & 0 & -(\omega_e-\omega_{r)} & R_r+L_r \end{bmatrix} \begin{bmatrix} i_{qs} \\ i_{ds} \\ i_{qr} \\ i_{dr} \end{bmatrix} + \begin{bmatrix} L_s & 0 & L_m & 0 \\ 0 & L_s & 0 & L_m \\ L_m & 0 & L_r & 0 \\ 0 & L_m & 0 & L_r \end{bmatrix} \frac{d}{dt} \begin{bmatrix} i_{qs} \\ i_{ds} \\ i_{qr} \\ i_{dr} \end{bmatrix} \quad (3)$$

Example

$$P = \begin{bmatrix} R_s & \omega_e.L_s & 0 & \omega_e.L_m \\ -\omega_e.L_s & R_s & -\omega_e.L_m & 0 \\ 0 & (\omega_e-\omega_r)L_m & R_r & (\omega_e-\omega_r)L_r \\ -(\omega_e-\omega_r)L_m & 0 & -(\omega_e-\omega_{r)} & R_r+L_r \end{bmatrix} \quad (4)$$

$$Q = \begin{bmatrix} L_s & 0 & L_m & 0 \\ 0 & L_s & 0 & L_m \\ L_m & 0 & L_r & 0 \\ 0 & L_m & 0 & L_r \end{bmatrix} \quad (5)$$

The above equation can be formed more simply, namely:

$$\begin{bmatrix} V_{qs} \\ V_{ds} \\ V_{qr} \\ V_{dr} \end{bmatrix} = P \begin{bmatrix} i_{qs} \\ i_{ds} \\ i_{qr} \\ i_{dr} \end{bmatrix} + Q \frac{d}{dt} \begin{bmatrix} i_{qs} \\ i_{ds} \\ i_{qr} \\ i_{dr} \end{bmatrix} \quad (6)$$

If you want to find the current value, the formula above becomes:

$$\frac{d}{dt} \begin{bmatrix} i_{qs} \\ i_{ds} \\ i_{qr} \\ i_{dr} \end{bmatrix} = -Q^{-1}P \begin{bmatrix} i_{qs} \\ i_{ds} \\ i_{qr} \\ i_{dr} \end{bmatrix} + Q^{-1} \begin{bmatrix} V_{qs} \\ V_{ds} \\ V_{qr} \\ V_{dr} \end{bmatrix} \quad (7)$$

2.3 Fuzzy Logic

In 1965, Lotfi A. Zadeh invented an intelligent control system, namely Fuzzy logic. the Fuzzy function is to distinguish a set according to the degree of membership from an uncertain boundary. This set theory is the development of a firm set theory that is created from the way humans understand an uncertain value. Fuzzy membership values are not only worth 0 or 1 but also produce a value that lies between 0 and 1. The Fuzzy structure can be seen in Figure 2.6 where the Fuzzy control design is divided into three stages, namely fuzzification, Fuzzy reasoning systems, and defuzzification [20].

JURNAL ECOTIPE
Electronic, Control, Telecommunication, Information, and Power Engineering
Volume 10, Issue 1, April 2023, pp. 111-120
ISSN 2355-5068 ; e-ISSN 2622-4852
DOI: 10.33019/jurnalecotipe.v10i1. 3925

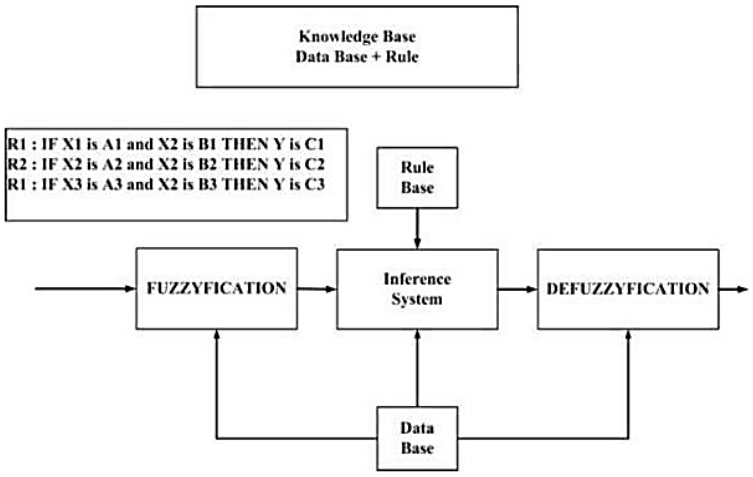

Figure 2. The general structure of the system based on Fuzzy altural calculations

2.4 Direct Torque Control (DTC)

DTC is a control method used to base the adjustment of the magnetic flux and stator torque and provides a fast and robust response for AC motors. The block diagram of the three-false induction motor DTC system is shown in Figure 3.

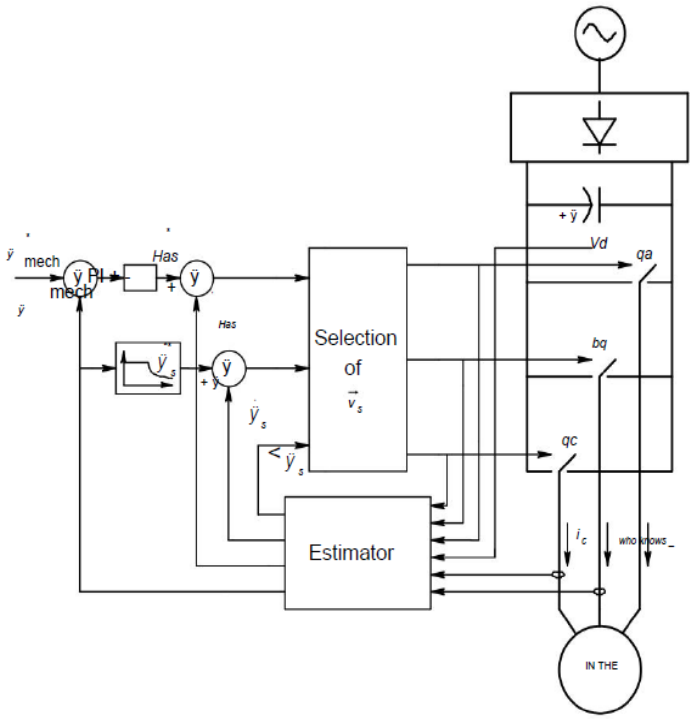

Figure 3. Diagram of a 3-Phase induction motor DTC system

2.5 Proportional and Derivative (PD) Control

PD control is a commonly used control system where each has different advantages and functions. Proportional control functions speed up the output of the system to reach the reference point by amplifying the driving error signal or error signal. Proportional control can produce an offset on the system by increasing the value of the proportional band or Kp. However, if the Kp value is too large, it will cause oscillations to arise because the system becomes unstable. P control can stand alone for system control.

JURNAL ECOTIPE
Electronic, Control, Telecommunication, Information, and Power Engineering
Volume 10, Issue 1, April 2023, pp. 111-120
ISSN 2355-5068 ; e-ISSN 2622-4852
DOI: 10.33019/jurnalecotipe.v10i1.3925

Derivative control is usually called the rate controller which is symbolized by D. It is called the rate controller because the output on the derivative control is proportional to the rate of change of the error signal.

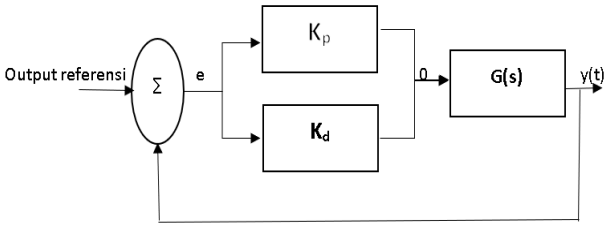

Figure 4. PD control

3. RESULTS AND DISCUSSION

The reference value for the stator flux is set at 1.46, while the reference value for speed is 100 rad/s. This speed reference value will later be used as a reference for the desired output response value of the system. The simulation response results are in the form of electromagnetic torque response, rotor speed, and estimated flux.

3.1 Results and Analysis of 3-Phase Induction Motor Speed System with DTC Controller

To analyze the output response of a 3-Phase induction motor system using DTC, it is necessary to do a simulation test first and in this circuit the reference value is 100 rad/s.

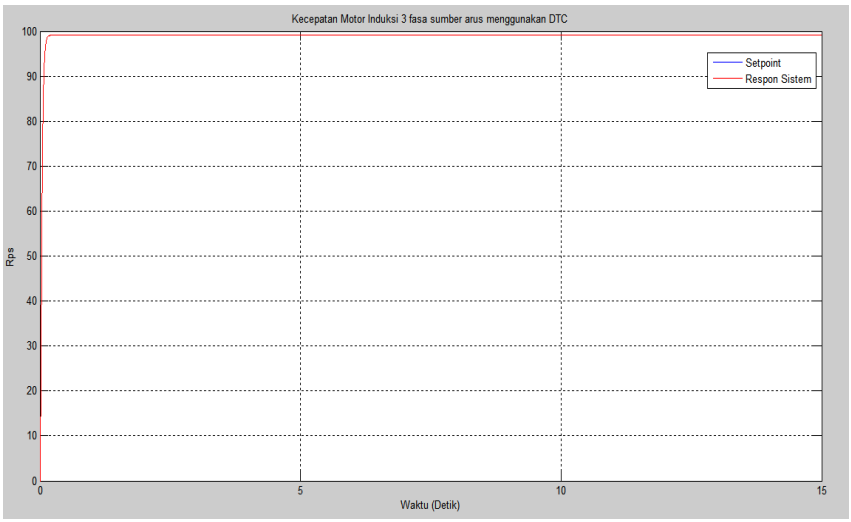

Figure 5. DTC control system output graph on 3-Phase induction motor

The rise time for a 3-phase induction motor with this trouble code is 0.0615 seconds. The settling time (ts) for a 3-Phase induction motor using this fault code is calculated for an output response of 98%, an output reading of 97.1474 rad/s, and a time to reach 97.1474 rad/s of 0.113 seconds. The deceleration time (td) for a 3-Phase induction motor with DTC is calculated for a 50% output response, an output reading of 49.565 rad/s, and a time to reach 49.565 rad/s of 0.034 seconds. The steady-state error (Ess) is obtained from the difference between the steady-state setpoint and the steady-state output. where the values are 100 rad/s and 99.13 rad/s respectively. Therefore, the steady-state error value for a 3-Phase induction motor with DTC is 0.87 rad/s.

3.2 Results and System Analysis of 3-Phase Induction Motor Speed with Fuzzy Sugeno DTC Controller

To analyze the output response of a 3-Phase induction motor system using DTC, it is necessary to do a simulation test first and in this circuit the reference value is 100 rad/s.

JURNAL ECOTIPE
Electronic, Control, Telecommunication, Information, and Power Engineering
Volume 10, Issue 1, April 2023, pp. 111-120
ISSN 2355-5068 ; e-ISSN 2622-4852
DOI: 10.33019/jurnalecotipe.v10i1. 3925

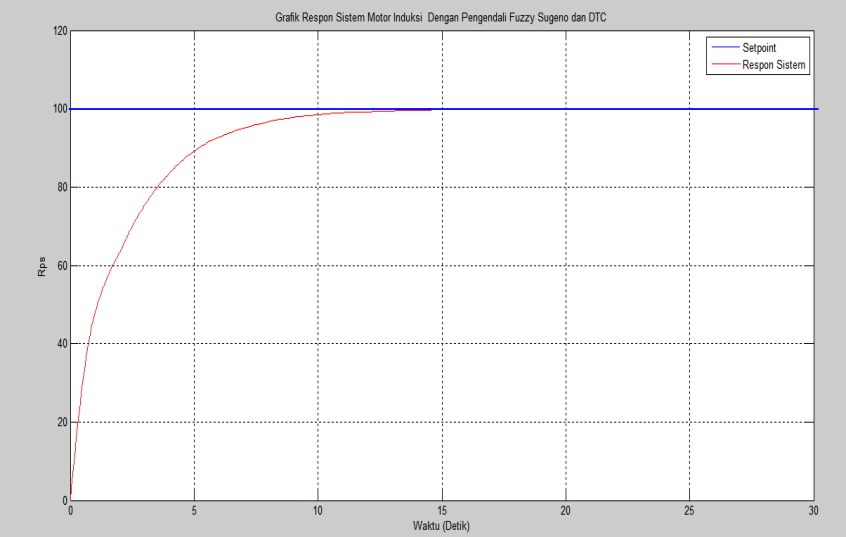

Figure 6. Graph of induction motor system response with Fuzzy Sugeno and DTC controllers

Therefore, the rise time of a 3-phase induction motor using DTC Fuzzy Sugeno is 5 seconds. The settling time (ts) of a 3-Phase induction motor using DTC Fuzzy Sugeno is calculated for 98% output response. Here the output value is 98 rad/s and the time to reach 98 rad/s is 9.15 seconds. For the deceleration time (td) of a 3-Phase induction motor, use the DTC with an output response of 50% when the output value is 50 rad/s and the time to reach 50 rad/s is 1.1 seconds.

3.3 Results and System Analysis of 3-Phase Induction Motor Speed with Fuzzy Sugeno-PD DTC Controller

Furthermore, the PD controller is added to speed up the time needed to reach the proposed reference value of 100 rad/s because when controlled using the DTC-Fuzzy controller it still takes a long time to reach its steady-state value.

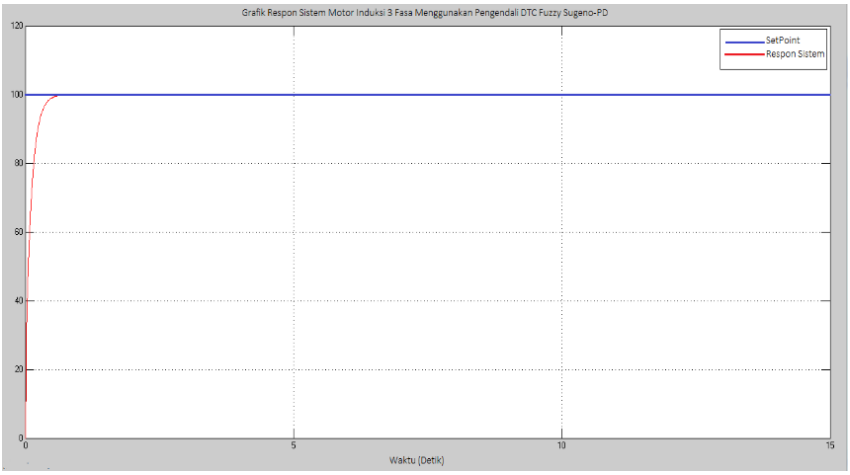

Figure 7. Graph of induction motor output using Fuzzy Sugeno-PD DTC controller

Therefore, the rise time of a 3-Phase induction motor using the Sugano PD Fuzzy DTC is 0.2 seconds. The settling time (ts) of a 3-Phase induction motor using DTC Fuzzy Sugeno-PD is calculated when the output response is 98% where the output value is 98 rad/s and the time needed to reach 98 rad/s is 0.45 seconds. For Delay Time (td) on a 3-Phase induction motor using DTC Fuzzy Sugeno-PD, it is calculated when the output response is 50% where the output value is 50 rad/s and the time needed to reach 50 rad/s is 0.1 second. The system time response using the DTC Fuzzy Sugeno-PD controller can be seen in Table 4.5 which displays the values of rise time, steady time, delay time, maximum overshoot, and steady-state error.

JURNAL ECOTIPE
Electronic, Control, Telecommunication, Information, and Power Engineering
Volume 10, Issue 1, April 2023, pp. 111-120
ISSN 2355-5068 ; e-ISSN 2622-4852
DOI: 10.33019/jurnalecotipe.v10i1.3925

3.4 Results and Analysis of 3-Phase Induction Motor Using DTC-Fuzzy Sugeno-PD Controller When Interrupted

To determine the performance of the Sugeno-PD Fuzzy DTC controller in overcoming disturbances in 3-Phase induction motors where disturbances are defined as changes in voltage up and voltage down. The disturbance given is 10% of the setpoint and the disturbance will be given at 10 seconds, then analyze the impact and changes in the system response from the controller.

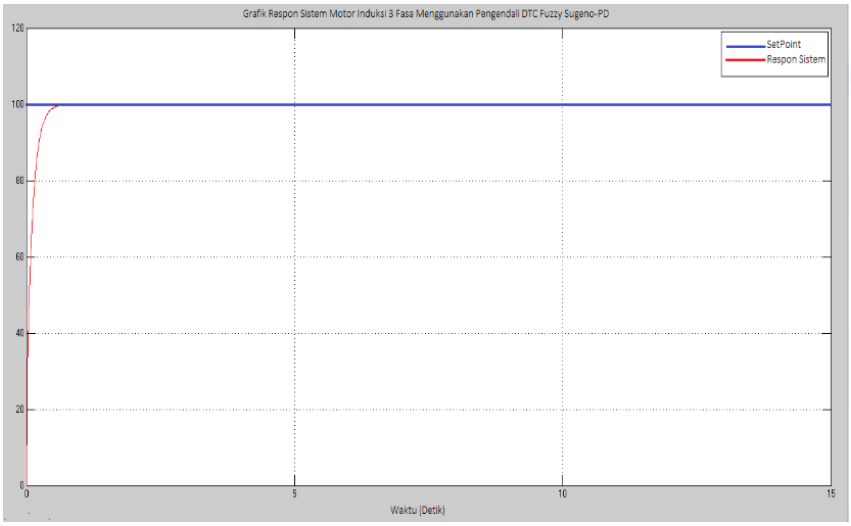

Figure 8. Graph of induction motor output using Fuzzy Sugeno-PD DTC controller with interference

Therefore, the rise time of a 3-Phase induction motor with a Sugeno PD Fuzzy DTC controller in this disturbance is 0.0268 seconds. Settling time (ts) For a 3-Phase induction motor using DTC Fuzzy Sugeno-PD controller with this disturbance is calculated when the output response is 98% where the output value is 97.9706 rad/s and the time needed to reach 97.9706 rad/s is 0.488 seconds. For Delay Time (td) on 3-Phase induction motor using DTC. A Fuzzy Sugeno-PD controller with disturbance, is calculated when the output response is 50% where the output value is 49.985 rad/s and the time needed to reach 49.985 rad/s is 0.1088 seconds.

4. CONCLUSION

Conclude, based on the simulations performed and response analysis, that by using the Sugeno-PD DTC Fuzzy controller on a 3-Phase asynchronous motor, the controller was able to achieve performance with a setpoint of 100 rad/s. I can. The settling time is 0.45 seconds, the rise time is 0.2 seconds, and the delay time is 0.1 seconds. It can be seen that the Sugeno PD Fuzzy DTC controller can achieve results that match the setpoint while eliminating overshoots and steady-state errors. There is a 5 rad/s steady-state error, a 5.4111% overshoot, and still some oscillation from the state of the planned output response before being fed to the controller. The state of the planned output response when presented to the DTC controller has a steady-state error of 0.87 rad/s and a settling time of 0.113 seconds. Adding the DTC controller to the Sugeno Fuzzy controller gives better results as the result reaches the set point in 9.15 seconds of steady-state time with no steady-state error and no overshoot. From the simulation results obtained, it can be concluded that studies using the Sugeno Fuzzy DTC controller can eliminate overshoots, oscillations, and steady-state errors. Apart from that, it is also said to be superior to previous studies.

Based on the research conducted and the analysis performed on a 3-Phase induction motor using the Sugeno-PD DTC Fuzzy controller, the authors used the 7x7 membership function in further studies to estimate the resulting system response I suggest you can check if is better. 5x5 membership function. Alternatively, add a PID controller to further improve the output response.

Volume 10, Issue 1, April 2023, pp. 111-120
ISSN 2355-5068 ; e-ISSN 2622-4852
DOI: 10.33019/jurnalecotipe.v10i1. 3925

REFERENCES

[1] N Evalina, Abdul Azis H, Zulfikar " Pengaturan Kecepatan Putaran Motor Induksi 3 Fasa Menggunakan *Programmable Logic Controller ",*Journal of Electrical Technology Vol. 3, No. 2. 2018 ISSN: 2598 – 1099.

[2] D. Mursyitah, A. Faizal, and E. Ismaredah, "Design of Fuzzy - PID Controller for Controlling Position In Magnetic Levitation Ball System", *JurnalEcotipe*, vol. 6, no. 2, pp. 61 - 66, Oct. 2019.

[3] Endro Wahjono "Pengaturan Kecepatan Motor Induksi Sebagai Penggerak Mobil Listrik *Dengan* Kontroler *Fuzzy Logic* Berbasis *Direct Torque Control",* Jurnal Ilmiah Mikrotek Vol. 1, No.3 2015

[4] F. Arvianto Dan Mochammad Rameli "Pengaturan Kecepatan Motor Induksi Tiga Fasa Menggunakan Metode *Flux Vector Control* Berbasis *Self-Tuning PI* ". JURNAL TEKNIK ITS Vol. 6, No. 2 ISSN: 2337-3539, 2017.

[5] M. Nur Faizi, Marzuarman "Pengontrolan Fluks Dan Torsi Pada Motor Induksi 3 Fasa Menggunakan Metode *Direct Torque Control* (Dtc) Berbasis Pi Dan *Fuzzy Logic Controllers* (Flc)". Jurnal Inovtek Polbeng, Vol. 07, No. 2, November 2017. ISSN 2088-6225. E-ISSN 2580-2798

[6] Gafur Nugroho "Lampiran A Perbandingan Sistem Pengendalian Motor Induksi Tiga Fasa Dengan Metode Field Oriented Control Menggunakan Pi Controller Dan Fuzzy Logic Controller". Jurnal Teknik Elektro, Vol. 9, No. 03 2020.

[7] Halim Mudia "Perancangan *Model Predictive Torque Control* (Mptc) Untuk Pengaturan Kecepatan Motor Induksi 3 Phasa Dengan *Robust Stator Flux Observer"*. JIMP - Jurnal Informatika Merdeka Pasuruan, Vol 3 No1 Maret 2018. ISSN 2503-1945

[8] I Putu Sutawinaya "Pengembangan Model Fuzzy Mamdani Untuk Pengaturan Kecepatan Motor Induksi Tiga Fasa Berbasis Metode Kontrol Field Oriented ". Jurnal Logic. Vol. 13. No. 2. Juli 2013

[9] Yoki Permana, Rusdhianto Effendie AK, Dan Josaphat Pramudijanto " Perancangan Dan Implementasi Pengaturan Kecepatan Motor 3 Fasa Pada Mesin Sentrifugal Menggunakan Metode *Model Reference Adaptive Control (MRAC)".* JURNAL TEKNIK POMITS Vol. 2, No. 1, (2014)

[10] Ramesh, T., Panda, K. A., "Direct Flux and Torque Control of There Phase Induction Motor Drive Using PI and Fuzzy Logic Controllers for Speed Controller for Regulator and Low Torque Ripple". Department of Electrical Engineering, National Institute of Tecnology, India, 2012

[11] K. R. S. Suda, E. Purwanto, B. Sumantri, M. R. Rusli, H. H. Fakhruddin, A. A. Muntashir "Pengaturan Kecepatan Motor Induksi 3 Fasa Dengan Menggunakan Pemodelan Sistem (Dtc) *Direct Torque Control*" Jurnal Pendidikan Teknologi dan Kejuruan, Vol. 18, No. 2, Juli 2021. P-ISSN : 0216-3241 E-ISSN : 2541-0652

[12] Sri Kusuma Dewi, Hari Purnomo "Aplikasi Logika Fuzzy Untuk Mendukung Keputusan EDISI 2." Graha Ilmu Yogyakarta 2010. ISBN: 978-979-756-632-6

[13] Ibrahim Nawawi, Bagus Fatkhurozzi "Studi Komparasi Kendali Motor DC Dengan Logika Fuzzy Metode Mamdani dann Sugeno" Jurnal Wahana Ilmuan, Vol. 2 No.2 2016.

[14] Sariman, Manlahima Padaridi, *Dindi Hamamie Mahfie*, Bhakti Yudho Suprapto " Perbandingan Pengendali Pi, Pd Dan Pid Pada Pengendalian Kecepatan Motor Induksi Tiga Fasa Dengan Memanfaatkan Supervisory Control And Data Acquisition (Scada)" Jurnal Surya Energy (JSE), Vol. 3, No. 2, 2019. JISSN: 2528-7400,.

[15] Rifdian Indrianto Sudjoko, Hartono " Desain Dan Simulasi Motor Induksi 3 Fasa Dengan Menggunakan Matlab" Jurnal Penelitian Politeknik Penerbangan

[16] Sukamto "Pengendalian Kecepatan Motor Induksi Menggunakan Kontroler Logika Fuzzy" Journal of Electrical Electronic Control and Automotive Engineering (JEECAE), Vol. 4 No.2 2019

Volume 10, Issue 1, April 2023, pp. 111-120
ISSN 2355-5068 ; e-ISSN 2622-4852
DOI: 10.33019/jurnalecotipe.v10i1.3925

[17] Endro Wahjono, Soebagio "Pengaturan Kecepatan Motor Induksi Tiga Fasa Dengan Metoda Direct Torque Control Menggunakan Fuzzy Logic Controller". Seminar Nasional Informatika (Semnasif 2009) UPN "Veteran", 2009. ISSN : 1979-2328

[18] Trzynadlowski, M. A,"Control of Induction Motors", Academic Press, Nevada, 2001

[19] Pratomo, Gilang. "Motor Induksi 3 Fasa" Tentang Motor Induksi 3 Fasa. (https://Www.Academia.Edu/26275174/Motor_Induksi_Tiga_Fasa) [Diakses Pada Tanggal : 29 November 2020]

[20] K. B. Bose, "Modern Power Electronics and AC Drives", *United State Of America: Prentice Hall, Knoxville,* 2002.

[21] Eddy Darmawan "Perancangan Sistem Kendali Hybrid Pid Dan Fuzzy Logic Pada Pengendalian Kecepatan Motor Dc Menggunakan Metode Quater Decay." Skripsi, Program Studi Teknik Elektro, Fakultas Sains dan Teknologi, UIN SUKA Riau, Pekanbaru 2020.

[22] Agung Setiawan S.Kom, M.M., M.Kom. Budi Yanto, S.T., M.Kom. Kiki Yasdomi, S.Kom., M.Kom. "LOGIKA FUZZY *Dengan* M A T L A B *(Contoh Kasus Penelitian Penyakit Bayi Dengan Fuzzy Tsukamoto)."* 2018. Perpustakaan Nasional Republik IndonesiaKatalog Dalam Terbitan (KDT). ISBN: 978-602-51483-7-8

[23] Supina Batubara "Analisis Perbandingan Metode Fuzzy Mamdani Dan Fuzzy Sugeno Untuk Penentuan Kualitas Cor Beton Instan" IT Journal Research and Development, Vol.2, No.1, Agustus 2017 ISSN: 2528-4053.

[24] Sri Widaningsih "Analisis Perbandingan Metode *Fuzzy* Tsukamoto, Mamdani Dan Sugeno Dalam Pengambilan Keputusan Penentuan Jumlah Distribusi Raskin Di Bulog Sub. Divisi Regional (Divre) Cianjur." Jurnal Informatika dan Manajemen STMIK, Vol 11 No.1 Mei 2017

[25] Katsuhiko Ogata, "Modern Control Engineering" fifth ed, United State Of America: Prentice Hall, 2010.

[26] Ned, M. "*Advanced Electric Drives*", MNPERE, *United States of America*: Jhon Wiley and Son, 2001.

[27] N. Mohan, "Advanced Electric Drives: Analysis, Control, and Modeling Using MATLAB/Simulink", *United States of America*: John Wiley & Sons, 2014.

[28] Cahyono, Budi. "Penggunaansoftware Matrix Laboratory (Matlab) Dalam Pembelajaran Aljabar Linier". Skripsi, Jurusan Pendidikan Matematika, Fakultas Ilmu Tarbiyah dan Keguruan, Institut Agama Islam Negeri Walsiongo, Semarang, 2013

[29] Ali, Muhammad. "Pembelajaran Perancangan Sistem Kontrol PID dengan Software Matlab". Jurnal Edukasi@Elektro, Vol. 1, No. 1, Oktober 2004.

[30] Mohammad Hafiz. "Kontrol Proporsional-Derivatif Pada Sistem Dinamik Pesawat Terbang Tipe Airbus A380-800". Jurnal Ilmiah Matematika, Vol. 3, No. 6, ISSN 23019115. 2017.

JURNAL ECOTIPE
Electronic, Control, Telecommunication, Information, and Power Engineering

Volume 10, Issue 1, April 2023, pp. 121-130
ISSN 2355-5068 ; e-ISSN 2622-4852
DOI: 10.33019/jurnalecotipe.v10i1.3802

Mobile Point of Sales (Mi-POS) Application for Cashiers Using React Native Framework A Case Study at Fajar Jaya Snack Shop

Dimas Fajar Saputro[1], Dedi Gunawan[2]
[1,2]Department of Informatics, Faculty of Communication and Informatics, Universitas Muhammadiyah Surakarta, Sukoharjo, 57169, Indonesia

ARTICLE INFO

Article historys:

Received : 25/01/2023
Revised : 11/02/2023
Accepted : 21/04/2023

Keywords:

Android; React Native; Point of Sale; Mi-POS; Mobile Application.

ABSTRACT

Toko Snack Fajar Jaya is one of the small and medium enterprises (UMKM) located in Surakarta. The store is selling snacks in both bulk and retail. The store's current system still relies on manual bookkeeping which causes errors and uncertainties in data management and sales reports. For example, the shop owner sometimes receives a monthly report that is not synced with the real product stock in the store. To solve these problems, a mobile application called Mi-POS is proposed using React Native framework to facilitate the development process. The application has functionalities to record customer transactions, view customer transaction history, manage product inventory, and print receipts. The development process of the system adopts the SDLC waterfall method. The method consists of several steps, starting from requirement analysis, design application, design interface, coding, testing, and, lastly maintenance. To ensure the application's quality and effectiveness, several testing strategies are involved such as using Black-box Testing and System Usability Scale (SUS). Results from Black-box Testing showed that all the features can run smoothly with an error rate of 0%. Meanwhile, SUS testing showed a score of 63.4, which falls in the "OK and usable" category indicating that the application can be adapted to support users' business activity.

Corresponding Author:

Dedi Gunawan
Universitas Muhammadiyah Surakarta, Jl. A. Yani, Mendungan, Pabelan, Kartasura, Sukoharjo Regency, 57169, Indonesia
Email: dedi.gunawan@ums.ac.id.

1. INTRODUCTION

Technology has had a significant impact on society over time, affecting not only the upper middle class but also the lower middle class. This is because of technology's ability to facilitate various activities. One example is the widespread use of Android smartphones, as said by [1], nearly 25% of the Indonesian population, or around 65 million people, use Android devices. Many of these users use them for both business and daily life [2] such as snack business. However, some individuals like the owner of Fajar Jaya Snack Shop, continue to rely on manual methods for tasks such as sales transactions and inventory management, instead of utilizing technology. This can lead to difficulties in running their business, as stated by [3].

One example of difficulties is the potential for errors when calculating the total purchase price for customers, particularly when buying in large quantities. These mistakes can lead to financial losses if not handled properly. As said by [4], using manual bookkeeping methods can lead to difficulties in record-keeping and can cause further issues.

JURNAL ECOTIPE
Electronic, Control, Telecommunication, Information, and Power Engineering
Volume 10, Issue 1, April 2023, pp. 121-130
ISSN 2355-5068 ; e-ISSN 2622-4852
DOI: 10.33019/jurnalecotipe.v10i1.3802

2. RESEARCH METHOD

The research was conducted at Fajar Jaya Snack Shop located in Surakarta. In order to gain a deeper understanding of the needs and requirements of the snack shop owners and cashiers, the research employed a qualitative approach. The data was collected through direct observation at the research site and interviews with the snack shop owners and cashiers. This allowed the researcher to gain a more subjective and personal perspective of the problems and needs of the shop owner and cashier. Then, in the application design, the method used is the Software Development Life Cycle (SDLC) model Waterfall Method. The method is adopted because of its systematic and sequential approach to software development and has been widely used in development [6]. The steps in this method include Requirement, Design, Implementation, Testing, and Maintenance. This can be seen in Figure 1.

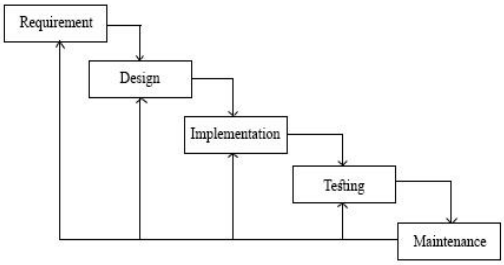

Figure 1. Waterfall Diagram

2.1. Direct Observation and Interviews

Direct observation at the research site and interviews were performed to gain a deeper understanding of the needs and requirements of the snack shop owner and cashier. The objective of direct observation was to observe the current processes of transactions that happen in the shop. The researcher spent several hours at the shop, observing the work of the shop owner and employees, and took notes on the processes and procedures used in the operation of the shop. In the meantime, interviews are performed to understand the experiences of the shop owner and employees during the transaction, using a questionnaire that covered various aspects of the business, including the types of products offered and the pricing. Their opinions and suggestions will be used for the development of the application to ensure the needs. The observation carries several findings such as the system needs two types of users i.e., cashier and administrator. It requires one database server to store the product and transaction record and also a Bluetooth printer to print the customer transaction receipt.

2.2. Requirement

The initial step is to identify the functional and non-functional requirements after gathering all necessary data. Functional requirements refer to the features and functions that the system should have, as per [7], while non-functional requirements include the software and hardware needed for the system's development, as stated by [8]. These requirements are described in Table 1.

Table 1. Requirement Analysis

No	Requirement	Description
1	Functional	• Admin can create, change and/or delete cashier accounts. • Admin can create receipts. • Admin can create, view, change and/or delete items. • Admin can view and delete transaction history. • Cashier can create receipts. • Cashier can view items. • Cashier can view transaction history. • Cashier can change their account password.
2	Non-functional	• The application is run on an Android device. • The application is made on a computer. • The application can print receipts. • The application is designed with a default computer program. • The application is made with the React Native framework. • Writing application code using Visual Studio Code.

JURNAL ECOTIPE
Electronic, Control, Telecommunication, Information, and Power Engineering
Volume 10, Issue 1, April 2023, pp. 121-130
ISSN 2355-5068 ; e-ISSN 2622-4852
DOI: 10.33019/jurnalecotipe.v10i1.3802

2.3. System Design

1. Use Case Diagram and Activity Diagram

According to [9], the use case diagram contains an explanation of the interactions that actors can have with the application. This designed application has two actors, namely the admin, and the cashier. Meanwhile, then Activity Diagram contains the system workflow of an application. This is as said by [10], this diagram describes the system process that users can do. This can be seen in Figure 2.

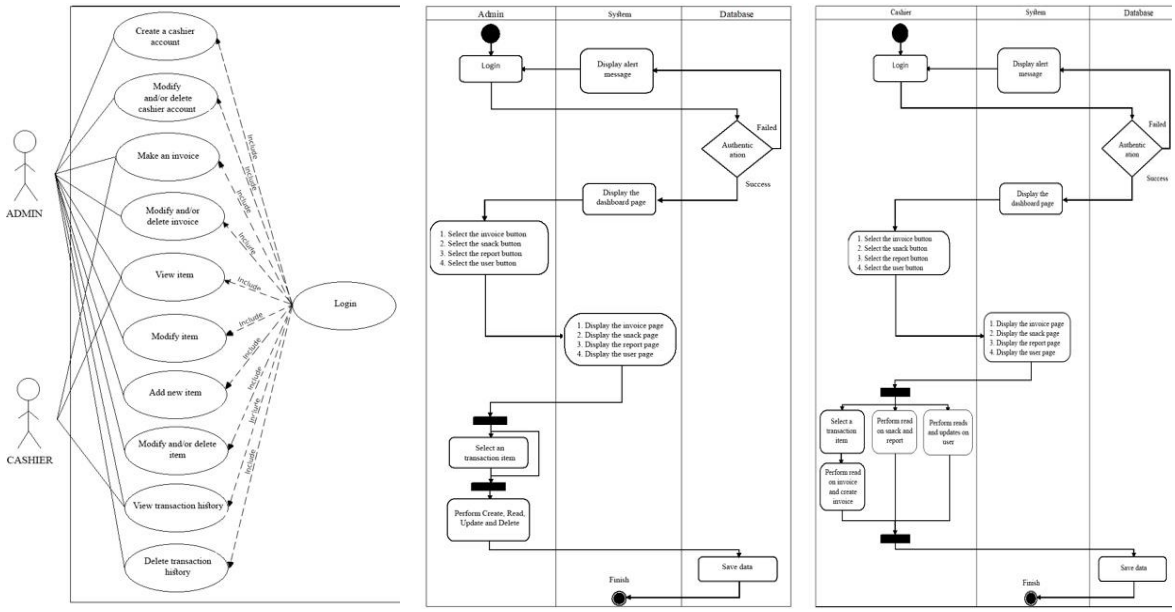

Figure 2. Use Case Diagram, Admin and, Cashier Activity Diagram

2. Entity Relationship Diagram (ERD)

An Entity Relationship Diagram (ERD) is a description or modeling of the relationship between one entity and another. This diagram helps to plan the database that will be used in the application later [11]. This is explained in the following Figure 3.

3. Mockup

Mockup is a representation of the application interface, and Balsamiq Mockup software will be used because it is a popular choice among developers [12]. In addition, according to [13], this software offers a variety of templates to aid. The interface that will be developed is divided into 5 sections.

a. Login page and dashboard page

The login page is the initial page that distinguishes the type of account. Once the user has logged in, the dashboard page appears, which contains a menu of features, as depicted in Figure 4.

JURNAL ECOTIPE
Electronic, Control, Telecommunication, Information, and Power Engineering
Volume 10, Issue 1, April 2023, pp. 121-130
ISSN 2355-5068 ; e-ISSN 2622-4852
DOI: 10.33019/jurnalecotipe.v10i1.3802

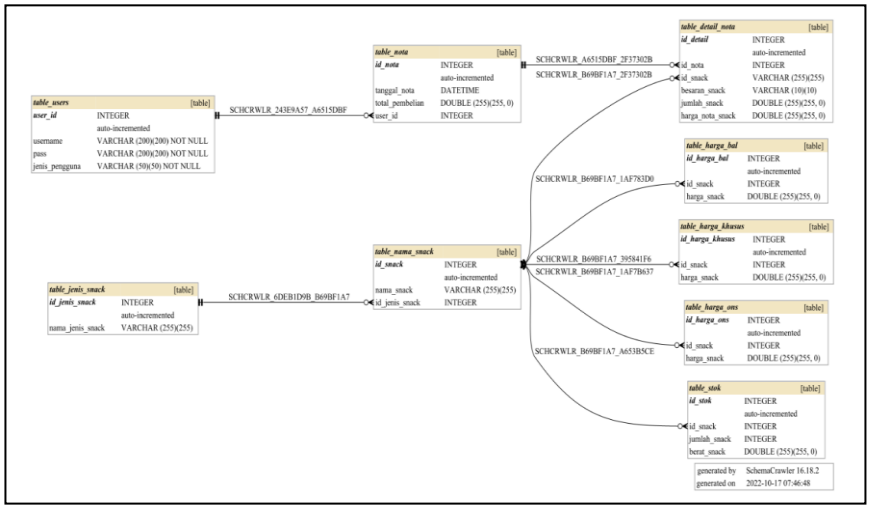

Figure 3. Entity Relationship Diagram

Figure 4. Login Page and Dashboard Page Mockup

b. Receipt Page

The page allows creation a receipt/transaction that will be printed and stored in the database. No functional restrictions between admin and cashier accounts, as seen in Figure 5.

Figure 5. Receipt Page Mockup

c. Snack Page

The snack page allows for the management of snack items, including adding, editing, and deleting. There is a difference in access between admin and cashier accounts, where the admin has full control over the snack items, while the cashier account is limited to viewing the items. This can be seen in Figure 6.

JURNAL ECOTIPE
Electronic, Control, Telecommunication, Information, and Power Engineering
Volume 10, Issue 1, April 2023, pp. 121-130
ISSN 2355-5068 ; e-ISSN 2622-4852
DOI: 10.33019/jurnalecotipe.v10i1.3802

Figure 6. Snack Page Mockup

d. Report Page

The report page contains transaction history. There is a difference in access between admin and cashier accounts, which the admin has full control over, such as deleting while the cashier account is limited to viewing. This can be seen in Figure 7.

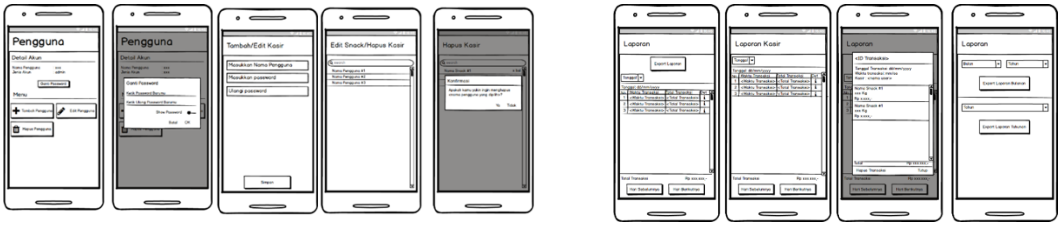

Figure 7. User Page and Report Page Mockup

e. User Page

This page is used to manage or manipulate user data. In the admin account, there are features to add, edit, and delete cashier accounts and change their passwords. However, in the cashier account, you can only see your username and change your password. This can be seen more clearly in figure 7.

2.4. Implementation

The next step is about creating the application using the modeled system design. This starts with creating an SQLite format database, which is used because it provides better performance than other Android databases such as Firebase [14]. Then, React Native framework is used for application development as it allows real-time code changes and is more popular than others [15]. Visual Studio Code is also preferred due to its lightweight nature and features that aid development as a text editor. During development, an emulator with Android version 5.1.1 is used to test the application's appearance and functions. The outcome is a "apk" file that can be installed on an Android device.

2.5. Testing

After the application is made, it will be tested using Black-box Testing and System Usability Scale (SUS). Black-box Testing focuses on the software's functional specifications with the test data sought as the output as expected, while SUS is a method of usability testing using 10 scales that provide a comprehensive view of the user experience. The basis for the assessment of this test is obtained from the experience felt by the user when using the application. SUS is done in the form of an online questionnaire with 10 questions as can be seen in Table 2, and scores range from 0 to 100. The SUS score assessment can be seen in Figure 9.

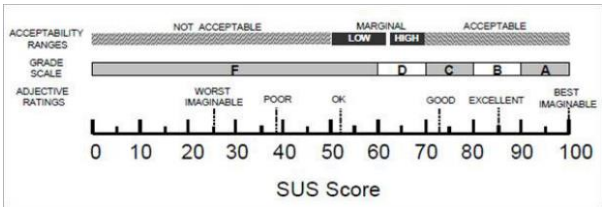

Figure 9. SUS Score

JURNAL ECOTIPE
Electronic, Control, Telecommunication, Information, and Power Engineering
Volume 10, Issue 1, April 2023, pp. 121-130
ISSN 2355-5068 ; e-ISSN 2622-4852
DOI: 10.33019/jurnalecotipe.v10i1.3802

The questionnaire scores are calculated by answered score will be subtracted with 1 (q-1) from odd questions and on even questions, the answered score will be subtracted from 5 (5-q). The final result is obtained by multiplying the total points by 2.5. This method is applied to all respondents, including 25 shop owners, cashiers, and members of the general public.

2.6. Maintenance

This step aims to monitor the performance of the application in the field. This step also includes fixing errors that were not present in the previous step.

Table 2. Requirement Analysis

Statement
I think I will use this app again
I find this app complicated to use
I find this app easy to use
I need help from other people or technicians in using this application
I feel that the features of this app are working properly
I feel there are many inconsistencies (mismatches in this app)
I feel others will understand how to use this app quickly
I find this system confusing
I feel no obstacles in using this application
I need to familiarize myself first before using this app

3. RESULTS AND DISCUSSION

3.1. Results

In this sub-chapter, we will discuss the results obtained from the application development process that has been carried out.

1. Login Page and Dashboard Page

Figure 10**.** Login Page and Dashboard Page

Figure 10 shows the login page, where the user must enter a correct user id and password to access the system according to the account rights. After logging in, the dashboard page appears, with four buttons; create a note for new transactions, snack for managing snack data, report for viewing transaction reports, user to manage user data, and a logout button to exit the system.

2. Receipt Page

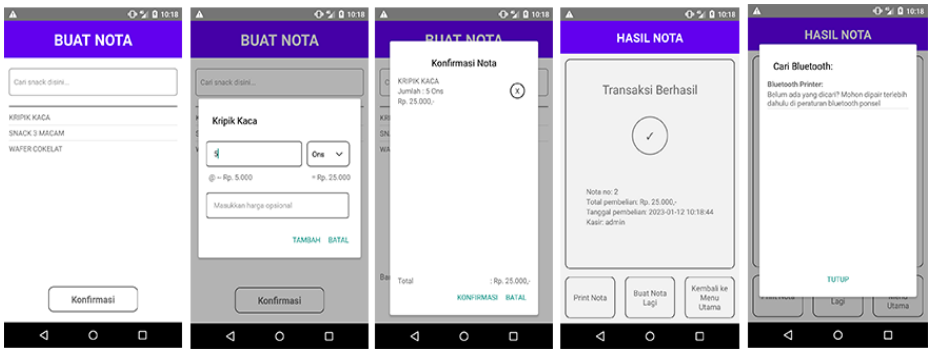

Figure 11. Receipt Page

JURNAL ECOTIPE
Electronic, Control, Telecommunication, Information, and Power Engineering
Volume 10, Issue 1, April 2023, pp. 121-130
ISSN 2355-5068 ; e-ISSN 2622-4852
DOI: 10.33019/jurnalecotipe.v10i1.3802

Figure 11 is a receipt page where the admin user or cashier will enter the snacks that the customer will buy into the cart. After finishing putting it into the cart, the user will confirm first before the transaction is entered into the database. When the transaction has been entered, the user can print the receipt or create another receipt.

3. Snack Page

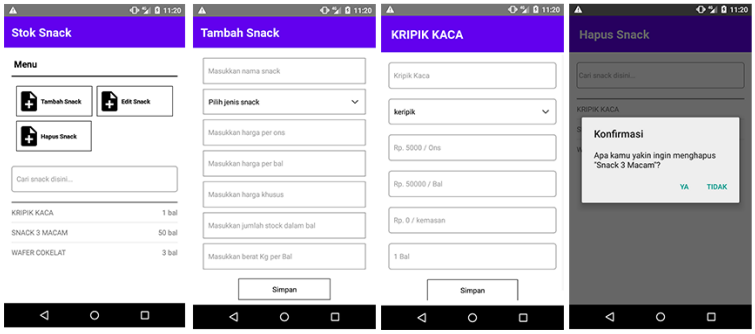

Figure 12. Snack Page

Figure 12 is a snack management page for checking, adding, editing, and deleting snacks. Users on this page are divided into cashiers and admins with different access rights. Cashier users can only check snacks while admin users have full access.

4. Report Page

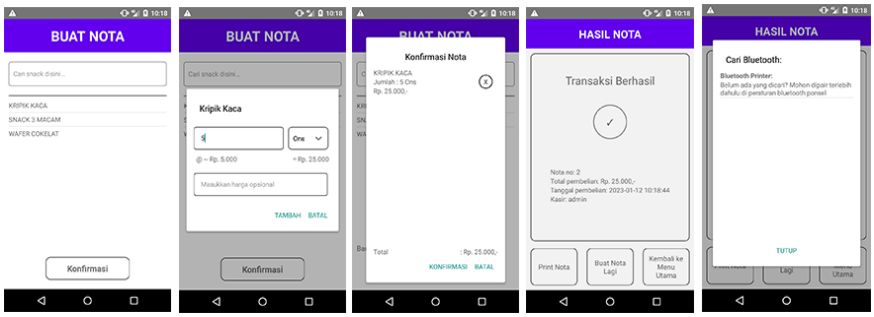

Figure 13**.** Report Page

Figure 13 is used to check reports, and delete transactions. Checking can be done per transaction on the selected date, per day in a month, and per month in a year. However, deletion can only be per transaction and can only be done by the admin.

5. User Page

Figure 14 is a user page used to manage user accounts. Users on this page are divided into 2 namely admin and cashier. Admin users can manage users by adding, editing, and deleting cashier accounts. Then, the cashier user can only edit the password on his account.

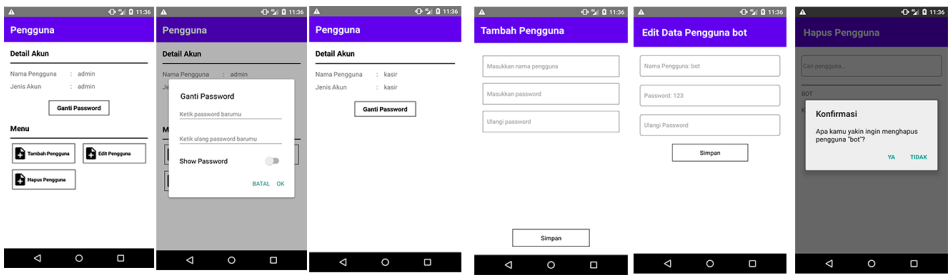

Figure 14. User Page

JURNAL ECOTIPE
Electronic, Control, Telecommunication, Information, and Power Engineering
Volume 10, Issue 1, April 2023, pp. 121-130
ISSN 2355-5068 ; e-ISSN 2622-4852
DOI: 10.33019/jurnalecotipe.v10i1.3802

3.2. Testing and Discussion

1. Black-box Testing

The following are the results of Black-box testing conducted on the Mi-Pos mobile application. These tests include functionality, ease of use, compatibility, performance, and security tests. The results of each test are shown in Table 3.

Table 3. Black-box Testing

Criteria	Scenario	Expected results	Test results
Login Page			
Login button	If user id and password are correct	Users can enter the dashboard page and access features that match their access rights.	Valid
	If user id and password are incorrect	The system displays an error message and the user cannot enter the application.	Valid
Dashboard Page			
Receipt Button	Pressing the create Receipt button	Users can enter the Receipt creation page	Valid
Snack Button	Pressing the snack button	Users can enter the snack page	Valid
Report Button	Pressing the report button	Users can enter the report page	Valid
User Button	Pressing the User button	Users can enter the user page	Valid
Receipt Page			
Click on the snack name	Pressing the snack to be made a receipt	The system displays the Receipt input dialog	Valid
Confirm button	If there is already data in the cart	The system displays a receipt confirmation dialog	Valid
	If there is no data in the cart	The system displays an error message	Valid
Back to the main menu button	Pressing the back to the main menu button	Users return to the dashboard page	Valid
Snack page			
Add, edit and delete Snack button	Pressing the add, edit, and delete snack button	Users enter the add, edit, and delete snack page	Valid
Report page			
Select month button	Pressing the select month button	The system displays a dialog to select the month and year	Valid
Select date button	Pressing the select date button	The system displays a dialog to select a date	Valid
Select Year	Pressing the select year button	The system displays a dialog to select the year	Valid
User page			
Password change button	Pressing the password change button	The system displays the password change dialog	Valid
Add, edit, delete User button	Pressing the add, edit and delete user button	Users enters the add, edit, delete user page	Valid

Volume 10, Issue 1, April 2023, pp. 121-130
ISSN 2355-5068 ; e-ISSN 2622-4852
DOI: 10.33019/jurnalecotipe.v10i1.3802

2. Usability Testing

Table 4. SUS score calculation

Respondents	Questionnaire Calculation Score										Total	Score (Total x 2.5)
	Q1	Q2	Q3	Q4	Q5	Q6	Q7	Q8	Q9	Q10		
1	3	3	4	3	3	3	3	1	0	3	26	65
2	3	3	3	3	3	3	3	1	3	3	28	70
3	3	2	3	3	3	2	3	1	2	1	23	57,5
4	4	0	4	2	4	0	4	0	4	0	22	55
5	4	2	2	1	3	1	2	2	4	0	21	52,5
6	3	3	3	2	3	2	3	1	3	3	26	65
7	2	3	2	1	2	1	3	1	1	2	18	45
8	3	4	3	4	3	3	4	1	1	4	30	75
9	0	1	4	3	3	4	3	0	1	4	23	57,5
10	3	3	3	3	3	2	2	2	3	3	27	67,5
11	4	4	4	4	4	4	4	0	0	4	32	80
12	1	3	3	3	3	3	3	1	1	3	24	60
13	4	3	3	3	4	3	3	1	1	3	28	70
14	3	3	3	3	3	3	3	1	3	3	28	70
15	3	3	3	3	4	4	3	1	1	2	27	67,5
16	2	2	3	1	2	2	3	1	2	2	20	50
17	2	3	3	2	2	1	3	1	3	2	22	55
18	3	3	3	4	3	3	3	1	1	3	27	67,5
19	3	4	4	3	4	4	2	0	2	4	30	75
20	3	3	3	3	2	3	3	1	1	3	25	62,5
21	2	3	3	3	3	3	3	1	3	3	27	67,5
22	3	3	3	2	3	3	3	1	3	3	27	67,5
23	3	3	3	1	3	3	3	1	1	2	23	57,5
24	3	2	2	1	3	1	2	1	3	2	20	50
25	3	3	3	3	3	3	3	3	3	3	30	75

Table 4 is the result of calculating the SUS score of 25 respondents. Then, after being calculated as a whole and averaged, a score of 63.4 is obtained which is Grade D which is included in the OK category with Marginal Low.

4. CONCLUSION

The mi-POS application has been successfully developed to meet the requirements of the Fajar Jaya Store in recording customer transactions, viewing transaction history, product inventory, and printing transaction receipts. The system is successfully deployed on Android phones. To access and store the data, the application requires communication between the application and its database using SQLite. Ensuring the quality of the system is a crucial part, and therefore; several tests are conducted such as using black-box testing and SUS testing. The results from Black-box Testing showed that all features ran smoothly with an error rate of 0%. Meanwhile, SUS testing showed a score of 63.4, which falls in the "OK and usable" category, indicating the application is acceptable to users but further improvement and development are still needed.

REFERENCES

[1] F. Irvansyah, S. Setiawansyah, and M. Muhaqiqin, “Aplikasi Pemesanan Jasa Cukur Rambut

Volume 10, Issue 1, April 2023, pp. 121-130
ISSN 2355-5068 ; e-ISSN 2622-4852
DOI: 10.33019/jurnalecotipe.v10i1.3802

Berbasis Android," *J. Ilm. Infrastruktur Teknol. Inf.*, vol. 1, no. 1, pp. 26–32, 2020, doi: 10.33365/jiiti.v1i1.253.

[2] U. Fadlilah, A. K. Mahamad, and B. Handaga, "The Development of Android for Indonesian Sign Language Using Tensorflow Lite and CNN: An Initial Study," *J. Phys. Conf. Ser.*, vol. 1858, no. 1, 2021, doi: 10.1088/1742-6596/1858/1/012085.

[3] P. D. A. Wiguna, I. P. A. Swastika, and I. P. Satwika, "Rancang Bangun Aplikasi Point of Sales Distro Management System dengan Menggunakan Framework React Native," *J. Nas. Teknol. dan Sist. Inf.*, vol. 4, no. 3, pp. 149–159, 2019, doi: 10.25077/teknosi.v4i3.2018.149-159.

[4] Karnadi and R. Suaidi Akbar, "Sistem Informasi Tata Kelola Surat Masuk Surat Keluar Prodi Teknologi Informasi Universitas Muhammadiyah Palembang Information System Governance Letter Management Information Technology Study Program Palembang Muhammadiyah University," *J. Digit. Teknol. Inf.*, vol. 2, 2019.

[5] Y. S. Nugroho, F. Y. Al Irsyadi, and E. W. Pamungkas, "Pelatihan Pemanfaatan Aplikasi Point Of Sales (POS) Bagi Industri Batik Mahkota dan Estu Mulyo Laweyan Surakarta," *Abdi Teknoyasa*, pp 2/2, 2021, [Online]. Available: https://journals2.ums.ac.id/index.php/abditeknoyasa/article/view/365/148.

[6] R. M. Firzatullah, "Development of XYZ University's Student Admission Site Using Waterfall Method," *Mobile-Based Natl. Univ. Online Libr. Appl. Des.*, vol. 3, no. 2, pp. 10–19, 2019, [Online]. Available: http://iocscience.org/ejournal/index.php/mantik/article/view/882/595

[7] L. Setiyani and E. Tjandra, "Analisis Kebutuhan Fungsional Aplikasi Penanganan Keluhan Mahasiswa Studi Kasus: Stmik Rosma Karawang," *J. Inov. Pendidik. dan Teknol. Inf.*, vol. 2, no. 1, pp. 8–17, 2021, doi: 10.52060/pti.v2i01.465.

[8] A. Aulia Aziiza and A. Nur Fadhilah, "Analisis Metode Identifikasi dan Verifikasi Kebutuhan Non Fungsional," *Appl. Technol. Comput. Sci. J.*, vol. 3, no. 1, pp. 13–21, 2020, doi: 10.33086/atcsj.v3i1.1623.

[9] F. Sonata and V. W. Sari, "Pemanfaatan UML (Unified Modeling Language) Dalam Perancangan Sistem Informasi E-Commerce Jenis Customer-To-Customer," *J. Komunika J. Komunikasi, Media dan Inform.*, vol. 8, no. 1, p. 22, 2019, doi: 10.31504/komunika.v8i1.1832.

[10] N. Musthofa and M. A. Adiguna, "Perancangan Aplikasi E-Commerce Spare-Part Komputer Berbasis Web Menggunakan CodeIgniter Pada Dhamar Putra Computer Kota Tangerang," *OKTAL J. Ilmu Komput. dan Sains*, vol. 1, no. 03, pp. 199–207, 2022.

[11] K. Afiifah', Z. F. Azzahra, and A. D. Anggoro, "Analisis Teknik Entity-Relationship Diagram dalam Perancangan Database: Sebuah Literature Review," *J. Intech*, vol. 3, no. 1, pp. 8–11, 2022.

[12] M. K. Zen Munawar, S.T., M. . Mira Ismirani Fudsyi, S.E., and M. K. Dadad Zainal Musadad, S.E., "Perancangan Interface Aplikasi Pencatatan Persediaan Barang Di Kios Buku Palasari Bandung Dengan Metode User Centered Design Menggunakan Balsamiq Mockups," *J. Inform. - Comput.*, vol. 06, pp. 12–13, 2019.

[13] Harfizar, D. Iskandar, and T. Nurbaiti, "Perancangan Sistem Informasi Pencarian Dan Pemasaran Barang Antik Berbasis E-Commerce Program Studi Teknik Informatika Stmik Raharja Abstrak," vol. 6, no. 1, pp. 28–38, 2019.

[14] A. T. Kabakuş, "A Performance Comparison of SQLite and Firebase Databases from A Practical Perspective," *Düzce Üniversitesi Bilim ve Teknol. Derg.*, vol. 7, no. 1, pp. 314–325, 2019, [Online]. Available: http://dergipark.gov.tr/doi/10.29130/dubited.44167.

[15] A. Biørn-Hansen, T.-M. Grønli, G. Ghinea, and S. Alouneh, "An Empirical Study of Cross-Platform Mobile Development in Industry," *Wirel. Commun. Mob. Comput.*, vol. 2019, 2019.

JURNAL ECOTIPE
Electronic, Control, Telecommunication, Information, and Power Engineering

Volume 10, Issue 1, April 2023, pp. 131-141
ISSN 2355-5068 ; e-ISSN 2622-4852
DOI: 10.33019/jurnalecotipe.v10i1.3964

The Design of Solar Cell-Based Street Lighting for School Area

Azriyenni Azhari Zakri[1], Muhammad Fauzan[2], Wahri Sunanda[3], Rudy Kurniawan[4]
[1,2] Department of Electrical Engineering, Faculty of Engineering, Riau University, Jl. H. R. Soebrantas Km. 12,5 Pekanbaru 28293 Riau Indonesia
[3,4] Department of Electrical Engineering, Faculty of Engineering, Bangka Belitung University, Kampus Terpadu Balunijuk, Bangka, 33172, Indonesia

ARTICLE INFO

Article historys:

Received : 18/04/2023
Revised : 27/04/2023
Accepted : 30/04/2023

Keywords:

Economical; Lighting; Solar Cell; Street Lightings

ABSTRACT

Currently, public street lighting using Solar-based Public Street Lighting has been widely used. Solar-based Public Street Lighting is an off-grid Solar Power Plant application for street lighting. This study aims to use Solar-based Public Street Lighting which has been designed for Inayah Islamic School according to the geographical features of the school. To design this Solar-based Public Street Lighting by considering the economic aspect. From the data obtained directly at the location, the road width is 4.5 meters and the total length is 330 meters. Road size is used to determine the need for lighting quality according to the Indonesian National Standard of 7391:2008. This Solar-based Public Street Lighting has been designed with a pole height of 5 meters and a 1.5-meter pole arm using a 20 Watt 2-in-1 LED lamp and a solar cell capacity of 50 Wp per pole. From the results of the design analysis, the component specifications used in the design have met the requirements according to SNI of 7391:2008, and the required poles for Solar-based Public Street Lighting are 22 points for the Inayah Islamic School Complex area

Corresponding Author:

Azriyenni Azhari Zakri
Department of Electrical Engineering, Faculty of Engineering, Universitas Riau, Kampus Bina Widya, Jl. H. R. Soebrantas Km. 12,5 Simpang Baru, Panam, Pekanbaru 28293 Riau Indonesia
Email: azriyenni@eng.unri.ac.id

1. INTRODUCTION

Inayah Islamic School plans to build Solar-based Public Street Lighting on the road of the school complex. Solar-based Public Street Lighting is an off-grid solar power generation application for street or regional lighting using batteries charged from sunlight as an energy source. Solar-based Public Street Lighting lamps are designed to stay on for 12 hours daily. The general rule of lighting is that too much light will not be better. Vision does not get better only with the amount or quantity of light but also with its quality, which is determined by the level of light reflection and the level of exposure ratio. This research examines the design of artificial lighting in terms of saving electricity on the Inayah Islamic School Complex Road. Street lighting must meet the SNI 7391:2008 [1] standard which discusses street lighting specifications because it aims to achieve uniformity in street lighting planning, especially street lighting in an area. With a road size that is not as big as a highway, economic calculations will be one of the references in this study. Thus, street lighting that can provide safety, comfort, and convenience for road users can be planned and provided.

This research is conducted on how to design street lighting that the solar power plant supplies. The type of road according to field data is a type of local road based on The National Standardization Agency SNI 7391:2008 which is related to the topic of Street Lighting Specifications in Urban Areas. This standard has provisions regarding lighting on various forms and sections of roads in urban areas that

JURNAL ECTIPE
Electronic, Control, Telecommunication, Information, and Power Engineering
Volume 10, Issue 1, April 2023, pp. 131-141
ISSN 2355-5068 ; e-ISSN 2622-4852
DOI: 10.33019/jurnalecotipe.v10i1.3964

have arterial, collector, and local road function classifications. The specifications referred to in this standard include function, type, size, installation, and placement/arrangement of street lighting as needed. Nurochim [2] in his writings related to Solar-based Public Street Lighting Planning for the Kendal sea road and its budget and in Pangkalpinang [3], in addition to using solar power in energy savings, and the cost of LED-type lights. Energy-efficient LED lamps are used in street lighting for better lumens per watt or efficacy. Thus, street lighting that uses LEDs requires less energy to illuminate an area. Therefore, this study will use the previous research as a reference in designing street lighting with energy and cost savings. The design of the lighting system on the road by taking a case study at the Inayah Islamic School Complex.

1.1. Lighting

Lighting is needed for humans to see an object, and inappropriate lighting will affect eye fatigue and nervous tension. To get the ideal lighting quality, the recommended lighting strength standard is set. The pole is part of Solar-based Public Street Lighting which is used to support the lights. Figure 1 is used to simplify calculations in the design and placement of lights for public road lighting so that the lighting angle can be calculated according to CIE 180:2007 [4,5] and SNI 7391:2008 [1] standards.

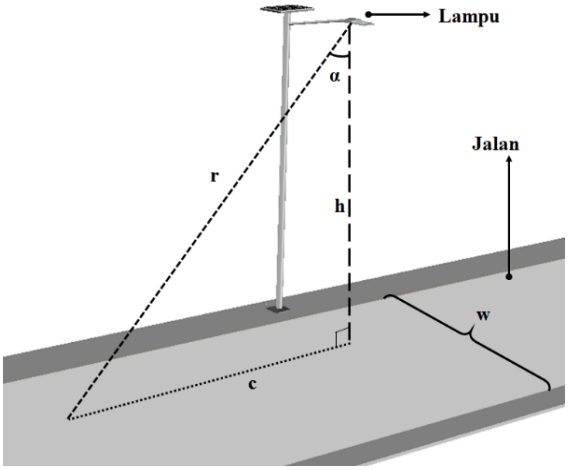

Figure 1. Determining lighting on the street size

Actual distance from the lamps to the middle of the road (r) can be obtained by Pythagoras theorem [6].

$$r = \sqrt{h^2 + c^2} \quad (1)$$

And to find out the angle α can be obtained with trigonometry ratios.

$$cos\ cos\ \alpha = \frac{h}{r} \quad (2)$$

Luminous flux is the amount of power of light emitted by a light source per second. Luminous flux is denoted by ϕ_v with units of lumens (lm). Luminance is the light intensity emitted or reflected on a surface area, symbolized by L_v with Candela per meter squared (Cd/m^2). Illumination (E_v) is the level of illumination on a surface expressed in lux or lm/m^2. The lighting level can be determined by CIE 115:2010 [9] and SNI 7391:2008 standards [1]. Table 1 shows the standard for lighting quality based on the type of road according to SNI 7391:2008 [1].

Table 1. Lighting level based on road type

Road Type or Classification	Average E_v (lux)
Local Street	2-5
Collector Street	3-7
Arterial Street	11-20

Source: SNI 7391 [1]

JURNAL ECTIPE
Electronic, Control, Telecommunication, Information, and Power Engineering
Volume 10, Issue 1, April 2023, pp. 131-141
ISSN 2355-5068 ; e-ISSN 2622-4852
DOI: 10.33019/jurnalecotipe.v10i1.3964

According to Lambert's law, Illumination (E_v) is related to the intensity of light (I_v) that is emitted in a direction with an angle of incidence (α) and is inversely proportional to the square of the distance traveled by the light (r) [7].

$$E_v = \frac{I_v}{r^2} cos\ cos\ \alpha \quad (3)$$

Efficacy (η_v) is the amount of flux produced by a lamp for every watt of electrical power used, with units of lumens per Watt (lm/W). Efficacy is closely related to the wavelength radiated by the lamp. LED efficacy continues to increase, and white LED sources have an efficacy approaching 100 lumens/Watt [4].

$$\eta_v = \frac{\phi_v}{P} \quad (4)$$

Light intensity (I_v) is the flux radiated in a certain direction in a space angle (Ω). The intensity of light in lumens per steradian is called candela (cd).

$$I_v = \frac{\phi_v}{\Omega} \quad (5)$$

Figure 2 shows the shape of the space angle (Ω). Steradian (sr) is the unit of space or solid angle from the midpoint of the ball between the radii, expressed by the surface area of the ball which is determined per the square of the radius [8].

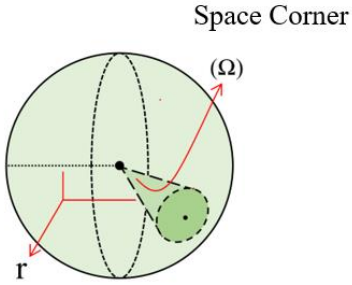

Figure 2. Space angle (Ω)

Space angle equation:

$$\Omega = 4\,\pi \quad (6)$$

1.2. Solar-based Public Street Lighting

Solar-based Public Street Lighting is the application of a solar power generation system as a generator of electricity to supply lights that illuminate the street. Based on the origin of the source, a solar power generation system is divided into two types. They are On-Grid and Off-Grid. Grid solar power generation system is a Solar-based Public Street Lighting that not only uses solar cells as a source of electric power to supply loads, but this type of solar power generation system is also generally connected to a source from PLN and a Generator Set (GenSet) as another source of electric power. In contrast to the On-Grid type, Off Grid solar power generation system only uses solar cells as the sole source of electric power to supply loads. Components of Solar-based Public Street Lighting are divided into several parts: the generator system, load section, and supporting equipment. The generating system includes solar cells, solar charge controllers, and batteries. The loading tool is the lamp. The supporting tools include poles, conductor cables, and panel boxes. There are several types of lamps used in lighting systems, namely incandescent lamps, halogen lamps, fluorescent lamps, mercury lamps, sodium lamps, and Light-Emitting Diode (LED) lamps. LED is a type of semiconductor diode that can emit light energy when given an electric voltage. By consuming less electrical energy, LEDs can produce light that has 60-100 lm/W. The battery is one of the PLTS components whose function is to store electricity generated from solar cells during the day. To determine the battery capacity to be used, first know the amount of energy used by the load in a day.

$$Electric\ Power = P \times usage\ time\ (jam) per - day \quad (7)$$

JURNAL ECOTIPE
Electronic, Control, Telecommunication, Information, and Power Engineering
Volume 10, Issue 1, April 2023, pp. 131-141
ISSN 2355-5068 ; e-ISSN 2622-4852
DOI: 10.33019/jurnalecotipe.v10i1.3964

Where P is the load power. Load reserves in Watt-hour units are converted to Ampere-hours (Ah) expressed in [10].

$$Ah = \frac{Electric\ Energy}{V} \quad (8)$$

Batteries have a maximum usage limit for battery capacity or Depth of Discharge (DoD). The day unit for storing and distributing energy to loads is generally determined as one day. Calculation of the required battery capacity is shown in the equation: [2].

$$Battery\ Capacity = \frac{Ah \times Day}{DoD} \quad (9)$$

or

$$Battery\ Capacity = \frac{Electric\ Energy \times Day}{V \times DoD} \quad (10)$$

Solar cells are devices that can convert sunlight into electricity. Solar cells generally take a maximum of about 5 hours to convert sunlight into electrical energy in a day. Electrical energy will be stored in batteries that are obtained from morning to evening so that electricity can be used whenever it is needed. The time equation needed for the module to get global light accurately is symbolized by t_{modul} as follows [6].

$$t_{modul} = \frac{GTI_{opta}}{G_{STC}} \quad (11)$$

Thus the size of the required solar panel module capacity (Wp) can be found by the equation:

$$Module\ Capacity = \frac{Energy\ Needed}{t_{modul}} \quad (12)$$

Solar panels, based on the type of material, are generally divided into three types: polycrystalline, monocrystalline, and thin film solar cells [11]. Solar Charge Controller (SCC) is an electronic device that is used as a charge regulator to limit the current and voltage flowing into the battery. SCC is used to prevent the battery from overcharging.

2. RESEARCH METHOD

This research method describes the initial stages carried out in research. In this research, a Solar-Based Public Lighting device is designed for Powered Public Street Lighting. At the research location, which is on the Inayah Islamic School complex, there was no street lighting, so the only data obtained were in the form of road size at the research location. Table 2 summarizes the measured road sizes at the study locations.

Table 2. Road size data

Part of the Street	Street Width	Street Length
Entrance	4.5 m	100 m
Inside Road	4.5 m	130 m
Exit Road	4.5 m	100 m

In designing Solar-Based Public Lighting, it uses an Off-Grid solar power plant system so that Solar-Based Public Lighting uses a DC electricity system and does not need to use an inverter. Street lighting is designed using Solar-Based Public Lighting type 2-in-1, this type has several advantages over the other two types of public lighting; unlike conventional Solar-Based Public Lighting which requires a panel box to store SCC and batteries, tilt solar cells can be adjusted freely without being affected by the tilt of the lamp, unlike the Solar-Based Public Lighting AIO. The specifications consist of a pole height of 5 m and a pole length of 1.5 m, a 2 in 1 20 W LED lamp, and a 50 Wp solar cell. The type of lamp to be used is a 2-in-1 LED lamp. The 2-in-1 LED lamp is integrated with the controller and battery

JURNAL ECTIPE
Electronic, Control, Telecommunication, Information, and Power Engineering
Volume 10, Issue 1, April 2023, pp. 131-141
ISSN 2355-5068 ; e-ISSN 2622-4852
DOI: 10.33019/jurnalecotipe.v10i1.3964

in the lamp housing. The lamp model proposed in the design with AutoCAD software, with power from a 20 Watt lamp with a battery capacity of 32 Ah and a battery voltage of 3.2 V as shown in Table 3.

Table 3. The specification of LED light 2-*in*-1

Explanation	Specification
Power	20 W
Battery Voltage	3.2 V
Battery Capacity	32 Ah

The type of solar cell that will be used in the design is a polycrystalline solar cell. This type is suitable for consumption needs that are not too large. Figure 4 shows the design of a polycrystalline solar panel using AutoCAD software. The image design was based on an online shop. The module power is 50 Wp with a maximum voltage of 18 V and a maximum current of 3 A. Table 4 summarizes the specifications of the solar panels used in the design of Solar-Based Public Lighting.

Table 4. Solar panel specifications

Explanation	Specification
Module Capacity	50 Wp
Peak Force (V_m)	18 V
Peak Current (I_m)	3 A

The lamp is directly connected to the solar cell because the battery and controller are already available in the lamp housing. The positive pin of the solar cell is connected to the positive SCC pin, and the negative pin of the solar cell is connected to the negative SCC pin as shown in the electrical system circuit in Figure 3.

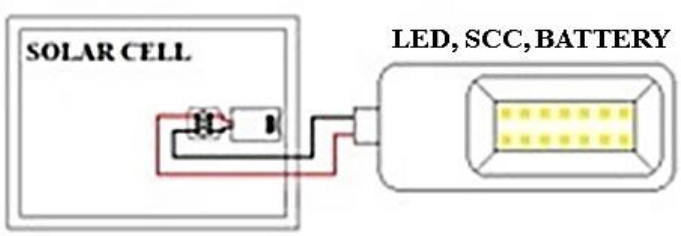

Figure 3. Electrical system circuit of solar cell-based street lighting 2-*in*-1

The work scheme for solar street lighting has two schemes. They are during the day and at night, the following is an explanation of how it works. When sunlight begins to shine on the solar cell, the solar cell begins to absorb sunlight and convert it into electrical energy. SCC regulates the electrical energy generated by solar cells to charge the battery and turn the lights off. When it is nighttime and the solar cells are no longer absorbing sunlight on the SCC, the SCC regulates the battery current to supply the LED lights and keeps the lights on. In making Solar Cell-Based Street Lighting sketches, a reference is needed to be used for component sizes. Due to the height of buses and trucks reaching 3.5 meters. To avoid collisions with vehicles, the pole height will use a measurement of 5 meters. The length of the lamppost arm is about 1.5 m and the pole is 0.5 meters away from the roadside. Figure 4 shows the initial design designed with AutoCAD software in centimeters. Solar Cell-Based Street Lighting is designed using a single arm.

JURNAL ECOTIPE
Electronic, Control, Telecommunication, Information, and Power Engineering
Volume 10, Issue 1, April 2023, pp. 131-141
ISSN 2355-5068 ; e-ISSN 2622-4852
DOI: 10.33019/jurnalecotipe.v10i1.3964

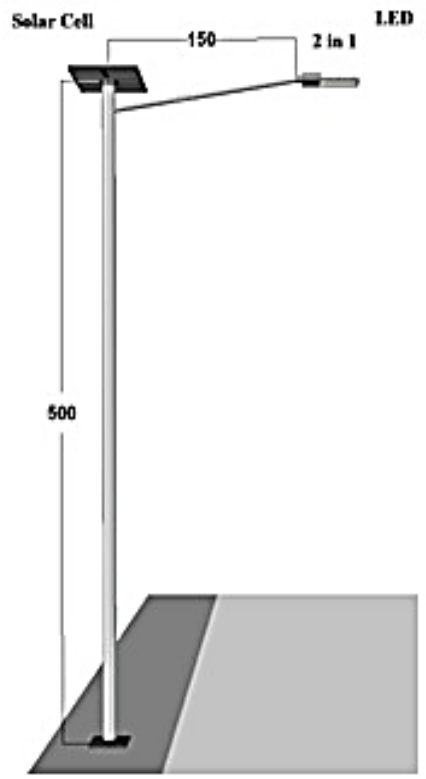

Figure 4. The design of solar cell-based street lighting for Inayah Islamic School

3. RESULTS AND DISCUSSION

Solar Cell-Based Street Lighting that has been designed will be reviewed and analyzed whether the design meets the applicable SNI. This chapter also explains how suitable the design of Solar Cell-Based Street Lighting is from the processed data and then economic calculations are carried out afterward. In the design, a 2-in-1 LED lamp with a power size of 20 watts is used, but it is not yet known whether the power size complies with SNI 7391:2008 or not. To calculate the distance and angle between the light rays on the end surface of the path. It is known that the height of the lamp is 4 m and the horizontal distance from the lamp to the middle of the road (c) is 1.5 m. The actual distance from the lamp to the end of the road (r) is obtained from equation (1) to be r = 5.154 meters, to calculate the angle β using equation (2) it is obtained $\alpha = 14{,}070°$. Calculating Light Intensity and Flux SNI 7391:2008 stipulates that the type of local road must have an illumination (E_v) of around 2 Lux to 5 Lux. And according to the parameters of CIE 115:2010, the research location is in class P4. In this calculation the illumination value used is 5 Lux, from equation (3) it can be found the required intensity $I_v = 136.920\ cd$. To calculate the luminous flux obtained using equation (5) it is obtained $\phi_v = 1720.663\ lm$. The light intensity required to comply with the provisions of SNI 7391:2008 is 136.920 candela and the luminous flux is 1720.663 lumens with an illumination of 5 Lux. Palaloi [12] in their scientific work said that LEDs generally have a light efficacy (η_v) of 65-100 lumens/watt and the average efficacy when used for a long time is 85.5 lumens/Watt [13]. So, by using equation (4), the power of the lights needed for the road of the Inayah Islamic School complex according to SNI is $P = 20.125\ W$. The light power required on the road of the Inayah Islamic School complex from the technical analysis is 20.125 Watt. The power of the lamp used in the design is 20 watts, this size is close to even greater than the size of the power needed on the road of the Inayah Islamic School complex.

Solar Cell-Based Street Lighting lamps are designed to be on for approximately 12 hours at night a day. To find out how much electrical energy is needed for a 20 Watt lamp to burn for 12 hours a day, you can use equation (7) to become 240 Watt-Hour. Lithium battery DoD [14] reaches 100%, with equation (10) you can find how much battery capacity is needed to supply lights in one working day. The capacity of the battery needed to supply a 20 Watt lamp for 12 hours in one day is 75 Ah. To find

JURNAL ECOTIPE
Electronic, Control, Telecommunication, Information, and Power Engineering
Volume 10, Issue 1, April 2023, pp. 131-141
ISSN 2355-5068 ; e-ISSN 2622-4852
DOI: 10.33019/jurnalecotipe.v10i1.3964

out the capacity of solar cells [15], a calculation is needed by considering how long the sun's peak time is to maximize energy absorption. From the statistical data on the Global Solar Atlas website, at the coordinates of the Inayah Islamic School, the GTI_{opta} value was obtained which is 4.756 kWh/m2 per day. So the time needed for the module to get global light can be obtained by equation (11) is $t_{modul} = 4.756\ hours$. The required solar panel capacity can be found by using equation (12). The internal solar panel capacity required in the design is 50.463 Wp rounded up to 50 Wp. The number of Solar-based Street Lighting needed along the road of Inayah Islamic School Complex can be found by determining the distance between the pillars with the following steps. To determine the distance between poles, it is necessary to calculate the maximum lighting distance (midpoint between poles). The lamp power used is 20 W with an average efficacy of 85.5 lm/W at a height of 5 m, with equation (4) for the light flux is$\phi_v = 1710\ lm$, and with equation (5) for the light intensity $I_v = 136{,}077\ cd$. The actual distance from the lamp to the farthest distance of illumination with 1 lux illumination (1 lux from each lamp, in SNI 7391:2008 the lowest illumination on local roads is 2 lux) with equations (3) and (2). So with equation (1) the horizontal distance of the lamp to the farthest street point with the smallest illumination is c = 7.235 m. The farthest horizontal distance of illumination of a 20 W LED lamp at a height of 5 m is 7.235 m. The distance between the poles is twice the farthest horizontal distance of the lighting so that 14.470 m is obtained, rounded up to 15 m. All sections of the Inayah Islamic School Complex have the same road width, but different lengths. The entrance road is 100 meters long, the inner road is 130 meters long and the exit is 100 meters long. From the entrance to the exit, the total length of the road is added up. So that the number of light pole points obtained is 22 poles. The number of light points from the entrance gate to the exit gate is 22 poles with a distance of 15 meters between poles. Figure 5 shows the placement and distance between pole points which are useful for knowing the approximate location of the Solar Cell-Based Street Lighting pole points on the site plan.

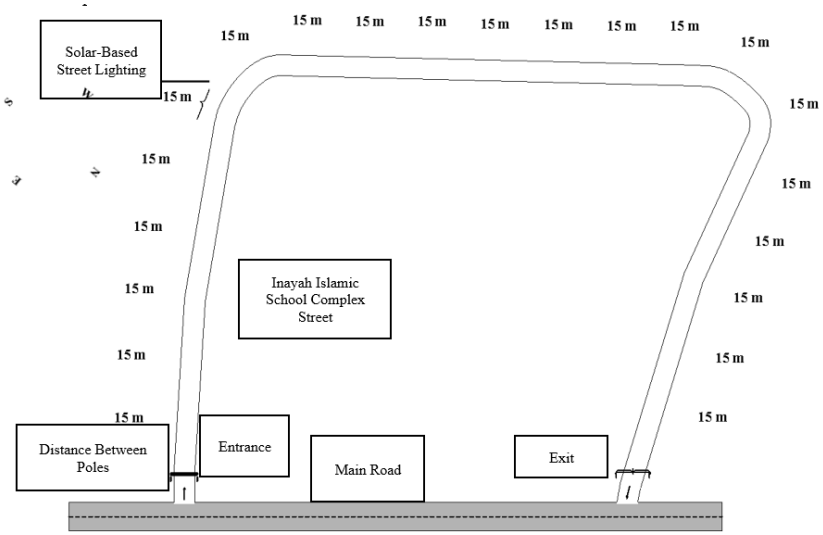

Figure 5. Estimation of point locations and distances between poles of solar cell-based street lighting

Figure 6 shows the placement and distance between the PJUTS pole points based on the original plan taken from a Google Map designed using AutoCAD software. This is useful for knowing the placement of poles in two-dimensional and three-dimensional views.

JURNAL ECTIPE
Electronic, Control, Telecommunication, Information, and Power Engineering
Volume 10, Issue 1, April 2023, pp. 131-141
ISSN 2355-5068 ; e-ISSN 2622-4852
DOI: 10.33019/jurnalecotipe.v10i1.3964

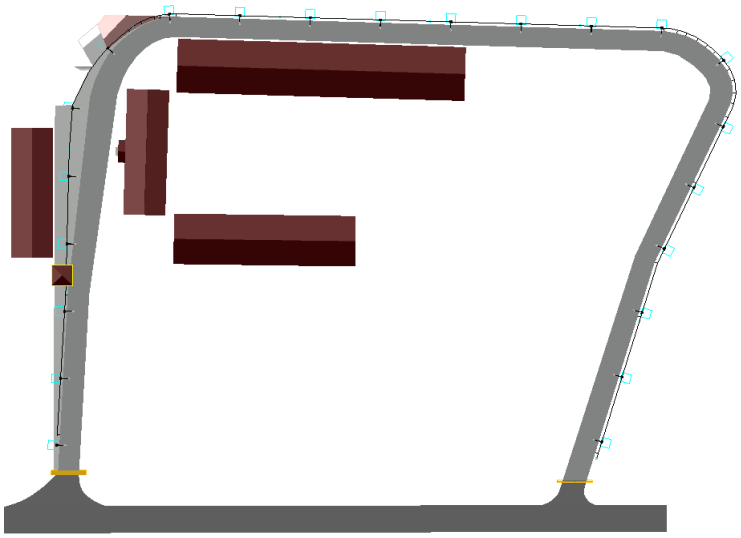

Figure 6. Pole points of solar cell-based street lighting on site plans with AutoCAD software

Three-dimensional design from the top view of the placement of the Solar Cell-Based Street Lighting pole points with AutoCAD software. The image is designed directly from a Google Map photo, the photo is coated with the specified colored line and then stores the three-dimensional version. The pole point in Figure 6 is symbolized by an empty cyan or light blue box and the school road in gray, while the red color shows the school roof.

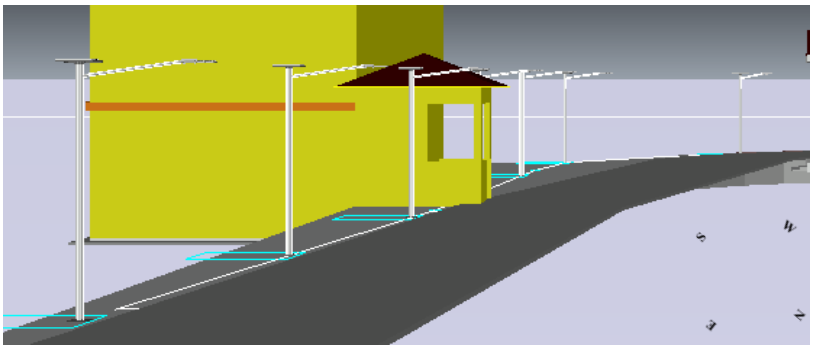

Figure 7. The display of solar cell-based street lighting at the entrance

Figure 7 shows a simulation in the AutoCAD software of the design of Solar Cell-Based Street Lighting at the entrance to the Inayah Islamic School Complex from the outside (entrance). It can be seen that Solar Cell-Based Street Lighting is placed on the left side of the road.

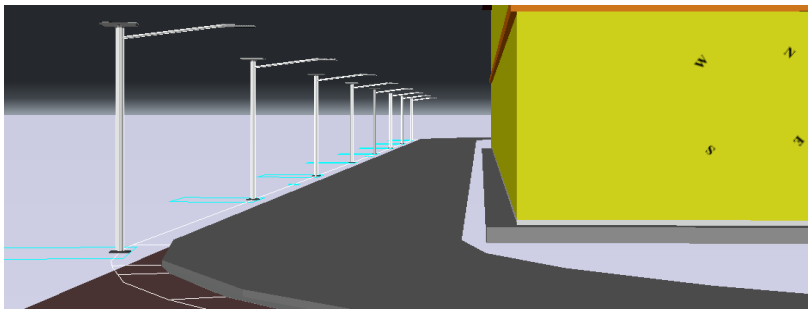

Figure 8. The display of solar cell-based street lighting the inside

Figure 8 shows a simulation in the AutoCAD software of the design of Solar Cell-Based Street Lighting on the inner road of the Inayah Islamic School Complex from the side of the entrance. Solar Cell-Based Street Lighting is placed on the left side of the road because there is no land on the right side of the road because it is adjacent to the school building.

JURNAL ECOTIPE
Electronic, Control, Telecommunication, Information, and Power Engineering
Volume 10, Issue 1, April 2023, pp. 131-141
ISSN 2355-5068 ; e-ISSN 2622-4852
DOI: 10.33019/jurnalecotipe.v10i1.3964

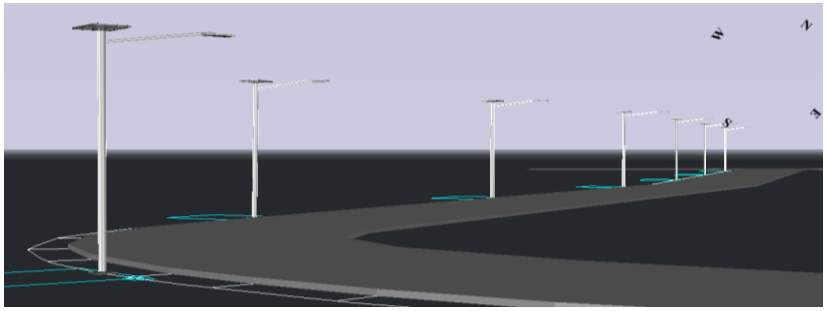

Figure 9. The display of solar cell-based street lighting in the exit

Figure 9 shows a simulation in the AutoCAD software of the design of Solar Cell-Based Street Lighting at the exit of the Inayah Islamic School Complex from the inside of the school. Solar Cell-Based Street Lighting is placed on the right side of the road from the outside because that side is the outer side of the Inayah Islamic School Complex. The table will show a comparison of the specifications of the components used with the components obtained from the calculations. Solar Cell-Based Street Lighting is placed on the right side of the road from the outside because that side is the outer side of the Inayah Islamic School Complex.

Table 5. Component specifications are designed with that into account

Component	Used	Estimation
LED	20 Watt	20.125 Watt
Battery	32 Ah	75 Ah
Solar Cell	50 Wp	50.463 Wp

From table 5, the capacity of the battery used and the one obtained from the calculation is quite different, the battery used has a capacity of 32 Ah and the battery obtained from the calculation has a capacity of 75 Ah. There are several reasons for still using a 2 in 1 LED lamp that is integrated with a 32 Ah battery, including a 2 in 1 LED lamp having a controller and the difficulty of finding suitable specifications on the market because it comes directly from the seller or factory. The two in one LED light controller is referred to as intelligent power control, when it adjusts the output power. The power used at the beginning is very small and over time will continue to increase until it reaches a maximum of one-third of the usage time and decreases again gradually from the last third of the usage time until the end of the usage time. Table 6 is the result of the first economic analysis, namely a comparison of the component prices for Solar Cell-Based Street Lighting and Conventional Street Lighting, showing the specifications and prices for the designed Solar Cell-Based Street Lighting. Meanwhile, the price and component specifications of conventional Street Lighting can be seen in Table 7. The specifications of conventional Street Lighting components follow the specifications of Solar Cell-Based Street Lighting.

Table 6. Estimated component prices of solar cell-based street lighting

Component	Type	Size	Price (Rp)
Pole	-	4 meters	2.000.000
Pole Arm	-	1.5 meters	250.000
Lamp	LED 2-*in*-1	20 Watt	990.000
Solar Cell	*Polycrystalline*	50 WP	650.000
Cable	NYY 2 × 1.5 mm^2	2 meters	30.000
Supporting Component	-	-	1.000.000
Total Cost per-pole			4.920.000
Total Cost of Solar Cell-Based Street Lighting (times poles)			108.240.000

JURNAL ECOTIPE Electronic, Control, Telecommunication, Information, and Power Engineering
Volume 10, Issue 1, April 2023, pp. 131-141
ISSN 2355-5068 ; e-ISSN 2622-4852
DOI: 10.33019/jurnalecotipe.v10i1.3964

Table 7. The estimated price of Conventional Street Lighting components

Component	**Type**	**Size**	**Price (IDR)**
Pole	-	4 meters	2.000.000
Pole Arm	-	1.5 meters	250.000
Lamp	LED	20 Watt	130.000
Component	**Type**	**Size**	**Price (IDR)**
Contact Cable	NYM 2 × 2.5 mm^2	4 meters	29.000
Connecting Cable for	NYFGBY 2 × 6 mm^2	32 meters	1.712.000
Supporting Components	-	-	500.000
Total cost per-pole			4.621.000
Total cost of all street lamps (times total poles)			101.662.000

Due to the energy source of conventional street lamps from State Electricity Company, there is a predetermined tariff fee. According to the State Electricity Company, schools are included in the social tariff category with a usage fee of IDR 455.00/kWh. The cost of using electricity for conventional street lamps as a whole in 1 year as a whole is 876,876 rupiah. The cost of using electricity for all conventional type street lamps in 1 year is IDR 1,392,120.95. The age of solar cells can reach 20 years. To find out the operational costs of conventional Street Lighting that uses State Electricity Company electricity, you can see the cost of electricity usage over the life of the solar cells. The operational cost of conventional street lamps for the next 20 years is IDR 17,537,520. In terms of investment costs, conventional street lamps are cheaper, but in terms of operational costs, Solar Cell-Based Street Lighting two-in-one is much more economical because Solar Cell-Based Street Lighting generates electrical energy from solar cells, so electricity usage rates are not charged.

4. CONCLUSION

Based on data analysis and calculation results on the design of street lighting at Inayah Islamic School Complex, it can be concluded that the design of street lighting at Inayah Islamic School Complex uses 2-in-1 LED lights with a power of 20 Watt, and the parameters of the poles with a road width of 4, 5 meters, namely the height of the pole is 5 meters, the distance between the poles is 15 meters and the Street Lightings point is 22 points, which is in accordance with SNI 7391:2008. By using 50 Wp solar cells, the design of Solar Cell-Based Street Lighting on the road of the Inayah Islamic School Complex requires a budget of around IDR 108,240,000.00 and conditional maintenance operational costs for the future. In terms of investment costs, conventional Street lighting is cheaper, but in terms of operational costs, 2-in-1 Solar Cell-Based Street Lighting is much more economical. This is because Solar Cell-Based Street Lighting generates electrical energy from solar cells, so electricity usage rates are not charged.

REFERENCES

[1] Indonesia, Standar Nasional. *Spesifikasi penerangan jalan di kawasan perkotaan*. Badan Standardisasi Nasional (BSN). 2008.

[2] A. Nurrohim, *Perencanaan Lampu Penerangan Jalan Umum*. Universitas Semarang. 2018.

[3] A. Febrianto, W. Sunanda, R. F. Gusa. "Penerangan Jalan Umum Tenaga Surya: Studi Kasus di Kota Pangkalpinang." *Jurnal Presipitasi*: *Media Komunikasi dan Pengembangan Teknik Lingkungan* vol. 16, no. 2, pp. 76-82. 2019.

[4] S. Almási, M. Bizjak, E. Burini, D. Coatham, D. Crawford, J. Hart, N. Hodson, D. Schreuder, R. Yates, J.S Yerrell, *CIE 180:2007 Road Transport Lighting for Developing Countries*. The International Commission on Illumination (CIE), 47, 2007.

JURNAL ECOTIPE
Electronic, Control, Telecommunication, Information, and Power Engineering
Volume 10, Issue 1, April 2023, pp. 131-141
ISSN 2355-5068 ; e-ISSN 2622-4852
DOI: 10.33019/jurnalecotipe.v10i1.3964

[5] IEC. International electrotechnical vocabulary (IEV) – Part 845: Lighting. In the International Electrotechnical Commission (2nd ed.). 2022

[6] I. B. Ramahani, Buku Instalasi PLTS. Jakarta : Deutsche Gesellscjsft fur Internastionale Zusammenarbit (GIZ. 2018.

[7] V.C Bender, F. B. Mendes, T.Maggi, M. A. D. Costa, T. B. Marchesan, "Design Methodology for Street Lighting Luminaires Based on a Photometrical Analysis". *IEEE*, pp. 1160–1165, 2013.

[8] S. Rolaskhi, "Inovasi Perancangan dan Perencanaan Bisnis Paket Panel Surya (Solar Home System)" [Universitas Komputer Indonesia]. In *Universitas Komputer Indonesia*. https://elibrary.unikom.ac.id/id/eprint/2608/

[9] T. Adams, A. Augdal, M. Bizjak, E. Bjeland, N. Bonne, C. Chain, M. Gillet, B. Hamel, B., P. Hautala, *CIE 115-2010 Lighting of Roads for Motor and Pedestrian Traffic*. The International Commission on Illumination (CIE), 35, 2010.

[10] A.A. Zakri, N. Nurhalim, D.P.H. Simanullang, I. Tribowo. "Photovoltaic Modeling Methods Based on Matlab Simulink Implementation". *Sinergi*, vol. *22*, no. 1, pp. 1-6, 2018.

[11] S. Rolaskhi, "Inovasi Perancangan dan Perencanaan Bisnis Paket Panel Surya (Solar Home System)" [Universitas Komputer Indonesia]. In *Universitas Komputer Indonesia*. https://elibrary.unikom.ac.id/id/eprint/2608/. 2019.

[12] S. Palaloi, S. Nafis, S.Emo. "Kajian Tingkat Efikasi Lampu LED Swabalast Untuk Pencahayaan Umum". *Ketenagalistrikan dan Energi Terbarukan*. vol. 14, no. 1, pp. 1–14. 2015.

[13] A.A. Zakri, R. Febriyursandi, A. Hamzah, *Teknik Pencahayaan Ruangan Via Dialux Evo*.2019.

[14] A.A Zakri, *et al*. "Alat Otomatis Pengisi Baterai Bersumber Solar Sel Menggunakan Pengendali Arduino. *Seminar Nasional Terapan Riset Dan Inovatif*, pp. 128–139. 2019.

[15] W. Sunanda, R. F. Gusa, Y. Tiandho, E.A Pratama, E. A. "Impact of shading net on photovoltaic cells performance". *Jurnal Teknik Elektro*, vol.11, no. 2, pp. 56-60. 2019.

JURNAL ECOTIPE
Electronic, Control, Telecommunication, Information, and Power Engineering

Volume 10, Issue 1, April 2023, pp. 142-151
ISSN 2355-5068 ; e-ISSN 2622-4852
DOI: 10.33019/jurnalecotipe.v10i1.3894

Design and Build a Website-Based Landslide Early Warning System

Muhammad Ghofinda Prasetia[1], Puji Cahniya Sari[2], M. Azwan[3], Inayatul Inayah[4], Fajar Mahardika[5]

[1,2,3,4]Program Studi Fisika, Fakultas Sains dan Teknologi, Institut Teknologi dan Sains Nahdlatul Ulama Pekalongan
[5]Program Studi Teknologi Komputer, Fakultas Sains dan Teknologi, Institut Teknologi dan Sains Nahdlatul Ulama Pekalongan
Jl. Karangdowo No.9 Kedungwuni Kab. Pekalongan, 51173, Indonesia.

ARTICLE INFO

Article history:

Received : 28/02/2023
Revised : 07/04/2023
Accepted : 30/04/2023

Keywords:

Landslide; Landslide Detector; MPU6050; Soil Moisture; Website

ABSTRACT

An early warning system is very important to implement to minimize losses received when a disaster occurs, one of which is a landslide disaster. An early warning system for landslides is carried out so that people can find out the signs of a disaster that can be accessed anywhere, so they can prepare themselves. For this reason, a tool is needed that can detect and provide early warning of landslides to the public which can be accessed through the website. In this study, a website-based landslide early warning system has been designed using a soil moisture sensor to measure it and the MPU6050 sensor to measure the slope of the soil. Sensor data will be displayed on the LCD and sent to the database and can be monitored through the website. The avalanche detector made is powered by a 15 V DC battery to provide 5V output to the NodeMCU ESP8266. Soil moisture sensor, MPU6050, LCD I2C, LED, and relay work at 5V. A Relay is used to turn on the siren at 12V voltage. Based on our research, the soil moisture measurement value between the sensor and the comparison device is around 1.55% and the soil slope measurement value between the sensor and measuring tool is around 0.14%, these two factors influence each other. The measurement error is still fairly normal according to the soil moisture sensor datasheet and MPU6050, which are ±3% together.

Corresponding Author:

Muhammad Ghofinda Prasetia
Jl. Karangdowo No.9 Kedungwuni Kab. Pekalongan, 51173, Indonesia.
Email: prasetia1805@gmail.com

1. INTRODUCTION

Landslides are a disaster that often occurs in hilly and mountainous areas [1]. The condition of the soil in parts of Indonesia is classified as prone to landslides. Based on the landslide vulnerability zone map according to the National Disaster Management Agency (BNPB) in 2023, there were 634 landslides in Indonesia [2].

Geographical conditions, which are generally mountainous areas with slopes, make the soil unstable. As a result, when the soil is moved, it becomes prone to landslides [3, 4]. Movement of soil and excess water content are the main causes of landslides. Landslides are also affected by the presence of a driving force on the ground which is greater than the resisting force [5, 6, 7]. In general, the Center for Volcanology and Geological Hazard Mitigation said that landslides have several symptoms that can be observed visually, including occurring after rain, cracks appearing on the slopes parallel to the direction of the cliff, buildings starting to crack, trees or electricity poles slanted, and

JURNAL ECOTIPE
Electronic, Control, Telecommunication, Information, and Power Engineering
Volume 10, Issue 1, April 2023, pp. 142-151
ISSN 2355-5068 ; e-ISSN 2622-4852
DOI: 10.33019/jurnalecotipe.v10i1.3894

new springs appear [8]. Landslide disasters can cause many losses, including causing casualties, disruption of transportation facilities, damaging agricultural land, and various other consequences that are detrimental to community activities [9]. The impact of this landslide disaster can be avoided with prevention efforts using an early warning system for landslides so that people can know the signs of landslides and receive warnings that landslides will occur [10, 11]. Information technology that is integrated into various aspects of life is often referred to as the Internet of Things (IoT) [12,13,14]. Its reliability makes everything connected, monitored, and controlled as expected [15]. The use of soil moisture sensors to detect soil moisture levels capacitively [16]. MPU6050 sensor to detect conditions at a certain level of slope that is integrated with the gyroscope sensor [17]. The ESP8266 module is complete and unified as an application provider that is integrated with sensors or with certain application tools [18].

In research conducted by Supriyatna entitled "Design and Build Early Warning Systems for Landslide Prone Areas". In this study designing a tool using an accelerometer sensor and LDR sensor, the system can be monitored wirelessly by adding a telemetry radio connected directly to Arduino and a computer using Labview [19]. However, it still has drawbacks, namely not using Android applications and not being based on IoT.

Research conducted by Muhammad Reza Maulana, et al entitled "Design of a Landslide Detection System Using IoT-based Gyroscope and Hygrometer Sensors" [20]. The designed system will provide information via telegram notifications. However, it has a drawback, namely sensor data is not stored in the database. So that the community cannot monitor the value of soil moisture and the slope of the land.

Based on previous research, the solution we want to offer is to create an avalanche detection design with the innovation we want to develop, namely by utilizing a soil moisture sensor to measure soil moisture and the MPU6050 sensor to measure the slope of the soil. Where sensor data can be monitored through the website so that it can be accessed from anywhere and at any time by the general public, which can complement a landslide early warning system that is reliable and user-friendly.

2. RESEARCH METHODS

2.1. Research procedure

In making this research the authors used the DSRM research method (Design Science Research Method). This method is used to create and design systematically to produce an output in the form of this design. The design of this website-based landslide detector tool begins with conducting a literature study of the research to be carried out to determine the tools and materials needed. The next step is to design a series of devices and do programming on the controller. After the program is successful, then the assembly of the device components is carried out. Further testing and analyzing the test results according to Figure 1.

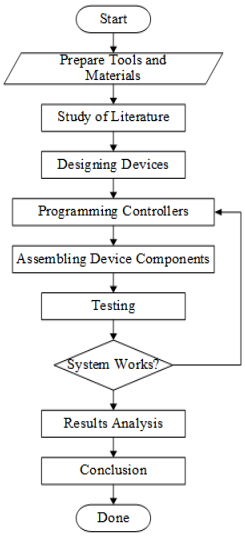

Figure 1. Research procedure

JURNAL ECOTIPE
Electronic, Control, Telecommunication, Information, and Power Engineering
Volume 10, Issue 1, April 2023, pp. 142-151
ISSN 2355-5068 ; e-ISSN 2622-4852
DOI: 10.33019/jurnalecotipe.v10i1.3894

2.2. Diagram Block System

This landslide detector was designed using Nodemcu ESP8266 as the main control system, a soil moisture sensor to measure soil moisture, and an MPU6050 sensor to measure soil slope. Both sensors will send data to MySQL as a database. Then the data that has been stored will be displayed on the website according to Figure 2. After that, the sensor value is also displayed on the LCD. The siren will sound and the LED will flash simultaneously if there are signs of an impending landslide. The system block diagram can be seen in the following figure.

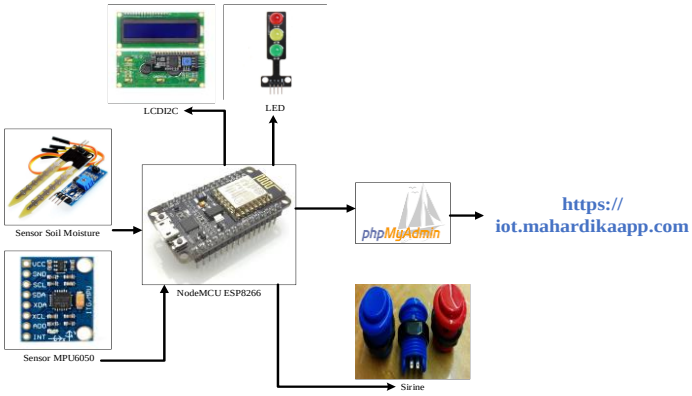

Figure 2. System block diagram

2.3. Device System

The series of systems in this study can be seen in Figure 3. All of these circuits function to read the parameters of soil moisture and soil slope in real-time through the website. So, the user can find out the sensor reading data remotely.

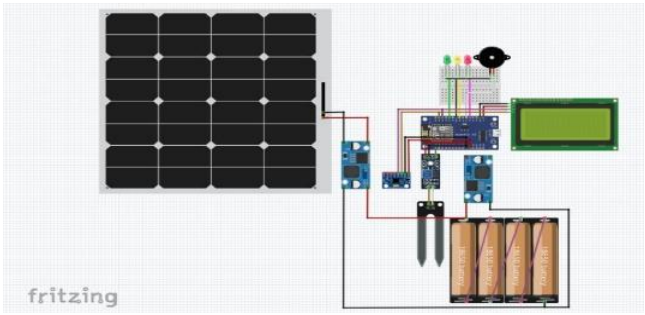

Figure 3. System Device

2.4. Flow Chart System

The working system of the avalanche detector design begins with initializing the data and then connecting the device to the internet using the ESP8266. Sensor data and ground state levels will be processed into three classifications, namely safe, alert, and dangerous. If the ground state is in Safe condition, the green LED will light up. However, if the ground is in an alert condition, the yellow LED will light up. And if the ground is in a Danger condition, the red LED and siren will light up simultaneously. Then the sensor data and soil condition classification will be displayed in real-time on the 12C LCD and the website if the serial number has been registered. The flow diagram of the avalanche detector work system can be seen in Figure 4.

JURNAL ECOTIPE
Electronic, Control, Telecommunication, Information, and Power Engineering
Volume 10, Issue 1, April 2023, pp. 142-151
ISSN 2355-5068 ; e-ISSN 2622-4852
DOI: 10.33019/jurnalecotipe.v10i1.3894

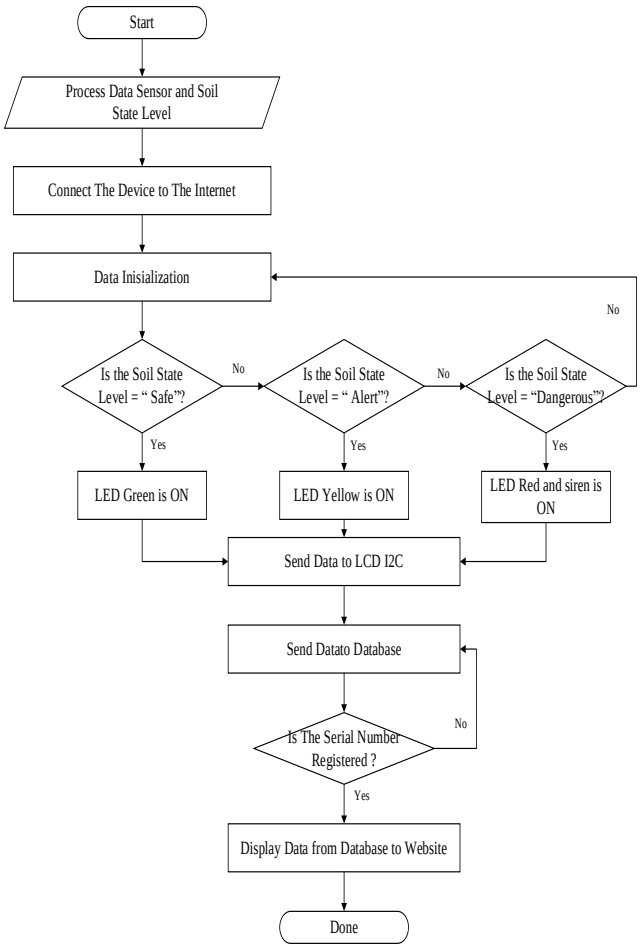

Figure 4. System flowchart

2.5. Software System

The use of the website as an IOT implementation is required to display sensor data that has been sent from ESP8266 to the database. To access the website, two types of users have been provided, namely admin and operator. Where both have different access rights.

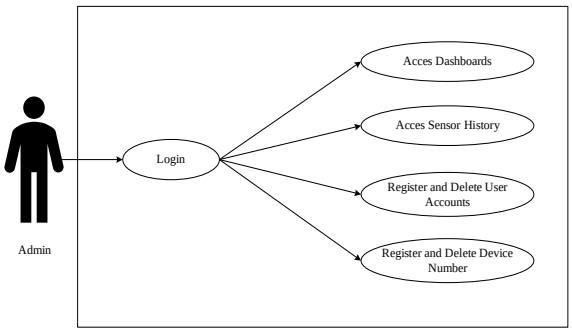

Figure 5. Admin charts

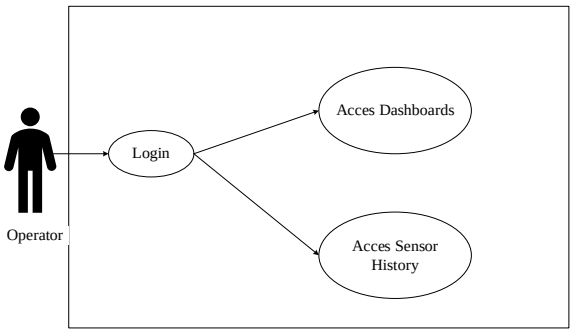

Figure 6. Operator charts

In Figure 5 the admin after logging in can access the dashboard, sensor history, users, and devices. Meanwhile, if you enter as a user, you can only access the dashboard and sensor history. As described in Figure 6.

In making the website, there are several menus, namely login, dashboard, sensor history, users, and devices.

JURNAL ECOTIPE
Electronic, Control, Telecommunication, Information, and Power Engineering
Volume 10, Issue 1, April 2023, pp. 142-151
ISSN 2355-5068 ; e-ISSN 2622-4852
DOI: 10.33019/jurnalecotipe.v10i1.3894

a. Login and Register

Figure 7. Login menu display

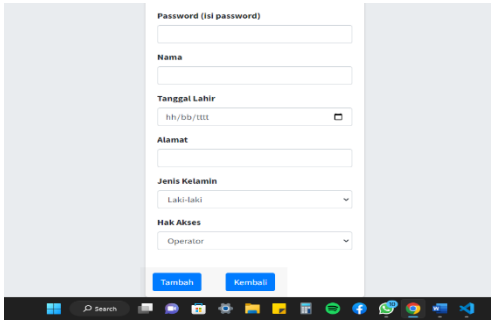

Figure 8. Display menu register

In Figure 7, we can see that the login menu must fill in the username and password for the account that has been registered. If the username and password do not match the database, a notification will appear "incorrect username or password". On the Register menu, if someone wants to visit the website but doesn't have an account, then he can press the "register" button to create an account. But accounts that have been registered are only as operators. More details can be seen in Figure 8.

b. Dashboard

On the dashboard menu, soil moisture and soil slope sensor data sent from NodeMCU ESP8266 to Mysql will be displayed in graphical form in real-time. The dashboard display can be seen in Figure 9.

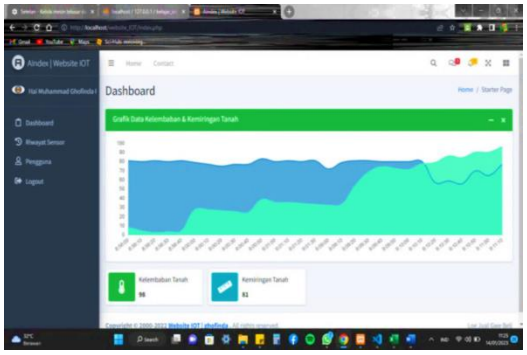

Figure 9. Dashboard view

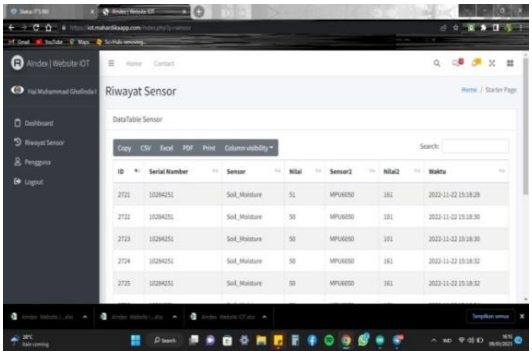

Figure 10. Display of sensor history

c. Sensor History

In addition to displaying data in graphical form on the dashboard menu. The sensor history menu is also used to display sensor data. However, the difference is that the data displayed in table form is based on the serial number on each controller that has been registered. In Figure 10 the sensor data shown comes from the Nodemcu ESP8266 controller with serial number 10284251. In addition, data on sensor history can also be printed to make it easier to analyze the design.

d. User

This menu can only appear if you are an admin user. The user menu contains registered user data in tabular form. Users who have access rights as admin can register, change or delete user data. The user menu display can be seen in Figure 11.

JURNAL ECOTIPE
Electronic, Control, Telecommunication, Information, and Power Engineering
Volume 10, Issue 1, April 2023, pp. 142-151
ISSN 2355-5068 ; e-ISSN 2622-4852
DOI: 10.33019/jurnalecotipe.v10i1.3894

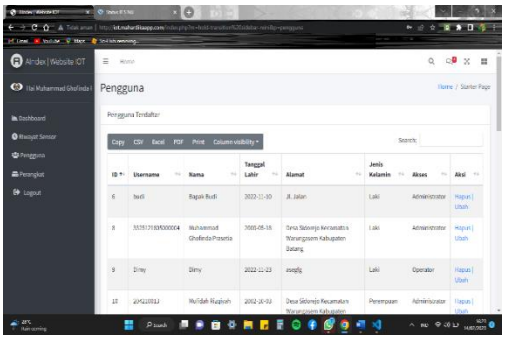

Figure 11. User menu display

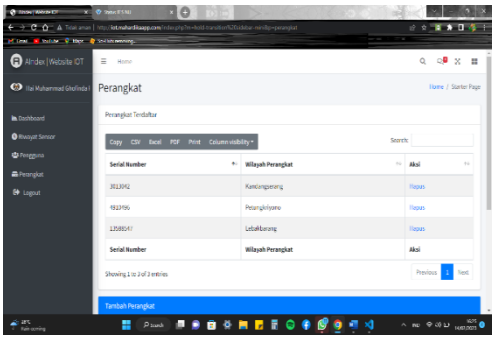

Figure 12. Device menu display

e. Device

The device menu functions to register the controller serial number in the design so that it can send sensor data to the database. Because only the controller on the device whose serial number has been registered can send sensor data to the website. In Figure 12 the device data contains the serial number that has been registered and the name of the area of the design device that is placed.

3. RESULTS AND DISCUSSION

3.1. Calibration

The calibration process of the soil moisture sensor and MPU6050 is used to determine and obtain the accuracy of the sensor when collecting data as a standard or reference in measuring soil moisture and soil slope.

The measurement of soil moisture is carried out by comparing the measurement of the soil moisture sensor and the measurement of the soil tester. Then, measuring the slope of the land is done by comparing the MPU6050 sensor measurements with protractor measurements.

a. Calibrate Soil Moisture with a Soil Tester

Before calibrating the soil moisture value, it is necessary to convert the soil moisture sensor resistance value into percentage units. Based on reading the value of the soil moisture sensor data, the resistance value of the soil moisture sensor reading is from the numbers 0 – 1023 bits which indicate the moisture value of the soil. The higher the value reading, the lower the soil moisture condition or it can be said to be dry. And conversely, the lower the value read by the sensor, the higher the soil moisture condition.

Therefore, to facilitate research, it is necessary to change the sensor value to a percent value (%). Refer to the manual calculation of soil moisture to change the sensor value to a percent value using equation (1).

$$\text{Percent Value} = \frac{1023 - sensor\ value}{1023} x\ 100\% . \quad (1)$$

Equation (1) explains that the sensor values obtained are reduced by the sensor value range, which amounts to 1023 and multiplied by 100%. The purpose of changing this value is so that the tool can directly detect the percentage of soil moisture so that it can be easily understood. The results of changing the sensor value from the resistance value to the percent value (%) are as follows.

Table 1. Conversion of sensor values to percent values

Sensor Value	Percent Value (%)
0	100%
353	65,5%
413	59,6%
560	45,2%
821	19,8%
1023	0%

JURNAL ECTIPE
Electronic, Control, Telecommunication, Information, and Power Engineering
Volume 10, Issue 1, April 2023, pp. 142-151
ISSN 2355-5068 ; e-ISSN 2622-4852
DOI: 10.33019/jurnalecotipe.v10i1.3894

After converting the unit value on the sensor to a percentage value, what needs to be done is calibrate the soil moisture sensor against similar comparison devices. Calibration is carried out by preparing varied soil samples based on the level of water content. Then the sample was measured using a soil moisture sensor and a soil tester as a comparison tool. Measurements were repeated three times for each sample. So that the measurement data is obtained in Table 2 as follows.

Table 2. Soil moisture calibration data with a soil tester

No	Soil Tester (%)	Soil Moisture (%)	Error (%)
1	23.3	21.3	2
2	24	22.3	1.7
3	31.7	30.3	1.4
4	33.3	30.7	2.6
5	41.3	40	1.3
6	43.3	43	0.3
Average			**1.55%**

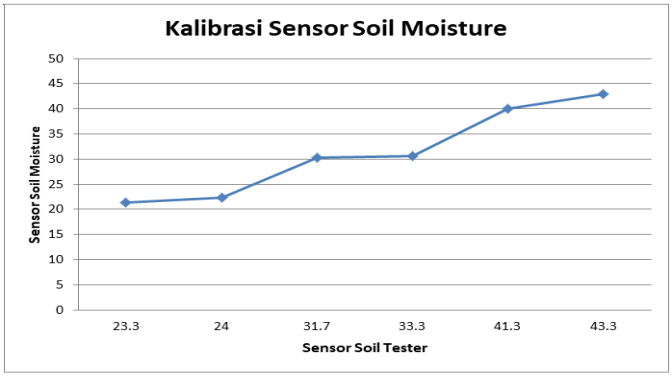

Figure 13. Average in the measurement results of the soil moisture sensor and the soil tester

Figure 13 shows that the average difference in the measurement results of the soil moisture sensor and the soil tester is 1.55%, so it can be interpreted that the soil moisture sensor can measure soil moisture with relatively good measurement results.

b. MPU6050 Calibration with Protractor

The test is carried out by comparing the slope of the tool with the slope of the protractor. Data collection is not carried out directly on the ground to determine the compatibility between the tool and the protractor directly. The reading results of the tool and the protractor must be the same because the tool is used as a detector of the slope of the land in degrees. Data collection at certain angles starting from 0º - 180º is carried out to ensure the accuracy of the tool and ensure that the status of the avalanche detector is displayed properly. The results of testing the tool can be seen in Table 3 as follows.

Table 3. MPU6050 calibration data with protractor

No	Protractor (°)	Sensor MPU6050 (%)	Error (%)
1	0	0	0
2	30	30	0
3	45	45	0
4	60	60.4	0.4
5	90	90.2	0.2
6	135	135	0
7	180	180.4	0.4
Average			**0.14%**

JURNAL ECOTIPE
Electronic, Control, Telecommunication, Information, and Power Engineering
Volume 10, Issue 1, April 2023, pp. 142-151
ISSN 2355-5068 ; e-ISSN 2622-4852
DOI: 10.33019/jurnalecotipe.v10i1.3894

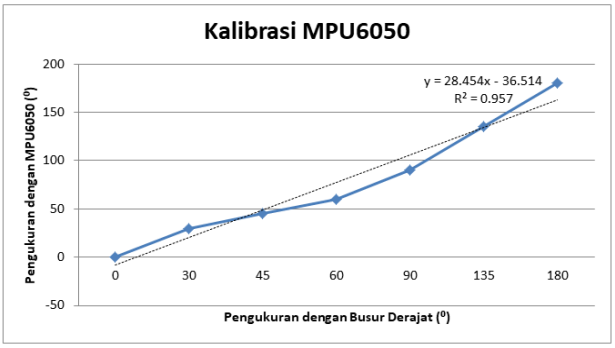

Figure 13. MPU6050 Calibration Measurement

It can be interpreted that the slope of the protractor with the results of the MPU6050 sensor reading is almost the same. The average difference in the measurement results of the MPU6050 sensor and the protractor is 0.14%, the difference between the slope of the protractor and the MPU6050 sensor is because the sensor is very sensitive so it easily changes when the sensor is exposed to small movements. Therefore, the sensor must be installed in a very stable position to produce more accurate data.

3.2. Testing

Tests on the design of the landslide detector are carried out based on the probability that the cause of the landslide will occur from the level of soil moisture and the slope of the soil. The probability of a landslide occurring is then tested every 10 seconds and repeated five times for each variable. So the following results are obtained:

Table 4. Test data sample

NO	ID	Serial Number	Nilai Sensor Soil Moisture	Nilai Sensor MPU6050	Waktu
1	1180	16723438	1023	100	2022-11-14 17:20:18
2	1185	16723438	415	41	2022-11-14 17:20:28
3	1190	16723438	413	40	2022-11-14 17:20:39
4	1195	16723438	416	41	2022-11-14 17:20:49
5	1200	16723438	1023	100	2022-11-14 17:20:59

In Figure 14 it can be seen that the average value changes every 50 seconds with a delay in sending data from the controller to the server average of approximately 1 second as shown in Table 4 because the design was tested with several treatments. In the first treatment, the design was in an upright position from an angle of about 80º, and the soil moisture sensor was planted in dry soil. In the second treatment, the design was at an angle <80º Soil moisture sensors were planted in soil that was sprinkled with a little water. In the third treatment, the design was at an angle of about 80º, and the soil moisture sensor was planted in the same soil and added a little water until it was moist. In the fourth treatment, the design was made at the same angle, and the soil moisture sensor was planted in water-soaked soil until the soil became soft. In the fifth treatment, the design was at an angle of <80º and planted in watery soft soil. Each treatment in design testing is classified into three conditions: safe, alert, and dangerous. This classification is distinguished from changes in the value of the soil moisture sensor and the MPU6050 sensor. According to the following table:

Table 5. Classification of Lanslide condition

No	Condition	Soil Moisture Value	MPU6050 Value
1	Safe	< 30	≥80⁰&≤91º
2	Alert	< 30	<80º& >91º
		≥ 40	≥80⁰&≤91º
		> 30 dan <50	≥80⁰&≤91º
3	Dangerous	≥ 40	<80º& >91º
		> 30 dan <50	<80º& >91º

JURNAL ECOTIPE
Electronic, Control, Telecommunication, Information, and Power Engineering
Volume 10, Issue 1, April 2023, pp. 142-151
ISSN 2355-5068 ; e-ISSN 2622-4852
DOI: 10.33019/jurnalecotipe.v10i1.3894

.

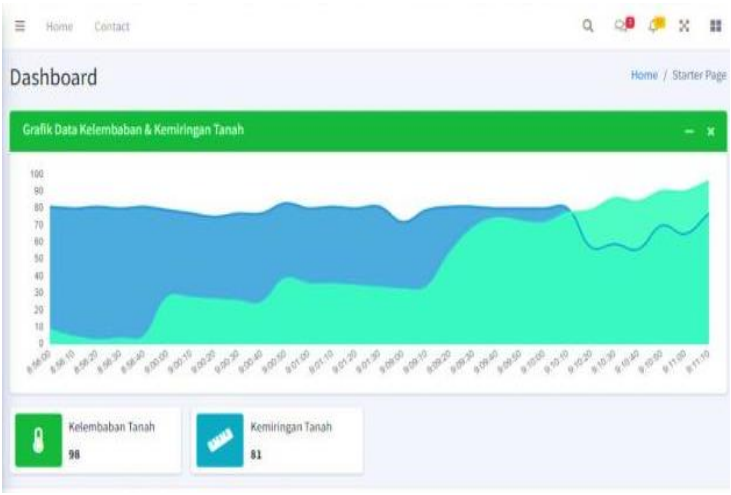

Figure 14. Graph of soil moisture and slope data

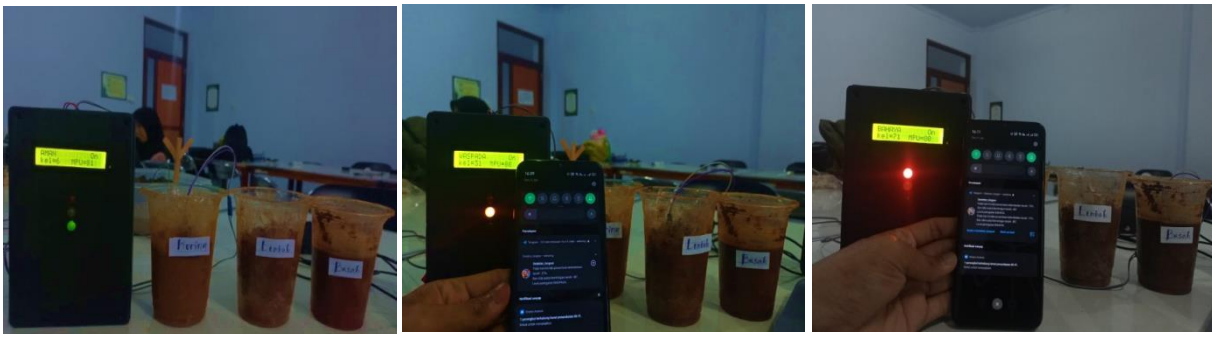

Figure 15. Equipment testing documentation

4. CONCLUSION

Based on the design, observation, and testing that has been done, the following conclusions can be drawn:

a. A landslide detection design has been made using the MPU6050 sensor as a soil slope detection and a soil moisture sensor as a soil moisture detector which can be monitored from the website.
b. The MPU6050 sensor can detect the slope of the land well, which only has an average error value of 0.14% for a square as a comparison tool. The Soil Moisture sensor can detect soil moisture well, where the average error value is 1.55% against the soil tester as a comparison tool.
c. Each treatment in design testing is classified into three conditions: safe, alert, and dangerous. The classification is distinguished from changes in the value of the soil moisture sensor and the MPU6050 sensor.
d. The design of this landslide detector device can run as expected, namely, it can provide notifications in real-time containing information on soil conditions, soil moisture values , and soil slope when in an alert and dangerous condition via the website optimally.

REFERENCES

[1] P. N. Fitriani, K. D. Lestari, H. D. Pratama, and F. Teknik, “Rancang Bangun Prototipe Deteksi Dini Tanah Longsor Berbasis Double Sensor,” *J. Inov. Fis. Indones.*, vol. 08, pp. 50–58, 2019.

[2] M. R. Amri *et al.*, *Risiko Bencana Indonesia*. 2016.

[3] R. M. Utama, I. Sucahyo, and M. YantiDewi, “Rancang Bangun Alat Deteksi Tanah Longsor Berbasis IOT dengan NODEMCU ESP8266 dan MPU6050,” *JIIF (Jurnal Ilmu dan Inov. Fis.*, vol. 06, no. 02, pp. 137–146, 2022.

Volume 10, Issue 1, April 2023, pp. 142-151
ISSN 2355-5068 ; e-ISSN 2622-4852
DOI: 10.33019/jurnalecotipe.v10i1.3894

[4] A. Susilo, D. R. Santoso, A. Rachmansyah, and Y. Zaika, "Desain Sistem Peringatan Dini Zona Rawan Longsor dengan Penerapan Sensor Kelembaban dan Getaran pada Tanah," *J. Meteorol. dan Geofis.*, vol. 12, no. 3, pp. 283–289, 2011.

[5] O. O. Artha, B. Rahmadya, and R. E. Putri, "Sistem Peringatan Dini Bencana Longsor Menggunakan Sensor Accelerometer dan Sensor Kelembaban Tanah Berbasis Android," *JITCE (Journal Inf. Technol. Comput. Eng.*, vol. 02, no. 02, pp. 64–70, 2018.

[6] J. Priyanto, H. Subagiyo, and P. Madona, "Rancang Bangun Peringatan Bahaya Longsor dan Monitoring Pergeseran Tanah Menggunakan Komunikasi Berbasis GSM," *J. Elem.*, vol. 1, no. 2, pp. 49–61, 2015.

[7] S. Y. Ulfa, G. A. Pauzi, and Warsito, "Desain dan Realisasi Alat Pendeteksi Perubahan Tingkat Kemiringan Tanah sebagai Penyebab Tanah Longsor Menggunakan Sensor Potensio Linier Berbasis Mikrokontroler ATMega 8535," *J. Teor. dan Apl. Fis.*, vol. 04, no. 01, pp. 29–36, 2016.

[8] D. M. M.Si, *Buku Referensi Bencana Tanah Longsor Penyebab dan potensi Longsor*. 2021.

[9] N. Luh *et al.*, "Rancang Bangun Sistem Pendeteksi Tanah Longsor Sederhana Berbasis Sensor Soil Moisture dan Sensor Ultrasonik," *Pros. SKF 2016*, pp. 348–356, 2016.

[10] N. Kadek, D. Parwati, D. M. Wiharta, and W. Setiawan, "Rancang Bangun Sistem Peringatan Dini Bahaya Tanah Longsor dengan Sensor Hygrometer dan Piezoelektrik," *E-Journal SPEKTRUM*, vol. 5, no. 2, pp. 183–190, 2018.

[11] I. N. Farikha, Hafidudin, and D. N. Ramadan, "Prototype Detektor Bencana Tanah Longsor Menggunakan Accelerometer dan Gyroscope Sensor dengan Konsep Internet Of Things (IoT)," *e-Proceeding Appl. Sci.*, vol. 6, no. 2, pp. 2442–2457, 2020.

[12] S. Birnadi, *Otomasi Sistem Penyiraman Untuk Beberapa Jenis Tanaman Sayuran pada Urban Agriculture*. 2019.

[13] N. Fauzia, N. Kholis, and H. K. Wardana, "Otomatisasi Penyiraman Tanaman Cabai Dan Tomat Berbasis IoT," *J. Reaktom*, vol. 6, no. 1, pp. 22–28, 2021.

[14] M. El Moulat, O. Debauche, A. B. Lahcen, P. Manneback, and F. Lebeau, "Monitoring System Using Internet of Things For Potential Landslides," *ScienceDirect*, vol. 134, pp. 26–34, 2018, doi: 10.1016/j.procs.2018.07.140.

[15] M. husnul Hakim and S. winardi, "Sistem Pendeteksi Dini Tanah Longsor Menggunakan Sensor Vibration Berbasis Internet of Things," *J. Pendidik. Teknol. Inf.*, vol. 5, no. April, pp. 1467–2621, 2022.

[16] Warner, "Soil Moisture Recorder," in *Madge Tech*, no. 603, 2012, pp. 2011–2012.

[17] B. Ave, D. Number, and R. Date, "MPU-6000 and MPU-6050 Product Specification," in *InvenSense*, vol. 1, no. 408, 2012, pp. 1–54.

[18] T. F. Siallagan and Juffi, "Rancang Bangun Sistem Peringatan Dini Terhadap Kebakaran Berbasis BOT Telegram Menggunakan Mikrokontroller ESP8266," *J. Glob.*, vol. VI, no. 1, pp. 61–70, 2019.

[19] Supriyatna, "Rancang Bangun Sistem Peringatan Dini Daerah Rawan Longsor." pp. 1–94, 2017.

[20] M. R. Maulana, G. Mukarrom, N. F. Aminy, J. Indriyanto, and A. Basit, "Rancang Bangun Sistem Deteksi Tanah Longsor Menggunakan Sensor Gyroscope dan Hygrometer Berbasis IOT," *J. Ilmu dan Inov. Fis.*, vol. 6, no. 2, pp. 137–146, 2022.

Publisher Address :

Electrical Engineering Department
Faculty of Engineering - Bangka Belitung University
Balunijuk, Kab. Bangka, Prov. Kep. Bangka Belitung
University Phone : (0717) 422145, 422965 Fax. (0717) 421303
Faculty Phone : (0717) 4260033 ext. 2122, 2124
Website : https://journal.ubb.ac.id/index.php/elektro
E-mail : jurnalecotipe@ubb.ac.id / jurnal.ecotipe@yahoo.com

ISSN 2355-5068
e-ISSN 2622-4852
Volume 10, Issue 1, April 2023